Effects of Genetic Deletion of Soluble Epoxide Hydrolase on Cardiac Function and Inflammation in Acute Lipopolysaccharide Injury

by

Deanna K. Sosnowski

A thesis submitted in partial fulfillment of the requirements for the degree of

Master of Science
in
Pharmaceutical Sciences

Faculty of Pharmacy and Pharmaceutical Sciences
University of Alberta

ABSTRACT

Acute inflammatory syndromes, such as endotoxemia, elicit detrimental multi-organ responses resulting in cardiac dysfunction often leading to death. Emerging evidence suggests epoxylipids can exert cardioprotective effects by modulating the NOD-like receptor family pyrin domain containing 3 (NLRP3) inflammasome pathway. However, these beneficial epoxylipids may be metabolized by soluble epoxide hydrolase (sEH). This study investigated whether cardiomyocyte-specific sEH-knockdown can attenuate inflammation and cardiac dysfunction in a model of acute lipopolysaccharide (LPS) injury via modulation of the NLRP3 inflammasome pathway.

Cardiomyocyte-targeted sEH-knockdown mice were produced by crossing *Ephx2*-floxed and Cre recombinase expressing mice. Male $sEH^{(Myo\ -/-)}$ (knockdown) and $sEH^{(Myo\ +/+)}$ (Cre control) mice were given tamoxifen (45 mg/kg, 6 i.p injections over 8 days) 5 weeks prior to LPS injection (10mg/kg, i.p.). Wild type (WT) and global sEH null mice were subjected to LPS treatment as comparators. Echocardiography was conducted pre-injection and 6 or 24 hours post-LPS. Plasma cytokine levels were determined with multi-plex assays. Neonatal rat cardiomyocytes were treated with LPS (1 μg/mL), 19, 20-epoxydocosapentaenoic acid (EDP, 1 μM) or sEH inhibitor, trans-4-[4-(3-adamantan-1-yl-ureido)-cyclohexyloxy]-benzoic acid (*t*AUCB, 10 μM), for 6 hours. NLRP3 and pro-IL-1β expression was assessed using immunoblotting. Extracellular release of MCP-1 and TNF-α were determined by ELISA. Caspase-1 activity was assessed by a fluorometric peptide substrate cleavage assay. Macrophage infiltration into the myocardium was assessed by immunohistochemical staining for CD68.

All groups experienced a decline in cardiac systolic function at 6 hours post-LPS. At 24 hours after LPS administration, the decline in cardiac function plateaued in mice with global and cardiomyocyte-specific sEH deletion while sEH expressing mice continued to deteriorate further. Plasma levels of pro-inflammatory cytokines post-LPS exposure were attenuated in mice lacking sEH. Cardiomyocytes treated with LPS had increased NLRP3 inflammasome and pro-IL-1β expression, which was not attenuated by co-treatment with 19,20-EDP or *t*AUCB. However, caspase-1 activity and the release of IL-1β, MCP-1 and TNF-α were reduced in 19,20-EDP and *t*AUCB treated cardiomyocytes. This was associated with reduced macrophage infiltration into the myocardium of LPS-treated sEH null and $sEH^{(Myo\ -/-)}$ mice.

In summary, cardiomyocyte-specific sEH deletion protects cardiac function and limits pro-inflammatory responses post-LPS exposure by limiting *local* cardiac inflammation and the activation of the *systemic* immune response. sEH inhibition does not prevent the expression of NLRP3 inflammasome machinery in cardiomyocytes but attenuates downstream activation of the pathway leading to release of fewer chemoattractant factors and recruitment of immune cells to the heart. Thus, limiting the inflammatory cascade to reduce LPS-induced cardiac and inflammatory injury.

PREFACE

This is an original work by Deanna K. Sosnowski. Currently, no part of this thesis has been previously published. Results in Chapter 3 were made possible through the collaboration with other individuals. K. Lockhart Jamieson assisted with the establishment of our tamoxifen protocol and preliminary echocardiographic measurements and analyses. Ahmed M. Darwesh assisted with caspase-1 assay troubleshooting. Xiuji Li and Kamala Lamsal assisted with Western immunoblotting and neonatal rat cardiomyocyte isolation. Suellen Lamb from the Li Ka Shing Institute of Virology conducted cryoslicing and staining for CD68 immunohistochemistry. Dr. Artiom Gruzdev and Dr. Darryl C. Zeldin from the National Institute of Environmental Health Sciences developed the Cre lox mouse model used for cardiomyocyte-specific sEH gene deletion. The research group of Dr. Bruce D. Hammock from the University of California, Davis synthesized and provided the small molecule, *t*AUCB, used in this study. Dr. John M. Seubert was the principle investigator responsible for the study design, interpretation of data, and guidance of the project.

"Science demands a tolerance for ambiguity. Where we are ignorant, we withhold belief. Whatever annoyance the uncertainty engenders serves a higher purpose: It drives us to accumulate better data. This attitude is the difference between science and so much else. Science offers little in the way of cheap thrills. The standards of evidence are strict. But when followed they allow us to see far, illuminating even a great darkness."

Dr. Carl Sagan, *Pale Blue Dot*

ACKNOWLEDGEMENTS

First and foremost, I want to thank my supervisor, Dr. John Seubert. Your guidance, patience, and understanding has made my experience truly fulfilling. I want to thank you for taking a chance on me. As a pharmacy student who wandered into your lab, I quickly realized that it was the place for me. Little did I know, the trajectory of my career (and life!) had been dramatically changed; and now I couldn't be more excited. I will always speak highly of you to my future peers and colleagues.

I would also like to thank the members of my committee, Dr. Paul Jurasz and Dr. Zam Kassiri. Your insight and expertise were so valuable to this project. As well, I want to thank Dr. Kassiri for your mentorship. Your words of advice 'Don't choose the easy thing' truly resonated with me. I will live by that going forward.

I would also like to acknowledge Dr. Artiom Gruzdev and Dr. Darryl Zeldin. I truly feel so privileged to have been given the opportunity to use the mouse model you developed. I also want to thank Dr. Matthew Edin, Dr. Bruce Hammock, and Dr. Gavin Oudit for their collaboration. For science to move forward, collaboration is invaluable, and I am so grateful to each of you.

I want to extend my gratitude to all the members of the Seubert Lab past and present. The late Dr. Victor Samokhvalov was a brilliant research associate and scientist who conducted the studies upon which my project was built upon. I also want to thank Dr. Lockhart Jamieson for taking me under her wing and her willingness to provide advice and wisdom over Zoom and a glass of wine. She is like the big sister I never had. Robert, I am glad I had the chance to work with you. I'm so happy I found someone who shares my sense of humor. I also could not have made it through without the steady reassurance, level-headedness, and words of encouragement from Ahmed. I am also grateful for Wessam, Kamala, Xiuju, Josh, Ala, and Liye for being such awesome lab colleagues. Also, thank you to Katryna, Emily, Tim, Lachlan, Yasir, Cassy, Dory, Rylee, Raye, and Anissa for your unwavering friendship. I am also so grateful for my pharmacist colleagues and everyone at Shoppers #2358 for being some of the coolest people I have ever met.

Of course, I would not be where I am today without my family. I realize how hard my parents have worked to give me the opportunities that they could have only dreamed of. I am so incredibly lucky and I hope I can make you proud.

Finally, I want to thank everyone in the Faculty of Pharmacy and Pharmaceutical Sciences. As well, I am grateful for the National Sciences and Engineering Research Council of Canada for funding and making this research possible.

TABLE OF CONTENTS

LIST OF TABLES

LIST OF FIGURES

AA	Arachidonic acid
ACEi	Angiotensin converting enzyme inhibitor
ALA	Alpha-linolenic acid
AMC	Amino-4-methylcoumarin
AngII	Angiotensin II
ANOVA	Analysis of variance
ARDS	Acute respiratory distress syndrome
ASC	Apoptosis-associated speck-like protein
ATP	Adenosine triphosphate
AUDA	12-(3-adamantan-1-yl-ureido)-dodecanoic acid
BME	Beta mercaptoethanol
BSA	Bovine serum albumin
Ca^{2+}	Calcium ion
CARD	Caspase recruitment domain
Cav-1	Caveolin-1
CD68, CD14	Cluster of differentiation
cGMP	Cyclic guanosine monophosphate
CHF	Congestive heart failure
CLP	Cecal ligation and puncture
COPD	Chronic obstructive pulmonary disease
COVID-19	Coronavirus disease 2019
COX	Cyclooxygenase
CVD	Cardiovascular disease
CYP450	Cytochrome P450

DAMP	Damage associated molecular patterns
DCM	Dilated cardiomyopathy
DHA	Docosahexaenoic acid
DHET	Dihydroxyeicosatrienoic
DiHOME	Dihydroxyoctadecenoic
DMSO	Dimethylsulfoxide
DNA	Deoxyribonucleic acid
DPA	Dihydroxyeicosapentaenoic
Drp-1	Dynamin-related protein-1
DTT	Dithiothreitol
ECM	Extracellular matrix
EDHF	Endothelial-derived hyperpolarizing factor
EDTA	Ethylenediaminetetraacetic acid
EEQ	Epoxyeicosatetraenoic acid
EET	Epoxyeicosatrienoic acid
EF	Ejection fraction
ELISA	Enzyme linked immunosorbent assay
EPA	Eicosapentaenoic acids
EpOME	Epoxyoctadecamonoenic acid
ER	Endoplasmic reticulum
ER	Estrogen receptor
FBS	Fetal bovine serum
Fis-1	Fission protein-1
FS	Fractional shortening
G-CSF	Granulocyte colony stimulating factor

GAPDH	Glyceraldehyde 3-phosphate dehydrogenase
GM-CSF	Granulocyte macrophage colony stimulating factor
H^+	Hydrogen ion
HETE	Hydroxyeicosatetraenoic acid
HIF-1α	Hypoxia-inducible factor-1
HMGB-1	High mobility group box 1
HRP	Horseradish peroxidase
ICAM-1	Intercellular adhesion molecule-1
IFN-y	Interferon gamma
IL	Interleukin
iNOS	Inducible nitric oxide synthase
I p.	Intraperitoneal
IP10	Interferon gamma-induced protein 10
iPSC	Induced pluripotent stem cell
IR	Ischemia-reperfusion
i.v.	Intravenous
IVRT	Isovolumetric relaxation time
K^+	Potassium ion
KC	Keratinocyte chemoattractant
LA	Linoleic acid
LAD	Left anterior descending coronary artery
LDH	Lactate dehydrogenase
LIF	Leukemia inhibitor factor
LIX	LPS induced CXC chemokine
LOX	Lipoxygenase

LPS	Lipopolysaccharide
LV	Left ventricle
LVAD	Left ventricular assist device
LVDP	Left ventricular developed pressure
LVEDV	Left ventricular end diastolic volume
LVESV	Left ventricular end systolic volume
M-CSF	Macrophage colony stimulating factor
MCP-1	Monocyte chemoattractant protein-1
mEH	microsomal epoxide hydrolase
MI	Myocardial infarction
MIG	Monokine induced by gamma interferon
MIP	Macrophage inflammatory protein
MnSOD	Manganese superoxide dismutase
mPTP	Mitochondrial permeability transition pore
mtDNA	Mitochondrial DNA
mtROS	Mitochondrial reactive oxygen species
MyD88	Myeloid differentiation primary response 88
Myh6-Cre$^{+/-}$sEH$^{(Myo\ -/-)}$	Cardiomyocyte-specific deletion of sEH
Myh6-Cre$^{+/-}$sEH$^{(Myo\ +/+)}$	Cre-expressing true control
NAD+	Nicotinamide adenine dinucleotide
NFkB	Nuclear factor kappa-light-chain-enhancer of activated B cells
NLR	NOD-like receptor
NLRP3	NOD-like receptor family pyrin domain containing 3
NO	Nitric oxide
OCT	Optimal cutting temperature

PAMP	Pathogen associated molecular patterns
PBS	Phosphate-buffered saline
PI_3K	Phosphatidylinositol-3-kinase
PLA_2	Phospholipase A2
PPARα	Peroxisome proliferator-activated receptor alpha
PPARγ	Peroxisome proliferator-activated receptor gamma
PRR	Pattern recognition receptor
PTUPB	4-(5-phenyl-3-(3-[3-(4-trifluoromethyl-phenyl)-ureido]-propyl)-pyrazol-1-yl)-benzenesulfonamide
PUFA	Polyunsaturated fatty acid
PVDF	Polyvinylidene difluoride
RAAS	Renin angiotensin aldosterone system
RANTES	Regulated on activation normal T cell expressed and secreted
ROS	Reactive oxygen species
SDS	Sodium dodecyl sulfate
sEH	Soluble epoxide hydrolase
SEM	Standard error of the mean
tAUCB	trans-4-[4-(3-adamantan-1-yl-ureido)-cyclohexyloxy]-benzoic acid
TLR	Toll-like receptor
TNF-α	Tumor necrosis factor alpha
TPPU	N-[1-(1-oxopropyl)-4-piperidinyl]-N'-[4-(trifluoromethoxy)phenyl)-urea
Trx	Thioredoxin
UA-8	13-(3-propylureido)tridec-8-enoic acid
VCAM-1	Vascular cell adhesion protein-1
VEGF	Vascular endothelial growth factor
WT	Wild type

CHAPTER 1

INTRODUCTION

1.1 SUMMARY

Rubor (redness), *calor* (heat), *tumor* (swelling), *dolor* (pain), and loss of function; these five 'pillars' have traditionally been used to describe inflammation.[1] However, our understanding of this biological process has advanced through scientific and medical innovation. Inflammation is critical for wound healing, tissue repair, and the body's defense against foreign pathogens.[1] However, a dynamic relationship exists between the defensive and potentially destructive actions of inflammation on the body.[1] Sepsis is a multifaceted syndrome which can occur in response to bacterial or viral infections.[2] Although the body mounts an immune response for protection, the inflammation generated is often robust, unregulated, and maladaptive.[2] Paradoxically, this inflammatory response causes further harm to the host. Systemic symptoms such as fever and hypotension, are also accompanied by direct organ damage.[3] Uncontrolled acute inflammation can directly damage the heart, which is a critical organ for providing an ongoing supply of oxygen and nutrients to the rest of the body.[4, 5] Even with antibiotic therapy and other supportive measures to restore intravascular volume and pressure, the prognosis is poor and mortality rate significantly higher for patients presenting with sepsis-induced cardiac dysfunction (septic cardiomyopathy).[3, 5]

Eicosanoids encompass a broad range of biologically active metabolites derived from N-3 and N-6 polyunsaturated fatty acids (PUFAs).[6] Biological stimuli, such as inflammation, can trigger the oxidation of PUFAs by cyclooxygenase (COX), lipoxygenase (LOX), and cytochrome P450 (CYP) enzyme systems to produce eicosanoids that can function as lipid mediators.[7, 8] PUFA-derived lipid mediators can have both beneficial and detrimental effects on the heart. Of particular interest are the CYP-derived lipid mediators, epoxylipids, which have been demonstrated to impact inflammation, cardiac function, reactive oxygens species (ROS) production, and mitochondrial quality; all of which are essential to the heart.[9] Some CYP-derived eicosanoids have demonstrated anti-inflammatory and cardioprotective properties in the context of acute inflammation.[10, 11] However, a mechanistic understanding of how these mediators and their subsequent metabolism exert their biological effects on the heart is still relatively unclear. Thus, it is an ongoing challenge for researchers to delineate tissue and cell type-specific mechanisms of these lipid mediators

for their use as potential pharmacological targets in different disease settings. This thesis will focus on providing a deeper understanding of how modulation of the CYP-derived eicosanoid profile affects the heart, and particularly the cardiomyocyte, during acute inflammatory injury using an experimental model of endotoxemia.

1.2 INFLAMMATION AND THE HEART

1.2.1 Cardiac dysfunction in sepsis: prevalence, prognosis, and management

Sepsis is an acute systemic inflammatory syndrome, where the body's immune response to a pathogen becomes dysregulated, leading to a hyperinflammatory state and overproduction of inflammatory mediators which are detrimental to the host.[12] It is one of the most common causes for inpatient hospital deaths in North America and is a critical global health problem.[13, 14] Disease progression follows a biphasic pattern (Figure 1.1).[2] An initial pro-inflammatory state is accompanied by a massive release of cytokines and activation of innate immune cells. This is later followed by an immunosuppressive state with mass apoptosis of immune cells, cardiac suppression, hypoperfusion, and potential for secondary infections to take hold.[15, 16]

Cardiac dysfunction induced by acute systemic inflammation, such as septic cardiomyopathy, is a serious complication and is challenging to clinically manage.[5] The incidence of acute cardiac dysfunction occurring during sepsis ranges from 10-40%, largely due to inconsistencies in diagnostic criteria and reporting between clinical studies.[17, 18] However, there is no doubt that prognosis is poor for patients who develop this complication, with mortality rates as high as 90%.[5, 17]

Septic cardiomyopathy often manifests as depressed systolic function, including reduced ejection fraction and cardiac output, hypotension, and left ventricular (LV) dilation.[5, 12, 18] This is detrimental to other organ systems in the body which rely on a steady, circulating supply of oxygen and nutrients. Current therapeutic management of septic cardiomyopathy includes hemodynamic supports such as vasopressors as well as inotropic agents such as dobutamine.[12, 19] However, current management strategies are often inadequate and mortality remains high. Other experimental therapeutics including agents targeting specific

pro-inflammatory cytokines, such as tumor necrosis factor alpha (TNF-α) and interleukin (IL)-1 were attractive, but have proven unsuccessful in clinical trials.[20-22] Hence, the need to understand mechanisms of sepsis-induced cardiac dysfunction and identify new pharmacological targets remains critical and ongoing.

1.2.2 Cellular and molecular mechanisms of septic cardiomyopathy

The pathophysiological mechanisms contributing to cardiac dysfunction in sepsis are numerous. Earlier theories suggested that decreased coronary flow leading to hypoperfusion of the heart muscle was the culprit for the decline in cardiac function.[23] However, more recent research demonstrates that this may be negligible and, instead, may be due to direct actions of cardiodepressant substrates produced during sepsis.[24, 25] Release of pro-inflammatory cytokines such as TNF-α and IL-1 may contribute to the early decline in cardiac function, whereas production of nitric oxide (NO) due to upregulation of inducible nitric oxide synthase (iNOS), may sustain cardiac depression into the later stages of the disease.[26, 27] Mitochondrial dysfunction is also another major player in septic cardiomyopathy.[28] The heart is a highly oxidative organ that relies on mitochondria not only for ATP production but also regulation of intracellular calcium (Ca^{2+}) homeostasis, essential for cardiac contractility.[29, 30] Disruption of cardiomyocyte mitochondrial respiratory chain function impairs energy production.[31] Cardiac mitochondria also endure loss of membrane potential, opening of the mitochondrial permeability transition pore (mPTP), and reactive oxygen species generation.[30, 32] Furthermore, the heart becomes less sensitive to catecholamine stimulation and damaged cardiomyocytes can secondarily release damage associated molecular patterns (DAMPs) such as high mobility group box 1 (HMGB1) which works in a paracrine manner to further perpetuate inflammatory damage of heart cells.[33, 34] In addition to a massive release of pro-inflammatory cytokines, metabolism of arachidonic acid into a plethora of inflammatory lipid mediators, or eicosanoids, including prostaglandins and leukotrienes can further damage the heart.[35] Upregulation of the expression of adhesion molecules on endothelial cells and cardiomyocytes also promotes the infiltration and accumulation of immune cells such as neutrophils and monocytes into the myocardium.[36, 37] Elements of the adaptive immune response are also engaged contributing to the

hyperinflammatory state.[38] Premature lymphocyte apoptosis facilitates sepsis-induced immunosuppression.[38] Overall, it is agreed upon that a variety of cardiodepressant factors are working in parallel, so targeting a single entity may not be sufficient to circumvent sepsis-induced cardiomyopathy.

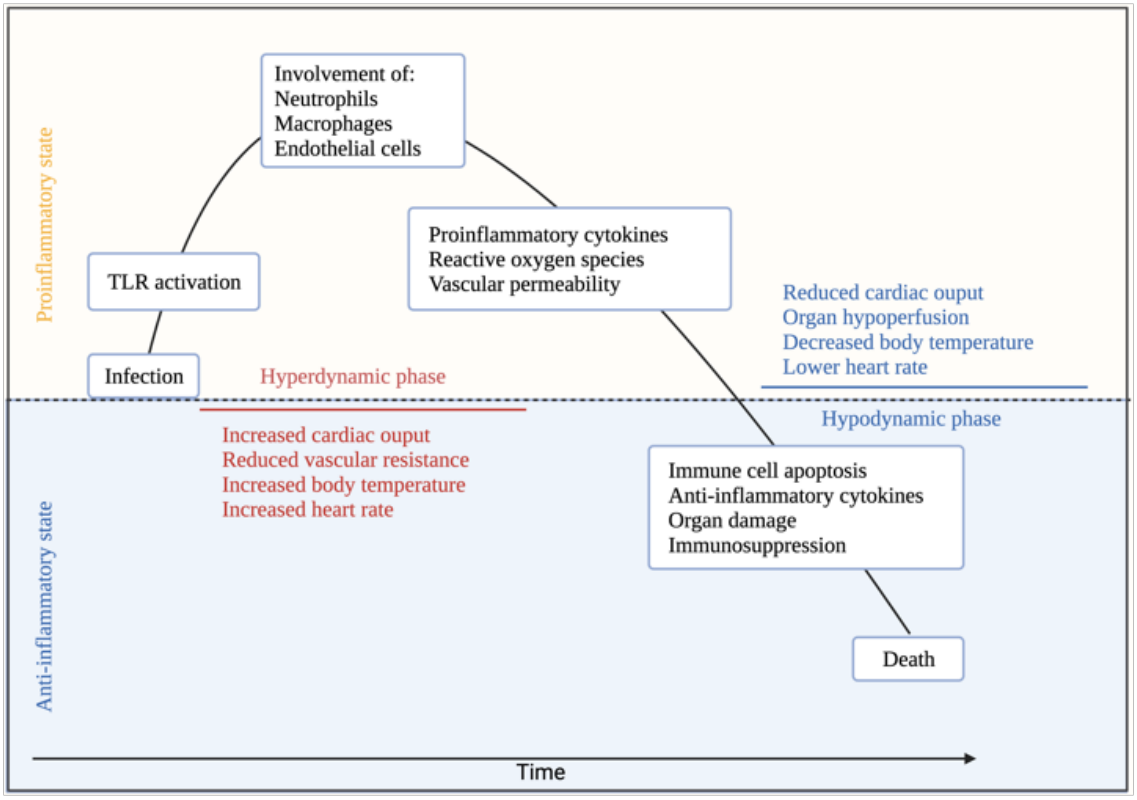

Figure 1.1. The biphasic pattern of sepsis disease progression. Adapted from the following sources.[3, 16]

1.2.3 The importance of understanding acute inflammation and the heart today: COVID-19 and cardiac inflammation

In 2019, the world was overtaken by a global pandemic caused by the coronavirus, SARS-Cov-2.[39] Over 5 million deaths and 250 million confirmed cases have occurred worldwide to date.[40] Fortunately, tireless work from scientists and clinicians led to the development of vaccines against the virus which began being administered early in 2021.[39] However, infections continue and many people remain suffering.

Not only does COVID-19 impact the lungs by causing acute respiratory distress syndrome (ARDS), severe infection with SARS-CoV-2 liberates an uncontrolled host inflammatory response which also damages other vital organs including the heart.[41] Cardiovascular involvement during severe SARS-CoV-2 infection can manifest as myocarditis, heart failure, acute coronary syndrome, arrhythmia, and an enhanced thromboembolic state.[41] Furthermore, SARS-CoV-2 infection can deteriorate the status of patients with underlying cardiovascular disease.[41] Despite the leaps and bounds made with respect to COVID-19 management over the past 2 years, a large amount of uncertainty remains about the etiology of cardiac involvement in SARS-CoV-2 infection and the long term impacts this may have on survivors. The disastrous and ongoing impact of COVID-19 further fuels the importance and critical need to research and understand how the heart is affected by unregulated acute inflammation.

1.2.4 Chronic inflammation and cardiovascular disease

In addition to acute inflammation, chronic, low-grade inflammation can also adversely impact the heart and has been demonstrated to be a key player in the pathogenesis of cardiovascular disease (CVD).[42-45] Aging is a non-modifiable risk factor for CVD.[46] Older individuals are more likely to experience an acute cardiac event and prognosis and recovery following an acute event tends to be poorer in elderly individuals.[47] The prevalence of CVD in older individuals has, in part, been linked to age-dependent cardiac structural and functional changes as well as systemic inflammation.[48, 49] CVD management in elderly individuals is often complicated by other chronic inflammatory disorders such as metabolic

syndrome, diabetes, and obesity.[43] Additionally, the innate and adaptive immune systems undergo remodelling with age, which may influence the development of CVD.[50-52] Thus, it is important that aging is also considered in the design of experimental models exploring the pathogenesis of chronic inflammation in CVD. Notably, chronic inflammation is also a main culprit in the pathobiology of atherosclerosis, acute myocardial infarction, and the progression to chronic heart failure.[53-60] Therefore, inflammation impacts the heart in both the acute and chronic setting. Understanding mechanisms of persistent, low-grade inflammation on the heart will provide valuable insight into age-dependent alterations of the cardiovascular system and chronic CVD.

1.3 LIPOPOLYSACCHARIDE

1.3.1 Overview: structure and function

Lipopolysaccharide (LPS), also known as endotoxin, is a glycolipid localized to the outer membrane of most gram-negative bacteria.[61] LPS serves as a barrier to protect bacteria from their extracellular environment. However, LPS is the main molecule which stimulates the host immune system upon infection with Gram-negative bacteria.[62] Structurally, LPS is composed of 3 main components – the O-antigen, the core oligosaccharide, and the lipid A moiety (Figure 1.2).[61] The O-antigen is a highly variable polysaccharide structure which induces antibody production in the infected host.[63] Its wide variability in composition allows for bacterial evasion of immune defenses.[63] The oligosaccharide core is also branched and heterogenous in structure.[64] Its stability allows separation of the lipid A and O-antigen components on the outer membrane.[64] Lastly, lipid A is the antigenic moiety of LPS, responsible for the activation of the host innate immune system and the robust and detrimental inflammatory response generated during endotoxemia and sepsis.[62]

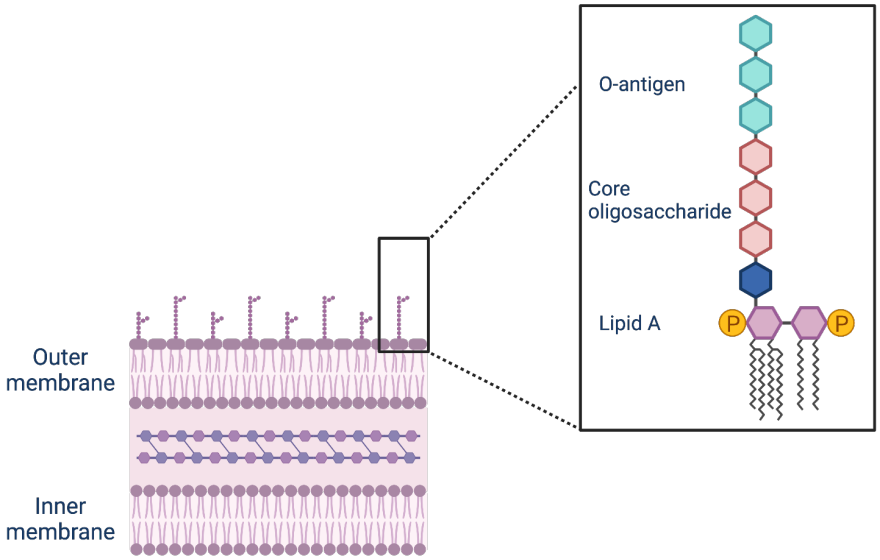

Figure 1.2. Structural composition of lipopolysaccharide. Adapted from the following sources. [61, 62, 64]

1.3.2 LPS as an experimental model of endotoxemia

Studies in humans have demonstrated that LPS is a main driver of cardiac dysfunction in sepsis.[65] To elicit acute systemic endotoxemia, purified LPS endotoxin is typically infused or injected either intravenously (i.v.) or intraperitoneally (i.p.) into experimental animals.[66] Since no bacteria are present, no active infection is established, but the host immune response is still activated.[16] The activation of innate immune cells, generation of pro-inflammatory mediators, and wide-spread organ damage models early-stage clinical sepsis, making LPS a widely used model.[16] Mice require a higher dose of LPS per body weight compared to humans in order to elicit a similar physiological response.[67] This may be due to the enhanced complexity of sepsis in humans, activation of different transcriptional responses due to LPS exposure, and variations in cellular composition of tissues between mice and humans.[68] However, when dose is properly titrated, there is striking similarity in the kinetics and composition of pro-inflammatory cytokines released between human sepsis and LPS-induced endotoxemia.[67]

1.3.3 Cell signal transduction

A class of transmembrane receptors, pattern recognition receptors (PRRs), recognize specific molecular structures and transduce intracellular signalling pathways to activate the innate immune system.[69] PRRs can recognize a class of conserved exogenous molecular structures termed pathogen associated molecular patterns (PAMPs) specific to foreign invaders and pathogens.[69] One of the most well-studied groups of PRRs are the toll-like receptors (TLRs). The immunogenic lipid A component of LPS is recognized by TLR4 as well as TLR2 isoforms.[70] TLR4 receptors are located on the surface of cells of the innate immune system.[69] Additionally, terminally differentiated cardiomyocytes also express TLR4 in high abundance, making the heart a susceptible target to the effects of endotoxin.[71]

Upon recognition of LPS by the cofactor, CD14, primarily found on monocytes and macrophages, the complex delivers LPS to cell-surface TLR4 receptors which form a homodimer structure.[71] Recruitment of the adapter protein, MyD88, to the cytosolic domain of TLR4 initiates the intracellular signalling pathway.[70] Activation of the inhibitory *k*B (I*k*B)

kinase induces phosphorylation of I*k*B and dissociation from the cytosolic nuclear factor kappa-light chain-enhancer of activated B cells (NF-*k*B) complex.[70] The transcription factor, NF-*k*B, is then free to translocate to the nucleus and upregulate the transcription of pro-inflammatory cytokines.[70] The production and release of inflammatory mediators and cytokines such as IL-1, IL-6, and TNF-α initiate the cascade of the innate immune response.[70]

1.3.4 LPS and chronic CVD: A clinical context

The contribution of chronic inflammation to heart disease has been a well-established concept in recent years, however the specific contribution of LPS to the pathobiology is less clear.[72] Living organisms are exposed to many types of pathogens, and thus LPS, in their environment on a daily basis. Humans are one of the organisms most sensitive to endotoxin.[67] Additionally, humans are also exposed to bacteria through current or chronic infections as well as microbiota via gut barrier dysfunction.[73] It was first proposed that the chronic immune activation and elevation of pro-inflammatory cytokines seen in congestive heart failure (CHF) patients may be due to a pathogenic process, known as *the endotoxin hypothesis*.[74] Despite optimal pharmacotherapy with diuretics and angiotensin converting enzyme inhibitors (ACEi), CHF patients may still experience edema, congestion, and hypoperfusion in their mesenteric venous system.[74] This can lead to enhanced gut permeability and the translocation of bacteria and LPS endotoxin into the systemic circulation.[75, 76] Enhanced interaction of LPS with monocytes and macrophages may explain significantly elevated levels of secreted CD14 and TNF-α in CHF patients.[74] As LPS is a potent simulator of inflammatory cytokines[77, 78], chronic LPS exposure in CVD may explain the low-grade inflammation and immune dysregulation which enhances disease progression and further promotes endotoxin translocation from the gut in a feed-forward cycle.[79] This hypothesis was built upon in a prospective cohort study from 1999 that directly quantified circulating endotoxin levels in heart failure patients.[80] It demonstrated that patients experiencing an acute CHF exacerbation had significantly higher levels of systemic endotoxin and other pro-inflammatory cytokines compared to stable CHF patients and healthy controls, and which reduced with resolution of the acute CHF exacerbation.[80] Since then, other studies have shown an association between endotoxin levels, immune activation,

and a wide range of cardiovascular disease.[75, 77, 78, 81-83] For example, chronic exposure to endotoxin from mild bacterial periodontitis infections can potentiate systemic inflammation which may be a risk factor for atherosclerosis and coronary artery disease.[84, 85] Therefore, LPS may not only acutely impact the heart during endotoxemia, but may contribute to CVD development through long term chronic exposure.

1.4 THE INNATE IMMUNE SYSTEM

1.4.1 Overview and function

The innate immune system serves as the body's first line of defense against invading pathogens as well in response to sterile inflammatory stimuli.[86] It consists of a variety of elements, including the skin barrier, epithelia and mucosa, as well as immune cells and their secreted components including cytokines and chemokines.[86] This system is also necessary to initiate the more specific and longer lasting response of the adaptive immune system.[86]

A dynamic relationship exists between the heart and the innate immune system.[87] For example, following acute cardiac injury, such as myocardial infarction (MI), cells of the innate immune system including monocytes, macrophages, and neutrophils are mobilized to the site of injury.[88] These cells can assist in clearing necrotic debris at the area of infarct but can also contribute to collagen deposition and detrimental cardiac remodeling.[88] Furthermore, tissue resident cardiac macrophages also help to regulate homeostatic functions of the heart including immune surveillance and electrical condution.[89-91] Our understanding of the relationship between the heart and the innate immune system is still unfolding, but is proving to be critical in our understanding of the heart in both health and disease.

1.4.2 Cells of the innate immune system

Neutrophils are typically the first group of innate immune cells to respond to acute infection or injury.[92] Neutrophils primarily function as phagocytes, engulfing debris and foreign material, as well as secretion of cytotoxic, oxidant, and lytic molecules.[92] However, these cells can also communicate with macrophages and release signalling molecules to

activate T helper cells.[92] Following acute MI, pro-inflammatory neutrophils rapidly infiltrate the myocardium to clear necrotic cells but can also contribute to dysregulation of the local inflammatory response.[93] Neutrophils also accumulate in organs, including the heart, during acute inflammatory injury such as sepsis.[37] During sepsis, there is a dysregulation of the neutrophil response. A larger proportion of immature neutrophils are released from the bone marrow and their apoptosis tends to be delayed.[94-97] Interestingly, blockade of neutrophil function during sepsis is insufficient to prevent septic cardiomyopathy.[36] This suggests that cardiac damage may occur through a combination of well-orchestrated responses from various immune cell types.

In addition to their hemostatic functions, platelets have also been attributed to the immune response.[98] In particular, the interaction between neutrophils and platelets enhances the host's defence to invading pathogens.[98] Platelets can attract neutrophils to infected tissues and organs through the secretion of chemoattractant factors and conditioning of endothelial beds to enhance neutrophil rolling, adhesion, and infiltration.[98, 99] The generation of neutrophil extracellular traps (NETs), a web of extracellular DNA, histones, and granules, through NETosis also relies on the interplay between neutrophil and platelet functions.[100] LPS stimulation of TLR4 receptors on platelets promotes their binding to surrounding adherent neutrophils and neutrophil formation of NETs to trap and kill invading pathogens.[100, 101] NETs then further promote thrombus formation, platelet activation, and aggregation.[98] Hence, a synergistic loop exists between neutrophil stimulation, NET formation, and platelet activation in the innate immune response during endotoxemia and sepsis.

Monocytes are also mobilized from the bone marrow and spleen in response to sterile injury as well as LPS where they can infiltrate peripheral tissues.[102] Once within the heart, monocytes can differentiate into macrophages and dendritic cells, which can function as phagocytes and secretory cells to mediate the innate immune response.[102] Macrophages can take on an array of phenotypes and are loosely referred to as pro-inflammatory and anti-inflammatory or reparative.[103] *In vitro* macrophages which are activated by interferon gamma (IFN-γ) or LPS are categorized as 'M1' or 'classically activated' macrophages and tend to take on a more pro-inflammatory phenotype.[103] This subset is efficient in the presentation of antigens to adaptive immune cells and the secretion of pro-inflammatory

cytokines and reactive oxygen species as a means of defense.[104, 105] Macrophages in culture which are activated by IL-4 are 'M2' or 'alternatively activated' and tend to be more reparative in function and work to dampen the inflammatory response.[103, 106]

However, *in vivo*, macrophage phenotypes are much more dynamic and tend to exist on a continuum rather than a polarized dichotomy.[106] *In vivo*, macrophages can adapt their functions based on circulating local mediators in their microenvironment, cellular stress, and disease states.[104] This plasticity makes concrete characterization of *in vivo* macrophages more challenging. However, researchers do have a comprehensive understanding of different macrophage functions in CVD. For example, following acute MI, peripheral monocytes are recruited to the site of cardiac damage.[107] These monocytes differentiate into macrophages that are more inflammatory in phenotype which partake in efferocytosis, release cytokines, and engulf necrotic cells and debris.[107] Within a day following the initial insult, a functionally different subset of macrophages populate the damaged myocardium. This subset fine-tunes the initial inflammatory response and assists in extracellular matrix (ECM) and collagen deposition.[107] A fine balance exists between macrophage functions to avoid rampant cardiac inflammation and maladaptive cardiac remodeling and fibrosis.[107] In sepsis, organs including the heart are rapidly overtaken by macrophages with more pro-inflammatory functions which contribute to tissue damage and the decline in cardiac function.[108] Macrophage polarization is also impaired with aging.[109] With increasing age, macrophage polarization accelerates towards a pro-inflammatory phenotype, which also may explain age-related cardiac functional decline.[110] Therefore, the temporal balance that exists in macrophage function could potentially be therapeutically exploited in various cardiac pathologies.

In addition to monocyte-derived macrophages, the myocardium also harbours resident macrophages important for homeostatic functions. This subset of macrophages enter the myocardium during the embryonic development stage where they persist into adulthood and turnover *in situ* during steady-state conditions with increasing contribution from differentiation of circulating monocytes over time.[91, 111-115] As tissue resident cells, cardiac macrophages are highly influenced by their local tissue microenvironment. Cardiac resident macrophages adapt a spindle-like morphology speculated to be due to the longitudinal alignment of surrounding myocardial fibres.[91] Their close association with

endothelial cells and cardiomyocytes suggests potential cross talk and signalling between cell types in the heart to maintain proper function and homeostasis.[116, 117] Expression of genes such as IL-10 and complement component 1q suggest that cardiac macrophages may have a role in dampening local inflammation.[117] In addition, enrichment in processes involving the uptake, processing, and presentation of antigens suggests an immunomodulatory and maintenance role in the heart under basal conditions. However, much of this data requires functional confirmation and perhaps organ-specific ablation of cardiac resident macrophages will help to delineate the role of these cells *in vivo* during homeostasis and injury.

The function of resident macrophage subsets in CVD have also been extended to the clinical setting. Outcomes in patients with end-stage CHF with left ventricular assist device (LVAD) implants awaiting cardiac transplant were examined.[118] Patients with persistent systolic dysfunction 6 months post-LVAD implantation had a significantly higher proportion of pro-inflammatory $CCR2^+$ macrophages in their LV biopsy at the time of LVAD implantation and removal than those whose systolic function had improved.[118] Although this is an association, these findings strengthen evidence that the heart contains phenotypically and functionally distinct macrophage subsets which may have clinical and prognostic implications in CVD. This also suggests that therapeutic strategies targeting a specific subset of cardiac resident macrophages, such as $CCR2^+$, may be a potential strategy to combat maladaptive immune response and cardiac dysfunction.

1.4.3 Pattern recognition receptors

A key feature of the innate immune system is its ability to distinguish self from non-self.[86] The innate immune system can sense certain molecules, broadly termed alarmins.[119] Alarmins can be components of foreign invaders including LPS from gram-negative bacteria, lipoteichoic acid from gram-positive bacteria, or viral genetic material.[120] These foreign molecules can also be called pathogen-associated molecular patterns (PAMPs).[120] Additionally, the innate immune system can sense damage-associated molecular patterns (DAMPs). These are molecules that are released from endogenous host cells in response to stressful stimuli or injury, such as cytokines, nuclear or mitochondrial DNA, and reactive

oxygen species.[121] PAMPs and DAMPs are recognized by their corresponding pattern recognitions receptors on innate immune cells.[122] An established class of PRRs include the toll-like receptors.[122] Notably, TLR4, and to a lesser extent, TLR2 recognize LPS as a PAMP and initiates the transduction of intracellular signalling pathways and production of pro-inflammatory cytokines in response to this molecule.[120, 123, 124]

TLR4 is ubiquitously expressed on innate immune cells including neutrophils, monocytes, macrophages, and also endothelial cells and platelets.[125, 126] Importantly, cardiomyocytes have also been demonstrated to express TLR4, which suggests a role for the cardiomyocyte in the detection and response to LPS. Stimulation of TLR4 receptors on cardiomyocytes activates NF-*k*B signalling and promotes the secretion of inflammatory IL-6, and neutrophil chemoattractants such as keratinocyte-derived chemokine (KC) and macrophage inflammatory protein (MIP).[127] Activation of cardiomyocyte TLR4 can augment acute cardiac injury, damage cardiomyocyte mitochondria, and promote apoptosis.[128, 129] Hence, the cardiomyocyte may also participate in the innate immune response to a larger degree than what has previously been anticipated.

1.4.4 Signalling molecules: cytokines

The innate immune system relies heavily on the sending and receiving of signals as a means of communication between cell types and tissues in response to infection or injury.[130] One such way these signals can be sent are through small molecules, called cytokines. These molecules are diverse in structure and function. Cytokines can travel throughout the systemic circulation or work locally in a receptor-mediated autocrine or paracrine manner.[130] During sepsis, there is a massive release of cytokines from immune cells, sometimes referred to as the 'cytokine storm'.[131] Release of these mediators can further activate and attract immune cells, integrate the adaptive immune response, and promote host cell damage contributing to a positive feedback loop of inflammation.[2] At the same time, the cytokine response is often necessary for host defense and clearance of infection.[132] Therefore, a delicate balance in cytokine regulation is imperative, which is often not the case in sepsis.

The release of cytokines and chemokines mirrors the biphasic disease progression of sepsis (Figure 1.1).[2, 133] In the early stages of sepsis, pro-inflammatory cytokines including IL-1, IL-6, IL-12, IL-17, IFN-γ, and TNF-α predominate.[132] Clinical studies have shown that non-survivors of sepsis have a persistent increase in these cytokines during the first 4 days compared to patients who recovered.[134] In patients who survive the hyperinflammatory state of sepsis, an immunosuppressive state follows. Apoptosis and dysfunction of T cells can stimulate phagocytes to release anti-inflammatory cytokines such as IL-10.[2, 94] The relative amount of IL-10 may be proportional to the destruction induced by the initial hyperinflammatory state, suggesting a close-knit relationship between the two phases of sepsis.[35, 135]

Low molecular weight cytokines, termed chemokines, can promote the differentiation, mobilization, and attraction of immune cells to infected or damaged tissue.[35] Notably, monocyte chemoattractant protein-1 (MCP-1) has been demonstrated to be elevated in sepsis and is important for the infiltration of circulating monocytes into tissues and organs.[134, 136] Furthermore, the chemokines MIP and KC activate and attract neutrophils.[137] Similarly, regulated on activation normal T cell expressed and secreted (RANTES) attracts T helper cells and monocytes, integrating both innate and adaptive immunity.[138, 139] As previously mentioned, neutralization of individual groups of pro-inflammatory cytokines in clinical trials have not improved patient mortality.[21] Hence, an intricate communication network exists between multiple cytokines and the innate and adaptive immune systems in sepsis.

1.4.5 The NLRP3 inflammasome

The NOD-like receptor (NLR) family pyrin domain containing 3 (NLRP3) inflammasome is a large cytosolic multi-protein complex implicated in the innate immune response.[140, 141] It consists of the multi-domain NLRP3 sensor molecule and apoptosis-associated speck-like protein (ASC), which is an adaptor protein that contains a caspase-recruitment domain (CARD), which allows the recruitment of the effector pro-caspase-1 to the multi-protein complex.[142]

Engagement of the NLRP3 inflammasome response is a multi-step process consisting of first priming, followed by activation (Figure 1.3).[142] Priming is initiated by the binding of danger signal molecules such as PAMPs and DAMPs to PRRs on the cell surface, such as TLR4.[143] Danger signals can constitute remnants from invading organisms, such as LPS or endogenous molecules released from damaged or dying cells.[143, 144] TLR4 stimulation causes activation of downstream intracellular MyD88 signalling and nuclear localization of the transcription factor NF-*k*B.[140] This upregulates the transcription and expression of inflammasome protein component, NLRP3, as well as inactive pro-IL-1β and pro-IL-18.[140] Following NLRP3 inflammasome priming the vital machinery comprising the NLRP3 inflammasome are assembled in the cytosol, awaiting further signal.[140]

A second signal is required for the activation of the dormant NLRP3 complex.[145] Signals are diverse and include potassium (K^+) efflux, release of intracellular ATP, mitochondrial DNA (mtDNA) and increased ROS from damaged mitochondria – all indications of cellular stress.[141, 145, 146] Nigericin, a K^+/H^+ ionophore is commonly used as an NLRP3 activator in the *in vitro* setting.[146] Signaling pathways upstream of NLRP3 activation are less clear. However, pro-caspase-1 is proteolytically activated inducing the maturation of pro-IL-1β and pro-IL-18 to their active forms.[140] Additionally, cytosolic gasdermin D is cleaved by caspase-1 allowing the cytotoxic N-terminal domain to translocate to the plasma membrane and assemble into pore-forming structures.[147, 148] These pores serve for the release of IL-1β and IL-18 from the cell where they can go on to induce further local and systemic inflammatory activation.[147, 149] Additionally, gasdermin D pores can induce cell lysis and pyroptosis, a form of inflammatory cell death.[150, 151]

Pyroptosis can be classified as a gasdermin D-dependent form of programmed inflammatory cell death.[150] This form of cell death is characterized by membrane blebbing and eventual cell lysis leading to the release of cellular content, danger signals, and inflammatory proteins.[148] The N-terminal portion of gasdermin D is able to interact with the inner portion of cell membrane phospholipids.[152] N-terminal monomers assemble into oligomers until a pore-like structure transverses the cell membrane causing disruption of the cellular osmotic gradient and cell swelling and lysis.[152]

In addition to LPS binding to cell surface TLR4 receptors, cytosolic LPS can also be sensed intracellularly leading to human caspase-4/5 and mouse caspase-11 activation.[147]

This signalling refers to the 'non-canonical' inflammasome pathway.[153] Activation of caspase-4/5 or 11 occurs leading to cleavage and liberation of the gasdermin D N-terminal.[147, 153] Pyroptotic pore formation permits the efflux of intracellular potassium and assembly of the NLRP3 inflammasome, followed by caspase-1 activation, and initiation of the canonical inflammasome signalling pathway.[153, 154]

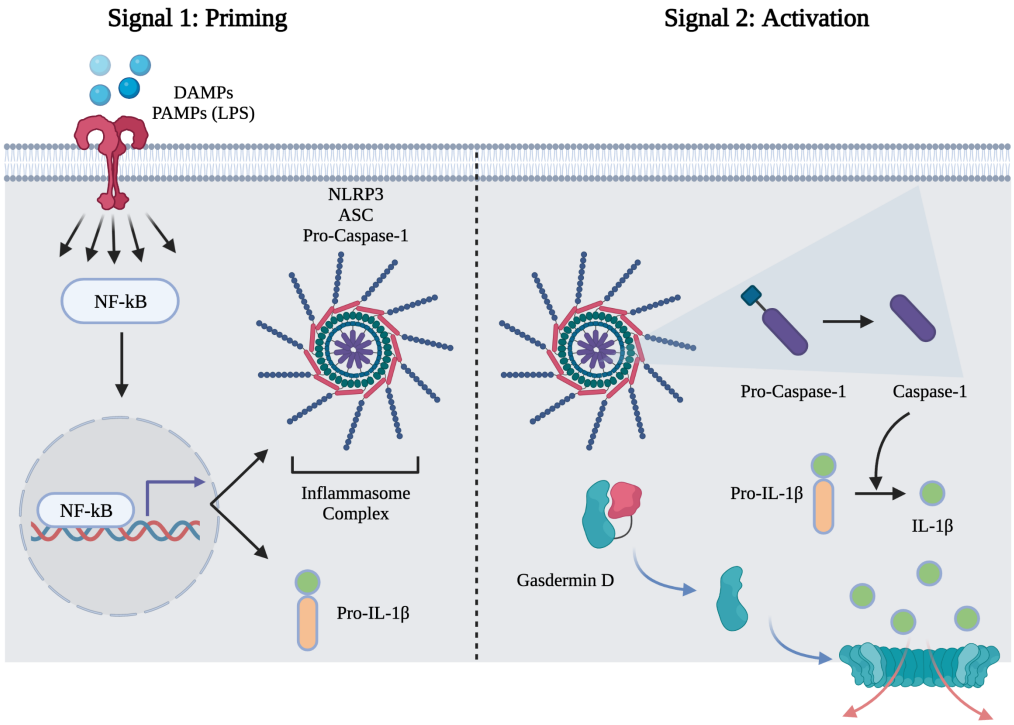

Figure 1.3. Priming and activation of the NLRP3 inflammasome. Adapted from the following sources.[140-142]

1.4.5.1 The role of mitochondria in NLRP3 inflammasome signalling

Mitochondrial damage and dysfunction is implicated in the activation of the NLRP3 inflammasome.[142] The liberation of mtDNA into the cytosol from damaged mitochondria can directly bind with the NLRP3 complex to cause secretion of IL-1β.[155] Cardiolipin is a mitochondrial phospholipid exclusively located on the inner membrane that is translocated to the outer membrane to act as a signalling molecule in response to mitochondrial stress.[156] The NLRP3 inflammasome can take advantage of this stress signal. The NLRP3 inflammasome can directly interact with exposed cardiolipin to activate caspase-1 and promote IL-1β secretion.[157] With aging, the NLRP3 inflammasome is also over-activated due to enhanced mitochondrial stress and impaired quality control mechanisms.[158] Aberrations in mitochondrial dynamics including fission and fusion can also trigger inflammasome activation.[159, 160] Thus it is clear, mitochondrial health and NLRP3 signalling are closely intertwined.

Sepsis notoriously promotes the damage of cardiac mitochondria.[161] LPS causes pathological fragmentation of cardiomyocyte mitochondria via dynamin-related protein-1 (Drp1) and its interaction with the adaptor, fission-1 (Fis1) on the mitochondria.[162, 163] Cardiac mitochondrial function is also impaired with LPS exposure.[164] Enzymatic activities of respiratory chain complexes are reduced, which compromises the ability for the heart to generate a sufficient amount of ATP and sustain proper function.[161, 164] Furthermore, mitochondria produce higher amounts of ROS which can further perpetuate mitochondrial dysfunction.[28, 165] Hence, there is strong evidence to suggest that LPS-induced mitochondrial damage may provide a connection to NLRP3 inflammasome activation in the pathogenesis of septic cardiomyopathy.

1.4.5.2 Implications of the NLRP3 inflammasome in CVD

The NLRP3 inflammasome pathway is dysregulated in a variety of inflammatory diseases.[166] It has also been implicated it acute and chronic cardiac inflammation.[167] It provides a critical link between the heart, mitochondrial dysfunction, and the innate immune system. Following acute MI, release of DAMPs induces cardiac NLRP3 priming and

activation which promotes pathologic hypertrophy leading to heart failure.[168] Pathogenesis of diabetic cardiomyopathy and atrial fibrillation have also been linked to cardiac NLRP3 inflammasome signalling.[169, 170] A small molecule inhibitor of the NLRP3 inflammasome, MCC950, has been synthesized.[171] MCC950 selectively works to interfere with ASC oligomerization without affecting the priming step or expression of inactive pro-IL-1β and pro-caspase-1 in cells.[171, 172] The use of MCC950 has been successful in attenuating cardiac dysfunction in models of MI, atherosclerosis, doxorubicin-induced cardiotoxicity, and sepsis-induced myocardial dysfunction, further attributing the involvement of this signalling mechanism to a range of cardiac pathologies.[173-176] Although commonly studied in immune cells such as monocytes and macrophages as well as whole tissue lysate, NLRP3 inflammasome signalling has recently been demonstrated in cardiomyocytes and cardiac fibroblasts.[167, 170] However, the role and regulation of this pathway in non-immune cells such as cardiomyocytes is still poorly defined.

1.5 LONG CHAIN PUFAS AND THE CARDIOVASCULAR SYSTEM

Long chain N-3 and N-6 PUFAs are essential fatty acids which must be obtained from the human diet. Alpha-linolenic acid (ALA), eicosapentaenoic acids (EPA), and docosahexaenoic acid (DHA) found in fish, flax, nuts, and canola and soybean oil are the main sources of the essential N-3 PUFAs.[6] N-6 PUFAs, including arachidonic acid (AA) derived from linoleic acid (LA), are found in vegetable oils, corn oil, and sunflower oil.[6] It is recognized that fatty acids can have pleiotropic effects on the cardiovascular system. The Canadian Cardiovascular Society recommends that PUFAs should be incorporated into the diet to replace trans and saturated fatty acids to reduce the risk for CVD.[177] However, the relationship between long chain PUFAs and cardiovascular health are complex.

Early observational studies showed that the Inuit population of Greenland consumed a diet rich in N-3 PUFAs from fish.[178-180] Those living in Greenland had lower plasma triglyceride levels, a risk factor for CVD, as well as incidence of ischemic heart disease and diabetes compared to people in Denmark who consumed a more traditional Western diet.[178-181] These observational studies prompted health scientists to further investigate the role of PUFAs in CVD. EPA was shown to exert an inhibitory effect on platelet aggregation and

lowered plasma triglycerides which may possibly explain the lower rate of thrombotic events observed in the Greenland observational studies.[182, 183] The GISSI-Prevenzione study was a randomized controlled trial that investigated the role of N-3 PUFA supplementation as secondary prevention for patients who had recently experienced acute MI.[184] Results demonstrated that N-3 supplementation significantly reduced the risk of morality, non-fatal MI and stroke, suggesting that N-3 PUFAs may provide some benefit in the setting of secondary prevention.[184] Furthermore, the Diet and Reinfarction Trial (DART) demonstrated that increasing N-3 PUFA intake through dietary interventions also significantly reduced all-cause mortality in men who had suffered a previous MI.[185] High-dose N-3 PUFA supplementation can also work acutely.[186] Administration to patients presenting in hospital with acute MI prevented left ventricular remodeling, fibrosis, and systemic inflammation throughout the following months of recovery.[186]

In contrast, the SU.FOL.OM3 trial was a randomized and placebo-controlled study that assessed the effects of supplementation of folate and N-3 PUFAs in patients who experienced an acute MI or ischemic stroke in the previous year.[187] Despite supplementation, there was no significant reduction in CVD related deaths or non-fatal MI or stroke events.[188] The role of PUFAs in primary prevention of CVD is also conflicting.[189] The ORIGIN trial found no significant reduction in the primary prevention of CVD events or mortality in patients with diabetes or dysglycemia following EPA and DHA supplementation despite a reduction in circulating triglyceride levels.[190] The American Heart Association has proposed some potential reasons which may explain the discrepancies between the outcomes of clinical trials. In recent years, there has been increased emphasis to the public about the health benefits of N-3 PUFA consumption.[191] An increasing number of individuals have made the effort to incorporate N-3 PUFA-rich sources such as fish into their diet.[191] Therefore, the additional supplementation of EPA and DHA provided in clinical trials may deliver little additional cardiovascular benefit if an individual's N-3 PUFA consumption is already at the recommended intake levels.[191] Advancements have also been made regarding the overwhelming benefit of other drug therapies in CVD, including statins, ACEi, and beta blockers.[191] Clinical practice has improved over the years and many patients who meet the criteria to be on these drugs have been prescribed them by their physician or pharmacist.[191] So, patients' risks for primary or secondary cardiovascular events are substantially reduced.

The additional supplementation of N-3 PUFAs may provide little additional clinical benefit for high risk patients in clinical trials who are already using optimal drug therapy.[191] Therefore, it still remains inconclusive and under debate whether PUFAs provide any clinical cardiovascular benefit besides altering surrogate markers such as plasma triglycerides.

Other studies suggest that N-3 PUFAs may play a role in the modulation of inflammation.[192, 193] The Western diet is rich in N-6 PUFAs, LA and AA, compared to N-3 PUFAs at a ratio of nearly 15:1.[194] AA is a precursor for a variety of pro-inflammatory, platelet activating, and pro-thrombotic lipid mediators including prostaglandins, such as thromboxane A_2, and leukotrienes produced by COX and LOX metabolic pathways which may increase the risk for the development of CVD.[194-196] Interestingly, a diet enriched with EPA and DHA promotes the incorporation of these N-3 PUFAs into the phospholipid membrane of cells including macrophages, neutrophils, and lymphocytes, reducing the N-6/N-3 membrane composition ratio.[197-201] Upon cellular stimulation or stress, PUFAs are released from the phospholipid membrane by phospholipase A_2 (PLA_2).[202, 203] EPA and DHA can compete with AA as substrates for COX and LOX enzyme systems.[197] When a larger proportion of N-3 PUFAs are present in the membrane due to supplementation, fewer N-6-derived COX and LOX pro-inflammatory mediators are produced, thus helping to control excessive inflammation.[197, 204] Furthermore, this can also reduce the expression of the pro-inflammatory COX-2 enzyme isoform.[205] Therefore, higher N-3 intake may reduce the production of pro-inflammatory AA-derived COX and LOX mediators. In the clinical setting, healthy volunteers who supplemented their diet with N-3 PUFAs for 6 weeks had reduced production of IL-1α and TNF-α upon stimulus with endotoxin.[192] Incorporation of N-3 PUFA supplementation into the diet of patients with rheumatoid arthritis, psoriasis, and ulcerative colitis demonstrated clinical improvement in symptoms however did not affect serum levels of acute phase reactants and cytokines.[195] As inflammation is often a common denominator in the pathobiology of CVD, beneficial effects of N-3 PUFAs on the heart may be exerted through their anti-inflammatory properties.[206, 207]

1.6 BIOSYNTHESIS OF N-3 and N-6 PUFA EPOXYLIPIDS

1.6.1 The cytochrome P450 enzyme system

The CYP450 enzyme system encompasses a broad family of monooxygenases that catalyse epoxidation and hydroxylation chemical reactions.[208] The insertion of an oxygen molecule through olefin epoxidation of the unsaturated double bond moiety of N-3 and N-6 PUFAs generates epoxylipids (Figure 1.4).[208] Hydroxylation and allylic oxidation of AA results in the formation of terminal HETEs and mid-chain HETEs, respectively.[208] These enzymes are primarily located at the endoplasmic reticulum in mammalian cells and can metabolize a broad range of xenobiotics including pharmaceuticals, as well as endogenous molecules such as lipids.[209] Additionally, a subset of CYP450s are found at the mitochondrial membrane in some tissues including the lungs and kidneys.[209] Primarily expressed in the liver, CYP450s are also abundant in the heart, brain, kidneys, and the vasculature. In human cardiac tissue, CYP2C8, CYP2C9, and CYP2J2 are the predominant isoforms involved in the maintenance of tissue homeostasis and CVD pathophysiology.[210] These CYP450 isoforms also exhibit some substrate selectively as preferential epoxygenases for AA, EPA, and DHA where the last double bond is the preferred epoxidation site.[208] Furthermore, AA, EPA, and DHA can compete as metabolic substrates for CYP2J and CYP2C enzymes, thus influencing the profile of metabolites produced.[194]

The human *CYP2C8* and *CYP2C9* genes exhibit conserved homology to the murine genes.[211] However, the single human *CYP2J2* gene is represented as a cluster of at least 8 different *Cyp2j* genes in mice, hence a directly homologous gene does not exist.[194, 212, 213] However, a transgenic murine model has been developed to over-express the human CYP2J2 isoform in the cardiomyocyte to enhance the production of beneficial epoxylipids.[214] These mice have enhanced left ventricular recovery following IR injury and a lower incidence of diabetic cardiomyopathy, heart failure, and susceptibility to arrhythmia.[214-216] In humans, CYP2J2 is most abundant in ventricular cardiomyocytes and may be implicated in cardiac disease pathogenesis.[217] Gene expression of *CYP2J2* is upregulated in the cardiomyocyte by the presence of ROS which enhances cell viability, indicating a potential compensatory and protective mechanism.[218] In patients with non-ischemic cardiomyopathy, protein levels of

CYP2J2 are significantly reduced.[217] Knockdown of *CYP2J2* gene expression alters other transcriptional programs in the adult cardiomyocyte including genes involved in cardiac ion channel signalling and extracellular matrix functions.[217] Hence, CYP2J2 may play a role in cardiac homeostasis and perturbations in its expression and activity may be involved in cardiac diseases involving arrhythmogenesis, fibrosis, and remodeling.

Drugs targeting other PUFA metabolizing pathways include COX enzyme inhibitors to prevent the formation of prostaglandins and thromboxanes.[219, 220] These drugs are widely used on the market to reduce inflammation.[219] Unfortunately chronic use of some of these agents can increase the risk of cardiac events in high risk patients, acute kidney dysfunction and serum electrolyte disturbances in patients on ACEi and thiazide diuretics for hypertension, and risk of bleeding in patients taking anticoagulants or antiplatelet drugs.[220] However, no pharmacologic agents on the market therapeutically modulate the CYP450 enzyme system for CVD indications, making the CYP450 enzymes an underutilized but perhaps promising pharmacological target.

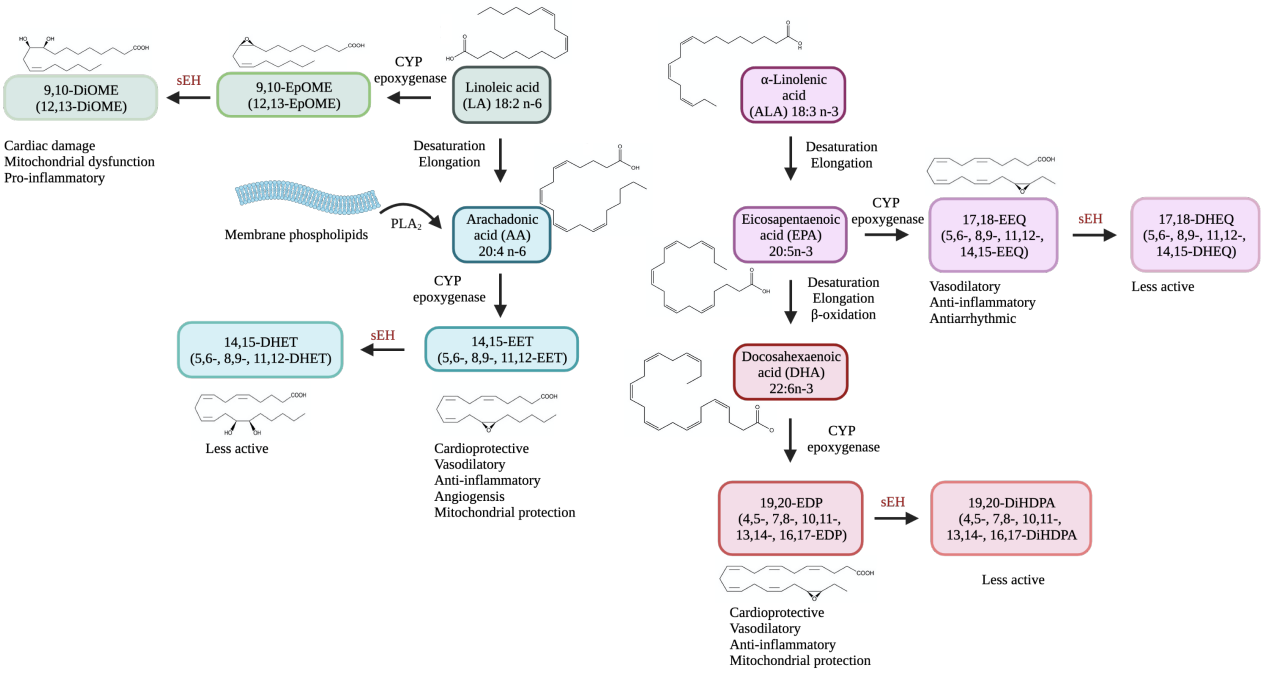

Figure 1.4. Schematic depicting the CYP450 metabolic pathways of N-3 and N-6 PUFAs. Adapted from the following sources.[6, 9, 202, 221]

1.6.2 N-3 and N-6 PUFA-derived epoxylipids

As previously discussed, N-3 PUFAs EPA and DHA obtained from the human diet can undergo an endogenous epoxidation reaction by CYP enzymes to form their corresponding epoxy metabolites. EPA can be metabolized into five regioisomers, 5,6-, 8,9-, 11,12, 14,15-, and 17,18-epoxyeicosatetraenoic acid (EEQ) (Figure 1.4).[6, 194] Furthermore, DHA can either be obtained from the diet or be produced from EPA as its precursor through elongase and desaturase reactions.[202] CYP epoxygenase can then metabolize DHA into the six regioisomers 4,5-, 7,8-, 10,11-, 13,14-, 16,17-, and 19,20- epoxydocosapentaenoic acid (EDP) (Figure 1.4). The metabolism of the N-6 PUFA, AA, by CYP epoxygenases produces the four regioisomers 5,6-, 8,9-, 11,12-, and 14,15-epoxyeicosatrienoic acid (EET) (Figure 1.4).[6] These epoxylipid metabolites have a range of biological functions. In particular, 17,18-EEQ, 19,20-EDP, 11,12-EET, and 14,15-EET have been the most well-characterized in the literature and pre-clinical studies and will be discussed in further detail.[222]

1.7 BIOLOGICAL ACTIONS OF N-3 AND N-6 PUFA-DERIVED EPOXYLIPIDS ON THE HEART

Despite the inconclusive clinical evidence surrounding the effects of N-3 and N-6 PUFAs on the cardiovascular system and the risk for CVD, it is believed that the beneficial effects of PUFAs may largely be mediated, instead, by their epoxylipid metabolites.[222] Biological effects and potencies of N-3 and N-6 derived epoxylipids are regio- and stereoselective, thus enhancing the complexity of their actions.

1.7.1 Cardioprotective effects of PUFA-derived epoxylipids

Epoxylipids have potent effects on the cardiovascular system. These effects include modulation of vascular bed tone. 19,20-EDP functions as a vasodilator of coronary artery smooth muscle by activating Ca^{2+}-activated K^+ channels.[223] The metabolic precursor, DHA is also able to mediate vasodilatory effects. However, it is unable to do so when the activity of CYP450 epoxygenase is inhibited, confirming that 19,20-EDP is responsible for the

biological activity of DHA on the vasculature.[223] 17,18-EEQ, the epoxylipid metabolite derived from EPA, also stimulates Ca^{2+}-activated and ATP-sensitive K^+ channels in vascular smooth muscle cells to promote hyperpolarization.[224-226] Vasodilatory effects of 17,18-EEQ have also been demonstrated in coronary, cerebral, pulmonary, and mesenteric vascular beds.[225-228] The other four EEQ regioisomers do not possesses the same vasodilatory potency, highlighting the importance of regioselectivity in the elicitation of epoxylipid biological effects.[224] All 4 EET regioisomers are also potent regulators of vascular tone and may function as endothelial derived hyperpolarizing factors (EDHF).[229] Physiological plasma concentrations of EETs are typically within the nanomolar range (0.75-300 nM).[230, 231] Relaxation of coronary arteries and resistance arterioles can be achieved at even picomolar concentrations of 11,12-EET indicating a physiological role for these compounds.[231] Mechanistically, this occurs through the activation of Ca^{2+}-activated K^+ channels on vascular smooth muscle cells independent of the endothelium.[231] Currently, epoxylipid-mimetic compounds are being advanced to clinical trials as they are proving to be a promising pharmacologic strategy for the treatment of hypertension.[232]

Epoxylipids also have demonstrated benefit in cardiac injury models of ischemia-reperfusion (IR) and myocardial infarction. In IR injury, perfusion of hearts with 19,20-EDP and DHA exerted profound improvement in post-ischemic functional recovery.[233] Importantly, the cardioprotective effect of DHA was abolished in IR injury when co-perfused with a CYP450 epoxygenase inhibitor, indicating these effects are also primarily mediated by the epoxylipid metabolite, 19,20-EDP.[233] The 11,12- and 14,15-EET regioisomers effectively reduced infarct size in an *in vivo* model of coronary ligation followed by reperfusion.[234, 235] This cardioprotective effect is thought to be primarily mediated through the action of 11,12- and 14,15-EET on ATP-activated K^+ channels.[235]

However, these cardioprotective effects of epoxylipids have also been associated with their anti-inflammatory actions and their ability to preserve cardiac mitochondrial quality. In IR injury, 19,20-EDP mediated cardioprotection may be attributed to the preservation of mitochondrial function, sustained efficiency of ATP generation, and reduction of mitochondrial ROS (mtROS) generation. [233, 236] In an *ex vivo* model of IR injury, perfusion of hearts with 17,18-EEQ was more effective at preserving cardiac and mitochondrial function compared to its EPA precursor.[233] Mitochondria may also be direct

targets of the actions of EETs. Pathological fragmentation of cardiac mitochondria was reduced in 14,15-EET perfused hearts which underwent IR injury. 14,15-EETs also prevented the loss of cardiomyocyte mitochondrial membrane potential and mPTP opening under acute stressful conditions which could attenuate cardiomyocyte apoptosis and preserve cell viability.[237] By maintaining a healthy pool of cardiomyocyte mitochondria via engagement of the autophagic response and mitobiogenesis, 14,15-EETs can preserve the efficiency of cardiomyocyte ATP production during nutrient starvation.[238] [239] The heart relies heavily on the oxidation of fatty acids and glucose for a constant supply of energy.[240] Mitochondria produce more that 90% of cardiomyocyte ATP and occupy more than 30% of the volume of the cell.[240] Hence, it is likely that the effects of epoxylipids on cardiac mitochondrial quality are contributing to their cardioprotective actions.

As previously discussed, acute and chronic inflammation can have a detrimental impact on the heart.[42] Inflammation is also a common factor in many CVD pathologies.[43, 45, 59] Epoxylipids have also shown to possess anti-inflammatory and immune resolving properties which may contribute to their cardioprotective effects.[10, 222] The cardioprotective mechanism of 19,20-EDP in cardiac IR injury may involve the attenuation of pathological inflammation, particularly the NLRP3 inflammasome.[233] 11,12-EET potently inhibits NF-kB signalling reducing endothelial cell expression of adhesion molecules in response to LPS and TNF-α preventing the attraction of leukocytes.[241] Following the acute exposure of cardiomyocytes to LPS, 14,15-EET treatment prevented NF-kB inflammatory signalling, TNF-α production, and loss of mitochondrial function via PPARγ DNA binding and singalling.[11] Furthermore, pro-inflammatory macrophage polarization and macrophage NLRP3 signalling can also be reduced with 11,12- and 14,15-EET treatment which may contribute to the preservation of cardiac and lung function in acute LPS endotoxemia.[108, 242] Thus, the complex mechanisms underlying the cardioprotective properties of epoxylipids highlight the tight relationship between the preservation of mitochondrial quality and attenuation of inflammation on heart function.

1.8 EPOXIDE HYDROLASE DEPENDENT METABOLISM

Despite their cardioprotective effects, epoxylipids are metabolically and structurally labile, thus the biological actions of epoxylipids are relatively short-lived.[243, 244] Epoxylipids can be further metabolized by epoxide hydrolase enzymes.[245] The epoxide ring is converted to two hydroxyl moieties by the addition of a water molecule to form the corresponding diol metabolite.[245] The characterization and biological effects of two isoforms, soluble epoxide hydrolase (sEH) and microsomal epoxide hydrolase (mEH) have been most extensively studied in the literature and play important roles in biological function due to their broad substrate selectivtiy.[245]

1.8.1 Overview of microsomal epoxide hydrolase

The mEH isoform is encoded by the *EPHX1* gene in humans and *Ephx1* gene in mice and rats which is relatively well-conserved between species.[246, 247] Originally identified in the endoplasmic reticulum fractions from liver tissue, mEH is also constitutively expressed in most tissues including epithelial tissue, immune cells, the brain, and heart and skeletal muscle.[248] mEH is primarily a xenobiotic-metabolizing enzyme responsible for the conversion of a wide range of reactive epoxide substrates to more water soluble and less toxic diols, which may have implications not only in detoxification but also in drug metabolism.[249, 250] Furthermore, mEH may also have a role in the metabolism of some endogenous substances including steroid hormones and limited PUFA-derived epoxides.[245, 251, 252] Upon the recent recognition that mEH can hydrolyze 5,6-, 8,9-, 11,12-, and 14,15-EET, there is speculation that mEH may also play a role in cardiovascular biology and disease.[253 254] Preliminary research suggests that mEH-induced epoxylipid metabolism may influence the regulation of vascular tone, however the understanding of the role of mEH in CVD is still limited.[255]

Aside from its role in detoxification, mEH may also be implicated in some diseases. Polymorphisms have been identified in the human *EPHX1* gene which may contribute to lung and ovarian cancer, lymphoid malignancies, as well as chronic obstructive pulmonary disease (COPD) and hepatitis.[256] Interestingly, a prospective cohort study concluded that

individuals with polymorphisms constituting a slower mEH metabolic rate had a larger decline in lung function due to occupational endotoxin exposure over a 20 year period.[257] Thus, mEH metabolic actions may actually provide some protection from the toxic effects of endotoxin.

1.8.2 Soluble epoxide hydrolase: structure, activity, and function

sEH is another predominant epoxide hydrolase enzyme which efficiently metabolizes CYP450-derived N-3 and N-6 epoxylipids.[258] It is encoded by the *EPHX2* gene in humans and *Ephx2* gene in rodents.[254, 259] sEH is expressed ubiquitously throughout the body in most tissues including the kidney, liver, heart, digestive tract and brain.[260] The functional sEH protein resides in the cytosolic compartment of cells and possesses two catalytic domains – an N-terminal phosphatase and, importantly, a C-terminal epoxide hydrolase which function independently of each other.[254, 261, 262] Notably, sEH hydrolyzes EETs to dihydroxyeicosatrienoic acids (DHETs), EpOMEs to dihydroxyoctadecenoic acids (DiHOMEs), and EDP to dihydroxyeicosapentaenoic acids (DPAs). The diol metabolites of EET and EDP are considered less potent.[263] On the other hand, DiHOMEs derived from EpOME precursors may be more biologically active and will be discussed in further detail below.[6, 264]

Since sEH is implicated in the metabolism and inactivation of cardioprotective epoxylipids, polymorphisms in the sEH gene contribute to the risk and development of a range of cardiovascular pathologies, some of which include coronary artery calcification, coronary heart disease, hypertension and ischemic stroke.[265-269] Changes in sEH gene expression are also correlated with some cardiac disease models. For example, sEH expression is upregulated in the heart and vasculature in models of angiotensin II (AngII), isoproterenol, and doxorubicin-induced cardiac hypertrophy indicating a possible role in cardiac remodeling.[270-274] sEH may also be involved in regulation of blood pressure and pathogenesis of hypertension through the renin-angiotensin aldosterone system (RAAS) due to its metabolism of vasoactive 8,9-, 11,12-, and 14,15-EETs.[275, 276] Furthermore, sEH is also involved in inflammatory processes. sEH activity positively correlates with the infiltration of inflammatory macrophages into the kidney in acute nephropathy.[277]

Interestingly, sEH may also be an endogenous regulator in obesity-induced gut barrier dysfunction which causes systemic inflammation due to the translocation of gut bacteria and endotoxin into the circulation.[278] Importantly, sEH activity is also implicated in the inflammatory response to acute LPS challenge. Changes in the expression of sEH in response to LPS appear to be tissue-dependent.[164, 279, 280] However, there is overwhelming evidence that inhibition of sEH activity attenuates the inflammatory complications of acute LPS administration, including cardiac dysfunction, hypotension, pain, and acute respiratory distress.[281-283] Thus, the wide involvement of sEH in CVD and inflammation makes sEH an attractive pharmacological target and experimental therapeutic for the treatment of cardiovascular and inflammatory disorders.

1.8.3 Pharmacological inhibitors of sEH

A variety of small molecule inhibitors have been synthesized to target sEH activity with the hope to translate into therapeutic treatments.[284, 285] The pharmacologic inhibition of sEH activity preserves the pool of beneficial epoxylipids and prevents their metabolism to their less active, and sometimes detrimental, diol metabolites.[284] Pharmacologic sEH inhibitors consist of a wide range of molecular structures, however those with substituted urea moieties have shown to be more potent and possess favourable pharmacokinetic properties.[284, 286, 287] Early sEH inhibitors such as 12-(3-adamantan-1-yl-ureido)-dodecanoic acid (AUDA), have demonstrated beneficial effects in models of acute inflammation and CVD including hypertension.[288-290] Another small molecule, N-[1-(1-oxopropyl)-4-piperidinyl]-N'-[4-(trifluoromethoxy)phenyl)-urea (TPPU), improved survival and also attenuated the systemic inflammatory response in a model of cecal ligation and puncture (CLP)-induced polymicrobial sepsis and acute lung injury.[283, 291]

More recent molecules have been designed to possess dual action.[292] For example, 4-(5-phenyl-3-(3-[3-(4-trifluoromethyl-phenyl)-ureido]-propyl)-pyrazol-1-yl)-benzenesulfonamide (PTUPB) is an inhibitor of sEH activity and simultaneously attenuates the formation of arachidonic acid-derived pro-inflammatory lipid mediators via inhibition of COX-2 metabolic activity.[293] PTUPB has shown efficacy in ameliorating systemic inflammation in models of CLP-induced sepsis and LPS-mediated acute lung injury, by

attenuating the NLRP3 inflammasome pathway.[293, 294] Another recently developed sEH inhibitor that possesses dual properties is 13-(3-propylureido)tridec-8-enoic acid (UA-8). UA-8 functions not only as an sEH inhibitor but also as an EET-mimetic compound to reduce inflammation and provide cardiac protection through a variety of mechanisms.[239] Research shows that UA-8 induces autophagic, mitochondrial protective, and cell survival responses in stressed cardiomyocytes enduring nutrient starvation.[239] Moreover, this compound attenuates LPS-stimulated inflammatory response and mitochondrial function decline in cardiomyocytes through peroxisome proliferator-activated receptor gamma (PPARγ) nuclear receptor signalling.[11] UA-8 has also demonstrated efficacy in *ex vivo* models. Left ventricular recovery was improved following IR injury in Langendorff perfused hearts treated with UA-8 which may be mediated through the phosphatidylinositol-3-kinase (PI3K) signalling pathway.[295] Hence, small molecules possessing sEH inhibitory activities have shown applicability in a variety of *in vitro* and *ex vivo* CVD and inflammatory disease models.

Lastly, trans-4-[4-(3-adamantan-1-yl-ureido)-cyclohexyloxy]-benzoic acid (*t*AUCB), is another sEH inhibitor molecule which has demonstrated superior potency and pharmacokinetic and oral bioavailability properties *in vivo*.[296, 297] Cardioprotective effects of *t*AUCB have been validated in models of acute MI and IR injury.[298-300] Mechanistically, this compound may attenuate NLRP3 priming and activation as well as prevent pathological mitochondrial fission and oxidative stress in IR injury.[299] *t*AUCB has also demonstrated *in vivo* efficacy in acute LPS-induced inflammation.[296, 297] Given the remarkable properties of *t*AUCB, this small molecule inhibitor is proving to be an excellent experimental drug candidate in a variety of disease models including endotoxemia.[292] But, despite the protective effects demonstrated with sEH inhibitor analogues and dual-acting compounds, none are currently approved for use in the clinical setting and still require further validation and assessment through ongoing and future clinical trials.

1.8.4 In vivo models of sEH gene expression disruption

Use of pharmacologic sEH inhibitor molecules have demonstrated *in vivo* efficacy. Furthermore, genetic disruption of sEH gene expression has also been incorporated into *in*

vivo animal models for mechanistic studies of sEH activity in different disease models.[301] Briefly, the first genetic model was developed at the start of the new millennium and was done via the disruption of exon 1 of the murine *Ephx2* gene using the insertion of a Neo cassette.[301] Chimeric males were crossed with C57/BL6 females to produce heterozygotes, which were further crossed to produce homozygous knockout offspring.[301] Homozygous global sEH null offspring exhibited no differences compared to their wild type counterparts. So, despite the physiological and homeostatic roles of sEH, the gene likely does not play a major role in embryonic and fetal development or reproduction.[301] Plasma epoxylipid to diol metabolite ratios were strikingly elevated in sEH null mice, indicating successful interference with sEH metabolic activity.[301] Interestingly, young adult (10-14 weeks) male sEH null mice had drastically reduced systolic blood pressure suggesting a homeostatic function of sEH in the regulation of vascular tone which may be sexually dimorphic.[301] Marked systolic hypotension is not sustainable with life, which could have influenced selection pressure for survival to eventually reduce the frequency of this phenotype. Later generations of *Ephx2* knockout mice were backcrossed with C57/BL6 mice to re-derive the colony. Following re-derivation of the colony, anomalies in the basal systolic blood pressure were resolved.[302] These generations of sEH null mice are now widely used in laboratories around the globe conducting sEH and epoxylipid research.

The use of *Ephx2* gene knockout animal models in research has allowed further insight into the physiological and pathophysiological mechanisms regulated by sEH activity. Global genetic deletion of sEH has demonstrated cardioprotective and anti-inflammatory effects in a variety of models including acute LPS injury, MI, IR injury, AngII-induced heart failure, lipotoxic cardiomyopathy, and cardiac hypertrophy.[299, 303-306] These cardioprotective effects are mediated through diverse mechanisms including attenuation of inflammation, mitigation of oxidative stress, and preservation of mitochondrial quality and function. Interestingly, lack of global sEH activity also exerts cardioprotective effects throughout the normal biological aging process, further attesting to its homeostatic functions. Middle-aged global sEH null female mice have preserved cardiac function compared to their female wild type and male sEH null middle-aged counterparts.[307] Hence, sEH null genetic models have proven to be a useful tool for gaining a mechanistic understanding of the role of sEH in both health and disease.

1.9 sEH-DERIVED METABOLITES: VICINAL DIOLS

1.9.1 Physiological and pathophysiological effects of DiHOMEs

Epoxyoctadecamonoenic acid (EpOME), formed by the epoxidation of linoleic acid (LA), is hydrolyzed to 9,10- or 12,13-dihydroxyoctadecenoic acid (DiHOME)[6]. It has been proposed that the detrimental actions of EpOMEs on the heart can, in fact, be attributed to the biologic activity of DiHOMEs.[264, 308] Endothelial-targeted over-expression of CYP2C8 led to significantly poorer recovery following ischemia-reperfusion injury in murine hearts.[309] The impaired recovery was also associated with increased cardiac tissue 9,10- and 12,13-DiHOME levels and ROS production. DiHOMEs have been shown to contribute to oxidative stress in the cardiovascular system.[310, 311] Additionally, these compounds can impair mitochondrial function via inhibition of the electron transport chain and activation of mitochondrial apoptotic signalling pathways.[312, 313]

In contrast, one study demonstrated that acute exposure to 30 μM of 12,13-DiHOME improved contractile function and coronary flow in perfused hearts without causing any disturbances in heart rhythm or rate.[314] However, in transgenic aged mice with overexpression of cardiomyocyte CYP2J2, post-ischemic functional recovery was impaired.[311] This is thought to be due to the accumulation of diol metabolites with age, as young CYP2J2 over-expressing mice had lower levels of 12,13-DiHOME, ROS production, and experienced cardioprotection in contrast to their aged counterparts.[311] Therefore, the duration of exposure and subsequent accumulation of DiHOMEs may be critical in mediating their differential biological effects on the heart.

Importantly, inhibition of sEH activity attenuates the formation of 9,10- and 12,13-DiHOME and circumvents their detrimental actions.[311, 315] Perfusion of aged hearts with *t*AUCB attenuated the decline in cardiac functional recovery in hearts from aged CYP2J2 over-expressing mice following IR injury.[311] Co-perfusion of murine hearts with the precursor 12,13-EpOME and sEH inhibitor, AUDA, demonstrated nearly full recovery of left ventricular developed pressure (LVDP) following IR injury compared to aerobic controls.[315] However, AUDA was unable to avert the detrimental effects on hearts directly treated with 12,13-DiHOME.[315] These data strengthen the notion that the metabolism of

EPOMEs to DiHOMEs is detrimental and that sEH inhibition is an effective way to protect the heart from these effects.

Recent and emerging research is focussing on the role of DiHOME metabolites in cardiac function as well as other physiological and pathophysiological processes. 12,13-DiHOME has been identified as a metabolic stimulating molecule, which induces lipid uptake into brown adipose tissue to promote lipid tolerance.[316, 317] This in turn can negate the effects of high-fat diet on the heart and directly stimulate cardiomyocyte respiration and contractility.[318] Furthermore, bone marrow cell colony formation, proliferation, and mobilization is enhanced by 12,13-DiHOME which may promote tissue repair.[319] Importantly, these data highlight the versatile role of DiHOMEs and that their effects may be tissue and disease-specific.

DiHOMEs also have a critical role in the immune response and inflammation. Intestinal bacteria can produce 12,13-DiHOME which acts on dendritic cells to reduce anti-inflammatory cytokine section and levels of T regulatory cells.[320, 321] Mediation of inflammatory pain signals in neurons may also be attributed to 12,13-DiHOME.[322] Additionally, 9,10- and 12,13-DiHOME can modulate neutrophils and reduce the oxidative respiratory burst.[323] Of current clinical relevance, patients with severe COVID-19 infection have dramatically elevated levels of plasma 9,10- and 12,13-DiHOMEs, which may contribute to acute lung injury and vascular permeability.[324]

Early research suggested that DiHOMEs may be a contributor to the cardiac injury observed with acute systemic inflammatory syndromes due to its prolongation of the cardiac action potential and disruption of ion channel currents and electrical activity.[325] Likewise, our previous work demonstrated that acute LPS inflammatory injury resulted in cardiac accumulation of 9,10- and 12,13-DiHOME metabolites.[164] The accumulation of plasma 9,10- and 12,13-DiHOME in hospitalized septic patients also corroborates our findings.[326, 327] LPS-induced cardiac functional decline and DiHOME accumulation were mitigated in sEH-deficient mice.[164] Importantly, 9,10- and 12,13-DiHOMEs directly induce mitochondrial damage, and an inflammatory and cytotoxic response in cardiomyocytes. Therefore, DiHOMEs may be partially responsible for mediating the detrimental effects of acute LPS inflammation on the heart and may represent another protective mechanism of sEH disruption in this model.

1.9.2 Bioactivity of DHETs

Hydrolysis of EETs by sEH produces their respective group of diol metabolites, dihydroxyeicosatrienoic acids (DHETs).[6] Four regioisomers can be produced; 5,6-, 8,9-, 11,12-, and 14,15-DHET. It is widely accepted that DHETs are less potent and biologically less active than their respective EET precursors.[6] Research focussing on the biological effects of DHETs are limited but existing evidence suggests they may also possess bioactivity in certain systems. 8,9-, 11,12-, and 14,15-DHETs are potent vasodilators through the modulation of ion channel kinetics.[231, 328-330] Some studies suggest that these agents could be used to regulate diastolic function and coronary flow.[231, 330] 14,15-DHET can also stimulate transcription factor activity including hypoxia inducible factor (HIF)-1α and may be an endogenous ligand of PPARα.[331, 332] However, the direct physiological implications of DHET as a selective transcription factor activator remain to be explored. Furthermore, 14,15-DHET can depress neutrophil-mediated ROS production and migration, indicating a possible role in the innate immune response.[333] Whether these effects result in immunosuppression and impaired ability for the host to defend itself from invading pathogens, or protects against detrimental immune activation is unknown and may be highly specific on the disease model used.

1.10 OVERVIEW OF THESIS

1.10.1 Rationale

Acute inflammation has detrimental effects on the heart.[5] Unregulated production of pro-inflammatory mediators causes local tissue and organ damage which impacts cardiac function.[18] Proper heart function is critical for a constant supply of oxygen and nutrients to other organs and the removal of metabolic by-products from the body. Cardiomyocytes make up 30% of the cell population in the human atria and 50% in the ventricular regions.[334] These cells are the main contractile components of the heart and can also facilitate electrical conduction; imperative for proper cardiac function.[335] Adult cardiomyocytes are terminally differentiated and have low proliferative capacity, making any damage to the myocardium detrimental.[335] In models of cardiac injury and damage, inhibition of the cytosolic enzyme, sEH, has demonstrated cardioprotective, anti-inflammatory, and mitochondrial protective actions.[6] Global genetic deletion of sEH preserves cardiac function and attenuates the production of systemic pro-inflammatory mediators in mice following acute LPS-induced inflammatory injury.[164] Despite the important role of the cardiomyocyte in the heart, the cardiomyocyte-specific effect of sEH *in vivo* has not been investigated. Furthermore, mechanisms by which impairment of sEH enzymatic activity exerts its protective effects at the level of the cardiomyocyte are still elusive. The NLRP3 inflammasome signalling pathway is upregulated in damaged myocardial tissue.[233] NLRP3 inflammasome activation can be triggered by mitochondrial dysfunction and its activation can propagate systemic inflammation.[140] Importantly, LPS injury damages cardiomyocyte mitochondria.[164] Our group has demonstrated that disruption of sEH activity ameliorates NRLP3 inflammasome activity in IR hearts, which is associated with preservation of cardiac mitochondrial quality.[233, 299] The overall aim of this thesis is to determine how sEH activity in the cardiomyocyte contributes to LPS-induced inflammatory cardiac dysfunction, with a focus on the contribution of the NLRP3 inflammasome pathway and systemic inflammatory cell signalling.

1.10.2 Hypothesis

Global hypothesis: Cardiomyocyte-specific sEH deletion attenuates the inflammatory response, which preserves cardiac function due to acute LPS-induced inflammatory injury.

1.10.3 Objectives

1. To compare the effects of cardiomyocyte-specific and global sEH deletion on cardiac function and systemic inflammatory response

2. To determine whether sEH inhibition can attenuate NLRP3 inflammasome signalling in the cardiomyocyte

3. To investigate if cardiomyocyte-specific sEH inhibition can ameliorate immune cell recruitment to the myocardium

CHAPTER 2

EXPANDED MATERIALS AND METHODS

2.1 MOUSE COLONIES

Mouse colonies were maintained at the University of Alberta, Health Sciences Laboratory Animal Services facility. Experimental protocols were approved by the University of Alberta Health Sciences Welfare Committee and carried out in accordance with the Canadian Council on Animal Care's *Guide to the Care and Use of Experimental Animals.*[336] Mice were maintained on a C57Bl/6 background. Global sEH knockout (sEH null) mice with targeted deletion of the *Ephx2* gene were compared to littermate C57Bl/6 wild type (WT) controls.[164, 301, 302] A murine model of cardiomyocyte-specific sEH gene deletion was developed by colleagues at the National Institute of Environmental Health Sciences (NIEHS, NC, USA) employing the use of tamoxifen-dependent CreER recombinase.[337] The Cre recombinase gene is driven by the myosin heavy chain 6 (Myh6) promoter. LoxP sites flank exons 11 and 12 on the *Ephx2* locus, responsible for the hydrolase activity of sEH. Mice with cardiomyocyte-specific sEH gene deletion (Myh6-$Cre^{+/-}$sEH$^{(Myo\ -/-)}$) were compared to their Cre-expressing true controls (Myh6-$Cre^{+/-}$sEH$^{(Myo\ +/+)}$) which lack LoxP sites on the *Ephx2* locus. Both male and female sexes were used experimentally, and sex was analyzed as a co-variant. Mice were stratified into the following age cohorts; young adults (2-5 months) and middle-aged adults (15-19 months). Results pertaining to female mice as well as middle-aged mice are presented in Chapter 6: Future Directions and Pilot Data.

2.2 KNOCKDOWN OF CARDIOMYOCYTE sEH EXPRESSION

Activation of Cre recombinase was done through a series of tamoxifen injections.[338] Briefly, tamoxifen (Sigma-Aldrich, Cat# T5648-1G) was dissolved in warm corn oil to make an 8 mg/mL homogenous solution. Each cohort of Cre lox mice were weighed and had their surface body temperature measured using an infrared thermometer. Mice 2-3 months in age were given an intraperitoneal (i.p.) injection of tamoxifen solution at a dose of 45 mg/kg/day for a total of 6 injections over a span of 8 days. Mice were given a 5 week wash-out period to recover from the systemic effects of tamoxifen and cardiac activation of Cre recombinase. Baseline transthoracic echocardiography and a physiological assessment (described in

further detail below) were performed to ensure no underlying cardiac dysfunction was present before the mice were utilized experimentally.

2.3 INDUCTION OF ACUTE LIPOPOLYSACCHARIDE INFLAMMATORY INJURY

Lyophilized lipopolysaccharide (LPS) was purchased from Sigma-Aldrich (Cat# L4391-1MG). Each batch was freshly reconstituted on the day of use to a final concentration of 1 mg/mL with normal saline. To induce a robust systemic inflammatory response, mice were given a single i.p. injection of LPS at a dose of 10 mg/kg or normal saline as control.[16, 164, 339, 340]

2.4 PHARMACOLOGIC INHIBITION OF sEH *IN VIVO*

The pharmacologic sEH inhibitor, trans-4-[4-(3-adamantan-1-yl-ureido)-cyclohexyloxy]-benzoic acid (*t*AUCB), was kindly gifted from Dr. Bruce Hammock (University California, Davis, United States). Mice were given a 4-day pre-treatment of *t*AUCB (10 mg/L) in their drinking water *ad libitum* or 0.1% DMSO as control.[297, 298, 300] Water intake was measured at the end of the 4-day pre-treatment. Immediately following the LPS i.p. injection, mice received an oral gavage bolus dose of *t*AUCB (1 mg/kg) dissolved in glycerin trioleate vehicle (Acros Organics, 368120050) as previously established.[296]

2.5 PHYSIOLOGICAL ASSESSMENT

Mice underwent a physiological assessment both at baseline and at 6 or 24 hours after LPS administration. Physiological impairment was quantified using an adapted validated scale and was used to assess overall function as well as changes in body weight and body surface temperature with each experimental intervention (Figure 2.5.1).[341] Each parameter was visually assessed and scored using a 3-point scale (0 = absent, 0.5 = mild, 1 = severe). An impairment score was determined by the sum of the scores for each parameter . The mean

and standard deviation for body weight and body surface temperature was determined for each experimental group. Individual mice with a body weight and/or surface temperature ≥ 1 standard deviation from the mean had an addition 0.25 points added to their impairment score. If body weight or surface temperature were ≥ 2 standard deviations from the mean, an additional 0.5 points was added. Total impairment points were then divided by a factor of 31, to account for each parameter assessed, to give a total score between 0 and 1.

2.6 TRANSTHORACIC ECHOCARDIOGRAPHY

2D transthoracic echocardiography was conducted at baseline and at 6 or 24 hours post-LPS injection to assess cardiac structure and function.[342] Mice were anesthetized by inhalation of 1% isoflurane. Cardiac measurements were taken using the Vevo 3100 high-resolution imaging system and a 40 MHz transducer (MX550S; Visual Sonics). Acquired images were analyzed using the Visual Sonics VevoLab software system. Ejection fraction (EF%), fractional shortening (FS%), left ventricular end diastolic volume (LVEDV) and end systolic volume (LVESV) measurements were taken from m-mode images of the left ventricle. A 4-chamber view of the heart was used to acquire measurements of diastolic function in pulse-wave doppler mode including E and A wave velocity, E/A ratio, and isovolumetric relaxation time (IVRT). At the mitral annulus, tissue doppler mode was used to obtain E' and A' wave velocities. Diastolic function was also calculated by E/E' ratios. Mice were given a minimum 4-day washout period from isoflurane anesthetic after baseline echocardiography before their use experimentally.

2.7 ORGAN AND TISSUE COLLECTION

Following 6 or 24 hours post-LPS injection, mice were given a lethal dose of sodium pentobarbital (100 mg/kg i.p.). Hearts were excised and flash frozen in liquid nitrogen. Whole blood was collected into EDTA-coated tubes and centrifuged at 2000 rpm for 10 minutes. Plasma was collected and flash frozen in liquid nitrogen. Samples were stored at -80°C for future processing.

2.8 HEART TISSUE HOMOGENIZATION AND FRACTIONATION

Frozen hearts were ground to a fine, homogenous powder using a ceramic mortar and pestle on dry ice. Tissue powder was homogenized using conical glass manual homogenizers with tissue homogenization buffer (sucrose 250 mM, tris-HCl 10 mM, EDTA 1 mM, sodium orthovanadate 1 mM, sodium fluoride 1 mM, aprotinin 10 μg/L, leupeptin 2 μg/L, pepstatin 100 μg/L). Subcellular fractionation was performed by differential centrifugation. Briefly, whole heart tissue homogenate was centrifuged at 700 x g for 10 minutes to separate tissue debris. Supernatant was collected and spun at 10,000 x g for 20 minutes to isolate the crude mitochondrial fraction in the pellet. Supernatant was further centrifuged at 100,000 x g for 1 hour to separate the microsomal fraction in the pellet and remaining cytosolic proteins in the supernatant. Mitochondrial and microsomal pellets were re-suspended in tissue homogenization buffer. Cytosolic, microsomal, and mitochondrial tissue fractions were frozen at -80°C until further use.

2.9 PLASMA CYTOKINE ARRAY

Frozen plasma samples were thawed on ice and aliquots were diluted 2-fold with phosphate buffered saline (PBS, pH 7.4). The Mouse Cytokine Array/Chemokine Array 31-Plex (MD31) was performed by Eve Technologies (Calgary, Alberta, Canada) using a multiplex colour-coded bead assay. Chemokine and cytokine concentrations were reported in pg/mL for each sample relative to an external standard.

2.10 CELL CULTURE AND TREATMENT

Cardiomyocytes were isolated from 2-4-day old neonatal rat pups in accordance with an established protocol.[343] To improve cell adherence prior to plating, plastic cell culture plates were coated with laminin which was removed after 24 hours. Excised hearts were manually minced in PBS and digested with 2% w/v collagenase, 0.5% w/v Dnase, and 2% w/v trypsin. Neonatal rat cardiomyocytes were plated at a density of 1.0 $x10^6$ cells/mL in standard DMEM/F12 plating media (Gibco Cell Culture, Cat# 11320-033) supplemented

with 10% FBS, 10% horse serum, and 1% penicillin-streptomycin. Cells were incubated at 37°C with 5% CO_2 and allowed to adhere to plates for 24 hours before their experimental use. On the day of treatment 80% cell confluency, cardiomyocyte beating, and adherence were confirmed using a phase contrast light microscope. Cells were washed with PBS and the standard plating media was replaced. Cells were treated with 1 μg/mL LPS (Sigma-Aldrich Cat# L4391-1MG) or 0.1% DMSO control for 6 hours.[11, 344] In addition, a cohort of cells were treated with 1 μM 19,20-epoxydocosapentaenoic acid, EDP (Cayman Chemicals, #10175), 1 μM 11,12-epoxyeicosatrienoic acid, EET (Cayman Chemicals, #50511), or 10 μM *t*AUCB at the same time or 1 hour before the addition of LPS.[11, 164] After 6 hours incubation at 37°C and 5% CO_2, cells were harvested and lysed using cell lysis buffer (20 mM tris-HCl, 50 mM sodium chloride, 50 mM sodium fluoride, 5mM sodium pyrophosphate, 0.25 M sucrose, 1 M DTT, 1% Triton X-100, pH 7.4). Lysate was centrifuged at 6000 x g for 10 minutes to separate debris. Supernatant containing whole cell lysate was flash frozen in liquid nitrogen. Aliquots of cell media were also collected in Eppendorf tubes. All samples were stored at -80°C for later use.

2.11 PROTEIN IMMUNOBLOTTING USING NEONATAL RAT CARDIOMYOCYTE CELL LYSATE AND HEART TISSUE FRACTIONATES

Aliquots from whole cardiomyocyte cell lysate and cytosolic heart tissue fractions were diluted 10-fold using distilled water or tissue homogenization buffer. A 3 μl volume of diluted sample was loaded onto a 96-well plate and 200 μl of Bradford Protein Assay Dye Reagent Concentrate (Bio-Rad #500-0006) diluted 1 in 5 using distilled water was added to each sample well. A standard curve was constructed with a protein concentration ranging from 1 μg/μl to 5 μg/μl. Absorbance of the colorimetric substrate was read at 595 nm wavelength using a spectrophotometer. Protein concentration in each sample was calculated using the standard curve.

Then, 35 μg of protein from each sample was prepared in distilled water and SDS sample buffer containing 1 in 10 β-mercaptoethanol (BME). Samples were heat denatured at 95ºC for 5 minutes. Samples were resolved onto Mini-PROTEAN TGX precast gradient gels (4-15%, Bio-Rad #4561084) at 90 V for 1 hour in tris-glycine-SDS running buffer.

Protein was transferred onto 0.2 μm polyvinylidene difluoride (PVDF) membranes (Bio-Rad #162-0177) at 100 V for 1 hour in ice cold tris-glycine transfer buffer with 20% methanol.

Membranes were blocked with 5% bovine serum albumin (BSA) dissolved in tris-buffered saline with 0.1% Tween-20 (TBS-T) for 1 hour. Membranes were incubated with primary antibodies to sEH (1:500, polyclonal rabbit antibody, Elabscience, EAB60489), NLRP3 (1:500, rabbit monoclonal antibody, Cell Signalling Tech., cs15101), pro-IL-1β (1:500, rabbit polyclonal antibody, Abcam, ab9722), GAPDH (1:1000, rabbit monoclonal antibody, Cell Signalling Tech., cs5174), or α-tubulin (1:1000, rabbit polyclonal antibody, Abcam, ab4074) overnight at 4ºC. Following 24h incubation, primary antibodies were removed and the membranes were washed 3 times with TBS-T for 5 minutes. Next, the membranes were incubated with horse radish peroxidase (HRP)-conjugated goat anti-rabbit IgG polyclonal antibody (1:2000, Cell Signalling Tech., cs7074) for 1 hour at room temperature. Following washing 3 times for 5 minutes with TBS-T, Amersham ECL Prime Western Blotting Detection Reagent (RPN2232) and the Bio-Rad ChemiDoc Imaging System were used to visualize proteins of interest. Protein densitometry was quantified with ImageJ software (NIH, United States) and normalized to loading controls.

2.12 IMMUNOBLOTTING FOR EXTRACELLULAR PROTEINS IN CELL CULTURE MEDIA

Cytokines can be secreted by stressed cells which can act in a paracrine or autocrine manner to further perpetuate cell damage and inflammation.[345] So, we assessed the levels of mature IL-1β released into the extracellular media from LPS-stimulated neonatal rat cardiomyocytes. Frozen media aliquots were thawed on ice and centrifuged at 6000 x g for 5 minutes to remove debris. Precipitation of media proteins released from treated neonatal rat cardiomyocytes was performed using a published methanol-chloroform precipitation protocol.[346] Briefly, precipitated proteins were reconstituted in 70 μl of 1x SDS sample buffer with 1 in 10 BME. Heat denatured samples were loaded onto Mini-PROTEAN TGX precast gradient gels (4-20%, Bio-Rad #4561094). Gels were run at 100 V for 1 hour in tris-glycine-SDS running buffer. Proteins were transferred from the gel onto a 0.2 μm nitrocellulose membrane (Bio-Rad #1704158) using the Bio-Rad Trans-Blot Turbo dry

transfer system at 25 V and 2.5 A for 5 minutes. Nitrocellulose membranes were blocked using a solution of 5% BSA in TBS-T for 1 hour. Membranes were incubated overnight with the anti-IL-1β rabbit polyclonal primary antibody (Abcam, ab9722) at a concentration of 1:500. Membranes were washed 3 times with TBS-T for 5 minutes and then incubated with HRP-conjugated goat anti-rabbit IgG polyclonal antibody (Cell Signalling Tech., cs7074) at a concentration of 1:2000 for 1 hour. Secondary antibody solution were removed, membranes were washed 3 times with TBS-T for 5 minutes and then exposed to the Amersham ECL Prime Western Blotting Detection Reagent (RPN2232). Chemiluminescent signal was detected using the Bio-Rad ChemiDoc Imaging System. Accuracy of protein loading and total secreted protein content was determined using a Ponceau stain (0.1% Ponceau red in 5% acetic acid). Protein densitometry of IL-1β was quantified using ImageJ software (NIH, United States). Protein band intensity was expressed as a fold change relative to the control group and normalized to total membrane protein levels.

2.13 LACTATE DEHYDROGENASE ACTIVITY

Assessment of lactate dehydrogenase (LDH) activity in EDTA-plasma samples was done using the LDH colorimetric assay kit (Abcam, ab102526) as per the manufacturer's instructions. Briefly, aliquots of plasma samples were diluted 30-fold using the manufacturer's assay buffer. Samples and LDH substrate were loaded onto a 96-well plate. LDH activity was proportional to the reduction of nicotinamide adenine dinucleotide ($NAD^{+)}$ to NADH which then interacts with a colorimetric probe. The absorbance was read at 450 nm using a spectrophotometer. LDH enzymatic activity was quantified using an NADH standard curve and normalized to the volume of original sample added to each well.

2.14 CASPASE-1 ENZYMATIC ACTIVITY

Neonatal rat cardiomyocytes were lysed using ice-cold cell lysis buffer without protease-phosphatase inhibitor. Heart powder was manually homogenized as described above using homogenization buffer without protease-phosphatase inhibitor. Cardiomyocyte cell lysate and whole heart tissue homogenate were centrifuged at 700 x g for 10 minutes to

remove debris, whole cells, nuclei, and cytoskeletal proteins. Supernatant containing intracellular organelles and protein was collected for assay use. Protein concentration of each sample was determined using a Bradford protein assay, described above. A 5x stock of reaction buffer (50 mM HEPES, 100 mM NaCl, 0.5% CHAPS, 1 mM EDTA, 10% glycerol, 10 mM DTT, pH 7.4) was prepared. A working solution containing 200 μM of 7-amino-4-methylcoumarin (AMC)-tagged caspase-1 peptide substrate, Ac-YVAD-AMC (Enzo Life Sciences Inc. ALX-260-024-M005) was prepared in 2x reaction buffer. Working solution and aliquots containing the same volume of sample were loaded into a 96-well plate in the dark. The plate was read at 340 nm excitation/440 nm emission with 70% gain every 5 minutes for a total of 90 minutes using a microplate reader. Caspase-1 activity was proportional to the generation of a fluorescence signal following cleavage and release of AMC from the peptide substrate. At 80 minutes into the reaction, the AMC generated by caspase-1 activity in each sample was quantified using an AMC standard curve. Caspase-1 activity was then normalized to protein concentration to determine specific caspase-1 activity in nmol/mg protein/minute.

2.15 CARDIOMYOCYTE RELEASE OF MCP-1 AND TNF-α

The release of MCP-1 and TNF-α by neonatal rat cardiomyocytes into the surrounding extracellular media was assessed using sandwich ELISA assay kits (Millipore-Sigma, RAB0057; R&D Systems, RTA00) as per the manufacturer's instructions. Briefly, media aliquots from treated cardiomyocytes were first thawed on ice. Next, samples were diluted 1000-fold for MCP-1 and 3-fold for TNF-α in manufacturer's diluent before loading into wells coated with capture antibody. Wells were washed and incubated with detector antibody followed by substrate solution. Plates were read at an absorbance of 450 nm in a spectrophotometer, following the generation of a colorimetric signal. Quantification of MCP-1 and TNF-α concentrations in the media was done with the use of a standard curve and normalized to sample volume.

2.16 IMMUNOHISTOCHEMISTRY

Upon euthanization of experimental mice, hearts were excised, rinsed in PBS, and sliced along the sagittal plane. Heart slices were embedded in optimal cutting temperature compound (OCT) in cryo-base molds, flash frozen in liquid nitrogen and stored at -80°C for later use. Cryostat sectioning and staining of tissue was done by Histology Lab Services, Li Ka Shing Institute of Virology, at the University of Alberta. Following slicing, heart sections were fixed in acetone and blocked with a solution containing 2% normal goat serum, 1% BSA, 0.1% Tween20 in PBS for 1 hour. Slices were then incubated with primary rabbit anti-CD68 polyclonal antibody (Abcam, ab125212) at 1:750 concentration overnight. Isotype controls were incubated with rabbit IgG 1 mg/mL (Sigma, I5006). Following washing, slices were stained with HRP-conjugated goat anti-rabbit polyclonal secondary antibody solution for 1 hour (Agilent Dako, K400311-2). To visualize positive staining, heart slices were incubated for 5 minutes in 3,3'-diaminobenzidine (Agilent Liquid DAB+ chromogen system, K346811-2). Nuclei in the hearts sections were counterstained with fresh hematoxylin (Fisher Chemical, SH30-4D). Slides were washed and a glass coverslip was set with Permount Mounting Medium (Fisher Chemical, SP15-100). CD68 positive staining was visualized at 40x magnification using the Zeiss AxioScope A1 light microscope and captured using the Zeiss AxioCam and ZEN 2 Imaging Software. The entire area of the heart slice was imaged in a total of 6-8 images to obtain a full representation of CD68 expression throughout the heart. The number of CD68 positive cells in each image from individual hearts were counted. The sum of all CD68 positive cells for each individual heart was divided by the total number of images taken of the heart slice. Quantification of CD68 positive cells in each image was conducted by an independent and blinded investigator.

2.17 ASSESSMENT OF MITOCHONDRIAL REACTIVE OXYGEN SPECIES

Generation of mitochondrial superoxide in live neonatal rat cardiomyocytes was performed using MitoSOX red dye - hydroethidine conjugated to triphenylphosphonium cation .[347] Oxidation of MitoSOX by mitochondrial superoxide and other ROS traps the positively charged compound in the negatively charged mitochondrial interior.[347] The

interaction of MitoSOX with mitochondrial DNA generates a fluorescent signal which can be measured and is proportional to mitochondrial-specific ROS production.[347]

Neonatal rat cardiomyocytes were plated at a density of 2.0 x 10^4 cells/well in 96-well plates using media without phenol red dye. Cells were allowed to adhere for 24 hours. On the day of experiment, cells were pre-treated with 1μM 19,20-EDP, 1 μM 11,12-EET, or 10 μM *t*AUCB for 1 hour before the addition of 1 μg/mL LPS. A solution containing MitoSOX red dye (Invitrogen, M36008) was prepared in phenol-red free media and added to each well for a final concentration of 2.95 μM. The fluorescent probe, MitoTracker green, (Invitrogen, M7514), which covalently binds to thiol groups on mitochondrial inner membrane proteins, was used to determine total mitochondrial content in each well.[348] MitoTracker green dye was used at a final concentration of 50 nM. Plates were read every hour for 6 hours using a fluorescent microplate reader. For MitoSOX, readings were taken at 510 nm excitation/580 nm emission. MitoTracker readings were taken at 490 nm excitation/516 nm emission. The amount of mitochondrial superoxide generation (MitoSOX signal) per well was normalized to total mitochondrial content (MitoTracker signal) from each well, respectively.

2.18 STATISTICS

In vivo data was analyzed with two-way ANOVA with Tukey's multiple comparisons test. *In vitro* data analysis was based on ordinary one-way ANOVA with multiple comparisons test. Data is presented as mean ± SEM. A p-value of < 0.05 was considered statistically significant. GraphPad Prism 9 software was used for computation of all statistics.

Table 2. Mouse Frailty Assessment Form©

Date: _____

Mouse #: _____ **Date of Birth:** _____ **Sex:** F M
Body weight (g): _____ **Body surface temperature (°C):** _____

Rating: 0 = absent 0.5 = mild 1 = severe

➢ **Integument:**				**NOTES:**
❖ Alopecia	0	0.5	1	_____
❖ Loss of fur colour	0	0.5	1	_____
❖ Dermatitis	0	0.5	1	_____
❖ Loss of whiskers	0	0.5	1	_____
❖ Coat condition	0	0.5	1	_____
➢ **Physical/Musculoskeletal:**				
❖ Tumours	0	0.5	1	_____
❖ Distended abdomen	0	0.5	1	_____
❖ Kyphosis	0	0.5	1	_____
❖ Tail stiffening	0	0.5	1	_____
❖ Gait disorders	0	0.5	1	_____
❖ Tremor	0	0.5	1	_____
❖ Forelimb grip strength	0	0.5	1	_____
❖ Body condition score	0	0.5	1	_____
➢ **Vestibulocochlear/Auditory:**				
❖ Vestibular disturbance	0	0.5	1	_____
❖ Hearing loss	0	0.5	1	_____
➢ **Ocular/Nasal:**				
❖ Cataracts	0	0.5	1	_____
❖ Corneal opacity	0	0.5	1	_____
❖ Eye discharge/swelling	0	0.5	1	_____
❖ Microphthalmia	0	0.5	1	_____
❖ Vision loss	0	0.5	1	_____
❖ Menace reflex	0	0.5	1	_____
❖ Nasal discharge	0	0.5	1	_____
➢ **Digestive/Urogenital:**				
❖ Malocclusions	0	0.5	1	_____
❖ Rectal prolapse	0	0.5	1	_____
❖ Vaginal/uterine/penile prolapse	0	0.5	1	_____
❖ Diarrhoea	0	0.5	1	_____
➢ **Respiratory system:**				
❖ Breathing rate/depth	0	0.5	1	_____
➢ **Discomfort:**				
❖ Mouse Grimace Scale	0	0.5	1	_____
❖ Piloerection	0	0.5	1	_____
❖ **Temperature score:** _____				
❖ **Body weight score:** _____				

Total Score/ Max Score:

© Susan E. Howlett, 2013

Figure 2.1. Scoring table used to assess physiological function of mice at baseline and after 6 or 24 hours of LPS exposure. From the following source.[341]

CHAPTER 3

RESULTS

3.1 VALIDATION OF *IN VIVO* MODELS

3.1.1 sEH expression levels in murine hearts

Western immunoblotting was performed in order to confirm that sEH expression was indeed absent or significantly reduced in sEH null and sEH$^{(Myo\ -/-)}$ hearts. sEH expression was quantified in the cytosolic fractions from heart homogenate. Expression was absent in sEH null mice and significantly reduced in the hearts of sEH$^{(Myo\ -/-)}$ mice (Figure 3.1.1), indicating that our models are valid and could be used confidently for future experiments.

3.2 GENETIC DELETION OF sEH CONFERS PHYSIOLOGICAL TOLERANCE TO ACUTE LPS

Physiological effects of acute LPS exposure in mice include reductions in body weight, blood glucose, and locomotor activity, as well as deviations from normal body temperature. [164, 349] Using a validated assessment scale adapted from Whitehead et. al.[341] the overall physiological function of mice was quantitated at baseline and 6 or 24 hours following acute LPS exposure.

3.2.1 Degree of LPS-induced physiological impairment in young male mice

Mice from all groups had similar baseline physiological function. Following 6 hours of LPS exposure, all groups of mice experienced increased physiological impairment compared to their baseline (Figure 3.2.1). LPS-treated mice had a slower and more unsteady gait compared to saline treated controls. Mice also began to experience piloerection of their coat, a slightly hunched posture, and a weaker forelimb grip strength on their wire cage top by 6 hours LPS. WT and sEH$^{(Myo\ +/+)}$ groups continued to physiologically deteriorate between 6 and 24 hours post-LPS administration. Nearly all WT and sEH$^{(Myo\ +/+)}$ mice presented with a tremor, reduced surface body temperature, irregular abdominal breathing rate, eye discharge and swelling, as well as very slow gait. Furthermore, these mice were minimally responsive to physical or auditory stimuli by 24 hours LPS. The decline in physiological

function between 6 and 24 hours LPS exposure was significantly less in sEH null and sEH $^{(Myo\ -/-)}$ mice compared to their true LPS-treated controls. sEH null and sEH $^{(Myo\ -/-)}$ groups still exhibited some impairment at the 24 hour time point similar to their status at 6 hours. Most of these mice remained alert and responsive throughout the course of the experiment. Therefore, all groups of mice still experienced physiological dysfunction due to acute LPS injury. However, the degree and progression of dysfunction is significantly attenuated in mice lacking sEH expression.

3.2.2 Degree of LPS-induced physiological impairment in tAUCB-treated mice

At 6 hours post-LPS administration, mice treated with the sEH pharmacological inhibitor, *t*AUCB, experienced physiological dysfunction (Figure 3.2.2). Both WT and *t*AUCB-treated mice continued to physically deteriorate between 6 and 24 hours post-LPS. Although the physiological impairment of *t*AUCB-treated mice was trending lower than their WT counterpart, there were no significant differences between WT or sEH null, and *t*AUCB treated mice at 6 or 24 hours. *t*AUCB treatment has shown benefit in other models of cardiovascular injury and inflammation.[307] This lack of physiological tolerance to LPS in *t*AUCB-treated mice suggests that administration and dosing of *t*AUCB may need to be optimized for our acute LPS-induced injury model and sample size expanded to increase power of this study.

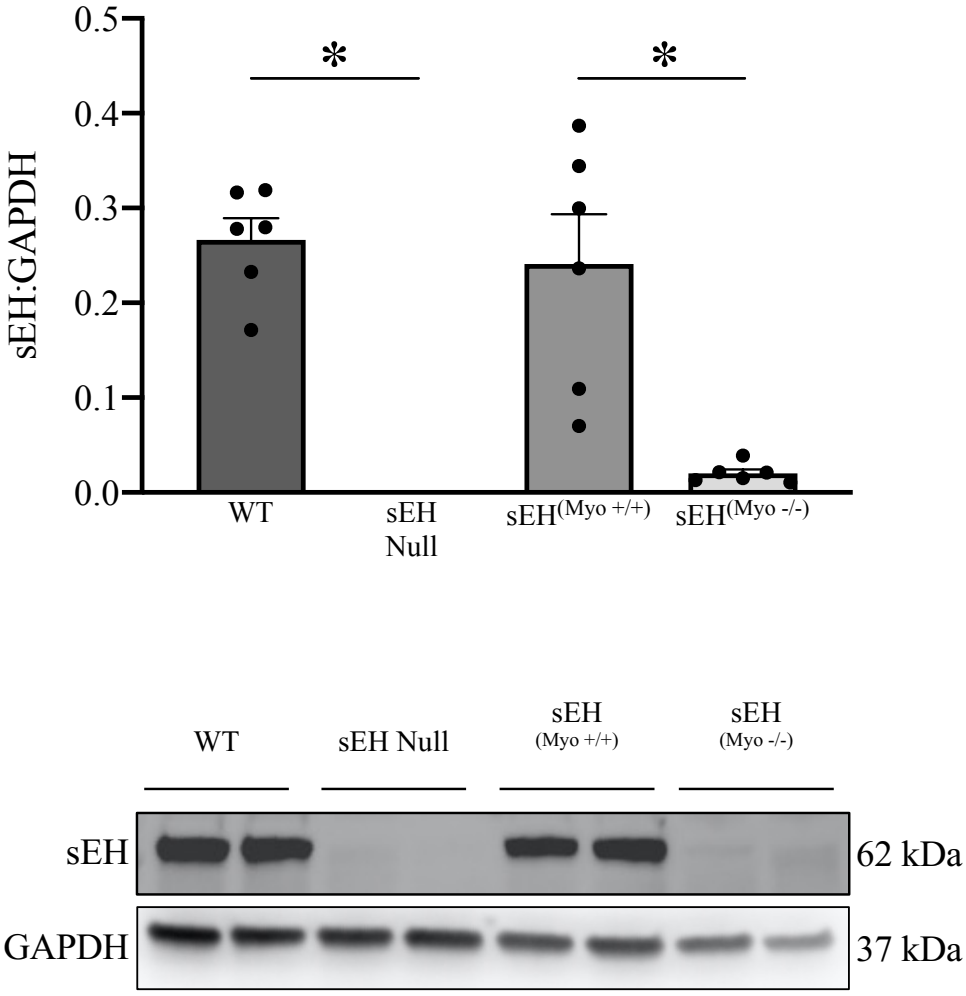

Figure 3.1.1. Western immunoblot of sEH expression in the hearts of experimental mice. Data are means ± SEM, N = 6, $p < 0.05$; * vs sEH expressing true control.

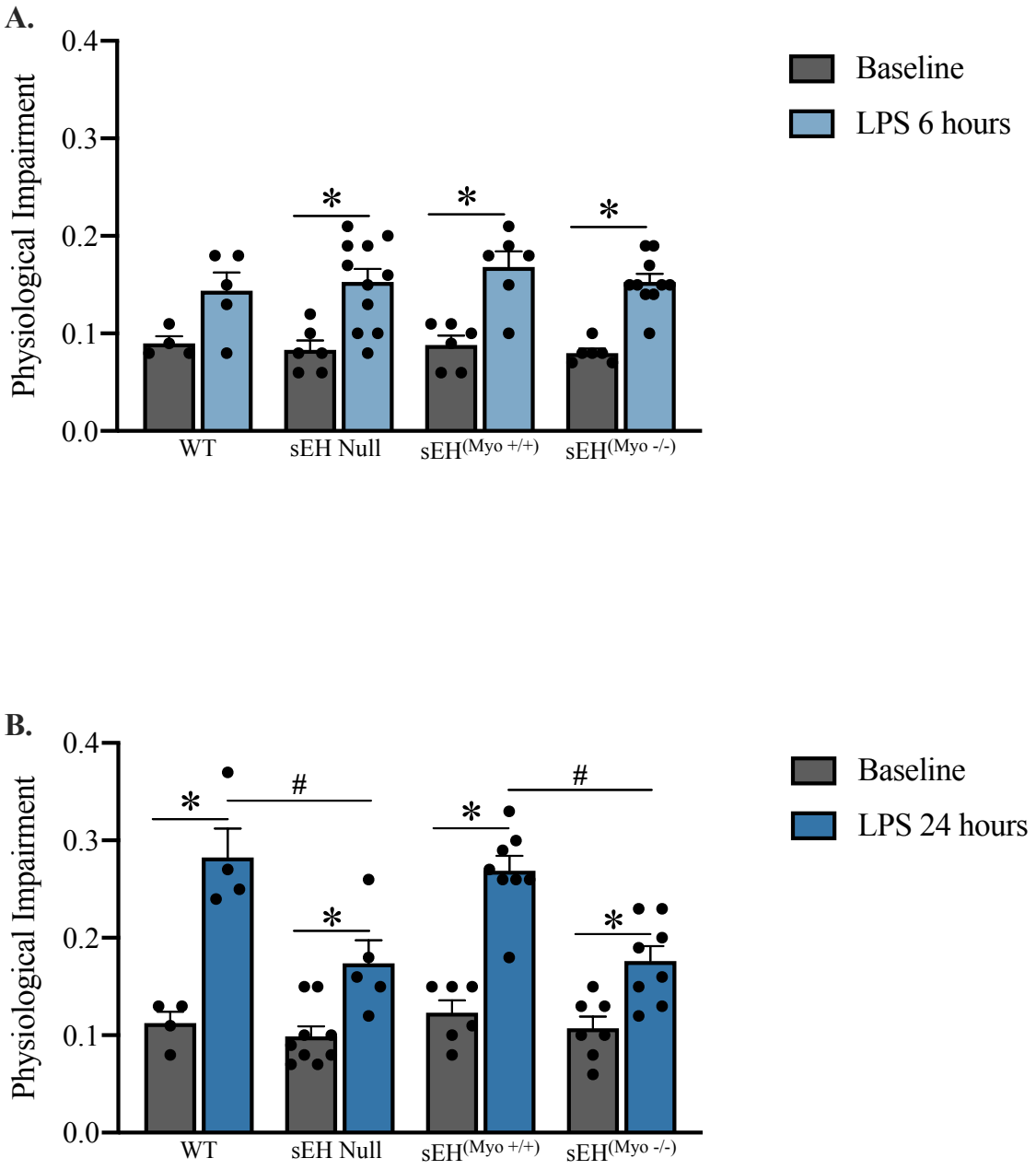

Figure 3.2.1. Level of physiological impairment in young male mice at baseline and at **A.)** 6 or **B.)** 24 hours after LPS administration. Data are means ± SEM, N = 4-11, $p < 0.05$; * vs baseline; # vs true control post-LPS.

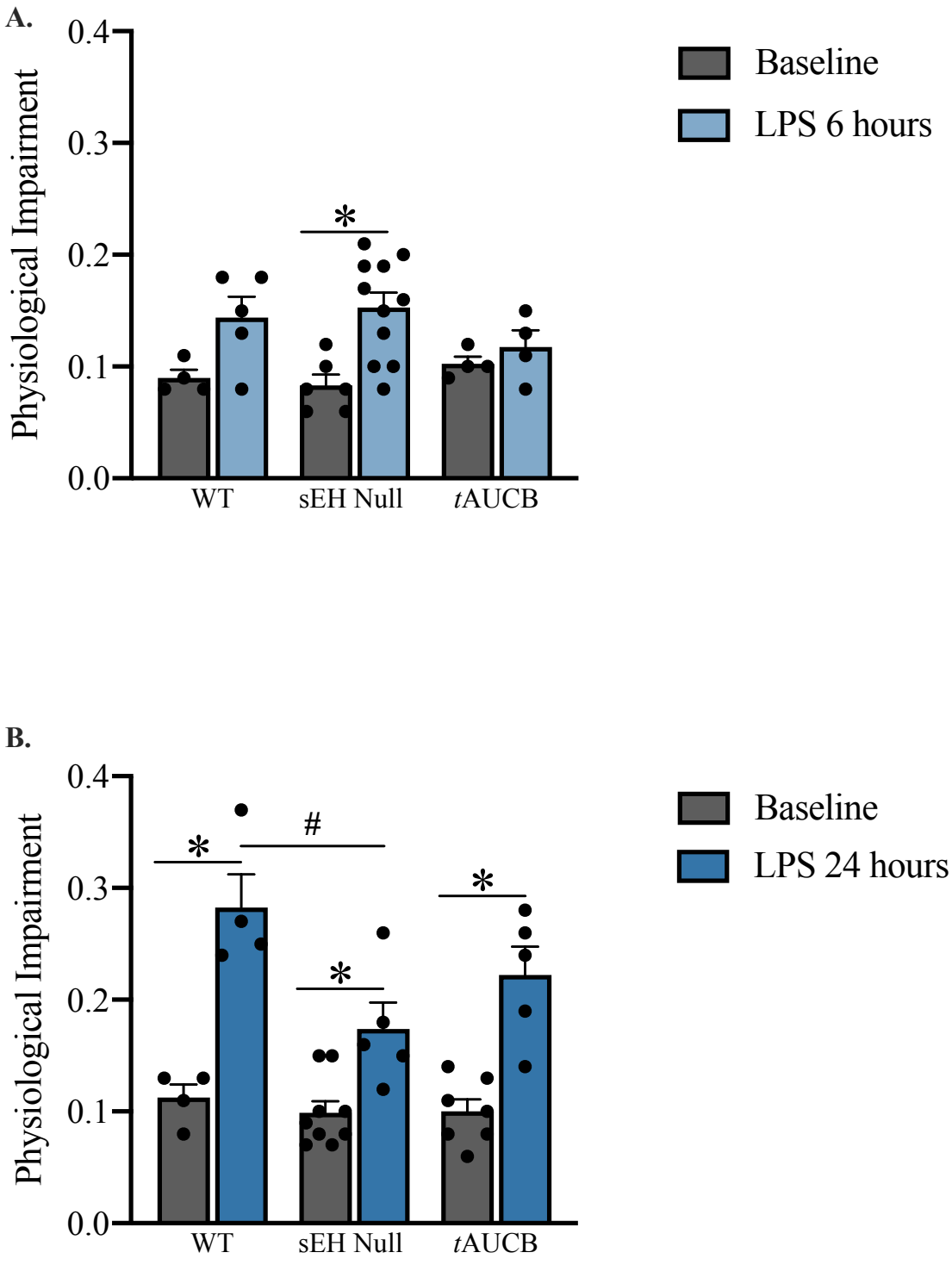

Figure 3.2.2. Level of physiological impairment in young male mice treated with *t*AUCB at baseline and at **A.)** 6 or **B.)** 24 hours after LPS administration. Data are means ± SEM, N = 4-11, $p < 0.05$; * vs baseline; # vs WT post-LPS.

3.3 ACUTE LPS INFLAMMATION EVOKES SYSTEMIC INJURY

Since LPS was injected intraperitoneally, and all groups of mice experienced a degree of physiological decline, we investigated if each group also experienced systemic cellular injury. Lactate dehydrogenase (LDH) is a cytosolic enzyme responsible for the interconversion between lactate and pyruvate.[350] Upon cellular injury, LDH is released from damaged and dying cells and can be detected in the systemic circulation.[350]

3.3.1 Plasma lactate dehydrogenase activity is increased with LPS exposure

Following 6 hours of acute LPS exposure, all groups of mice experienced an increase in LDH activity in their plasma, suggesting acute cell and tissue damage in response to LPS (Figure 3.3.1). Between 6 and 24 hours post-LPS exposure, LDH activity continued to increase in WT and sEH$^{(Myo\ +/+)}$ groups and was significantly higher compared to their saline-treated controls. However, LDH activity in sEH null and sEH$^{(Myo\ -/-)}$ mice plateaued and did not increase much beyond the activity levels measured at 6 hours post-LPS (Figure 3.3.1). This LDH activity pattern mirrors the decline in physiological function described in section 3.2.1. Furthermore, this suggests that all groups of mice are broadly and systemically affected by acute LPS injury. However, sEH expressing mice progressively deteriorate over time with increased length of exposure to LPS.

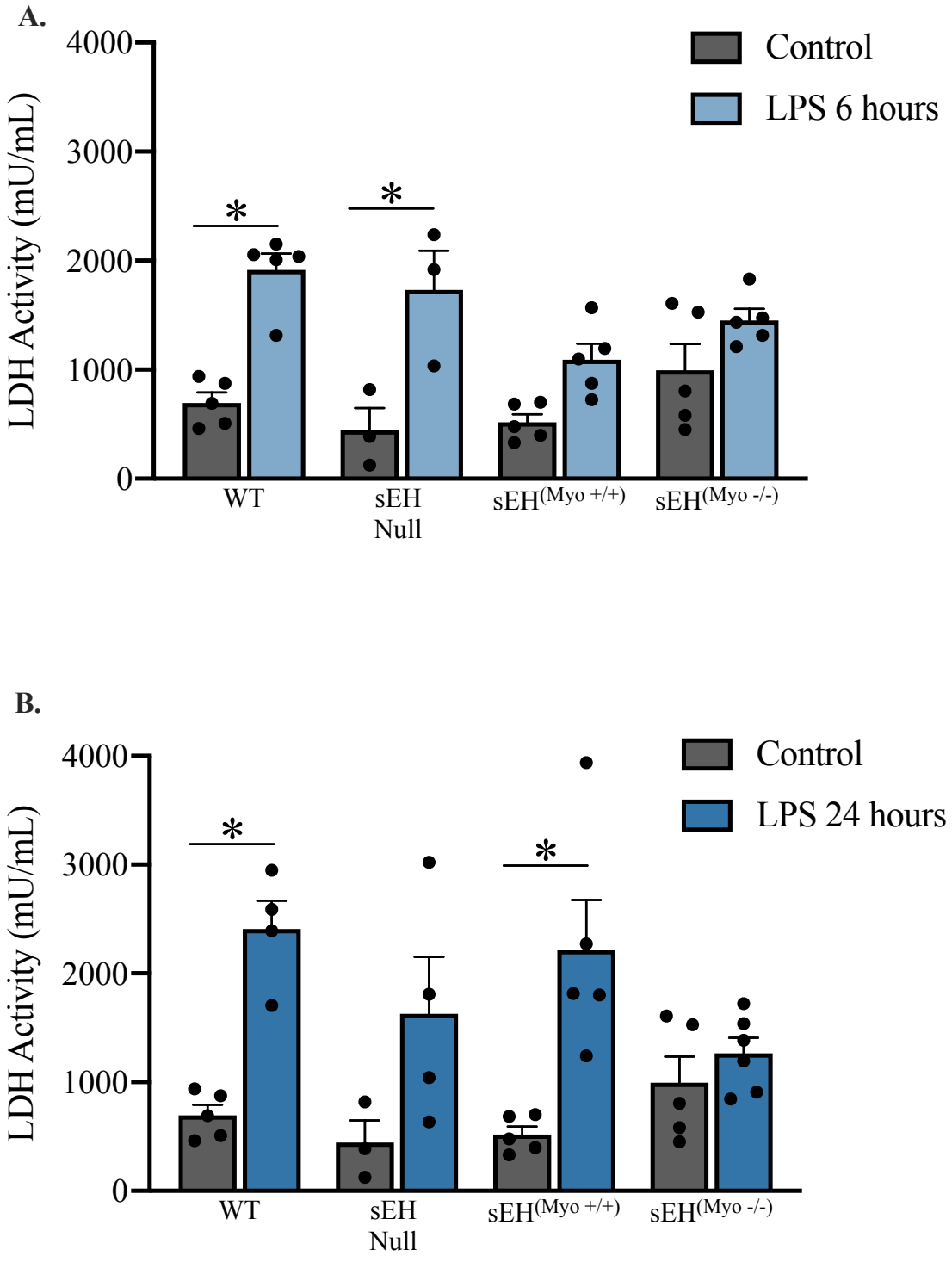

Figure 3.3.1. Plasma levels of LDH activity in control mice and in mice exposed to LPS for **A.)** 6 or **B.)** 24 hours. Data are means ± SEM, N = 3-6, $p < 0.05$; * vs respective control.

3.4 GENETIC DELETION OF sEH IS CARDIOPROTECTIVE IN ACUTE LPS INJURY

It has been previously established that global genetic deletion of sEH is cardioprotective in young male mice following 24 hours of acute LPS injury.[164] However, whether cardioprotection can be maintained with cardiomyocyte-specific deletion of sEH is unknown. Additionally, the effects of different lengths of LPS exposure and pharmacological inhibition of sEH on cardioprotection in acute LPS injury has not been explored.

3.4.1 An initial decline in cardiac function occurs at 6 hours post-LPS exposure

Heart rate and baseline cardiac function were similar between all groups mentioned below. Following 6 hours of LPS exposure, sEH null and sEH $^{(Myo\ -/-)}$ mice experienced a decline in systolic function including ejection fraction and fractional shortening parameters, which was also seen in WT and sEH$^{(Myo\ +/+)}$ mice (Table 3.4.1) and (Figure 3.4.1). LPS-treated mice also had a decline in their cardiac output and stroke volume. Geometric measurements of the heart during systole and diastole were also altered. With LPS, the width of the posterior wall of the left ventricle during systole was reduced in all groups except sEH null mice. Additionally WT and sEH$^{(Myo\ +/+)}$ groups experienced an enlargement of their left ventricular internal diameter during systole. There were no significant differences in mitral E/A wave ratios or the E/E' wave ratios at 6 hours. This suggests that systolic dysfunction may precede alterations in diastolic parameters. All groups had a significant increase in their Tei index compared to their baseline. This suggests that all groups still experienced a degree of cardiac functional decline by the 6 hour timepoint. Despite that sEH null mice experienced a systolic cardiac dysfunction with 6 hours LPS, sEH null heart function was still significantly preserved compared to WT counterparts. However, no significant differences in heart function were determined between sEH $^{(Myo\ -/-)}$ and sEH$^{(Myo\ +/+)}$ groups, indicating that cardiac function in both these groups declined at a similar rate between the time of LPS injection and the 6 hour time point.

3.4.2 Cardiac functional decline plateaus by 24 hours post-LPS in sEH-deficient mice

At 24 hours post-LPS, the rate of decline in cardiac function in sEH null and sEH $^{(Myo\ -/-)}$ slowed, while WT and sEH $^{(Myo\ +/+)}$ groups continued to deteriorate further and at a faster rate beyond the 6 hour time point. Ejection fraction and fractional shortening were significantly preserved in mice with global and cardiomyocyte-specific sEH gene deletion mice compared to their sEH expressing counterparts (Table 3.4.2) and (Figure 3.4.1). Cardiac output and stroke volume were also significantly reduced in all groups except sEH null mice. By the 24 hour time point, changes in ventricular volumes also arose, which were not present at 6 hours. All groups except sEH null mice had an increase in the volume of blood remaining in the left ventricle at the end of systole, which may explain the decline in cardiac output and stroke volume. The left ventricular internal diameter remained enlarged during systole. However, this did not occur in sEH null mice, and the degree of the enlargement was less in the sEH$^{(Myo\ -/-)}$ group compared to their sEH$^{(Myo\ +/+)}$ counterparts. Furthermore, changes in diastolic parameters became apparent at the 24 hour time point. sEH expressing mice experienced a significant increase in their isovolumetric relaxation time (IVRT), whereas the change was not nearly as robust in sEH null and sEH$^{(Myo\ -/-)}$ mice. WT mice also had an enlarged E/E' wave ratio further indicative of diastolic dysfunction. These data provide important information about the temporal progression of cardiac dysfunction in LPS treated mice. Changes in systolic parameters may occur earlier than diastolic alterations. Importantly, sEH disruption localized to the cardiomyocyte still has the capacity to exert a significant degree of cardioprotection and slow the rate of cardiac functional decline.

3.4.3 Pharmacologic inhibition of sEH does not provide the same degree of cardioprotection as sEH genetic deletion

Systolic function was significantly reduced in *t*AUCB-treated mice at both 6 and 24 hours (Table 3.4.3), (Table 3.4.4) and (Figure 3.4.1). This was indicated in the significant decline in ejection fraction, fractional shortening, cardiac output, and stroke volume. Interestingly, ejection fraction and fractional shortening measurements in *t*AUCB-treated

mice were trending higher compared to their WT counterparts. But, these measurements were still significantly less than sEH null mice. Additionally, the left ventricular end systolic volume and systolic internal diameter was also increased with LPS treatment in the *t*AUCB group. However, the decline in these parameters was more robust at 6 hours post-LPS whereas partial resolution of the abnormalities was present at the 24 hour time point. Moreover, *t*AUCB-treated mice also had an increased IVRT and reduced mitral E/A wave ratio indicating a degree of diastolic dysfunction similar to WT mice. These data further attest that sEH inhibition may work in a time-dependent manner to slow the rate of cardiac functional decline over time. However, pharmacologic inhibition of sEH was less effective at preserving cardiac function compared to genetic deletion in sEH null and sEH$^{(Myo\ -/-)}$ groups.

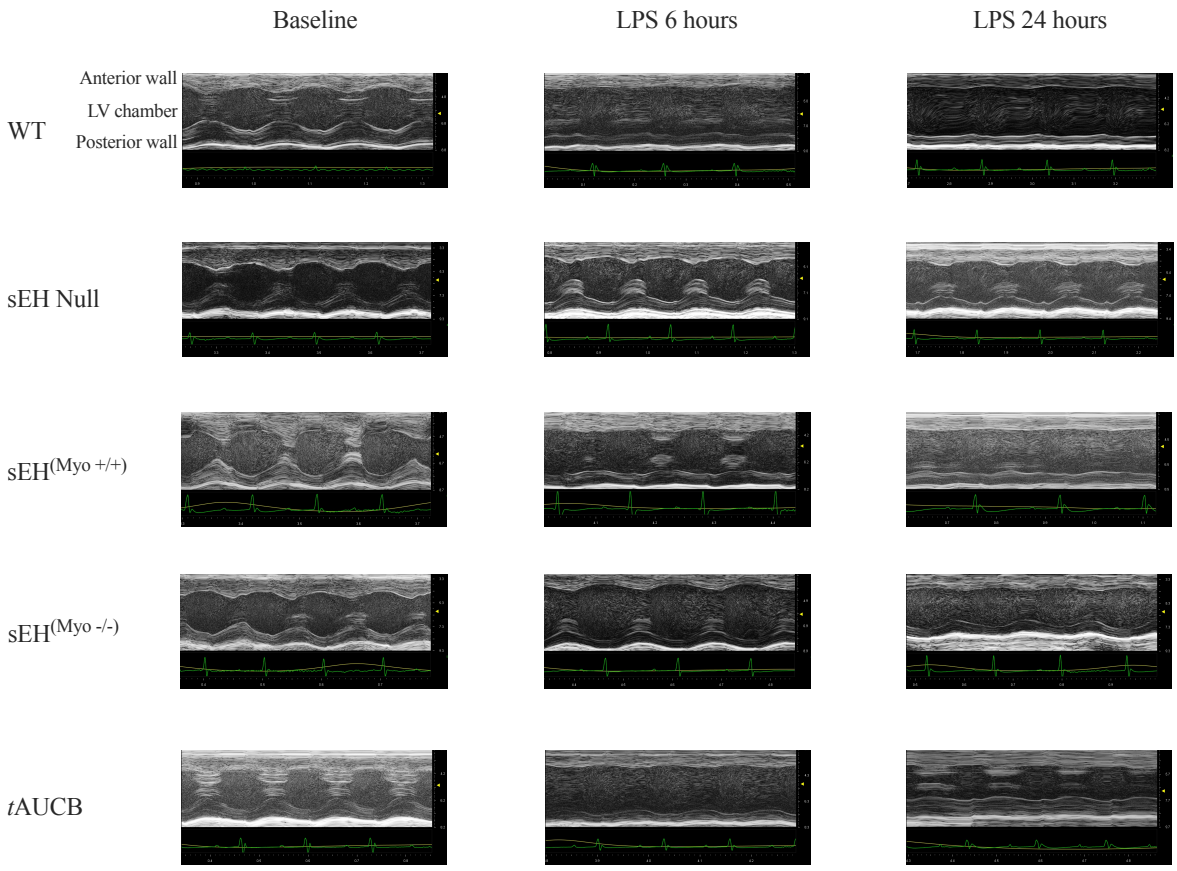

Figure 3.4.1. Representative M-mode images taken in the short axis view of the left ventricle acquired using 2D transthoracic echocardiography.

	WT		sEH Null		$sEH^{(Myo +/+)}$		$sEH^{(Myo -/-)}$	
	Baseline	LPS-6h	Baseline	LPS-6h	Baseline	LPS-6h	Baseline	LPS-6h
Heart rate (beats/min)	448 ± 14	460 ± 12	453 ± 10	475 ± 11	443 ± 21	490 ± 6.29	444 ± 23	477 ± 14
Wall Measurements								
Corrected LV mass, mg	76.71 ± 8.71	108.47 ± 4.43*	80.09 ± 6.85	91.17 ± 4.33	105.06 ± 8.57	98.12 6.34	89.36 ± 5.49	85.33 ± 8.68
IVS-diastole, mm	0.75 ± 0.09	0.90 ± 0.05	0.89 ± 0.03	0.96 ± 0.04	0.86 ± 0.07	0.91 ± 0.04	0.82 ± 0.05	0.89 ± 0.04
IVS-systole, mm	1.13 ± 0.09	1.09 ± 0.05	1.37 ± 0.07	1.25 ± 0.06	1.35 ± 0.07	1.18 ± 0.06	1.19 ± 0.06	1.22 ± 0.06
LVPW-diastole, mm	0.75 ± 0.06	0.76 ± 0.06	0.73 ± 0.05	1.00 ± 0.07*	0.81 ± 0.06	0.74 ± 0.04	0.79 ± 0.07	0.87 ± 0.05
LVPW-systole, mm	1.24 ± 0.08	0.90 ± 0.05*	1.27 ± 0.06	1.26 ± 0.08#	1.25 ± 0.06	0.95 ± 0.06	1.22 ± 0.09	1.12 ± 0.08
LVID-diastole, mm	3.67 ± 0.13	4.24 ± 0.13	3.57 ± 0.14	3.28 ± 0.17#	4.11 ± 0.17	3.99 ± 0.16	3.79 ± 0.14	3.69 ± 0.14
LVID-systole, mm	2.43 ± 0.11	3.82 ± 0.12*	2.27 ± 0.06	2.54 ± 0.20#	2.73 ± 0.11	3.28 ± 0.08	2.61 ± 0.12	2.84 ± 0.16
Cardiac Function								
Ejection Fraction (%)	63.99 ± 2.33	25.34 ± 1.51*	68.59 ± 1.79	50.46 ± 4.28#*	64.00 ± 2.23	39.86 ± 1.29*	60.79 ± 3.97	48.58 ± 3.01*
Fractional Shortening (%)	34.36 ± 1.80	11.59 ± 0.74*	37.75 ± 1.41	24.93 ± 2.93#*	34.64 ± 1.68	19.15 ± 0.78*	32.41 ± 2.70	24.22 ± 1.77*
LVEDV, µl	58.18 ± 4.42	79.25 ± 4.55	56.56 ± 5.66	46.02 ± 4.60#	73.55 ± 6.63	69.23 ± 6.28	64.45 ± 6.14	57.96 ± 6.10
LVESV, µl	21.16 ± 2.30	59.34 ± 4.12*	17.42 ± 1.47	24.54 ± 3.81#	29.37 ± 4.22	41.39 ± 2.90	25.09 ± 3.11	27.38 ± 2.44
CO, ml/min	16.56 ± 1.13	8.67 ± 0.33*	16.44 ± 1.42	10.23 ± 0.97*	19.93 ± 1.49	12.75 ± 1.91	17.55 ± 2.19	12.15 ± 1.34
SV, µl	37.02 ± 2.59	19.91 ± 1.12*	39.14 ± 4.36	21.48 ± 2.06*	44.18 ± 4.31	27.84 ± 3.41	39.36 ± 4.83	27.38 ± 2.44
Doppler Imaging								
IVRT, ms	11.67 ± 0.86	25.38 ± 1.56*	13.08 ± 1.06	17.89 ± 1.59#	12.96 ± 0.75	15.64 ± 0.85	13.47 ± 1.51	19.25 ± 1.77*
IVCT, ms	12.08 ± 1.21	13.19 ± 3.60	12.84 ± 2.31	11.25 ± 1.15	12.64 ± 0.79	14.89 ± 2.06	12.18 ± 1.64	8.90 ± 0.50#
ET, ms	40.94 ± 2.46	30.03 ± 3.22	43.27 ± 1.86	29.18 ± 2.37*	36.85 ± 3.55	32. 25 ± 3.72	44.80 ± 3.76	33.12 ± 1.32*
Mitral E/A ratio	1.40 ± 0.07	1.17 ± 0.15	1.35 ± 0.06	1.46 ± 0.10	1.59 ± 0.11	1.43 ± 0.23	1.57 ± 0.08	1.29 ± 0.09
E/E' ratio	30.20 ± 2.10	25.98 ± 4.55	31.32 ± 3.00	32.96 ± 3.56	30.73 ± 4.05	42.66 ± 5.59	32.62 ± 1.97	34.97 ± 5.74
Tei index	0.60 ± 0.08	1.28 ± 0.08*	0.60 ± 0.06	1.07 ± 0.13*	0.68 ± 0.06	0.98 ± 0.07*	0.58 ± 0.04	0.85 ± 0.04*
Body Weight (g)	31.20 ± 0.73	29.36 ± 0.64	26.96 ± 0.83	25.97 ± 0.66#	25.47 ± 1.01	24.25 ± 0.94	23.53 ± 0.89	24.81 ± 1.36
N value	7	5	7	9	6	5	7	10

Table 3.4.1. Cardiac functional parameters at baseline and after 6 hours post-LPS administration in young male mice measured by 2D transthoracic echocardiography. Data are means ± SEM, N = 5-10, $p < 0.05$; * vs baseline; # vs WT LPS-6h or $sEH^{(Myo +/+)}$ LPS-6h.

	WT		sEH Null		$sEH^{(Myo +/+)}$		$sEH^{(Myo -/-)}$	
	Baseline	LPS-24h	Baseline	LPS-24h	Baseline	LPS-24h	Baseline	LPS-24h
Heart rate (beats/min)	437 ± 17	399 ± 8	451 ± 11	422 ± 13	463 ± 19	390 ± 12	475 ± 22	420 ± 13
Wall Measurements								
Corrected LV mass, mg	84.65 ± 8.06	79.24 ± 2.91	93.06 ± 4.01	80.59 ± 7.08	88.55 ± 5.10	88.41 ± 5.53	80.00 ± 4.35	81.34 ± 2.74
IVS-diastole, mm	0.77 ± 0.04	0.90 ± 0.03	0.91 ± 0.05	0.90 ± 0.04	0.78 ± 0.03	0.88 ± 0.04	0.82 ± 0.03	0.85 ± 0.04
IVS-systole, mm	1.19 ± 0.06	1.03 ± 0.03	1.39 ± 0.06	1.25 ± 0.05	1.18 ± 0.07	1.05 ± 0.05	1.26 ± 0.04	1.13 ± 0.05
LVPW-diastole, mm	0.78 ± 0.06	0.79 ± 0.05	0.82 ± 0.04	0.84 ± 0.09	0.79 ± 0.04	0.73 ± 0.06	0.73 ± 0.03	0.72 ± 0.03
LVPW-systole, mm	1.23 ± 0.07	0.95 ± 0.05*	1.28 ± 0.06	1.21 ± 0.09	1.28 ± 0.06	0.86 ± 0.05*	1.15 ± 0.03	0.97 ± 0.04*
LVID-diastole, mm	3.80 ± 0.13	3.45 ± 0.15	3.73 ± 0.08	3.38 ± 0.25	3.90 ± 0.10	3.83 ± 0.15	3.73 ± 0.09	3.74 ± 0.13
LVID-systole, mm	2.47 ± 0.11	3.03 ± 0.15*	2.47 ± 0.09	2.42 ± 0.22#	2.58 ± 0.11	3.43 ± 0.12*	2.49 ± 0.11	3.04 ± 0.14*
Cardiac Function								
Ejection Fraction (%)	65.65 ± 1.63	28.75 ± 1.49*	64.76 ± 1.80	54.64 ± 6.11#	64.90 ± 2.41	26.89 ± 2.53*	63.13 ± 2.53	42. 03 ± 3.40*#
Fractional Shortening (%)	35.65 ± 1.28	13.07 ± 0.72*	34.95 ± 1.28	28.81 ± 4.01#	35.38 ± 1.82	12.38 ± 1.35*	34.17 ± 1.95	20.86 ± 1.98*#
LVEDV, µl	63.06 ± 6.18	49.82 ± 4.91	59.73 ± 3.52	48.83 ± 7.70	69.77 ± 6.97	64.76 ± 5.52	61.45 ± 3.13	63.11 ± 4.86
LVESV, µl	22.14 ± 2.84	35.73 ± 3.80*	21.32 ± 2.00	21.83 ± 5.00	24.66 ± 3.08	46.33 ± 2.97*	23.30 ± 2.27	37.60 ± 4.21*
CO, ml/min	17.12 ± 1.74	5.54 ± 0.55*	15.59 ± 1.79	10.66 ± 2.07	14.08 ± 2.57	5.20 ± 0.85*	13.65 ± 1.17	8.44 ± 0.86*
SV, µl	40.92 ± 3.60	14.09 ± 1.30*	38.41 ± 2.22	27.01 ± 5.75	45.11 ± 4.67	18.44 ± 3.28*	38.16 ± 1.73	25.51 ± 2.00*
Doppler Imaging								
IVRT, ms	15.06 ± 1.08	31.24 ± 2.69*	13.93 ± 0.87	21.74 ± 2.84#*	12.56 ± 1.24	26.21 ± 3.83*	14.99 ± 1.03	22.17 ± 2.39
IVCT, ms	12.05 ± 1.42	15.73 ± 2.04	9.23 ± 0.71	18.54 ± 5.78	10.51 ± 1.88	15.63 ± 2.28	11.34 ± 1.74	13.20 ± 1.77
ET, ms	44.85 ± 2.38	34.08 ± 2.22*	39.12 ± 1.74	35.49 ± 2.82	47.04 ± 2.93	36.39 ± 1.88*	44.77 ± 1.48	38.86 ± 1.38
Mitral E/A ratio	1.47 ± 0.08	1.06 ± 0.21	1.47 ± 0.09	1.29 ± 0.12	1.44 ± 0.08	1.05 ± 0.08	1.60 ± 0.11	1.26 ± 0.05
E/E' ratio	28.93 ± 1.94	58.46 ± 11.85*	30.78 ± 3.27	25.12 ± 3.71#	31.75 ± 3.51	25.69 ± 3.96	32.19 ± 2.75	38.50 ± 2.87
Tei index	0.62 ± 0.05	1.38 ± 0.08*	0.60 ± 0.02	1.24 ± 0.22*	0.52 ± 0.06	1.19 ± 0.14*	0.60 ± 0.05	0.88 ± 0.10
Body Weight (g)	26.50 ± 0.80	24.71 ± 0.97	29.01 ± 0.89	26.40 ± 1.00	31.07 ± 0.55	27.11 ± 0.62*	27.88 ± 0.69	24.32 ± 0.59*
N value	14	10	13	10	12	10	16	17

Table 3.4.2. Cardiac functional parameters at baseline and after 24 hours post-LPS administration in young male mice measured by 2D transthoracic echocardiography. Data are means ± SEM, N = 10-17, $p < 0.05$; * vs baseline; # vs WT LPS-24h or $sEH^{(Myo +/+)}$ LPS-24h.

	WT		sEH Null		*t*AUCB	
	Baseline	LPS-6h	Baseline	LPS-6h	Baseline	LPS-6h
Heart rate (beats/min)	448 ± 14	460 ± 12	453 ± 10	475 ± 11	437 ± 13	480 ± 17
Wall Measurements						
Corrected LV mass, mg	76.71 ± 8.71	108.47 ± 4.43	80.09 ± 6.85	91.17 ± 4.33	69.06 ± 6.32	82.16 ± 7.09
IVS-diastole, mm	0.75 ± 0.09	0.90 ± 0.05	0.89 ± 0.03	0.96 ± 0.04	0.98 ± 0.04	0.83 ± 0.05
IVS-systole, mm	1.13 ± 0.09	1.09 ± 0.05	1.37 ± 0.07	1.25 ± 0.06	1.38 ± 0.03	1.01 ± 0.07
LVPW-diastole, mm	0.75 ± 0.06	0.76 ± 0.06	0.73 ± 0.05	1.00 ± 0.07*	0.73 ± 0.03	0.74 ± 0.02
LVPW-systole, mm	1.24 ± 0.08	0.90 ± 0.05*	1.27 ± 0.06	1.26 ± 0.08$^{\#}$	1.22 ± 0.02	0.97 ± 0.02
LVID-diastole, mm	3.67 ± 0.13	4.24 ± 0.13	3.57 ± 0.14	3.28 ± 0.17$^{\#}$	3.11 ± 0.19	3.71 ± 0.11
LVID-systole, mm	2.43 ± 0.11	3.82 ± 0.12*	2.27 ± 0.06	2.54 ± 0.20$^{\#}$	1.98 ± 0.17	3.14 ± 0.12*
Cardiac Function						
Ejection Fraction (%)	63.99 ± 2.33	25.34 ± 1.51*	68.59 ± 1.79	50.46 ± 4.28*$^{\#}$	68.45 ± 2.28	32.43 ± 3.13*†
Fractional Shortening (%)	34.36 ± 1.80	11.59 ± 0.74*	37.75 ± 1.41	24.93 ± 2.93*$^{\#}$	37.21 ± 1.59	15.10 ± 1.65*
LVEDV, µl	58.18 ± 4.42	79.25 ± 4.55	56.56 ± 5.66	46.02 ± 4.60$^{\#}$	40.94 ± 5.68	61.67 ± 3.96
LVESV, µl	21.16 ± 2.30	59.34 ± 4.12*	17.42 ± 1.47	24.54 ± 3.81$^{\#}$	13.24 ± 2.90	41.87 ± 3.86*$^{\#}$†
CO, ml/min	16.56 ± 1.13	8.67 ± 0.33*	16.44 ± 1.42	10.23 ± 0.97*	11.16 ± 1.21	9.56 ± 1.10
SV, µl	37.02 ± 2.59	19.91 ± 1.12*	39.14 ± 4.36	21.48 ± 2.06*	27.70 ± 2.81	19.80 ± 1.86
Doppler Imaging						
IVRT, ms	11.67 ± 0.86	25.38 ± 1.56*	13.08 ± 1.06	17.89 ± 1.59$^{\#}$	17.61 ± 1.94	25.14 ± 2.43†
IVCT, ms	12.08 ± 1.21	13.19 ± 3.60	12.84 ± 2.31	11.25 ± 1.15	14.89 ± 1.90	17.25 ± 3.26
ET, ms	40.94 ± 2.46	30.03 ± 3.22	43.27 ± 1.86	29.18 ± 2.37*	45.28 ± 4.90	33.98 ± 2.69
Mitral E/A ratio	1.40 ± 0.07	1.17 ± 0.15	1.35 ± 0.06	1.46 ± 0.10	1.33 ± 0.05	1.13 ± 0.19
E/E' ratio	30.20 ± 2.10	25.98 ± 4.55	31.32 ± 3.00	32.96 ± 3.56	39.35 ± 5.67	29.05 ± 2.89
Tei index	0.60 ± 0.08	1.28 ± 0.08*	0.60 ± 0.06	1.07 ± 0.13*	0.75 ± 0.10	1.16 ± 0.16
Body Weight (g)	31.20 ± 0.73	29.36 ± 0.64	26.96 ± 0.83$^{\#}$	25.97 ± 0.66	26.85 ± 1.66	25.58 ± 1.72
N value	7	5	7	9	4	4

Table 3.4.3. Cardiac functional parameters at baseline and after 6 hours post-LPS administration in young male tAUCB-treated mice measured by 2D transthoracic echocardiography. Data are means ± SEM, N = 4-9, $p < 0.05$; * vs baseline; # vs WT LPS-6h; † vs sEH Null LPS-6h.

	WT		sEH Null		*t*AUCB	
	Baseline	LPS-24h	Baseline	LPS-24h	Baseline	LPS-24h
Heart rate (beats/min)	437 ± 17	399 ± 8	451 ± 11	422 ± 13	459 ± 15	415 ± 8
Wall Measurements						
Corrected LV mass, mg	84.65 ± 8.06	79.24 ± 2.91	93.06 ± 4.01	80.59 ± 7.08	83.01 ± 5.23	73.52 ± 2.81
IVS-diastole, mm	0.77 ± 0.04	0.90 ± 0.03	0.91 ± 0.05	0.90 ± 0.04	0.80 ± 0.03	0.94 ± 0.05
IVS-systole, mm	1.19 ± 0.06	1.03 ± 0.03	1.39 ± 0.06	1.25 ± 0.05	1.27 ± 0.05	1.18 ± 0.07
LVPW-diastole, mm	0.78 ± 0.06	0.79 ± 0.05	0.82 ± 0.04	0.84 ± 0.09	0.79 ± 0.07	0.87 ± 0.05
LVPW-systole, mm	1.23 ± 0.07	0.95 ± 0.05	1.28 ± 0.06	1.21 ± 0.09	1.26 ± 0.07	1.07 ± 0.06
LVID-diastole, mm	3.80 ± 0.13	3.45 ± 0.15	3.73 ± 0.08	3.38 ± 0.25	3.72 ± 0.12	3.09 ± 0.12*
LVID-systole, mm	2.47 ± 0.11	3.03 ± 0.15	2.47 ± 0.09	2.42 ± 0.22	2.35 ± 0.13	2.53 ± 0.12
Cardiac Function						
Ejection Fraction (%)	65.65 ± 1.63	28.75 ± 1.49*	64.76 ± 1.80	54.64 ± 6.11#	68.62 ± 2.62	39.69 ± 4.24*†
Fractional Shortening (%)	35.65 ± 1.28	13.07 ± 0.72*	34.95 ± 1.28	28.81 ± 4.01#	38.28 ± 2.06	19.40 ± 2.65*†
LVEDV, µl	63.06 ± 6.18	49.82 ± 4.91	59.73 ± 3.52	48.83 ± 7.70	58.28 ± 4.54	40.02 ± 3.99
LVESV, µl	22.14 ± 2.84	35.73 ± 3.80*	21.32 ± 2.00	21.83 ± 5.00	18.87 ± 2.78	23.96 ± 3.11
CO, ml/min	17.12 ± 1.74	5.54 ± 0.55*	15.59 ± 1.79	10.66 ± 2.07	14.83 ± 1.75	6.47 ± 1.15*
SV, µl	40.92 ± 3.60	14.09 ± 1.30*	38.41 ± 2.22	27.01 ± 5.75	39.41 ± 2.68	16.06 ± 2.44*
Doppler Imaging						
IVRT, ms	15.06 ± 1.08	31.24 ± 2.69*	13.93 ± 0.87	21.74 ± 2.84#	15.32 ± 1.05	27.94 ± 2.52*
IVCT, ms	12.05 ± 1.42	15.73 ± 2.04	9.23 ± 0.71	18.54 ± 5.78	10.59 ± 1.95	18.50 ± 1.80
ET, ms	44.85 ± 2.38	34.08 ± 2.22*	39.12 ± 1.74	35.49 ± 2.82	41.71 ± 3.00	32.67 ± 1.61*
Mitral E/A ratio	1.47 ± 0.08	1.06 ± 0.21	1.47 ± 0.09	1.29 ± 0.12	1.63 ± 0.08	1.16 ± 0.10*
E/E' ratio	28.93 ± 1.94	58.46 ± 11.85*	30.78 ± 3.27	25.12 ± 3.71#	28.77 ± 3.06	31.91 ± 7.60
Tei index	0.62 ± 0.05	1.38 ± 0.08*	0.60 ± 0.02	1.24 ± 0.22*	0.66 ± 0.08	1.49 ± 0.15*
Body Weight (g)	26.50 ± 0.80	24.71 ± 0.97	29.01 ± 0.89	26.40 ± 1.00	27.58 ± 0.81	25.10 ± 0.68
N value	14	10	13	10	14	15

Table 3.4.4. Cardiac functional parameters at baseline and after 24 hours post-LPS administration in young male tAUCB-treated mice measured by 2D transthoracic echocardiography. Data are means ± SEM, N = 10-15, $p < 0.05$; * vs baseline; # vs WT LPS-24h; † vs sEH Null LPS-24h.

3.5 CARDIOMYOCYTE-SPECIFIC DELETION OF sEH ATTENUATES THE SYSEMIC INFLAMMATORY RESPONSE

Global genetic deletion of sEH can reduce systemic inflammation.[164] However, it is unknown whether cardiomyocyte-specific sEH deletion has the capacity to modulate the systemic inflammatory response. The use of a colour-coded multi-plex bead assay allowed for the quantification of the levels of 31 different cytokines, growth factors, and chemoattractant factors in plasma aliquots from saline and LPS treated mice. Surprisingly, levels of circulating chemokines and cytokines were significantly lower in the plasma from $sEH^{(Myo\ -/-)}$ mice compared to the $sEH^{(Myo\ +/+)}$ true controls after LPS administration (Figure 3.5.1). The impact of sEH disruption on attenuation of systemic cytokines and chemokines was more robust at the 24 hour post-LPS timepoint, with all groups experiencing a degree of systemic inflammation at 6 hours post-LPS. This time-dependent attenuation in systemic inflammatory response mirrors the plateau in physiological impairment and cardiac functional decline at 24 hours post-LPS in sEH null and $sEH^{(Myo\ -/-)}$ groups. Therefore, sEH expression at the level of the cardiomyocyte has the capacity to modulate systemic inflammation in acute inflammatory injury.

3.5.1 Effects on pro-inflammatory mediators

Elevation of pro-inflammatory interleukins, including IL-1β, IL-6, IL-13, IL-17, and the IL-12p40 subunit, were significantly attenuated in sEH null and $sEH^{(Myo\ -/-)}$ groups after 24 hours of LPS exposure (Figure 3.5.1). Other mediators of the systemic inflammatory response including TNF-α, IFN-γ, KC, RANTES, and MIP were also suppressed in the plasma of sEH deficient mice (Figure 3.5.2). Interestingly, LPS-induced CXC chemokine (LIX) was elevated in saline-treated control $sEH^{(Myo\ +/+)}$ and $sEH^{(Myo\ -/-)}$ plasma but not in control WT or sEH null mice (Figure S3.5.1). This suggests baseline phenotypic alterations in our Cre Lox mouse colony, which may require further characterization.

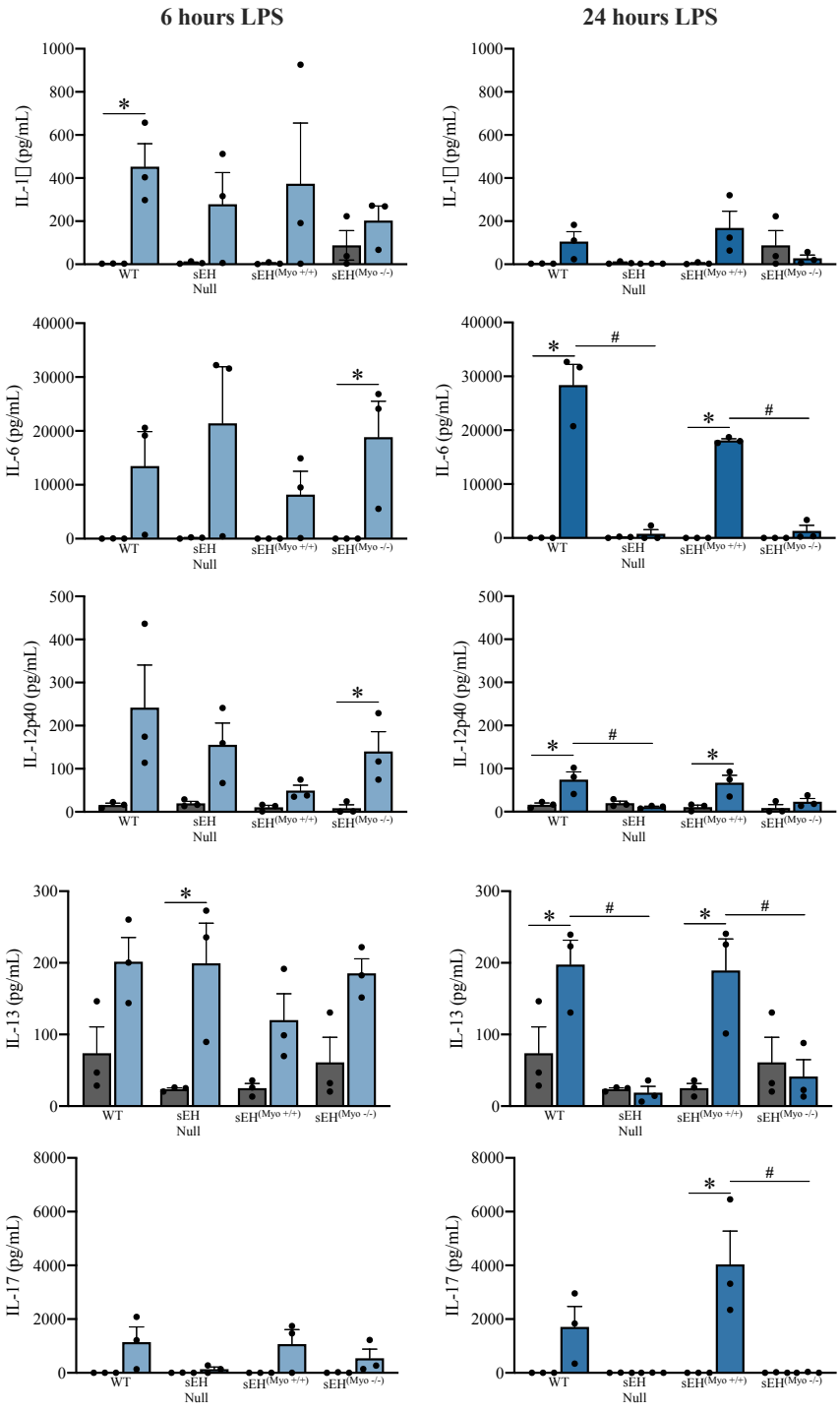

Figure 3.5.1. Plasma levels of pro-inflammatory interleukins in control mice and mice treated with LPS for 6 (light blue) or 24 (dark blue) hours measured using a multi-plex assay. Data are means ± SEM, N = 3, $p < 0.05$; * vs control; # vs true control WT or $sEH^{(Myo\ +/+)}$ post-LPS.

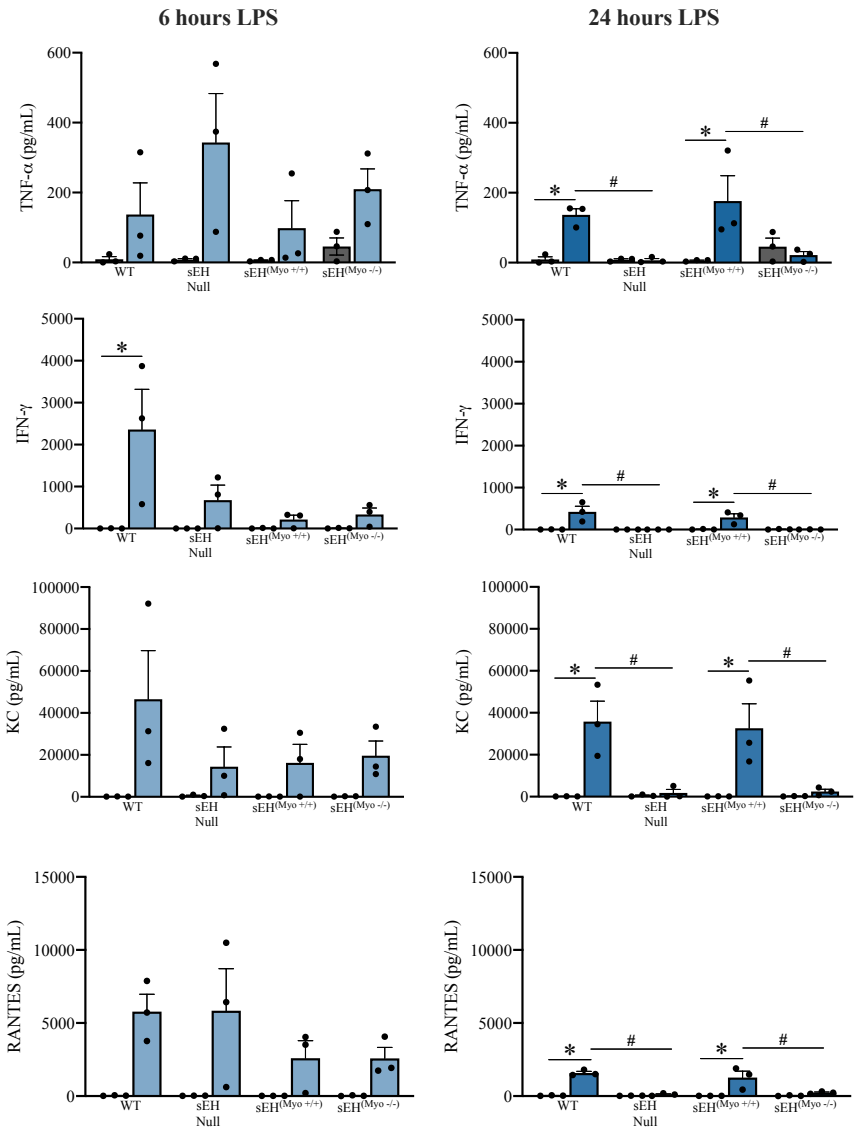

Figure 3.5.2. Plasma levels of other pro-inflammatory mediators in control mice and mice treated with LPS for 6 (light blue) or 24 (dark blue) hours measured using a multi-plex assay. Data are means ± SEM, N = 3, $p < 0.05$; * vs control; # vs true control WT or $sEH^{(Myo +/+)}$ post-LPS.

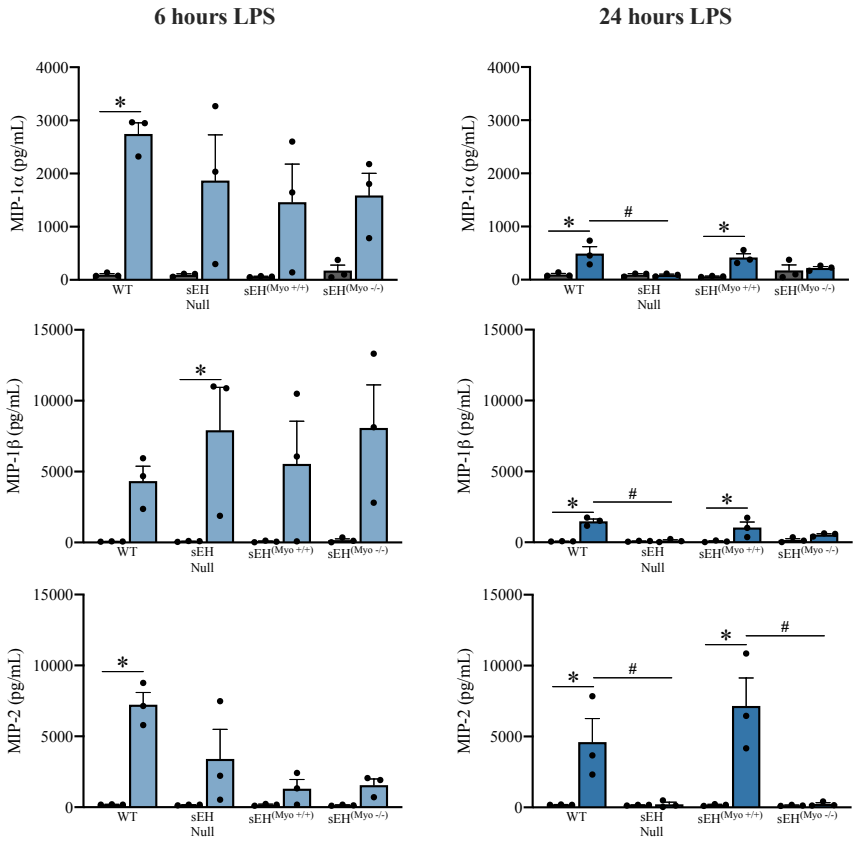

Figure 3.5.2. Plasma levels of other pro-inflammatory mediators in control mice and mice treated with LPS for 6 (light blue) or 24 (dark blue) hours measured using a multi-plex assay. Data are means ± SEM, N = 3, $p < 0.05$; * vs control; # vs true control WT or $sEH^{(Myo +/+)}$ post-LPS.

3.5.2 Effects on anti-inflammatory mediators

Due to the vast inflammatory immune response caused by endotoxemia, release of interleukins with anti-inflammatory properties can also be stimulated.[132] IL-10 plasma levels were significantly reduced in sEH null mice but not in the sEH$^{(Myo\ -/-)}$ group following 24 hours of LPS exposure (Figure 3.5.3). No changes in IL-4 were observed between groups with or without LPS treatment (Figure S3.5.1). Interestingly, these data suggest that anti-inflammatory responses to acute endotoxemia may be differentially regulated by sEH deficiency localized to the cardiomyocyte compared to global genetic deletion.

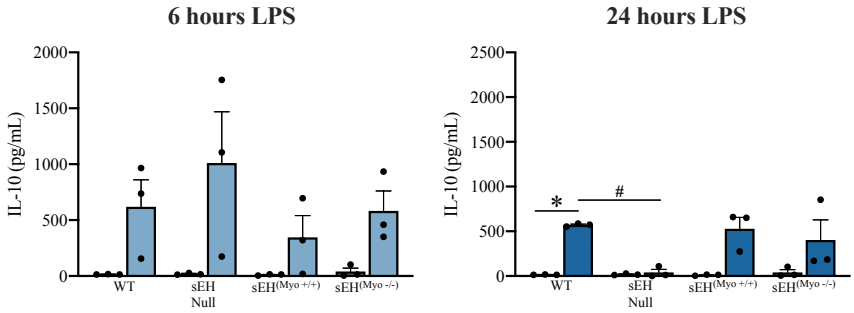

Figure 3.5.3. Plasma levels of the anti-inflammatory interleukin, IL-10, in control mice and mice treated with LPS for 6 (light blue) or 24 (dark blue) hours measured using a multi-plex assay. Data are means ± SEM, N = 3, $p < 0.05$; * vs control; # vs true control WT or sEH$^{(Myo\ +/+)}$ post-LPS.

3.5.3 Effects on stimulating factors and growth factors

Growth factors that stimulate the proliferation and maturation of cells of hemopoietic lineage increase in response to acute endotoxemia to aid in the innate immune response against foreign invaders.[132] Plasma concentrations of macrophage colony-stimulating factor (M-CSF) were markedly increased in all groups following 6 hours of LPS exposure. Conversely, at the 24 hour time point, M-CSF levels were reduced in sEH null and sEH$^{(Myo\ -/-)}$ mice compared to their sEH expressing controls (Figure 3.5.4). Monocyte chemoattractant protein-1 (MCP-1), also known as CCL2, is one of the central chemokines responsible for monocyte migration and infiltration into organs and tissues.[136] MCP-1 plasma levels mirror the time dependent change observed with M-CSF at 6 and 24 hours LPS (Figure 3.5.4). These data suggest a possible time-dependent connection between monocyte proliferation and chemoattraction and that sEH deficiency may contribute to early resolution of these signals. In contrast, changes in levels of granulocyte colony-stimulating factor (G-CSF) and granulocyte macrophage colony-stimulating factor (GM-CSF) were not nearly as robust, suggesting that monocytes and macrophages may be a particular cell population of interest (Figure 3.5.5.D). Furthermore, the plasma level of vascular endothelial growth factor (VEGF) can be interpreted as a marker of angiogenesis but also may indicate the activation of platelets and that the vascular endothelial barrier is compromised.[351-353] During the course of 24 hours of LPS exposure, VEGF levels increased in WT and sEH$^{(Myo\ +/+)}$ mice, whereas levels remained relatively unchanged in sEH null and sEH$^{(Myo\ -/-)}$ groups over time (Figure 3.5.4).

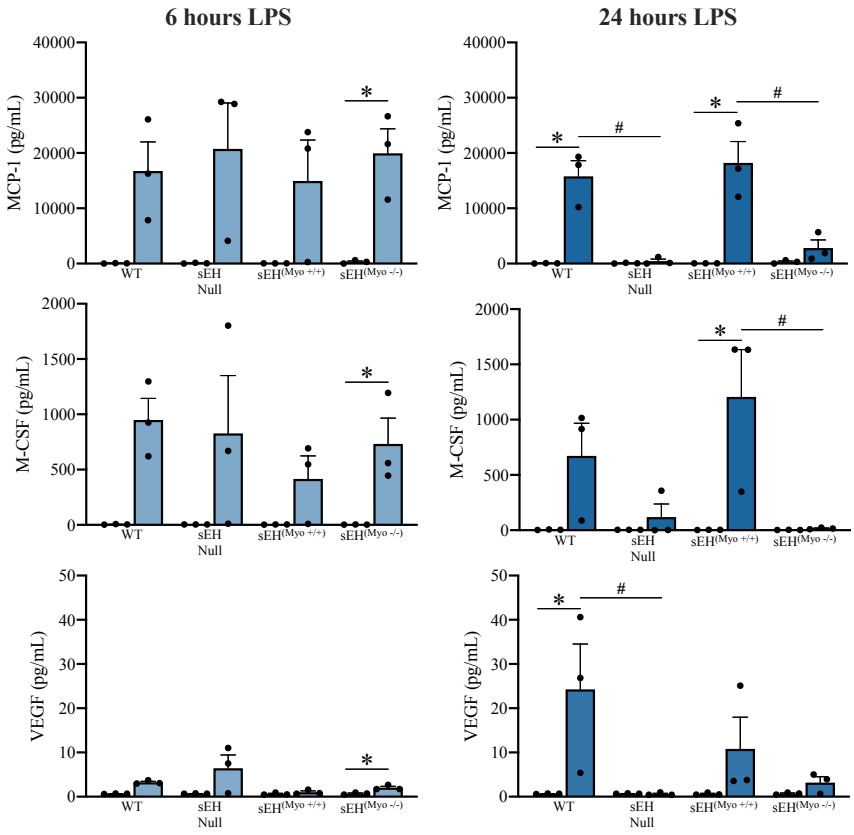

Figure 3.5.4. Plasma levels of chemoattractants and growth factors in control mice and mice treated with LPS for 6 (light blue) or 24 (dark blue) hours measured using a multi-plex assay. Data are means ± SEM, N = 3, $p < 0.05$; * vs control; # vs true control WT or sEH$^{(Myo +/+)}$ post-LPS.

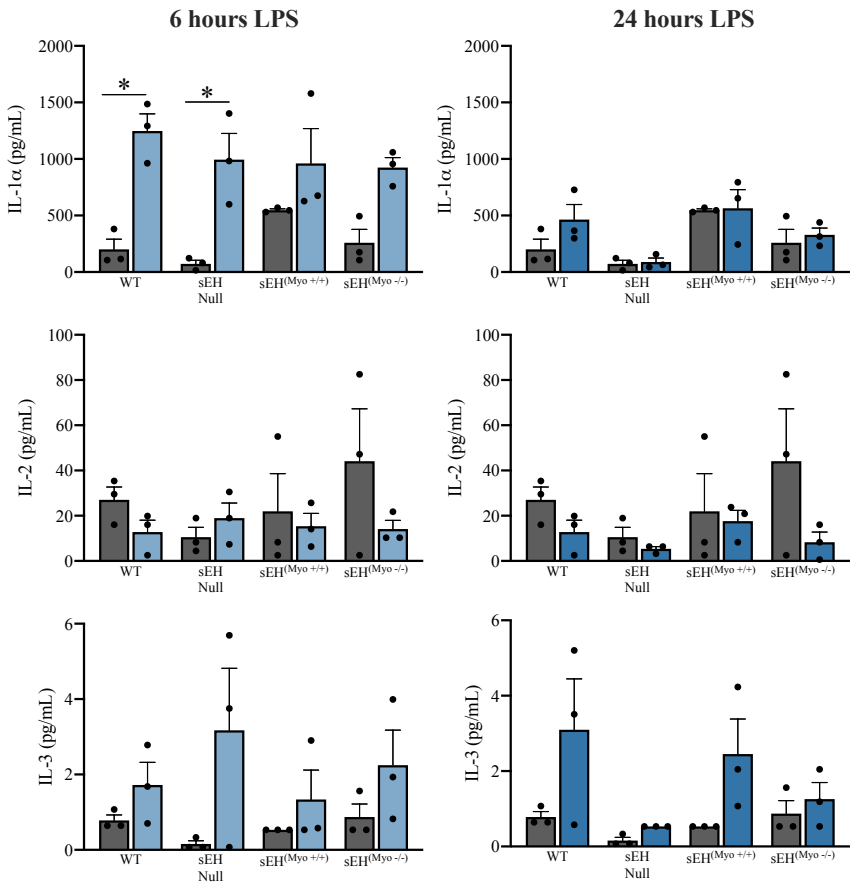

Figure 3.5.5.A. Plasma levels of other cytokines in control mice and mice treated with LPS for 6 (light blue) or 24 (dark blue) hours measured using a multi-plex assay. Data are means ± SEM, N = 3, $p < 0.05$; * vs control; # vs true control WT or sEH$^{(Myo\ +/+)}$ post-LPS.

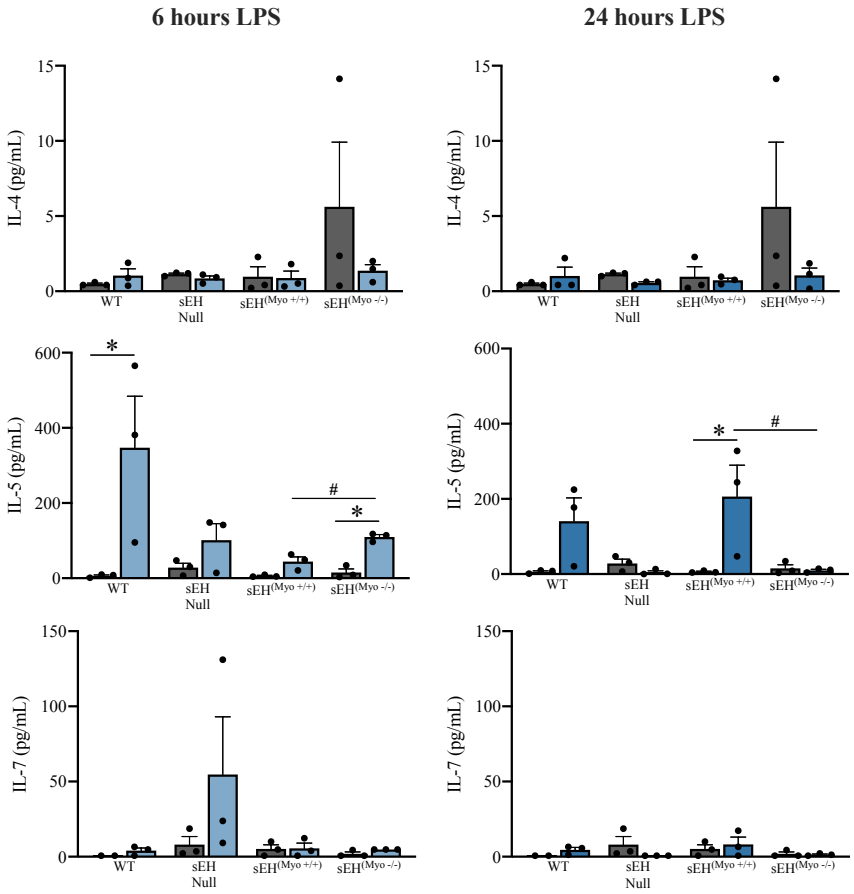

Figure 3.5.5.B. Plasma levels of other cytokines in control mice and mice treated with LPS for 6 (light blue) or 24 (dark blue) hours measured using a multi-plex assay. Data are means ± SEM, N = 3, $p < 0.05$; * vs control; # vs true control WT or $sEH^{(Myo\ +/+)}$ post-LPS.

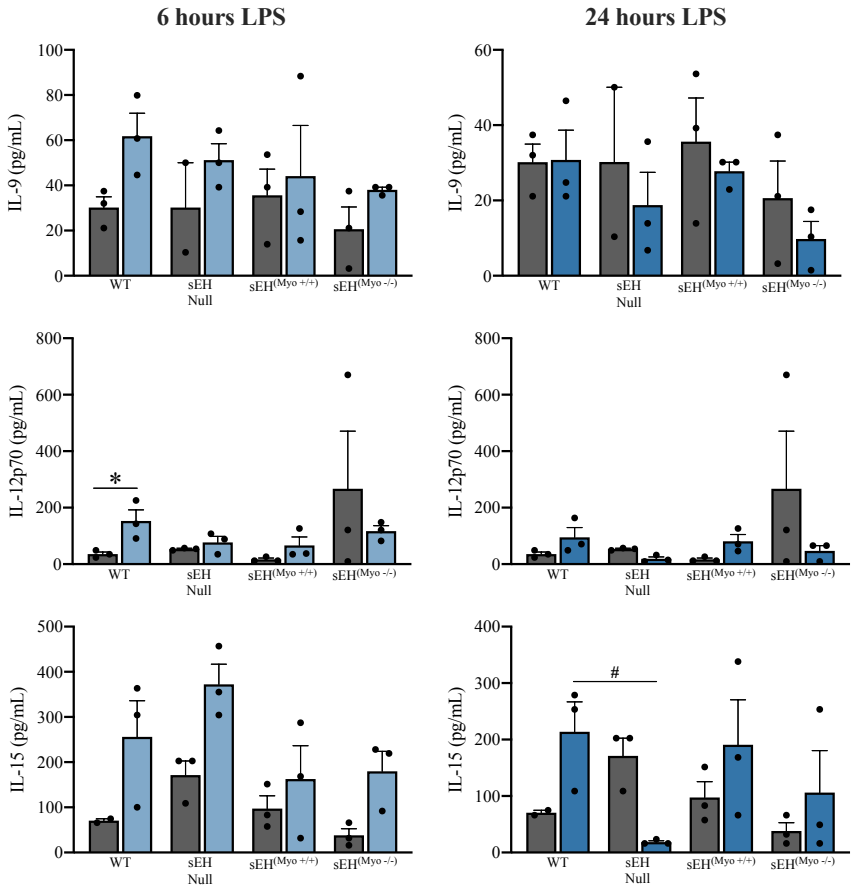

Figure 3.5.5.C. Plasma levels of other cytokines in control mice and mice treated with LPS for 6 (light blue) or 24 (dark blue) hours measured using a multi-plex assay. Data are means ± SEM, N = 3, $p < 0.05$; * vs control; # vs true control WT or $sEH^{(Myo\ +/+)}$ post-LPS.

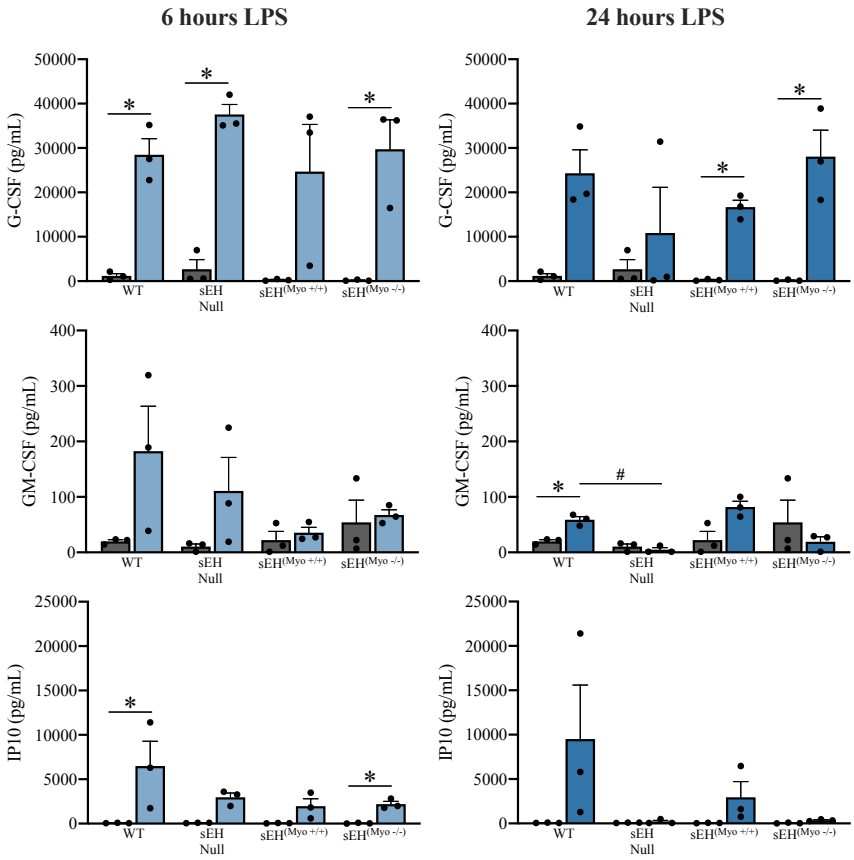

Figure 3.5.5.D. Plasma levels of other cytokines in control mice and mice treated with LPS for 6 (light blue) or 24 (dark blue) hours measured using a multi-plex assay. Data are means ± SEM, N = 3, $p < 0.05$; * vs control; # vs true control WT or sEH$^{(Myo\ +/+)}$ post-LPS.

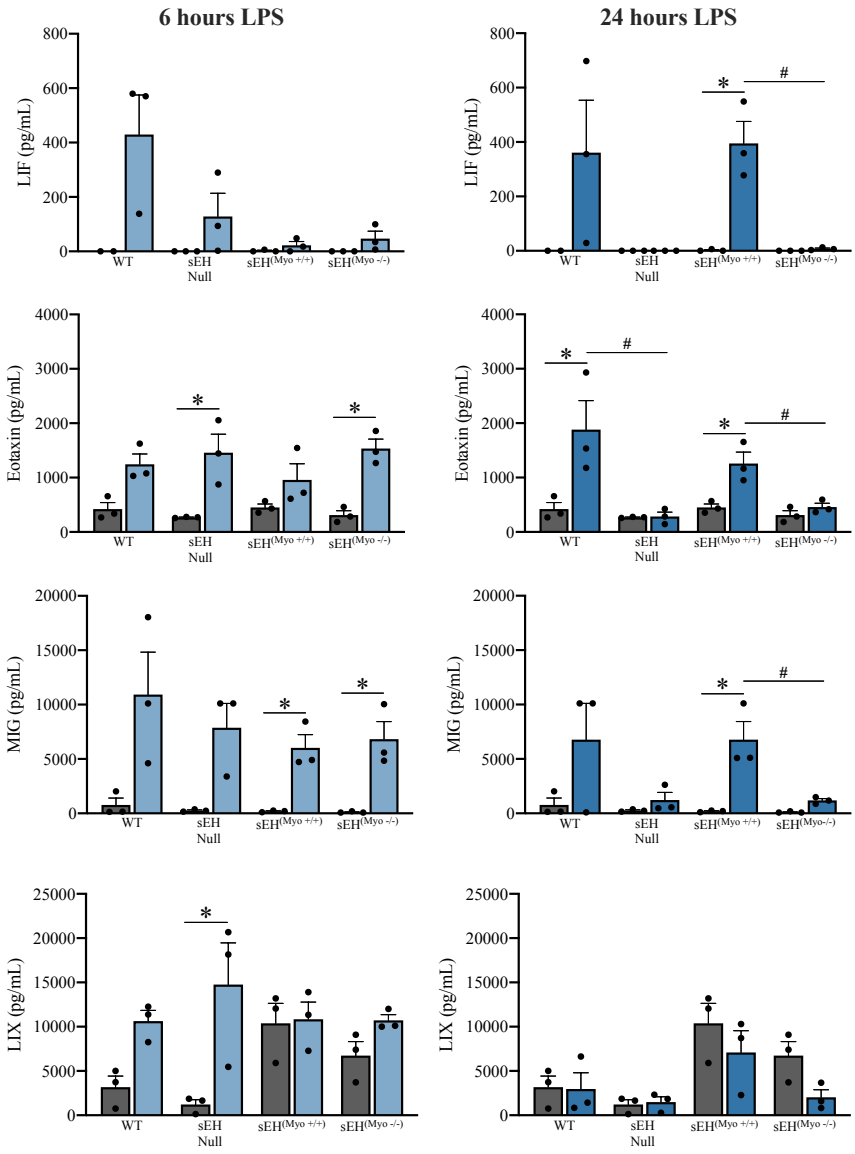

Figure 3.5.5.E. Plasma levels of other cytokines in control mice and mice treated with LPS for 6 (light blue) or 24 (dark blue) hours measured using a multi-plex assay. Data are means ± SEM, N = 3, $p < 0.05$; * vs control; # vs true control WT or $sEH^{(Myo\ +/+)}$ post-LPS.

3.6 GENETIC DELETION OF sEH MODULATES THE NLRP3 INFLAMMASOME

3.6.1 NLRP3 inflammasome activation is attenuated with global and cardiomyocyte-specific sEH deletion

The priming step of the NLRP3 inflammasome causes upregulation of the expression of the NLRP3 protein and the inactive cytokine, pro-IL-1β.[142] Following 6 hours of LPS exposure, protein levels of NLRP3 and pro-IL-1β were significantly higher in cytosolic heart fractions of sEH expressing WT and $sEH^{(Myo\ +/+)}$ mice (Figure 3.6.1) and (Figure 3.6.2). A similar pattern was also observed in the hearts from mice exposed to LPS for 24 hours (Figure 3.6.1) and (Figure 3.6.2). Activation of the NLRP3 inflammasome, which can occur through a variety of signals, stimulates the proteolytic activity of caspase-1 to cleave pro-IL-1β, eventually leading to the release of the mature inflammatory cytokine, IL-1β, from the cell.[142] The activity of caspase-1 was assessed in whole heart lysate from control and LPS-treated mice (Figure 3.6.3). Specific activity of caspase-1 was increased in WT and $sEH^{(Myo\ +/+)}$ hearts after enduring 6 hours of LPS inflammatory injury. Notably, these groups also had higher plasma concentrations of IL-1β (Figure 3.5.1). Conversely, no differences in caspase-1 activity were observed between groups after 24 hours of LPS exposure. Additionally, levels of plasma IL-1β were reduced in all groups at 24 hours compared to the 6 hour time point (Figure 3.5.1). These data not only confirm that cardiomyocyte-specific and global deletion of sEH interferes with inflammasome activation in the heart, but that it does so in a time-dependent manner. Therefore, the early attenuation of the NLRP3 inflammasome pathway may serve to protect cardiac function at later time points throughout the inflammatory process.

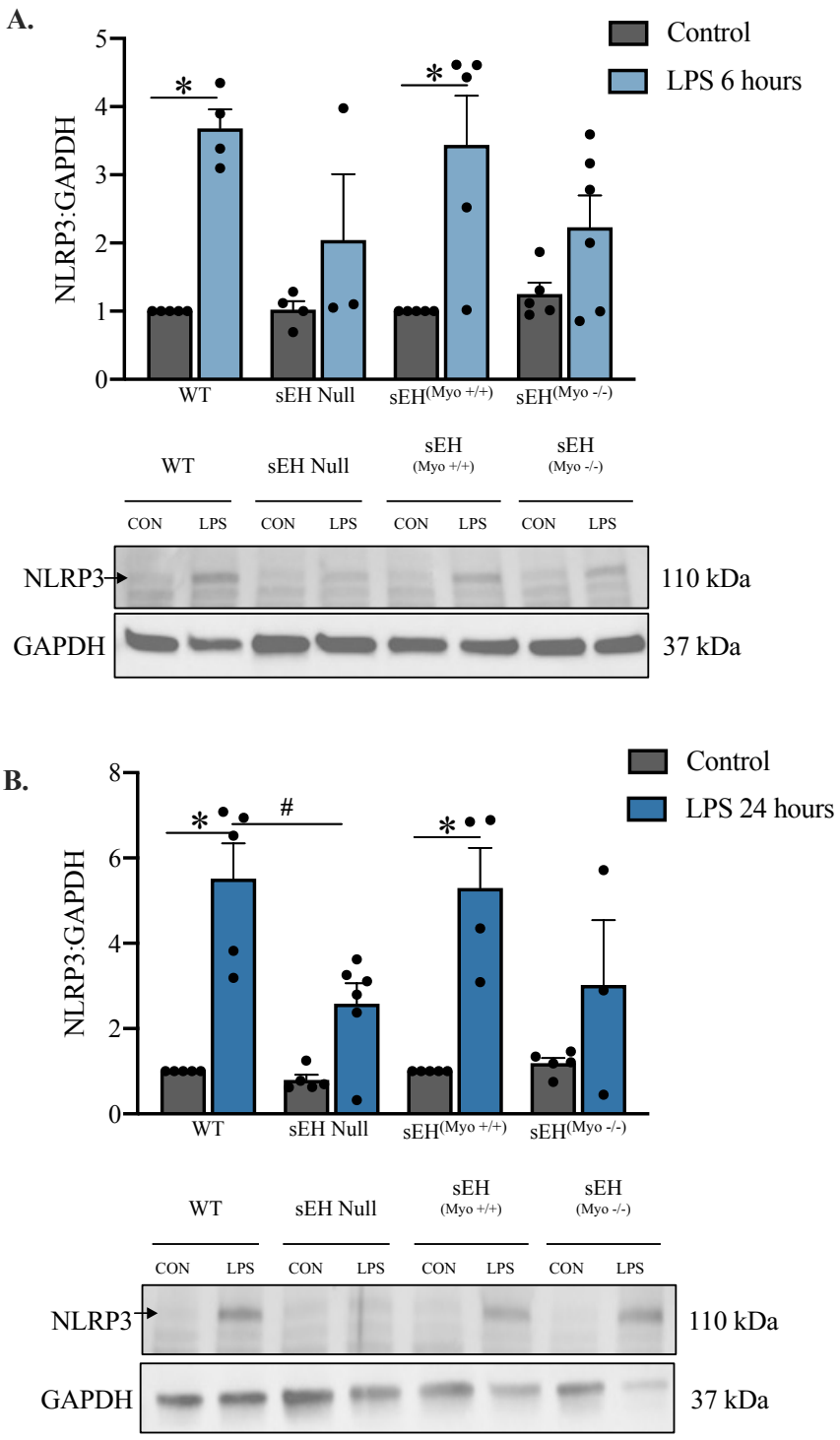

Figure 3.6.1. Western immunoblot of NLRP3 expression in the cytosolic heart fractions of control and **A.)** 6 and **B.)** 24 hour LPS-treated mice. Data are means ± SEM, N = 3-6, $p < 0.05$; * vs respective control; # vs WT LPS-24h.

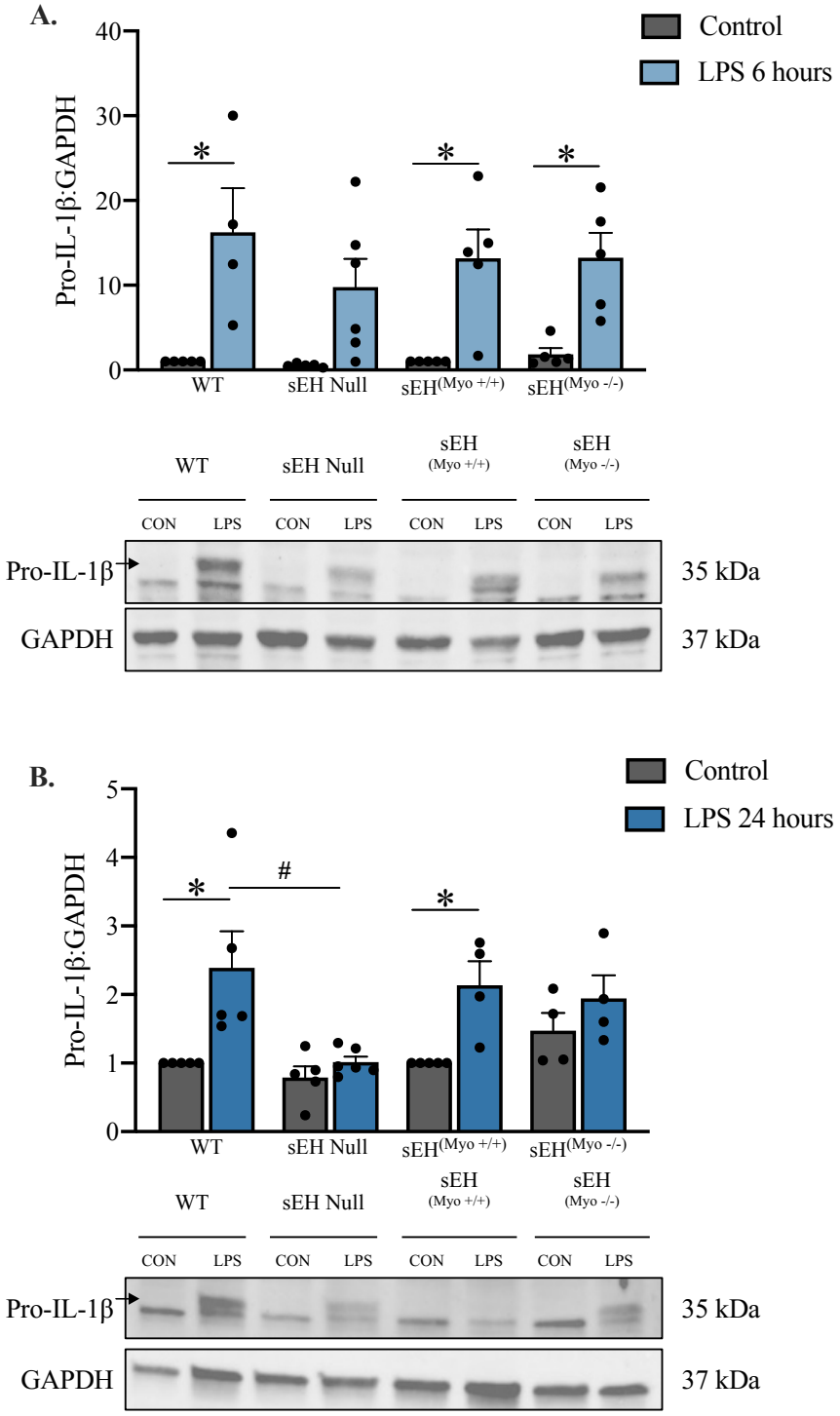

Figure 3.6.2. Western immunoblot of pro-IL-1β expression in the cytosolic heart fractions of control and **A.)** 6 and **B.)** 24 hour LPS-treated mice. Data are means ± SEM, N = 4-6, $p < 0.05$; * vs respective control; # vs WT LPS-24h.

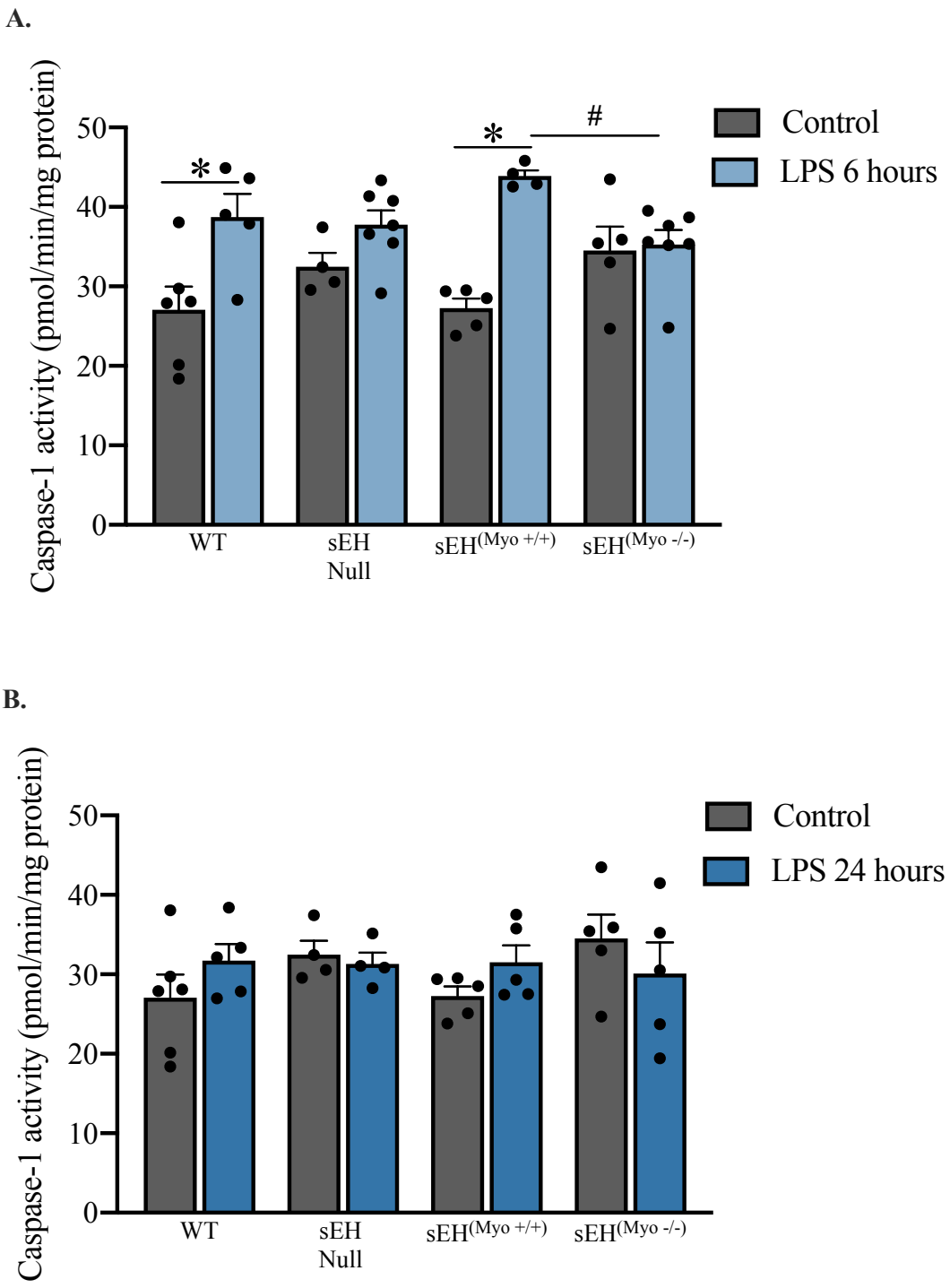

Figure 3.6.3. Specific caspase-1 proteolytic activity from the hearts of control and **A.)** 6 and **B.)** 24 hour LPS-treated mice. Data are means ± SEM, N = 4-7, $p < 0.05$; * vs respective control; # vs $sEH^{(Myo +/+)}$ LPS-6h.

3.7 EPOXYLIPID TREATMENT AND PHARMACOLOGICAL INHIBITON OF sEH IN PRIMARY CARDIOMYOCYTES MODULATES THE NLRP3 INFLAMMASOME RESPONSE

3.7.1 Epoxylipids and sEH inhibition slow the release of mitochondrial ROS

The NLRP3 inflammasome can be activated by mitochondrial damage, including the release of mitochondrial ROS.[142, 158] To determine whether LPS treatment damages cardiomyocyte mitochondria and if this damage can be mitigated by sEH inhibition or epoxylipids, we employed the use of MitoSOX dye which can be used to detect the presence of mitochondrial ROS as a fluorescent signal.[347] We followed the generation of mitochondrial ROS over a 6 hour time period. ROS levels were significantly elevated after 3 hours in LPS treated cardiomyocytes (Figure 3.7.3). When cardiomyocytes were co-treated with LPS and 19,20-EDP or *t*AUCB, mitochondrial ROS generation was significantly less after 3 hours. Therefore, LPS exposure triggers the generation of cardiomyocyte mitochondrial ROS which may contribute to the activation of the NLRP3 inflammasome. Importantly, inhibition of sEH activity and epoxylipid treatment of cardiomyocytes can slow the release of mitochondrial ROS, which may in part, attenuate the activation of the NLRP3 inflammasome.

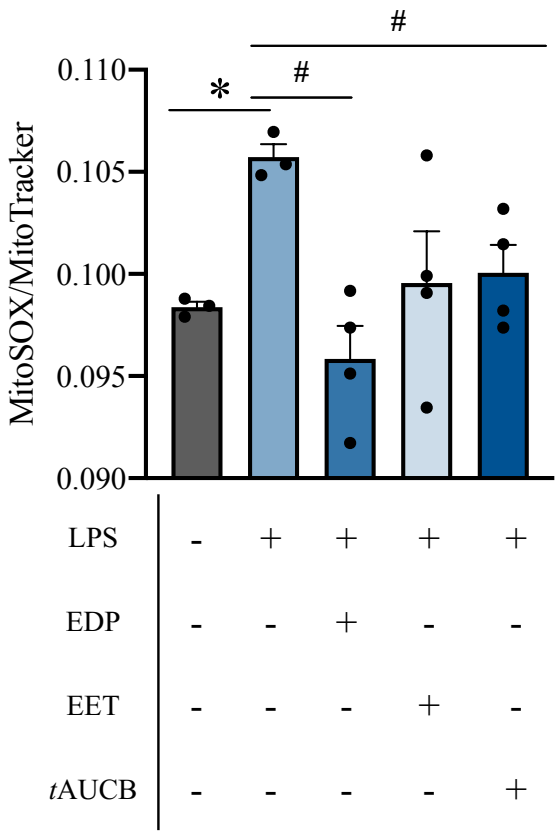

Figure 3.7.1. Relative mitochondrial ROS production (MitoSOX red fluorescence) normalized to total mitochondrial content (MitoTracker green fluorescence) after 3 hours of LPS stimulation of neonatal rat cardiomyocytes. Data are means ± SEM, N = 3-4, $p < 0.05$; * vs control; # vs LPS.

3.7.2 LPS triggers the NLRP3 inflammasome in cardiomyocytes which is attenuated by sEH inhibition or epoxylipid treatment

It is well established that the NLRP3 inflammasome pathway can be activated in innate immune cells in response to acute inflammatory stimuli.[142] Additionally, NLRP3 expression in heart tissue is increased by ischemia-reperfusion injury.[236] However, whether the NRLP3 inflammasome pathway could be modulated in non-immune cells such as cardiomyocytes in response to LPS stimulation is still elusive. So, we treated neonatal rat cardiomyocytes with LPS for 6 hours. These cardiomyocytes had significantly higher protein expression of NLRP3 and pro-IL-1β, indicating that the inflammasome response can be directly triggered in cardiomyocytes (Figure 3.7.2). Caspase-1 activity was also significantly higher in LPS-treated cells and the levels of mature IL-1β released into the surrounding cell media were also increased, suggesting that cardiomyocyte-specific inflammasome activity is enhanced in response to LPS (Figure 3.7.3). Furthermore, this activation of the NLRP3 inflammasome in the cardiomyocyte may, in part, be due to the generation of mitochondrial ROS caused by LPS exposure.

Neonatal rat cardiomyocytes pre-treated for 1 hour with 19,20-EDP, 11,12-EET, or *t*AUCB before the addition of LPS did not have a significant attenuation of NLRP3 or pro-IL-1β protein expression in the cytosol compared to LPS treated cells (Figure 3.7.2). However, caspase-1 activity in 19,20-EDP and *t*AUCB treated cardiomyocytes was nearly absent in response to LPS stimulation (Figure 3.7.3). The levels of mature IL-1β released into the cell media was also reduced with *t*AUCB, 19,20-EDP, and 11,12-EET treatment. Signals such as mitochondrial ROS affect the activation of caspase-1 and release of IL-1β from the cell, rather than NLRP3 or pro-IL-1β protein expression.[140] So, sEH inhibition and epoxylipid treatment may exert their protective effects via modulation of the activation step of the NLRP3 inflammasome in cardiomyocytes in response to LPS by delaying the generation of mitochondrial ROS.

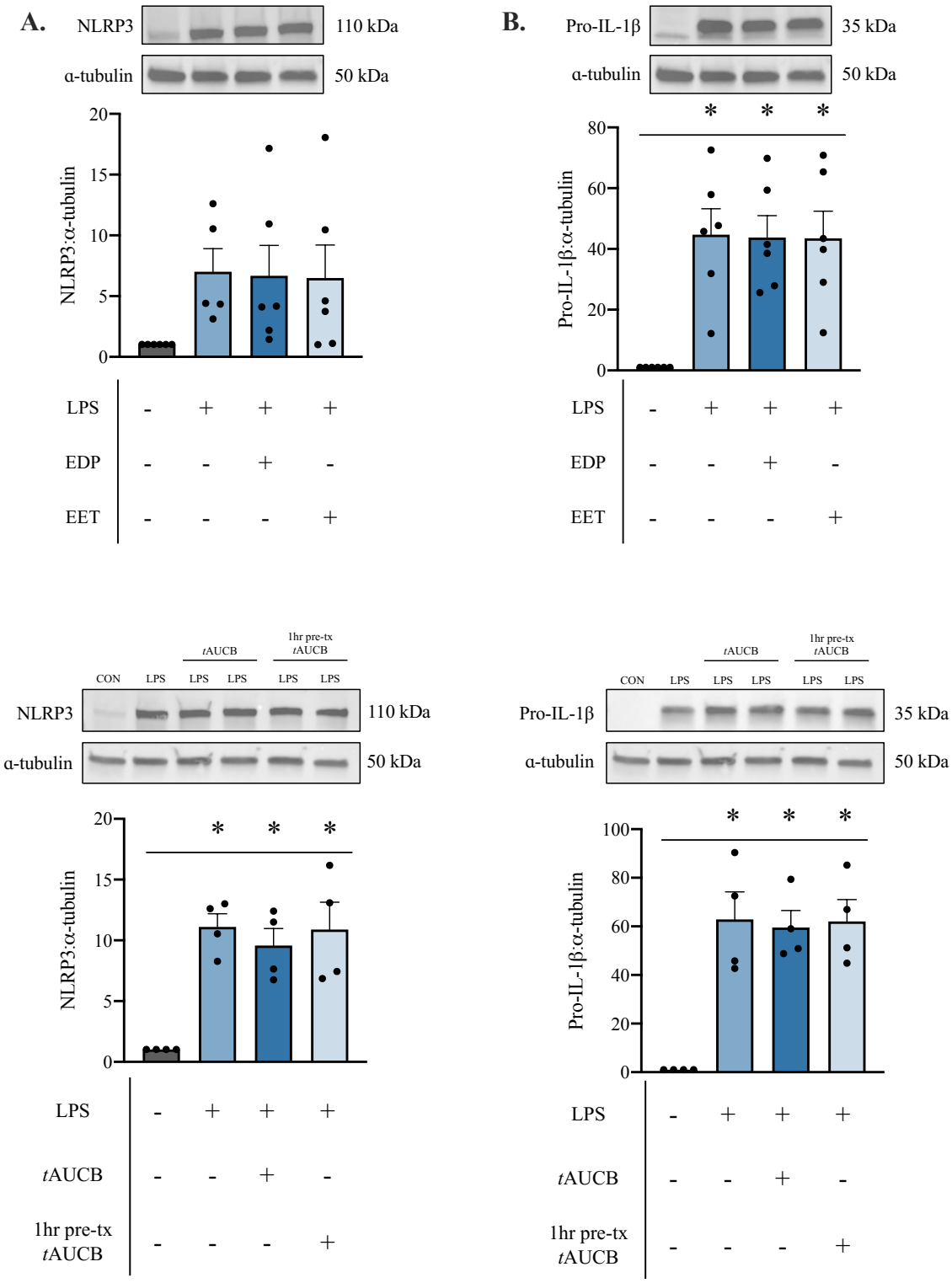

Figure 3.7.2. Western immunoblot of **A.)** NLRP3 and **B.)** pro-IL-1β expression in neonatal rat cardiomyocytes. Data are means ± SEM, N = 4-6, $p < 0.05$; * vs control.

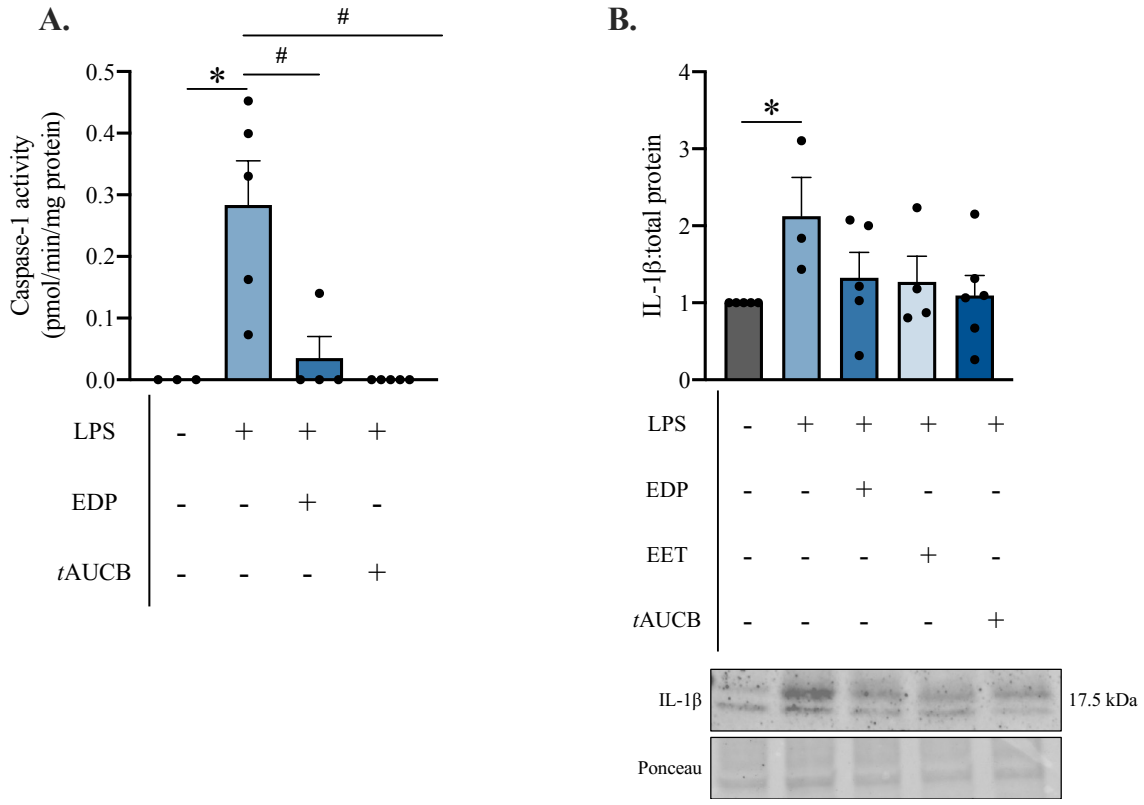

Figure 3.7.3. A.) Specific caspase-1 activity in LPS-treated neonatal rat cardiomyocytes. **B.)** Western immunoblot of mature IL-1β protein released from cardiomyocytes into the extracellular media. Data are means ± SEM, N = 3-6, $p < 0.05$; * vs control; # vs LPS.

3.8 EFFECTS ON INFLAMMATORY CELL RECRUITMENT TO THE MYOCARDIUM

3.8.1 sEH gene disruption impairs macrophage recruitment to the myocardium

The plasma from sEH null and sEH$^{(Myo\ -/-)}$ mice possessed lower levels of circulating chemoattractants including MCP-1 and TNF-α after LPS treatment, compared to their sEH expressing counterparts. These findings prompted us to investigate whether there was a lesser degree of inflammatory cell infiltration into the heart, which could account for the preservation of cardiac function. Macrophages can be identified by unique glycoprotein surface markers.[106] CD68 is a surface glycoprotein that is highly expressed by macrophages.[106] Immunohistochemical staining of heart slices demonstrated enhanced CD68^{+} cell presence in the myocardium after 24 hours of LPS exposure in WT and sEH$^{(Myo\ +/+)}$ groups compared to saline treated controls (Figure 3.8.1) and (Figure 3.8.2). Interestingly, the number of CD68^{+} cells in sEH null and sEH$^{(Myo\ -/-)}$ hearts after 24 hours of LPS exposure was significantly less compared to their sEH expressing controls (Figure 3.8.1) and (Figure 3.8.2). These data suggest that impaired expression of cardiomyocyte sEH may protect the heart by interfering with the recruitment and infiltration of monocytes and accumulation of macrophages in the heart. Interestingly, levels of CD68^{+} cells were elevated in saline-treated control sEH$^{(Myo\ +/+)}$ and sEH$^{(Myo\ -/-)}$ hearts, suggesting a possible baseline cardiac phenotype in our Cre lox mice which requires further investigation.

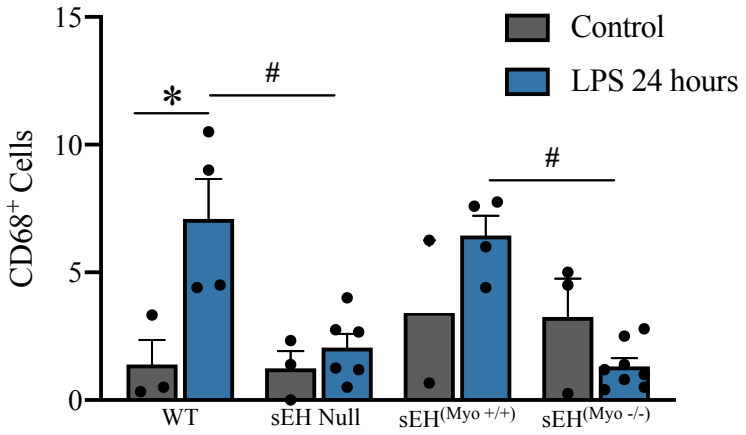

Figure 3.8.1. Quantitation of CD68+ cells. Each point (N) represents the average number of $CD68^{+}$ cells from all images (4-6) taken of a heart from each individual mouse. Data are means ± SEM, N = 2-8, $p < 0.05$; * vs respective control; # vs true control WT or $sEH^{(Myo\ +/+)}$ post-LPS.

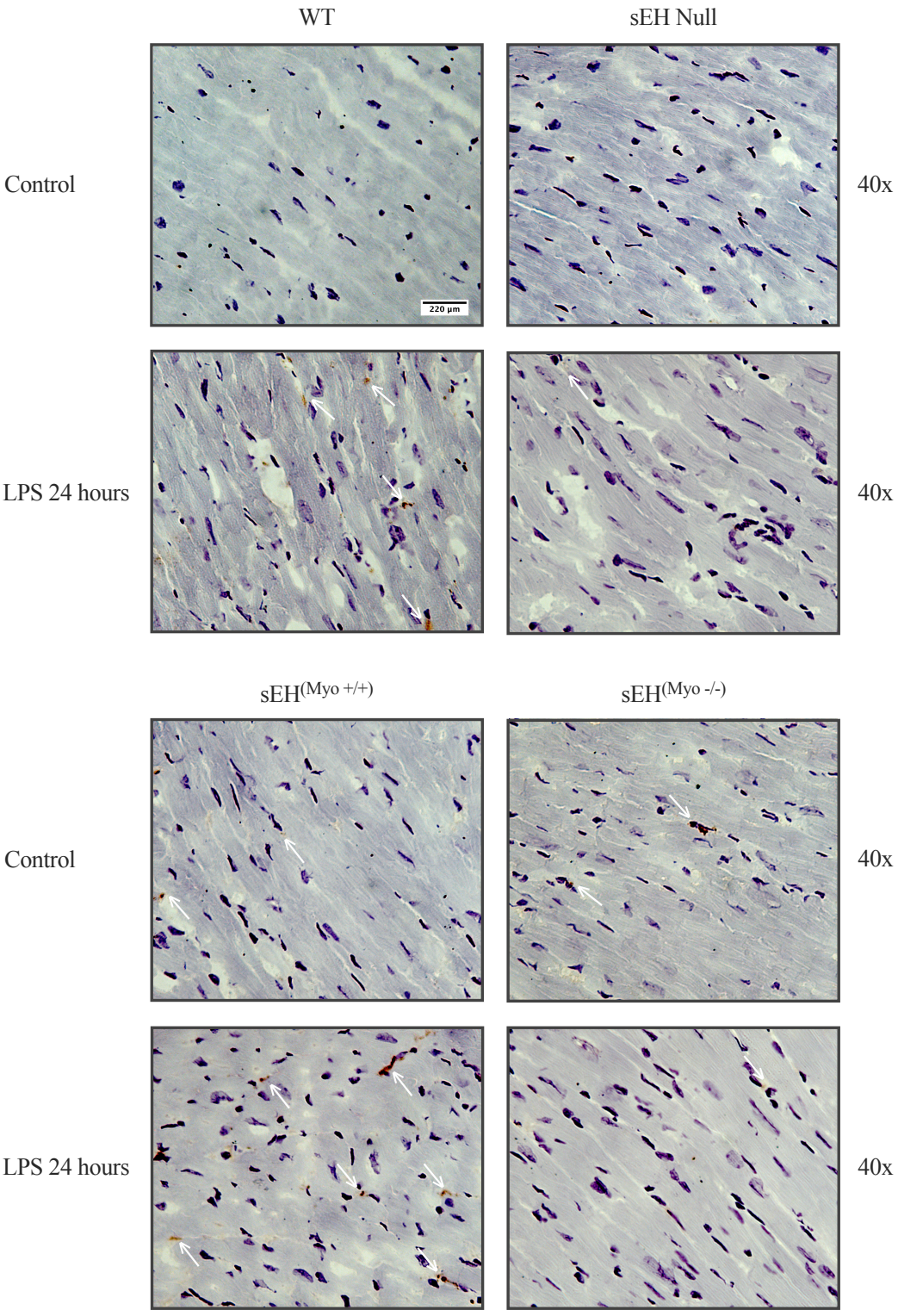

Figure 3.8.2. Representative images of CD68 immunohistochemistry in control heart slices and hearts from mice exposed to LPS for 24 hours. $CD68^{+}$ cells are denoted by white arrows.

3.8.2 Cardiomyocyte sEH inhibition or epoxylipid treatment impairs the release of chemoattractant factors

Cellular release of chemoattractant mediators such as MCP-1 and TNF-α can recruit innate immune cells such as neutrophils and monocytes to organs and tissues which can exacerbate inflammatory damage.[102] Release of these mediators from endothelial cells, macrophages, and other phagocytes is well established.[136] Given the reduced presence of $CD68^+$ cells in the $sEH^{(Myo\ -/-)}$ myocardium following LPS exposure, we investigated whether cardiomyocytes could also play a direct role in the recruitment of inflammatory cells in response to acute inflammation. Cardiomyocytes treated with LPS released significant levels of MCP-1 and TNF-α into their surrounding media (Figure 3.8.3). However, these levels were significantly attenuated when the cells were pre-treated with 19,20-EDP, 11,12-EET, or *t*AUCB before the addition of LPS. Critically, this demonstrates that the cardiomyocyte has a direct role in the release of chemoattractant mediators, which can recruit inflammatory cells to the heart. Moreover, epoxylipids and sEH inhibition can attenuate this effect, which may contribute to their cardioprotective mechanisms in acute systemic inflammatory injury.

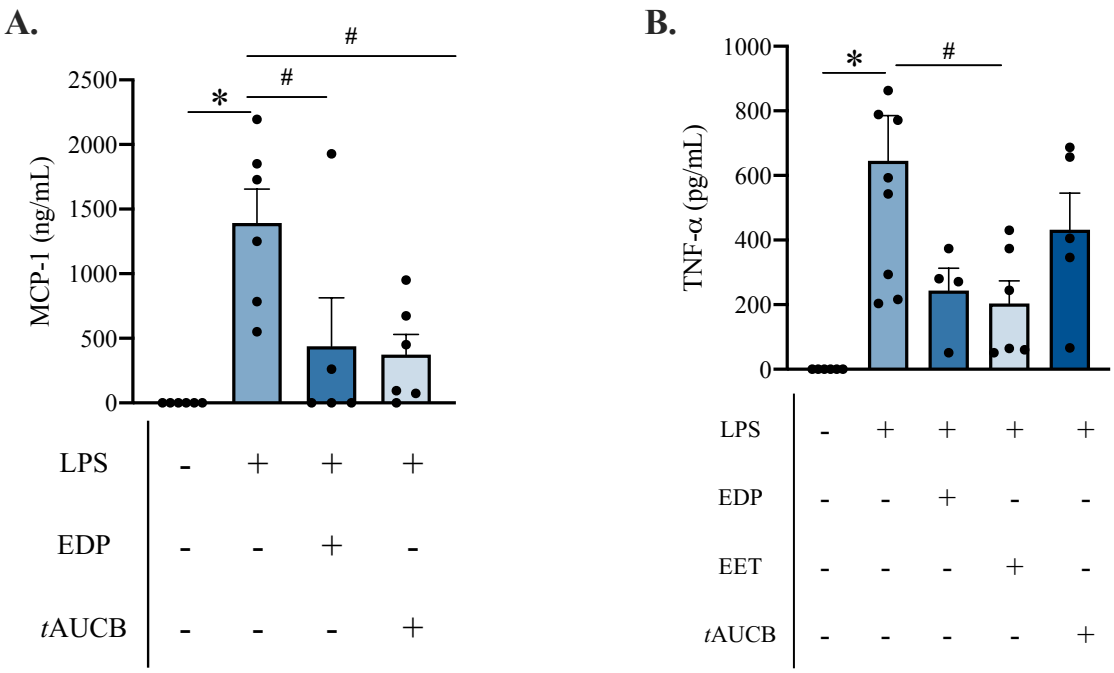

Figure 3.8.3. Levels of **A.)** MCP-1 and **B.)** TNF-α secreted by cardiomyocytes into their surrounding media after 6 hours post-LPS treatment determined by ELISA. Data are means ± SEM, N = 4-9, $p < 0.05$; * vs control; # vs LPS

CHAPTER 4

DISCUSSION

Overview of findings

In this study, we demonstrate for the first time that cardiomyocyte-specific deletion of sEH is cardioprotective and anti-inflammatory in systemic LPS inflammatory injury. The heart is detrimentally impacted in acute endotoxemia resulting from a variety of mechanisms.[5, 12, 18, 23] By specifically targeting cardiomyocyte sEH activity, we can interfere with a detrimental feed-forward process; where endotoxemia induces excess inflammation that fuels further inflammatory responses, leading to organ dysfunction and severe physiological deterioration. The data presented in this thesis, highlights how cardiomyocytes are a critical participant in the innate immune response and that cardiomyocyte sEH expression is vital in mediating these effects. First, we have demonstrated that cardiomyocyte-specific sEH deletion is cardioprotective in acute inflammatory injury. $sEH^{(Myo\ -/-)}$ mice experienced less cardiac dysfunction with LPS treatment than their $sEH^{(Myo\ +/+)}$ counterparts. Then by focussing on the direct effects of epoxylipid treatment and sEH inhibition at the level of the cardiomyocyte we demonstrate that the NLRP3 inflammasome pathway is disrupted. Lastly, it is demonstrated that engagement of the systemic inflammatory response and recruitment of macrophages to the myocardium play a major role in LPS-induced cardiac dysfunction. Importantly, cardiomyocyte-specific sEH deletion has the capacity to attenuate systemic cytokine levels and interfere with macrophage infiltration of the heart. Importantly, the *systemic* effects of *local* cardiomyocyte-specific sEH deletion may contribute to preservation of cardiac function and overall physiological tolerance to the effects of acute LPS inflammatory injury.

4.1 CARDIAC EFFECTS: CARDIOPROTECTION OF CARDIOMYCOYTE-SPECIFIC sEH DELETION

Our previous work demonstrated the global genetic deletion of sEH was cardioprotective and reduced the inflammatory response following 24 hours of LPS exposure in mice.[164] Acute LPS exposure causes profound disruption of cardiac function, which is attenuated in sEH null mice. However, the effect of sEH deletion localized to the

cardiomyocyte, as well as use of a pharmacological sEH inhibitor on cardioprotective and anti-inflammatory outcomes had yet to be explored.

4.1.1 Preserved cardiac function

Endotoxemia and sepsis elicit widespread multi-organ damage. The heart is no exception to this destruction.[5, 18] Cardiac function is a serious problem in septic patients and its presence leads to significantly poorer prognosis and higher mortality rates.[4, 5] However, therapies to treat sepsis-induced cardiac dysfunction are lacking, where the majority of treatments rely on antibiotics and supportive therapies such as vasopressors, fluid resuscitation, and inotropic agents.[5, 354] In our model of acute LPS-induced endotoxemia, we observed similar alterations in heart function consistent with septic cardiomyopathy.[15, 18, 355] Mice experienced a profound reduction in systolic function accompanied by left ventricular dilation and increased LV volumes. However, these changes were significantly more robust in WT and sEH$^{(Myo\ +/+)}$ mice which had unaltered expression of sEH.

Genetic deletion of sEH has known cardioprotective effects in a variety of models. sEH null mice which underwent myocardial infarction via left anterior descending (LAD) coronary artery ligation fared significantly better in terms of heart function compared to their WT counterparts.[300, 303] *Ex vivo* ischemia-reperfusion of hearts from sEH null mice had markedly improved functional recovery compared to sEH expressing comparators.[299] Additionally, we have previously demonstrated that global sEH deletion preserves cardiac function following 24 hours of acute LPS exposure.[164] Our findings in this study further validate the versatile cardioprotective properties attributed to sEH genetic disruption.

However, the heart consists of a heterogeneous population of cell types including myocytes, endothelial cells, fibroblasts, and resident macrophages.[334] By selectively deleting sEH expression only in the cardiomyocyte, we were able to delineate the effects of sEH in this particular cell type towards overall cardioprotection. sEH$^{(Myo\ +/+)}$ and sEH$^{(Myo\ -/-)}$ mice had striking differences in cardiac response to LPS treatment. Systolic parameters including EF% and FS% were significantly preserved in sEH$^{(Myo\ -/-)}$ compared to their true controls. sEH$^{(Myo\ +/+)}$ mice also had significant alterations in diastolic functional parameters and LV dimensions that were not nearly as robust in the sEH$^{(Myo\ -/-)}$ group. This highlights

the critical role that sEH plays within the cardiomyocyte and its contribution to LPS-induced cardiac dysfunction.

Despite the protection conferred by cardiomyocyte-specific deletion of sEH, it is not all-encompassing. Global sEH null mice were still significantly more protected than sEH$^{(Myo\ -/-)}$ groups. At 24 hours post-LPS exposure, sEH$^{(Myo\ -/-)}$ still exhibited a significant decline in systolic heart function that was not present in sEH null mice. Importantly, this suggests that although absence of sEH in the cardiomyocyte elicits a cardioprotective response, the unaltered activity of sEH in other cell types of the heart and the rest of the body still contribute to the detrimental effects of acute LPS injury.

The cardioprotection of sEH deletion may be, in part, due to its impact on the changing oxylipid profile in response to LPS. mRNA expression of epoxylipid-producing CYP enzymes of the *Cyp2j* and *Cyp2c* isoforms have been shown to decline in the liver, kidney, duodenum, and lungs of endotoxemic mice.[293, 294, 356] The reduction in CYP enzyme expression may suggest a reduced capacity to produce epoxylipids with known protective properties, including EETs. So, inhibition of sEH may serve as a factor to prevent the hydrolysis and subsequent inactivation of these epoxylipids and thus preserve their presence in tissues during acute inflammation. However, LPS-induced changes in CYP enzyme mRNA expression appear to be tissue-dependent.[356] In brain tissue from LPS challenged mice, *Cyp2j* and *Cyp2c* mRNA doubled in expression.[356] Changes in CYP enzyme expression with acute LPS have yet to be characterized in the myocardium, and may provide important insights into the protective mechanisms of sEH deletion in the heart.

Our previous work has shown that plasma 8,9-, 11,12-, and 14,15-EET levels are unchanged with LPS in WT and sEH null mice.[164] But the formation of their 4 regioisomer diol metabolites, DHETs, are attenuated in sEH null groups suggesting an increase in EET half-life and thus the duration of their protective effects. Other studies have similarly found no changes in the levels of 5,6-, 8,9-, 11,12-, or 14,15-EETs and also DHETs in the hearts of LPS treated mice.[357] However, lower levels of DHA derived epoxides such as 10,11-, 13,14-, and 16,17-EDP were demonstrated in hearts following LPS exposure.[358] Mice overexpressing the human CYP2J2 transgene also had preserved cardiac function and hemodynamic parameters in an acute model of endotoxemia.[359] Therefore, cardiomyocyte-

specific sEH deletion may partially exert its protection by causing an accumulation of protective epoxylipids including EET and EDP in the heart.

4.1.2 Temporal changes

The pathological course of sepsis is time-dependent. Initially, patients experience a hyperdynamic state followed by a hypodynamic phase consisting of hypoperfusion and reduced cardiac output.[12, 15, 16] We assessed the effects of acute LPS treatment on cardiac function at 2 timepoints; 6 and 24 hours post injection. We observed an initial decline in cardiac function in all groups which stabilized in sEH null and sEH$^{(Myo\ -/-)}$ groups while WT and sEH$^{(Myo\ +/+)}$ mice continued on a steep trajectory of deterioration toward the end of the 24 hour time point. Therefore, the effects of sEH deletion may manifest in a temporal manner by slowing the development of cardiac depression in the hypodynamic phase of endotoxemia.

4.1.3 The effects of pharmacologic sEH inhibition on LPS-induced cardiac dysfunction

A range of pharmacological compounds have been developed to inhibit the hydrolase activity of sEH. Compounds of this class have been tested in models of acute endotoxemia and sepsis.[296, 360] Various studies have demonstrated that treatment with sEH inhibitors improves survival, reduces acute lung injury, hypotension, edema, and attenuates inflammatory cytokine release associated with experimental models of sepsis.[282, 283, 291, 293, 294, 360] However, the effect of pharmacological sEH inhibitors on LPS-induced cardiac dysfunction had not been investigated. We employed the use *t*AUCB as our pharmacologic compound of choice. *t*AUCB has established cardioprotective properties in other models of cardiovascular disease including myocardial infarction and cardiac ischemia-reperfusion injury.[300] Additionally, *t*AUCB possesses favourable pharmacokinetic properties including oral bioavailability when administered to mice in a model of acute LPS injury.[296] In contrast to the overwhelming benefit demonstrated by sEH inhibitors on endotoxemia in the literature, our findings on the effects of *t*AUCB in LPS-induced cardiac dysfunction were rather modest. Our findings demonstrated systolic cardiac function from *t*AUCB-treated

mice was significantly worse that sEH null mice but was trending better compared to their WT counterparts.

The pharmacokinetics of *t*AUCB have been extensively characterized in a model of acute LPS inflammation, which was why the modest effects on cardioprotection we observed were perplexing.[296] In the literature, a dose of 10 mg/kg of LPS was injected i.p. followed by a *t*AUCB oral gavage bolus of 1 mg/kg dissolved in triolein vehicle, similar to our protocol.[296] *t*AUCB was able to effectively maintain the epoxylipid to diol plasma ratio after LPS treatment and attenuated the development of hypotension.[296] However, the endpoints for the authors' experiments were 4 hours and 6 hours post-LPS administration, respectively. In contrast our experimental endpoints were at 6 and 24 hours after LPS injection. Furthermore, the authors did not assess cardiac functional parameters at 6 hours. So, our data may suggest that 6 hours is not enough time for *t*AUCB to affect cardiac function. We also did not confirm whether mice were experiencing the effects of *t*AUCB at 6 hours. Importantly, we will have to assess this by quantifying the plasma epoxylipid to diol ratio and *t*AUCB levels at this time point. Our choice to use a 24 hour endpoint also poses a challenge. The pharmacokinetics of *t*AUCB have not been characterized at 24 hours post-administration in an acute LPS model. Again, quantification of plasma levels of epoxylipids and diols and *t*AUCB levels will provide valuable information as to whether the effects of *t*AUCB are still present at 24 hours post-administration.

Furthermore, the effects of sEH inhibitors in LPS injury may be tissue specific. For example, 6 days of continuous administration of the sEH inhibitor, AUDA, through implanted osmotic mini-pumps in acute LPS inflammation did not affect the expression of pro-inflammatory genes such as *Il-6*, *Mcp-1*, *Tnf-α*, *Vcam-1*, or *Cox-2* in liver tissue.[279] AUDA treatment was also unable to attenuate the accumulation of neutrophils in the liver following a single 1 mg/kg LPS bolus dose.[279] In contrast, i.p. administration of AUDA 4 hours after intratracheal installation of LPS successfully attenuated MCP-1 and TNF-α levels and reduced neutrophil infiltration into the lung tissue.[288] These differential effects conferred by the same sEH inhibitor may be influenced by the model and the experimental design and protocol, making it a challenge to compare studies head-to-head. The modest cardioprotection we observed with *t*AUCB in our model may be due to a combination of all these factors. Importantly, a number of *t*AUCB administration protocols of varying

concentrations, pre-treatment lengths, and bolus dosing intervals will need to be assessed in our model of LPS-induced acute inflammation before any conclusions can be drawn about the efficacy of *t*AUCB on LPS-induced cardiac dysfunction.

4.2 CELLULAR EFFECTS: IMPAIRMENT OF CARDIOMYCOCYTE INFLAMMATORY SIGNALLING

4.2.1 Deficiency of sEH activity attenuates the NLRP3 inflammasome in the heart

The NLRP3 inflammasome is an innate immune system signalling complex. Activation of the NLRP3 inflammasome promotes caspase-1-mediated cleavage and release of mature IL-1β from the cell.[142] The NLRP3 signalling pathway is activated in acute endotoxemia throughout the body including the lungs, peritoneal macrophages, liver, and brain.[146, 242, 293, 294, 361] CLP-induced polymicrobial sepsis causes an increase in inflammasome protein expression and activation in heart tissue, which is associated with a decline in stroke volume and cardiac output.[176, 362] Inflammatory mechanisms are a major contributor to endotoxemia-induced cardiac dysfunction.[363] MCC950, a selective NLRP3 pharmacologic inhibitor, is able to attenuate sepsis-induced cardiac dysfunction in a murine model, which confirms the critical role of inflammation and the NLRP3 inflammasome in this pathological process.[176]

In agreement with the literature, we observed enhanced protein expression of NLRP3 and pro-IL1β, as well as caspase-1 activity in heart tissue from LPS-treated mice. Furthermore, sEH deletion attenuated expression of pro-IL-1β and NLRP3 in heart tissue, and reduced caspase-1 activity. These findings coincide with the current literature demonstrating that lack of sEH activity has the potential to blunt the inflammasome response in various models of cardiac and acute inflammatory injury. Our previous work has demonstrated that hearts which underwent IR injury from sEH null mice or which were perfused with *t*AUCB had attenuated NLRP3 protein expression and reduced caspase-1 activity and mature IL-1β levels.[299] Furthermore lack of sEH activity can attenuate NLRP3 priming and activation in the murine liver, kidneys, and lungs.[293, 294, 364, 365] In septic mice treated with the dual COX-2/sEH inhibitor, PTUPB, levels of NLRP3, IL-1β, and caspase-1

were reduced. Our study extends similar findings to the heart in acute LPS-induced inflammation and suggests that the cardioprotective effects of global and cardiomyocyte-specific sEH deletion may, in part, work by interfering with the cardiac NLRP3 inflammasome response.

4.2.2 Epoxylipid treatment and sEH inhibition ameliorates NLRP3 inflammasome activation in cardiomyocytes

There is evidence for the attenuation of the NLRP3 inflammasome in IR hearts directly treated with epoxylipids and their mimetic compounds.[233, 236] Furthermore, 14,15-EET and 19,20-EDP have protective effects on LPS-stimulated cardiomyocytes.[11, 366] Interestingly, we did not observe any differences in pro-IL-1β or NLRP3 protein expression in neonatal rat primary cardiomyocytes pre-treated with 19,20-EDP, 11,12-EET, or *t*AUCB before the addition of LPS. These data are in contrast to our *in vivo* findings which demonstrated a reduction in the protein expression of pro-IL-1β and NLRP3 in the cytosol from whole hearts in sEH null and sEH$^{(Myo-/-)}$ mice. These findings are also in contrast to other studies which demonstrated that 11,12-EET pre-treatment reduced the level of NLRP3 and pro-IL-1β protein expression in LPS-stimulated adult mouse primary cardiomyocytes.[344]

As previously discussed, the heart contains a heterogeneous population of cells and circulating immune cells can also infiltrate tissues and organs during acute inflammatory injury.[15, 334] Importantly, this may explain our observed discrepancies between the effects on NLRP3 and pro-IL-1β protein expression with LPS *in vivo* and *in vitro*. Pharmacologic sEH inhibition and 5,6-, 8,9-, 11,12-, and 14,15-EETs can impair NLRP3 protein expression in macrophages as well as hepatocytes.[242, 294, 364] Therefore, sEH and epoxylipid effects on the inflammasome may be dependent on cell type. Clodronate liposomal-induced depletion of macrophages was capable of attenuating acute lung injury and NLRP3 inflammasome signalling in the lungs of septic mice, highlighting an important role for macrophages in the tissue-specific NLRP3 activity in response to LPS.[294] Instead, our observation of reduced NLPR3 and pro-IL-1β protein levels from *in vivo* hearts in sEH deficient mice may be due to the attenuation of the inflammasome in recruited and resident cardiac tissue macrophages, fibroblasts, and endothelial cells rather than cardiomyocytes. This also suggests that a large

proportion of the inflammasome response in the heart may be driven by macrophage NLRP3 activity and that the impact of sEH on other cell types of the heart should also be explored.

However, there are also technical considerations to be taken into account for the discrepancies in our findings. For one, the assay we chose to assess this endpoint, immunoblotting, may not have sufficient sensitivity to detect more subtle changes in protein expression. LPS treatment of cardiomyocytes induced robust upregulation in protein expression of NLRP3 and pro-IL-1β. Because the density of the signal was intense in all groups, there is the potential that near saturation of the signal may have been reached, in which a linear relationship between band density and protein abundance may no longer exist.[367] Thus our use of chemiluminescent imaging and densitometry quantification may not be powerful enough to discern slight alterations in protein expression induced by *t*AUCB or epoxylipid treatment.

Furthermore, we chose a 6 hour treatment time point for our cardiomyocytes due to the toxicity of LPS.[11] We wanted to ensure that cell viability was minimally impacted so that at the time of cell harvest, we would have functional cells to analyze changes in protein expression and activity induced by LPS. However, a dynamic relationship exists between gene transcription, protein expression, and further post-translational modification.[368] A 6 hour timepoint may be too short to observe such robust changes in protein expression arising from NF-kB transcription factor activation all the way to functional protein status. The increased protein expression we observed on immunoblot, may be from an increase in the translation of pre-processed mRNA, and not NF-kB transcriptional activity. Instead, assessing mRNA levels of NLRP3 and pro-IL-1β to determine whether *t*AUCB or epoxylipid treatments directly regulate at the level of transcription may allow us to make more definitive conclusions. Therefore, qRT-PCR may be a more appropriate method to use in this instance which can easily be employed to validate our immunoblot findings.

Rather, we demonstrated that epoxylipid treatment and sEH inhibition reduced the activation of the NLRP3 inflammasome in the cardiomyocyte as indicted by lower cellular caspase-1 activity and secreted levels of mature IL-1β. Secreted IL-1β can act in a paracrine manner to sustain NLRP3 priming and activation in surrounding immune cells.[345] So, cardiomyocyte-specific deletion of sEH *in vivo* may work by impairing the release of mature IL-1β from the cardiomyocyte leading to attenuation of the priming and activation of the

NLRP3 inflammasome in other adjacent cell types of the heart contributing to the decline in overall cardiac tissue expression of inflammasome components.

4.2.3 DiHOMEs and the NLRP3 inflammasome

Our previous work has identified the accumulation of 9,10- and 12,13-DiHOME metabolites as a potential intermediate mechanism by which LPS induces myocardial damage and dysfunction.[164] Direct stimulation of cardiomyocytes with 9,10- and 12,13-DiHOME induced mitochondrial fragmentation, impaired respiratory capacity, and triggered release of inflammatory mediators including TNF-α and MCP-1.[164] We demonstrate the inhibition of sEH activity attenuates the activation of the cardiomyocyte NLRP3 inflammasome following LPS stimulation. However, we never directly assessed if this effect on the cardiomyocyte is associated with a decline in DiHOME levels. Furthermore, the effects of DiHOME treatment on the cardiomyocyte NLRP3 inflammasome response has not been directly investigated. In the future it will be important to determine if cardiomyocyte-specific deletion of sEH also has the capacity to influence the lipid mediator metabolite profile within the cardiomyocyte and even throughout the heart and the rest of the body. As well, whether attenuated DiHOME production can account for the effects we have observed on the NLRP3 inflammasome *in vitro* and *in vivo* will provide valuable insight into how modulation of the lipid mediator profile impacts cardiomyocyte-specific NLRP3 inflammasome activity.

4.2.4 Mechanisms of inflammasome activation in cardiomyocytes

Inflammasome activation requires a 'second signal'. This can include K^+ ion efflux, release of mitochondrial DNA, mitochondrial ROS production, and the presence of extracellular ATP.[140-142] We observed activation of the NLRP3 inflammasome with LPS treatment of cardiomyocytes as indicated by activation of caspase-1 activity and the release of mature IL-1β into the surrounding cellular media. However, we did not administer exogenous ATP or the K^+/H^+ ionophore, nigericin, to our cardiomyocyte culture to directly activate the NLRP3 inflammasome after LPS-induced priming. Lipopolysaccharide

promotes intracellular stress through oxidative and mitochondrial damage in a range of cell types and tissues, including the heart.[28, 162, 366, 369-378] LPS also causes the accumulation of detrimental diol metabolites which directly impact mitochondrial function.[164] Furthermore, attenuation of this response is cardioprotective.[162, 373, 375, 376, 379, 380] So, we investigated whether LPS induces the generation of intracellular stress signals which can endogenously promote the activation of the NLRP3 inflammasome. Using MitoSOX red fluorescent dye, we observed a marked time-dependent increase in the generation of mitochondrial ROS with LPS treatment of cardiomyocytes. Our findings demonstrate that 19,20-EDP and *t*AUCB treatment attenuates the early production of mitochondrial ROS. In agreement, the literature also demonstrates that NLRP3 inflammasome activation can be blunted by sEH inhibition or deletion, and epoxylipid treatment.[233, 236, 242, 294, 299, 344, 365] The attenuation of early mitochondrial ROS production may serve to reduce the activation of the NLRP3 inflammasome and thus attenuate the cardiomyocyte-specific inflammatory response.

Dysfunctional mitochondria are a major source of ROS.[381] The NLRP3 inflammasome is sensitive to ROS released from damaged mitochondria.[382, 383] The attenuated production of mitochondrial ROS suggests that *t*AUCB and 19,20-EDP may preserve cardiomyocyte mitochondrial quality to reduce activation of the NLRP3 inflammasome, leading to preserved cardiac function in acute endotoxemia. Epoxylipids can reduce the production of ROS and possess mitochondrial protective properties.[238, 384] These compounds can promote mitochondrial biogenesis and stimulate autophagic processes to remove damaged mitochondria, restore bioenergetic efficiency, and maintain mitochondrial membrane potential.[237, 366, 385, 386] Furthermore, they prevent the loss of anti-oxidant enzyme activity including manganese superoxide dismutase (MnSOD) and thioredoxins (Trx).[233, 387, 388] In fact, preservation of Trx anti-oxidant capacity by 19,20-EDP can attenuate the activation of the NLRP3 inflammasome. However, the exact mechanisms by which these compounds regulate cardiomyocyte mitochondria to attenuate mitochondrial ROS production and subsequent NLRP3 inflammasome activation in LPS-stimulated cardiomyocytes requires further investigation.

4.3 SYSTEMIC EFFECTS: ATTENUATED SYSTEMIC INFLAMMATION AND IMMUNE CELL RECRUITMENT

4.3.1 Evidence for systemic protection in cell-specific sEH gene deletion in vivo models

Deletion of sEH expression limited to the cardiomyocyte not only preserved cardiac function but reduced the systemic inflammatory response to LPS. Use of a cardiomyocyte-specific sEH deletion *in vivo* model has yet to be published in the literature. However, other studies have demonstrated deletion of sEH localized to murine kidney podocytes also provides systemic protection in acute inflammatory injury[389]. The authors demonstrated that a lack of podocyte sEH attenuates kidney injury in response to acute LPS exposure. Importantly, serum concentrations of pro-inflammatory cytokines, IL-1β, IL-6, and TNF-α were also significantly reduced in mice lacking podocyte sEH expression. The ability for podocyte-specific sEH deletion to exert a protective systemic response supports our findings that cardiomyocyte-specific sEH deletion also can have the capacity to attenuate the systemic inflammatory response. Furthermore, these findings highlight the interconnectedness between sEH expression in specific cell types and the far-reaching systemic impact it can have.

4.3.2 Modulation of the cytokine storm

Detrimental effects of endotoxemia and sepsis can be attributed to the maladaptive over-activation of the host immune response. A massive release of inflammatory mediators, also termed the 'cytokine storm', causes wide-spread tissue and organ damage.[35] In addition to their pro-inflammatory effects, these mediators can directly impair heart function.[390] In response to systemic LPS administration, the heart produces pro-inflammatory cytokines that can act in a paracrine and autocrine manner to promote cardiomyocyte apoptosis and cardiac dysfunction.[131, 391-393] Debris from damaged and dying cells can act as DAMPs to further ensue the inflammatory response in a detrimental feed-forward process. We examined the plasma cytokine profile in saline and LPS treated mice at 6 and 24 hours post-injection and

observed a massive increase in interleukins and other cytokines, colony stimulating factors, and chemoattractants in response to LPS.

Epoxylipids as well as disruption of sEH activity have well-established anti-inflammatory mechanisms of action in a range of disease models. Previously, we have demonstrated that global sEH deletion significantly attenuates systemic MCP-1 and TNF-α levels in response to LPS which is correlated with improved cardiac function.[164] Deficiency of sEH activity also interferes with cell signalling pathways responsible for the production of pro-inflammatory cytokines, including transcription factor NF-kB DNA binding.[164] However, the cardiomyocyte-specific role of sEH in the production of systemic inflammatory mediators had yet to be explored. To our surprise, sEH$^{(Myo\ -/-)}$ mice had significantly lower levels of plasma cytokines. This vast reduction in the systemic inflammatory response due to sEH disruption limited only to the cardiomyocyte suggests that cardiomyocytes serve as essential players in the systemic immune response to LPS. Stimulation of TLR4 receptors on cardiomyocytes enhances cytokine release and adhesion molecule expression.[127] So, cardiomyocytes are not only victims of acute inflammation, but also amplifiers of the response. Cardiomyocyte inflammatory mediator release may also augment the secretion of cytokines from other cell types within the local cardiac environment. Cardiomyocyte-specific sEH deletion may be working to interrupt intercellular communication and propagation of the inflammatory response. Therefore, deletion of cardiomyocyte sEH has systemic implications in the reduction of the global inflammatory response, which in turn can preserve cardiac function.

Interestingly, the protection provided by global and cardiomyocyte-specific sEH deletion was time-dependent. There is a kinetic relationship between cytokine production and release and the progression of endotoxemia.[35, 133] Initially, a massive production of pro-inflammatory cytokines occur within the first 24 - 48 hours resulting in overwhelming inflammation.[35, 94] Later, collapse of the immune system can cause severe immunosuppression and development of secondary infections.[94, 346] In our study at 6 hours post-LPS, all LPS-treated groups had an increase in the majority of plasma cytokine levels. The levels of systemic inflammatory mediators in sEH null and sEH$^{(Myo\ -/-)}$ mice were not substantially different from their sEH expressing counterparts at this time point. However, by 24 hours, plasma levels of cytokines were significantly lower in sEH null and sEH$^{(Myo\ -/-)}$

groups suggesting earlier or more rapid resolution of inflammation. This time-dependent fluctuation in plasma cytokines in sEH null and sEH$^{(Myo\ -/-)}$ mice may account for the temporal pattern of cardiac functional decline. An early impairment in cardiac function observed in sEH null and sEH$^{(Myo\ -/-)}$ mice coincides with a rise in systemic cytokine production at the 6 hour time point. Attenuation of the cytokine levels by 24 hours may account for the plateau in cardiac functional decline in sEH null and sEH$^{(Myo\ -/-)}$ mice. Whereas WT and sEH$^{(Myo\ +/+)}$ mice had a slower resolution in their levels of circulating cytokines and thus their cardiac function remained on a trajectory of decline.

4.3.2.1 Interferon-γ

IFN-γ has been identified as a master regulator of endotoxemia and works synergistically alongside LPS.[394] It enhances sensitization to LPS and the production pro-inflammatory cytokines such as TNF-α, which can propagate the inflammatory response.[394-396] MCP-1-mediated inflammatory cell recruitment in the heart is also regulated by IFN-γ.[397] Direct stimulation of cardiomyocytes with IFN-γ causes contractile dysfunction and cardiodepressant effects as well as cardiomyocyte-specific upregulation of pro-inflammatory cytokines.[397-399] Deletion of sEH has been demonstrated to protect neurons and microglia from the inflammatory effects of IFN-γ stimulation, however the effects on the heart have not been well established.[400] Importantly, we observed significant attenuation of circulating levels of IFN-γ in sEH null and sEH$^{(Myo\ -/-)}$ mice which may contribute to their enhanced overall tolerance to LPS and IFN-γ inflammatory effects. It has been demonstrated that constitutive overexpression of IFN-γ in the liver can lead to increased circulating levels of the cytokine.[397] So, if heart is more tolerant to the effects of IFN-γ due to sEH disruption, cardiac-induced IFN-γ production may also be supressed and contribute to overall lower systemic levels of this particular cytokine.

4.3.2.2 Interleukin-1β, interleukin-6, and tumor necrosis factor-α

IL-1β, IL-6, and TNF-α are highly implicated in the progression of endotoxemia and sepsis and are positively correlated with disease severity and mortality.[35, 134] These pro-

inflammatory mediators are directly involved in cardiomyocyte contractile dysfunction.[392, 401, 402] TNF-α also enhances DRP-1-mediated mitochondrial fragmentation and dysfunction in cardiomyocytes.[403] The systemic release of these mediators was significantly attenuated in sEH null and sEH$^{(Myo\ -/-)}$ groups. In agreement with our findings, exogenous administration of 11,12-EET or CYP2C8 overexpression are capable of attenuating the release of TNF-α and IL-6 from macrophages and endothelial cells.[404] Cells of the innate immune system, including macrophages, monocytes and dendritic cells, are the primary producers of these cytokines.[35] However, the attenuation of systemic IL-1β, IL-6, and TNF-α cytokine profiles were robust in sEH$^{(Myo\ -/-)}$ mice. This suggests that cardiomyocytes-specific deletion of sEH may not only work in a localized manner to protect the cardiomyocyte and local cardiac environment but may have the capacity to interfere with cytokine production and release by other cell types including immune cells.

4.3.2.3 Interleukin-13

IL-13 is typically associated with the allergic inflammatory response.[405] Interestingly, this cytokine was markedly increased with LPS treatment but attenuated in sEH null and sEH$^{(Myo\ -/-)}$ mice. Few studies have investigated the role of this cytokine in endotoxemia and sepsis. However, our findings suggest that this cytokine may play an important role and could possibly be regulated by cardiomyocyte-specific sEH activity. It has been demonstrated that exogenous IL-13 treatment can preserve mitochondrial function and limit damage in cardiomyocytes exposed to LPS.[405, 406] So, elevated levels of IL-13 observed in WT and sEH$^{(Myo\ +/+)}$ plasma may serve as a compensatory mechanisms in response to mitochondrial damage and ROS production in response to LPS injury.

4.3.2.4 Interleukin-10

IL-10 is an anti-inflammatory cytokine, which suppresses monocyte and macrophage function.[407] Levels of IL-10 are proportional to the degree of inflammation and are typically elevated in more critically ill septic patients.[35, 407] Despite the anti-inflammatory nature of this cytokine, its effects are often insufficient to counteract the increase in pro-inflammatory

mediators.[407] Additionally, IL-10 can promote worsening of the physiological state via sepsis-induced immunosuppression.[94] At 24 hours post-LPS, plasma levels of IL-10 were elevated in WT and sEH$^{(Myo\ +/+)}$ groups, proportional to the robust inflammatory response. Interestingly, IL-10 levels were also elevated in the sEH$^{(Myo\ -/-)}$ group but not sEH null mice. This discrepancy may suggest that cardiomyocyte-specific sEH activity may not be as important in the modulation of anti-inflammatory cytokines. Instead, the systemic protection conferred from cardiomyocyte-specific sEH deletion may be mainly attributed to the attenuation of pro-inflammatory cytokines. There is conflicting evidence in the literature as to whether sEH inhibition or deletion promotes or impairs IL-10 production in various models of disease.[388, 408-410] However, the data from our model suggests that IL-10 levels may be decreased in sEH null mice due to the overall attenuated inflammatory response. Additionally, IL-10 may be modulated by sEH activity in other cell types, such as monocytes and macrophages, which may explain why global sEH deletion but not cardiomyocyte-specific deletion had the capacity to reduce the systemic levels of this cytokine

4.3.2.5 Macrophage colony stimulating factor

Acute endotoxemia can stimulate the release of cytokines which function as hematopoietic growth factors including M-CSF, G-CSF and GM-CSF.[134] We observed increases in circulating plasma levels of these 3 growth factors with LPS-induced inflammation. Importantly, global and cardiomyocyte-specific sEH deletion significantly attenuated M-CSF levels in the plasma. M-CSF stimulates the differentiation and proliferation of hemopoietic progenitors into mature myeloid cells and can promote mobilization of myeloid cells into the circulation and differentiation of macrophages.[411] LPS stimulation of heart tissue causes an increase in the release of colony stimulating factors, highlighting the possibility of growth factor synthesis by the heart.[412] Interestingly, a clinical study showed that non-survivors of sepsis had undetectable levels of stimulating factors in their plasma, while survivors had a steady increase in levels over a 4-day period.[134] The gradual increase in stimulating factors may function to circumvent the late-stage immunosuppression, which typically follows the initial inflammatory phase of sepsis. Our sEH expressing mice experienced an immense systemic inflammatory burden. So, the

increase in colony stimulating factor levels may be compensatory for the later immunosuppression stage due to apoptosis and dysfunction of overwhelmed inflammatory cells to follow. However, the systemic inflammatory response was robustly attenuated in sEH deficient groups, so the proliferation and mobilization of myeloid cells by M-CSF may be unnecessary, which may explain the lower levels of this cytokine. Additionally, inhibition of sEH attenuates hematopoietic progenitor cell proliferation.[319] Interestingly, exogenous 12,13-DiHOME and 11,12-DHET treatment can rescue progenitor proliferation in sEH null mice. This suggests that attenuated growth factor levels in sEH deficient mice may partly be due to the reduced generation of diol metabolites.[319]

4.3.2.6 Monocyte chemoattractant protein-1

Previously, we have demonstrated that global sEH knockout reduces levels of circulating MCP-1 in mice following LPS injection.[164] Now, our findings extend to include a robust attenuation of circulating MCP-1 with sEH deletion limited to the cardiomyocyte. MCP-1, also known as the chemokine CCL2, is a chemoattractant molecule for monocytes and macrophages.[413] In septic patients, serum levels of MCP-1 are associated with poor prognosis and survival outcome.[134] In response to acute LPS inflammation, organs, including the heart, can release MCP-1 to attract circulating immune cells to the site of damage.[414] Previously demonstrated with LPS injury, local DHA-derived cardiac epoxylipids were reduced while MCP-1 levels were elevated.[358] This inverse correlation may explain why sEH inhibition in the heart is protective in the context of MCP-1 signalling. Inhibition of sEH impairs monocyte chemotaxis toward MCP-1which can be restored by the treatment with the diol metabolites, 5,6-, 8,9-, 11,12-, and 14,15-DHETs.[415] Because we observed a robust reduction in systemic MCP-1, this may suggest that the sEH disruption can impair MCP-1 release from the heart and that reduced production of circulating DHETs can interfere with migration of monocytes, thus affecting monocyte chemotaxis by disrupting both the stimulus and the response. However, reduced cardiomyocyte inflammatory signalling and damage may also attenuate MCP-1 release from other cell types including endothelial cells and tissue macrophages, thus reducing the overall MCP-1 burden on the host. Additionally, cardiomyocyte-specific sEH deletion may prevent inflammatory injury

to the cardiomyocyte, leading to diminished release of DAMPs, reducing the stimulation of adjacent cardiomyocytes and tissue resident immune cells to secrete MCP-1 and other inflammatory mediators.[416] Diminished MCP-1 may also attenuate the stimulation and infiltration of immune cells which otherwise would in turn cause further damage to cardiomyocytes, propagate local tissue inflammation, and promote cardiac dysfunction.[417]

4.3.2.7 Vascular endothelial growth factor

VEGF enhances vascular permeability in sepsis and correlates with severity of disease. [351, 352] This is a marker of endothelial dysfunction and contributes to intravascular fluid leak and organ hypoperfusion.[351, 418] Blockade of VEGF signalling reduces expression of intercellular adhesion molecule-1 (ICAM-1), inflammatory cell infiltration into the lungs, and cytokine production in sepsis.[419, 420] The limited increase in plasma VEGF in sEH null and sEH$^{(Myo\ -/-)}$ groups post-LPS exposure may contribute to preserved endothelial integrity, reducing inflammatory cell extravasation into the tissue including the myocardium. EET regioisomers have established pro-angiogenic properties.[229, 421] This has been established in the context of cancer where 11,12- and 14,15-EET can promote vascularization and hence tumor growth.[422] Angiogenic properties of endothelial-derived 11,12- and 14-15-EETs also have implications in wound healing and tissue repair through the enhanced expression of VEGF and establishment of collateral blood supply in ischemic tissue.[423-425] Additionally, inhibition of the sEH phosphatase domain activity increases VEGF-mediated angiogenesis.[426] In contrast to our findings, studies have shown sEH inhibition and preservation of endogenous EET levels enhances VEGF and angiogenesis in ischemic injury of the brain and heart.[427] Conversely, some preliminary evidence suggests that, 19,20-EDP and its N-3 PUFA precursor, DHA, could negatively regulate VEGF and angiogenesis.[428, 429] Additionally, in a model of endotoxemia, 11,12-EET has been shown to preserve endothelial barrier integrity and reduce hyperpermeability, which may explain the lower levels of VEGF we observed.[430] Since we observed an attenuation in VEGF with sEH inhibition, the effect on VEGF may be due to alteration in a range of lipid mediator metabolites and not just EETs. Therefore, sEH inhibition and reduced circulating cytokines may be working to primarily mitigate endothelial dysfunction, resulting in lower VEGF levels.[431]

4.3.3 Cardiomyocytes as a direct source chemoattractant factors

Due to the robust attenuation of systemic cytokine levels in mice with cardiomyocyte-specific sEH deletion, it is likely that inhibition of cardiomyocyte sEH activity may be working to reduce the stimulation of other cell types as well. One way this could occur is by reduced secretion of DAMPs and chemoattractants, preventing activation of adjacent cells, and disrupting the overall inflammatory cascade. MCP-1 production in cardiovascular disease has been mainly attributed to macrophages and endothelial cells.[136] However, limited studies have also shown that cardiomyocytes can be a direct and potent source of chemoattractant factors.[413] This could influence the recruitment of immune cells to the myocardium which can contribute to cardiac dysfunction and local inflammation. Stimulation of cardiomyocytes *in vitro* with LPS caused a robust release of TNF-α and MCP-1 into the surrounding cellular media. This suggests that cardiomyocytes are also active participants in the innate immune response to LPS challenge through the secretion of attractant mediators. Release of these mediators from cardiomyocytes may also work locally, inducing damage to surrounding cells. Evidence suggests that stimulation of cardiomyocytes with LPS can promote the production and release of TNF-α which can act in a paracrine fashion to promote cardiomyocyte apoptosis and cardiac dysfunction.[131, 393] Furthermore, TNF-α causes DRP-1 mediated fragmentation of cardiomyocyte mitochondria in sepsis.[403] As previously mentioned, mitochondrial damage and ROS production can trigger the NLRP3 inflammasome, which we have shown to be a critical signalling pathway in the myocardial response to LPS.[432] Additionally, cardiomyocyte release of TNF-α and MCP-1 can also function as systemic signals for the recruitment of circulating inflammatory cells into the cardiac tissue.[413, 417] This highlights the wide-spread effects that cardiomyocyte inflammatory signalling can have on the entire body. Pre-treatment of cardiomyocytes with 19,20-EDP, 11,12-EET, and *t*AUCB significantly attenuated the release of MCP-1 and TNF-α in response to LPS stimulation. These *in vitro* findings suggest a possible mechanism by which cardiomyocyte-specific sEH deletion may be protective *in vivo*. Importantly, we have confirmed that the cardiomyocyte is a direct source of MCP-1 and TNF-α in response to LPS stimulation. In addition to attenuating the systemic levels of these mediators, impaired cardiomyocyte production indicates a directly protective role at the local level of the heart.

4.3.4 Attenuated macrophage infiltration limits local immune response and cardiac damage

Neutralization of MCP-1 reduces the accumulation of inflammatory cells into the myocardium in endotoexemia.[417] Since LPS-induced cardiomyocyte release of chemoattractant factors was directly attenuated by epoxylipids and sEH inhibition, we investigated whether this correlated with reduced inflammatory cell recruitment to the myocardium *in vivo*. We assessed this by immunohistochemical staining of $CD68^+$ cells in the myocardium. CD68 is a cell surface glycoprotein found on macrophages and monocytes and is a useful cytochemical marker of inflamed tissue.[433, 434] Activation of recruited inflammatory leukocytes causes mitochondrial dysfunction and functional impairment of surrounding cardiomyocytes and exacerbation of cardiac injury in the LPS stimulated heart.[416, 435] Therefore, sEH-deficient cardiomyocytes likely release fewer chemoattractant factors which impairs the mobilization of monocytes via reduced circulating M-CSF levels. Infiltrating immune cells are a direct source of cytokine production and contribute to tissue damage. These actions can work synergistically to recruit fewer inflammatory cells to the heart so that overall cardiomyocyte and cardiac impairment can be attenuated.

LPS stimulates ICAM-1 and vascular cell adhesion molecule-1 (VCAM-1) expression on cardiac fibroblasts, promoting mononuclear cell adhesion.[436, 437] TNF-α, IFN-γ, and IL-1 cytokines can induce endothelial cell activation and the expression of adhesion molecules as well.[438-440] Myocardial expression of adhesion molecules such as VCAM-1 is associated with higher immune cell infiltration and worsen cardiac outcomes.[36, 441] Currently, it is accepted that adult cardiomyocytes are not a major source of ICAM-1 and VCAM-1 expression in the heart.[436, 442] However, whether cardiomyocytes can influence the expression of adhesion molecules on cardiac fibroblasts and endothelial cells which contributes to reduced myocardial inflammatory cell infiltration we observed in sEH null and $sEH^{(Myo\ -/-)}$ hearts is still elusive.

sEH expression is correlated with tissue infiltration of macrophages in various disease states including renal injury and atherogenesis.[277, 443, 444] Inhibition of sEH or 11,12-EET treatment can inhibit pro-inflammatory polarization of tissue macrophages.[277, 290, 409, 445] In acute endotoxemia, adenovirus mediated over-expression of CYP2J2 increased levels of 11,12- and 14,15-EETs which attenuated macrophage cardiac infiltration, NF-kB signalling,

release of pro-inflammatory mediators, and preserved cardiac function.[108] There is conflicting evidence whether genetic disruption of sEH can also modulate the expression of selectins and adhesion molecules to impair immune cell infiltration to tissues.[279, 444, 446, 447] Whether the attenuated inflammatory response in sEH deficient cardiomyocytes also modulates their immune microenvironment via the expression of adhesion molecules on other cell types as a mechanism of reduced macrophage recruitment to the heart still remains to be investigated.

4.3.5 Evidence for cardiomyocyte-induced immune cell recruitment is indirect

We demonstrated that LPS stimulation of cardiomyocytes directly enhances the release of TNF-α and MCP-1. These mediators can function as chemoattractant factors. Epoxylipids and *t*AUCB treatment attenuate this release *in vitro* which is correlated with less infiltration of $CD68^+$ cells into the myocardium of mice with sEH gene deletion. These results are promising and suggest that the cardiomyocytes may be important in the recruitment of systemic immune cells to the heart, where direct cardiac damage can be further propagated. However, it is important to acknowledge that a division exists between our *in vitro* and *in vivo* findings. Whether the reduced infiltration of $CD68^+$ cells into the myocardium is truly due to the attenuated MCP-1 and TNF-α secretion from cardiomyocytes in $sEH^{(Myo\ -/-)}$ mice cannot be firmly concluded. To strengthen our conclusions, it will be important to evaluate whether epoxylipids or pharmacological sEH inhibition in cardiomyocytes can directly interfere with the migration and infiltration of immune cells into the local microenvironment. One way this could be directly assessed is through the use of a chemotaxis assay. The effects of sEH-derived metabolites on MCP-1 induced monocyte migration have been demonstrated using this method.[415] Migration of monocytes either co-cultured with LPS-treated cardiomyocytes or conditioned with the extracellular media from cardiomyocytes could be assessed. Should migration of monocytes be impaired by cardiomyocyte sEH inhibition, this can serve as a mechanistic explanation to confirm our histological findings *in vivo* that chemotaxis and recruitment of leukocytes to the heart is directly impaired by the effects of cardiomyocyte-specific sEH activity inhibition. Antibody targeted antagonism of the MCP-1 receptor, CCR2, in the migration assay could also be used

to assess whether MCP-1 released from cardiomyocytes is functioning through a ligand-receptor interaction on proximal monocytes.

4.3.6 Assessment of neutrophil and T cell myocardial infiltration

We chose to assess the presence of macrophages in the myocardium as a marker of local inflammatory response and immune cell recruitment. During endotoxemia, it has been demonstrated that circulating monocytes infiltrate the myocardium and can contribute to cardiac dysfunction.[448-450] However, other immune cells including neutrophils, natural killer (NK) cells, and T cells are involved in LPS-induced organ dysfunction.[37, 451] Importantly, the results from the plasma cytokine profile suggest the chemoattraction and potentially the cardiac infiltration of other immune cell subtypes may also be altered, which could contribute to the cardioprotection caused by cardiomyocyte-specific sEH deletion.

KC is a chemoattractant factor for neutrophils. Some studies have shown that the diol metabolites of 14,15-EET, 14,15-DHET, attenuates neutrophil chemotaxis by downregulating the receptor, CXCR1, for KC.[333] Interestingly, with cardiomyocyte-specific sEH deletion, we observed reduced plasma levels of KC, which indicates impaired neutrophil migratory capacity. These data suggest that other metabolites beside DHETs may influence KC levels and neutrophil chemoattraction. Indeed, other findings show a dose-dependent decrease in KC with sEH inhibitor treatment.[285] Macrophage inflammatory protein, including MIP-1α, MIP-1β, and MIP-2 are also responsible for NK cell and neutrophil activation and chemotaxis.[137] sEH activity disruption significantly reduces MIP-2 levels from LPS stimulated microglia and neutrophil infiltration following traumatic brain injury.[400] Mice lacking sEH activity had reduced MIP-2 levels and tissue neutrophil infiltration in hyperoxia-induced acute lung injury.[452] Since plasma levels of these cytokines were significantly attenuated in LPS-treated sEH null and $sEH^{(Myo\ -/-)}$ groups, the myocardial accumulation of neutrophils would be important to assess as it may represent another protective mechanism of sEH activity inhibition in acute LPS injury. Innate immune cells can secrete cytokines and present antigens to engage the adaptive immune response during endotoxemia.[451] Hence, T cells are critical participants in the systemic inflammatory response during sepsis. Furthermore, the cytokine RANTES is chemotactic for leukocytes

and T cells. Systemic levels of RANTES were significantly lower in sEH null and sEH$^{(Myo\ -/-)}$ groups following LPS exposure. Thus, the assessment of myocardial infiltration of various T cell subtypes may provide valuable information about cardiomyocyte sEH activity on the adaptive immune response.

4.3.7 Preservation of cardiac function correlates with improved systemic tolerance to LPS

Increased plasma LDH activity is a non-specific marker for cellular injury and death.[453] In sepsis, hyperlactatemia is also an indication of poor tissue perfusion and inability to eliminate by-products of glycolysis.[350] At 6 hours post-LPS exposure, all groups experienced an increase in plasma LDH activity. These levels continued to increase through to the 24 hour time point where they were significantly elevated in WT and sEH$^{(Myo\ +/+)}$ groups. The fact that sEH null and sEH$^{(Myo\ -/-)}$ groups still experienced an increase in plasma LDH activity with LPS treatment, albeit levels plateaued after 6 hours post-LPS, highlights two important conclusions. First, global or cardiomyocyte-specific sEH deletion does not provide all-encompassing tolerance to the damaging systemic effects of LPS. Since plasma LDH activity is a non-specific marker of cell damage, it is highly unlikely that disruption in sEH activity would be sufficient to attenuate all mechanisms contributing to LPS-induced cellular stress. Thus, elevated LDH activity observed in all LPS-treated groups is logical and expected. Second, even though sEH null and sEH$^{(Myo-/-)}$ endured a degree of cell damage and stress in response to LPS, these groups had attenuated decline in physiological function. They had better tolerance to LPS. Mice with sEH deletion were more mobile and active and they had less of a decline in body surface temperature and body condition score. These observations are reflected in the scoring and quantitation of physiological impairment.

Overall, sEH$^{(Myo\ -/-)}$ mice were less impacted by the physiological effects of acute LPS than their sEH$^{(Myo\ +/+)}$ counterparts. Cardiomyocyte-specific deletion of sEH reduces immune cell recruitment to the heart through the attenuated release of cardiomyocyte-derived chemoattractant mediators. Attenuated immune cell recruitment and release of cytokines preserves the integrity of the cardiac microenvironment and also dampens the systemic inflammatory cascade. Activation of cellular inflammatory pathways, such as the NRLP3 inflammasome, is reduced. Decline in cardiac function is slowed and the organism becomes

more physiologically tolerant to LPS-induced acute inflammatory injury. This strongly attests to the importance of preservation of cardiac function to the overall state of the organism. The heart is critical for the ongoing supply of oxygen and nutrients to the rest of the body. The proper circulation of blood also prevents the accumulation of waste and metabolic by-products and maintains blood pressure. Therefore, preserved heart function contributes to the preservation of the overall physiological state organism. Overall, these findings demonstrate the multi-level interconnectedness of the organism from cells to organs to the whole body system *in vivo*.

4.4 CONCLUSION

In conclusion, cardiomyocyte-specific sEH deletion exerts profound protection on the heart but also demonstrates systemic effects. Cardiomyocytes act to condition the local cellular and cytokine microenvironment, reducing local cell damage, systemic release of cytokines and recruitment of leukocytes. Altogether, this culminates in attenuated over-exaggeration of the innate immune response and preserved cardiac function in acute LPS inflammatory injury (Figure 4.1). Through multi-level protection originating at the source of the cardiomyocyte, overall physiological tolerance to LPS is increased. Importantly, this study sheds light on the dynamic interactions between different cell types in orchestrating the innate immune response. Further efforts in combating septic-induced cardiac dysfunction should not only focus on cells of the innate immune system, but also cardiomyocytes and their communication with other cell types in the local myocardium and systemic circulation.

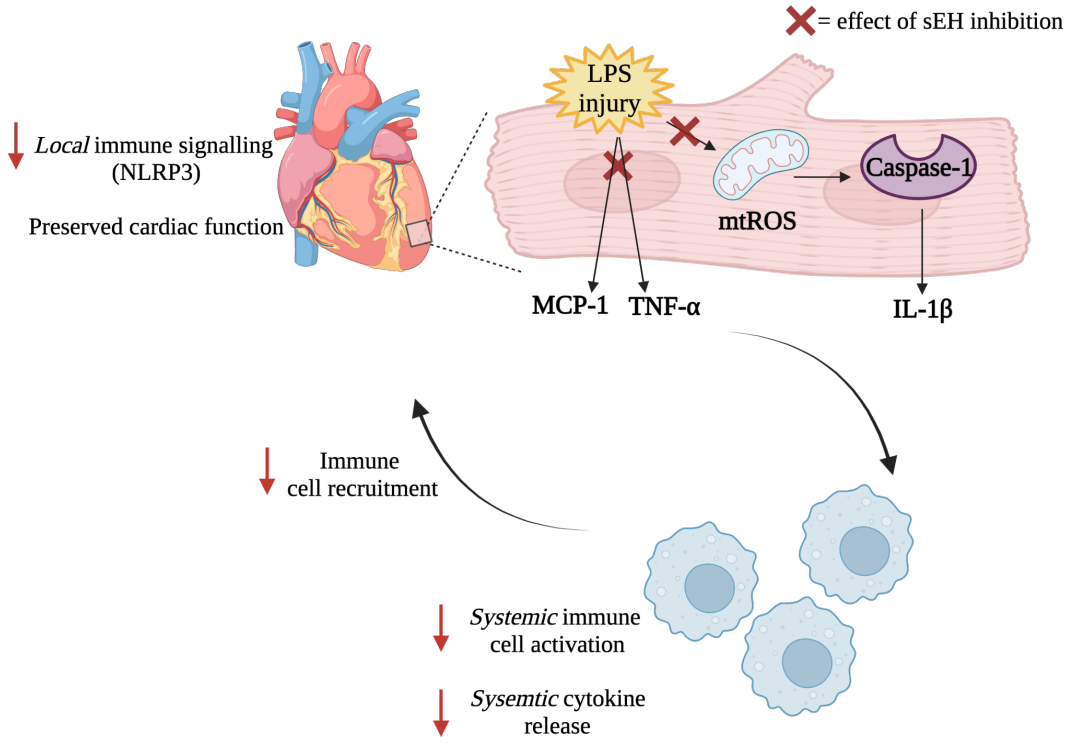

Figure 4.1. Graphical abstract. Cardiomyocyte-specific sEH deletion attenuates activation of cardiomyocyte NLRP3 inflammasome signalling and release of MPC-1 and TNF-α. Fewer systemic immune cells are activated and recruited to the myocardium. Local immune response in the heart is reduced, contributing to less cardiac damage and preserving cardiac function. With preserved cardiac function and reduced systemic inflammation, the host is more physiologically tolerant to the effects of acute LPS injury.

CHAPTER 5

LIMITATIONS

5.1 The use of LPS as a model for experimental endotoxemia: clinically relevant or just convenient?

The use of a single LPS injection to induce an acute systemic inflammatory response in mice is one of the most common ways to model endotoxemia in the literature.[65] But like most models, there are pros and cons. As with most experimental models, LPS represents a more simplistic way to represent sepsis seen in humans and to control for extraneous and potentially confounding parameters in the experimental setting.

In the clinical setting human sepsis is complex. As previously discussed, humans experience a biphasic pattern in the presentation of sepsis.[16] Initially, a hyperdynamic and pro-inflammatory state predominates. There is a massive release of pro-inflammatory cytokines and patients experience fever, enhanced cardiac output and other organ dysfunction.[16] Afterward, hemodynamic depression occurs with reduced cardiac output and a drop in body temperature. Antigen presenting cells begin to dysfunction and T cells become apoptotic, predisposing the patient to an immunosuppressed state and the potential for nosocomial infections to take hold.[16] However, there is potential for these phases to overlap to some degree, increasing the complexity of the disease state.[16] Ideally, animals models of sepsis should follow a similar pattern.

With direct LPS injection, the animal receives a single bolus dose of pure endotoxin.[454] The organism is not exposed to any live pathogenic bacteria, hence a state of bacteremia is not achieved. Use of LPS allows for a controlled and uniform dose of endotoxin to be given to each experimental animal. However, since no live bacteria are injected, the animal may not respond in the same way as in an active infection.[65] Live bacteria can replicate and other surface antigens other than endotoxin can act as alarmin molecules for the innate immune response.[455] Other models of sepsis include CLP as well as infusion of live bacteria into animals.[339] These models produce an active and ongoing state of infection for the body to respond to.[454] Additionally, polymicrobial sepsis can be achieved with CLP which may be more clinically relevant in human sepsis cases caused by gut barrier dysfunction and rupture.[339] However, to induce CLP in experimental animals, the abdominal cavity must be surgically opened so there is the potential for confounding inflammation and stress from the surgery.[454, 456]

Humans are very sensitive to endotoxin and nanogram concentrations can elicit a systemic response and changes in cardiac function.[65, 340] On the other hand, mice and other rodents are typically more tolerant to LPS.[340] Conveniently, the LPS dose can be adjusted in mice to model different severities of endotoxemia.[16] A dose of 0.5-1 mg/kg in mice causes a mild inflammatory response.[454] Doses of 10 mg/kg are typically used to initiate a robust systemic inflammatory response and 20 mg/kg is commonly used for survival studies, where time to mortality is the measured endpoint.[65, 457] Therefore, LPS allows researchers to control the level of inflammation they would like to generate with respect to the specific aims of their study.[455, 456]

Furthermore, there are also differences in the timing of the septic response between mice and humans. Mice injected with LPS tend to have an earlier and more robust increase in systemic inflammatory cytokines compared to human sepsis.[16, 339, 454] The pro-inflammatory state also tends to resolve faster in mice than humans.[339] We observed an initial increase in the plasma cytokines in all experimental groups at the 6 hour time point. In humans, it is possible that we might observe a later peak in the release of systemic pro-inflammatory cytokines which may be less robust but rather prolonged instead. Furthermore, sEH activity disruption appeared to affect the temporal resolution of the initial inflammatory response. The inflammatory and functional state of sEH null and $sEH^{(Myo\ -/-)}$ mice stabilized between the 6 and 24 hour time point, while WT and $sEH^{(Myo\ +/+)}$ continued to deteriorate beyond their 6 hour time point state. Therefore, the temporal effects of sEH activity inhibition in human sepsis may differ as well. These differences in timing of inflammation may be reflected in differences in temporal changes of cardiac function between mice and humans.

LPS treatment of human induced pluripotent stem cell (hiPSC)-derived cardiomyocytes has also been recently employed *in vitro* for cellular mechanistic studies of endotoxemia and sepsis.[393] The use of iPSCs allows more applicability to human disease compared to immortalized cardiac cell lines or primary cardiomyocytes isolated from mice or rats. However, the differentiation and maintenance of iPSCs can be quite expensive and tedious and requires extensive optimization before they can be used experimentally.[458]

Overall, for preliminary and standardized experimental work, LPS is a valuable endotoxemia model for deciphering a mechanistic understanding of the disease state and

experimental pharmacologic interventions.[339] Importantly, experimental therapeutic interventions tested in a model of LPS could also be further validated using CLP and bacterial infusion to further substantiate the applicability of the intervention.

5.2 Optimization of tAUCB pharmacokinetics for an acute inflammation model

Extensive pharmacokinetic profiling has been conducted on various pharmacological sEH inhibitors.[285, 296, 297] Our lab has optimized the administration and dosage of *t*AUCB in a chronic MI injury model.[298] A 4 day-pre-treatment of 10 mg/L *t*AUCB *ad libitum* in drinking water prior to MI and which is continued for 28-days thereafter is cardioprotective.[300] In contrast, the *t*AUCB administration protocol we employed for this study yielded modest results. Echocardiographic and functional data suggest trends toward cardioprotection, however, no significant protection could be concluded with our *t*AUCB treatment groups. Importantly, our model is one of acute and robust systemic inflammation, fundamentally different from chronic MI. We observe a rapid physical decline and reduction in mobilization of mice within the first few hours of LPS administration.[349] By the 6 hour LPS time point, mice on average lost 5% of their body weight. By 24 hours, upwards of 10% of the baseline body weight was lost. The rapid decline in body weight over this short period of time is likely not only due to reduced food intake, but also loss of water.[459, 460] We also observed an increase in skin turgor with LPS-treated mice, indicative of dehydration.[459, 460]

The elimination half-life for *t*AUCB is 8-10 hours.[296] Complete washout is achieved after 3 days following attainment of steady-state oral administration.[296] Given that it takes 3 to 5 half-lives for a drug to be eliminated and cease its pharmacological effects on the body, this may partially explain why the protective effects of *t*AUCB treatment are diminished in our model if the mice stop drinking soon after LPS injection. Thus, the dose as well as the length and time of pre-treatment administration may need to be adjusted. Furthermore, oral drug absorption can be dramatically reduced in the setting of acute pain and stress.[461] Endotoxemia-induced systemic hypotension may also reduce perfusion of the mesenteric vascular system, which could impair drug absorption into the systemic circulation.[462] Therefore whether the mice are efficiently absorbing *t*AUCB after acute LPS injection should be determined. LCMS/MS analysis of plasma levels of *t*AUCB and epoxylipid to

diol metabolite ratios could be monitored at various time points following LPS administration. A concentration-time dependent relationship could be constructed for different *t*AUCB administration protocols, which can be correlated to cardiac function post-LPS to determine a pharmacokinetic-pharmacodynamic relationship. Although *t*AUCB was designed for enhanced bioavailability in oral administration, it has also been administered by the i.v. and s.c. route.[296] Other routes of administration could be explored if oral *t*AUCB absorption is not sufficient following acute LPS stress. Lastly, sample size for each treatment group should be increased to ensure the study is adequately powered. Then, with all data considered together an optimized *t*AUCB administration protocol could be constructed for use in acute inflammatory injury models.

CHAPTER 6

FUTURE DIRECTIONS AND PILOT DATA

6.1 THE EFFECTS OF BIOLOGICAL SEX AND AGING ON RESPONSE TO ACUTE LPS INFLAMMATORY INJURY

6.1.1 Young female mice may experience less cardiac functional decline compared to males

A cohort of young female WT and sEH null mice were injected with LPS and cardiac function was assessed by 2D echocardiography after 24 hours. Compared to baseline, there was a significant decline in cardiac output and stroke volume (Table 6.1.1). However, this may, in part, be attributed to a decline in heart rate at 24 hours post-LPS. There were no other significant differences between baseline and LPS cardiac measurements in WT and sEH null female mice. This is in contrast to their male counterparts. WT males had significantly worse ejection fraction and fractional shortening with LPS treatment. Furthermore, male WT mice experienced diastolic dysfunction indicated by significantly higher IVRT and E/E' ratios as well as alterations in LV posterior wall and internal diameter measurements. There were significant differences in ejection fraction, fractional shortening, LV internal diameter, IVRT and E/E' ratio between young WT and sEH null males with LPS treatment. Interestingly, in young female mice, there were no significant differences between WT and sEH null mice after LPS treatment. This may be due to the small sample size we have at this time. However, these preliminary data suggest that young female mice may have less decline in cardiac function compared to males, regardless of whether sEH activity is disrupted.

Female $sEH^{(Myo\ +/+)}$ and $sEH^{(Myo\ -/-)}$ also underwent exposure to LPS for 24 hours. Physiological assessment indicated that $sEH^{(Myo\ +/+)}$ and $sEH^{(Myo\ -/-)}$ groups experienced a degree of physiological impairment significant to their baseline (Figure 6.1.1). However, there was no significant difference in impairment between female $sEH^{(Myo\ +/+)}$ and $sEH^{(Myo\ -/-)}$ groups post-LPS. This is in contrast to young male $sEH^{(Myo\ +/+)}$ mice which had more physiological impairment than their $sEH^{(Myo\ -/-)}$ counterparts with LPS. Echocardiographic data also exhibited a similar trend (Table 6.1.2). Both $sEH^{(Myo\ +/+)}$ and $sEH^{(Myo\ -/-)}$ males experienced cardiac functional decline in ejection fraction, fractional shortening, LV posterior wall width and internal diameter, as well as stroke volume and cardiac output compared to their baseline measurements. Male $sEH^{(Myo\ +/+)}$ had significantly worse ejection

fraction and fractional shortening compared to LPS-treated sEH$^{(Myo\ -/-)}$ mice. In contrast, there were no significant differences in heart function between female sEH$^{(Myo\ +/+)}$ and sEH$^{(Myo\ -/-)}$ mice post-LPS. Surprisingly, sEH$^{(Myo\ +/+)}$ female ejection fraction was an average of 55%, compared to 26% in males post-LPS. sEH$^{(Myo\ -/-)}$ female mice had a slight decline in stroke volume and LV end diastolic volume post-LPS compared to baseline. Interestingly, no cardiac functional measurements were significantly different between baseline and post-LPS in sEH$^{(Myo\ +/+)}$ female mice. The sample size for our male cohort is significantly larger than our females at this time. So, a small sample size may account for the lack of significant differences detected in our female cohort. However, these preliminary findings suggest that sex-specific differences may underly the cardiac functional response to LPS in young male and female mice.

6.1.2 Middle-aged female mice may experience less physiological and cardiac functional decline compared to males

The effect of LPS treatment in middle-aged (15-19 months) male and female WT and sEH null mice was also assessed in preliminary experiments. Both WT and sEH null males and females experienced physiological decline in response to LPS (Figure 6.1.2). At baseline, the physiological impairment in middle-aged WT and sEH null female mice was, on average, lower than their male counterparts. Following LPS treatment, middle-aged females also had less physiological impairment compared to males. WT and sEH null middle-aged males had more impairment compared to their young male counterparts both at baseline and after 24 hours of LPS exposure. After LPS exposure, sEH null young males had an average impairment score of 0.174, which was significantly lower compared WT mice. However, middle-aged sEH null mice had a score of 0.358, which was nearly equal to middle-aged WT mice. Importantly, this may suggest that the protection conferred from sEH deletion may be age-dependent and some of those protective effects may be lost with aging.

Middle-aged WT and sEH null males also experienced a similar degree of cardiac functional decline with LPS (Table 6.1.3). Ejection fraction and fractional shortening were reduced compared to baseline. IVRT and Tei index were also significantly increased.

Cardiac functional measurements in middle-aged sEH null males were not preserved compared to WT. In middle-aged females, ejection fraction, fractional shortening, and cardiac output were significantly less in sEH null groups after LPS compared to baseline. The Tei index was also increased in the sEH null group. Strikingly, middle-aged WT female mice only had a significant decline aortic ejection time with LPS treatment compared to baseline. There were no other significant differences between baseline and LPS cardiac measurements in middle-aged WT females.

Early findings demonstrating that WT middle-aged female mice exhibit preserved cardiac function post-LPS are surprising. Our preliminary data will need to be further validated. The disparity in baseline physiological function may partially explain why middle-aged females had less physiological and cardiac decline following LPS challenge compared to middle-aged males. As well, this suggests that there may be sex differences in the normal biological aging process. However, the sample size for our middle-aged cohort is still limited. As there is individual variation with aging, it will be important that sample size is increased before any firm conclusions can be drawn.

6.1.3 Systemic anti-inflammatory effects of global sEH deletion are reduced with aging in male mice

Initial analyses of plasma samples collected from WT and sEH null middle-aged male mice was also conducted. As previously mentioned, an increase in plasma LDH activity is a non-specific marker for cellular damage and death.[453] In middle-aged male mice, both WT and sEH null groups demonstrated an increase in plasma LDH activity after 24 hours of LPS exposure (Figure 6.1.3). Interesting, baseline LDH activity was more than 3 times higher in middle-aged sEH null mice than their young counterparts. The higher levels of LDH activity in untreated mice suggests that the biological aging process may be associated with non-specific forms of cellular stress and damage. This may partially explain our observation of a larger degree of baseline physiological impairment in middle-aged compared to young male mice. After LPS exposure, LDH activity was also 1.5 to 2 times greater in middle-aged mice in comparison to young mice. Importantly, middle-aged sEH null mice had similar LDH activity to the WT group, whereas LDH activity was lower in young sEH null mice

when compared to their WT counterparts. These data further support that some of the protective benefit attributed to sEH deletion in young mice may be lost with aging.

Measurement of plasma cytokine and stimulating factor levels also exhibited a similar pattern (Figure 1.6.4), (Figure 1.6.5), and (Figure 1.6.6). WT middle-aged mice had 10 fold higher levels of IL-1β, and TNF-α levels were more than double than their young counterparts post-LPS. Astoundingly, middle-aged sEH null mice had a 200 and 14 fold increase in these mediators compared to young mice, respectively. Hence, hyperinflammation in response to LPS is potentiated with increased age and global sEH deletion may not have the capacity to attenuate cytokine production to the same degree that it does in young mice. However, the plasma levels of IL-13 and IFN-γ were significantly higher in middle-aged WT mice compared to sEH null. Furthermore, other cytokines including MIP-1α, MIP-1β, RANTES, LIF, TNF-α, eotaxin, and MCP-1 levels were significantly higher compared to baseline levels in WT mice, but did not reach statistical significance in the sEH null cohort. Thus, sEH deletion may still provide some protection against LPS-induced hyperinflammation in middle-aged mice, albeit its protective capacity is significantly reduced.

6.1.4 The impact of age and biological sex: current knowledge and future directions

Our preliminary data in female and middle-aged mice suggest that disparities may exist in the response to acute LPS inflammation with aging and biological sex. Clinical data shows that elderly individuals are more susceptible to developing sepsis as well as sepsis-induced morbidity including cardiac dysfunction, and mortality.[463, 464] This may be due to a number of factors including other underlying comorbidities as well as a weakened host immune response, making the elderly more susceptible to infection.[132] Studies using aged animals show an larger degree of hyperinflammation and immune dysregulation in response to LPS compared to young adult animals.[465, 466] Hyperinflammation in aged mice and rats exposed to LPS are reflected by increased IL-6 and TNF-α levels compared to their younger counterparts.[465, 467] Furthermore, overactivation of the adrenergic system is shown to also account for excessive production of inflammatory cytokines with aging in endotoxemia.[466] This supports the higher systemic cytokine levels observed in middle-aged males post-LPS

compared to young males. In elderly human patients, elevated IL-6 and TNF-α are predictors of poorer outcomes and mortality, suggesting these cytokines may have clinical implications.[468]

Cardiac gene expression of IL-1β, ICAM-1, and IL-6 were also upregulated in aged mice treated with LPS.[467, 469] These effects were significant in middle-aged mice 16-17 months in age and most prominent in elderly mice older than 23 months.[469] Mechanistically, it has been proposed that the worsened cardiac function in LPS-treated aged mice may be due to impairment in cardiac autophagy and AMPK activation.[470] Aged endotoxemic mice were also less physiologically tolerant to LPS indicated by more severe and earlier onset of hypothermia, which supports the larger decline in physiological function in LPS-treated middle-aged mice.[467] Furthermore, CD14, which assists TLR4 cell surface receptors in the recognition of LPS is upregulated in some tissues, including the liver and spleen with aging during endotoxemia.[465, 466] Therefore, this may account for the increased sensitivity and response to LPS observed in our middle-aged mice. Endotoxemia studies have also shown that aged animals have a higher rate of splenic cell apoptosis following LPS injection compared to young counterparts which may contribute to immune cell dysfunction.[464] Therefore, not only does potentiation of the hyperinflammatory response complicate endotoxemia with aging but also the risk for enhanced immunosuppression.

Some of our pilot data also shows that female mice may have a lesser degree of cardiac functional decline in response to LPS regardless of whether sEH activity is disrupted, compared to their male counterparts. We have previously demonstrated that global sEH deficiency in female mice preserves cardiac function during the normal biological aging process compared to aged WT and global sEH null males.[307] These effects may be mediated by preserved cardiac SIRT3 activity and lower levels of oxidative stress. Similarly, our preliminary echocardiographic data suggest that female mice may also have a higher degree of cardioprotection following LPS administration. Interestingly, female mice with a functional sEH gene still demonstrated marked protection, which may question whether inhibition of sEH activity is as critical for protection for females in this model as it is for males. Epoxylipids and sEH activity demonstrate sexual dimorphic responses on cardiac function in health and disease.[300] Cardiac function in murine females may be more dependent on the function of EETs and associated with downregulation in sEH

expression.[471, 472] We have demonstrated that sEH expression is increased in aged male murine hearts but not in females.[307] Therefore, sEH inhibition may be less important in mediating cardiac protection in females compared to males. This may explain why cardiac function in young WT and sEH$^{(Myo\ +/+)}$ females is trending better than WT and sEH$^{(Myo\ +/+)}$ males post-LPS. Furthermore, if females have downregulation of sEH expression at baseline, this may explain why there are minimal differences between WT and sEH$^{(Myo\ +/+)}$ female mice compared to sEH null and sEH$^{(Myo\ -/-)}$ counterparts post-LPS. Some studies suggest that disparate mechanisms can also underly LPS-induced cardiac dysfunction in female and male mice.[473] Cardiac dysfunction in males may be related to lower Ca^{2+} transients whereas the dysfunction may lie downstream of Ca^{2+} signalling in female hearts and be dependent on cyclic guanosine monophosphate (cGMP) signalling.[473] Animal studies have shown for the male sex to generate higher levels of pro-inflammatory cytokines and have prolonged cardiac dysfunction in endotoxemia.[349, 474] Furthermore, some studies hypothesized that males are more susceptible to hyperinflammation in endotoxemia due to the protective effect attributed by female hormones including estrogens.[475-478] Conversely, in some clinical studies female sex was identified as an independent predictor for increased mortality in critically ill septic elderly patients.[468, 479] However, other studies have demonstrated that women may have a better prognosis compared to men which was correlated with enhanced anti-inflammatory IL-10 levels.[480, 481]

As the data presented represent preliminary findings, future experiments and analysis will need to be conducted in order to validate our results and investigate potential underlying mechanisms. The aging of mice constitutes a tedious process confounded by the development of other age-related health conditions. The COVID-19 pandemic also posed a significant challenge to the aging portion of this project. In March 2020 we were forced to cull more than 100 mice in anticipation of University shutdowns and staffing shortages. This significantly impaired the amount of mice we were able to age over the past 2 years. Slowly, the current situation appears to be improving and our lab has upcoming aged mice that will be ready to use in the next few months. These mice can be utilized to increase sample size in order to assess consistency in our preliminary echocardiographic data. We began an aging cohort of sEH$^{(Myo\ +/+)}$ and sEH$^{(Myo\ -/-)}$ mice. In spring 2022, the first group of these mice will be available for use, which will allow us to assess the effects of aging on the protection

conferred by cardiomyocyte-specific sEH deletion in acute LPS inflammatory injury. Importantly, assessment of the plasma cytokine panel in aged female WT and sEH null LPS-treated mice will be necessary to compare to our aging male data. Since the protection conferred by sEH genetic deletion appears to dampen with increasing age, the biochemical and molecular analysis of tissue will be of value to investigate which protective mechanisms of sEH inhibition are lost and which may be conserved. Importantly, very limited studies have assessed the intersection of aging *and* biological sex in response to acute LPS. Analysis of cardiac functional parameters and physiological impairment scores by 3-way ANOVA may be appropriate to incorporate treatment (control or LPS), genotype, and biological sex into a single statistical test. Nonetheless, pursuing further investigation of these pilot data presented will undoubtedly yield valuable information for future studies.

	Female				Male			
	WT		sEH Null		WT		sEH Null	
	Baseline	LPS-24h	Baseline	LPS-24h	Baseline	LPS-24h	Baseline	LPS-24h
Heart rate (beats/min)	473 ± 11	380 ± 23*	441 ± 14	408 ± 12	437 ± 17	399 ± 8	451 ± 11	422 ± 13
Wall Measurements								
Corrected LV mass, mg	78.38 ± 7.18	82.82 ± 10.95	94.48 ± 8.77	67.36 ± 8.31	84.65 ± 8.06	79.24 ± 2.91	93.06 ± 4.01	80.59 ± 7.08
IVS-diastole, mm	0.71 ± 0.06	0.98 ± 0.13	0.81 ± 0.04	0.68 ± 0.07	0.77 ± 0.04	0.90 ± 0.03	0.91 ± 0.05	0.90 ± 0.04
IVS-systole, mm	1.26 ± 0.14	1.33 ± 0.10	1.22 ± 0.08	1.12 ± 0.09	1.19 ± 0.06	1.03 ± 0.03	1.39 ± 0.06	1.25 ± 0.05
LVPW-diastole, mm	0.73 ± 0.07	0.73 ± 0.03	0.79 ± 0.07	0.73 ± 0.06	0.78 ± 0.06	0.79 ± 0.05	0.82 ± 0.04	0.84 ± 0.09
LVPW-systole, mm	1.07 ± 0.05	0.95 ± 0.03	1.12 ± 0.10	0.99 ± 0.06	1.23 ± 0.07	0.95 ± 0.05*	1.28 ± 0.06	1.21 ± 0.09
LVID-diastole, mm	3.90 ± 0.08	3.48 ± 0.10	3.98 ± 0.08	3.48 ± 0.32	3.80 ± 0.13	3.45 ± 0.15	3.73 ± 0.08	3.38 ± 0.25
LVID-systole, mm	2.43 ± 0.11	2.64 ± 0.11	2.64 ± 0.14	2.66 ± 0.28	2.47 ± 0.11	3.03 ± 0.15*	2.47 ± 0.09	2.42 ± 0.22#
Cardiac Function								
Ejection Fraction (%)	66.52 ± 2.65	50.79 ± 8.85	62.81 ± 2.59	47.98 ± 9.66	65.65 ± 1.63	28.75 ± 1.49*	64.76 ± 1.80	54.64 ± 6.11#
Fractional Shortening (%)	36.34 ± 2.00	25.72 ± 5.30	33.78 ± 1.99	24.39 ± 5.68	35.65 ± 1.28	13.07 ± 0.72*	34.95 ± 1.28	28.81 ± 4.01#
LVEDV, µl	65.05 ± 4.00	51.00 ± 4.14	69.63 ± 3.86	54.60 ± 9.00	63.06 ± 6.18	49.82 ± 4.91	59.73 ± 3.52	48.83 ± 7.70
LVESV, µl	21.97 ± 2.71	24.36 ± 2.14	26.28 ± 2.88	28.47 ± 7.50	22.14 ± 2.84	35.73 ± 3.80*	21.32 ± 2.00	21.83 ± 5.00
CO, ml/min	20.39 ± 1.28	9.88 ± 1.95*	19.12 ± 1.12	10.91 ± 3.44*	17.12 ± 1.74	5.54 ± 0.55*	15.59 ± 1.79	10.66 ± 2.07
SV, µl	43.08 ± 2.41	26.64 ± 6.28	43.35 ± 2.00	26.13 ± 7.51*	40.92 ± 3.60	14.09 ± 1.30*	38.41 ± 2.22	27.01 ± 5.75
Doppler Imaging								
IVRT, ms	17.55 ± 1.48	23.60 ± 1.87	15.70 ± 0.90	21.27 ± 6.82	15.06 ± 1.08	31.24 ± 2.69*	13.93 ± 0.87	21.74 ± 2.84#*
IVCT, ms	13.91 ± 2.96	14.12 ± 1.55	13.40 ± 1.65	13.35 ± 3.63	12.05 ± 1.42	15.73 ± 2.04	9.23 ± 0.71	18.54 ± 5.78
ET, ms	51.54 ± 2.94	48.30 ± 6.34	49.27 ± 2.45	45.11 ± 2.80	44.85 ± 2.38	34.08 ± 2.22*	39.12 ± 1.74	35.49 ± 2.82
Mitral E/A ratio	1.70 ± 0.08	1.32 ± 0.59	1.83 ± 0.31	1.72 ± 0.24	1.47 ± 0.08	1.06 ± 0.21	1.47 ± 0.09	1.29 ± 0.12
E/E' ratio	31.44 ± 3.08	64.85 ± 25.98	31.82 ± 3.02	47.22 ± 14.17	28.93 ± 1.94	58.46 ± 11.85*	30.78 ± 3.27	25.12 ± 3.71#
Tei index	0.61 ± 0.06	0.82 ± 0.17	0.60 ± 0.05	0.80 ± 0.25	0.62 ± 0.05	1.38 ± 0.08*	0.60 ± 0.02	1.24 ± 0.22*
Body Weight (g)	21.26 ± 1.31	19.99 ± 2.13	20.30 ± 0.40	17.96 ± 0.28	26.50 ± 0.80	24.71 ± 0.97	29.01 ± 0.89	26.40 ± 1.00
N value	5	3	8	4	14	10	13	10

Table 6.1.1. Cardiac functional parameters at baseline and after 24 hours post-LPS administration in young female and male WT and sEH null mice measured by 2D transthoracic echocardiography. Data are means ± SEM, N = 3-14, $p < 0.05$; * vs baseline; # vs WT LPS-24 hours.

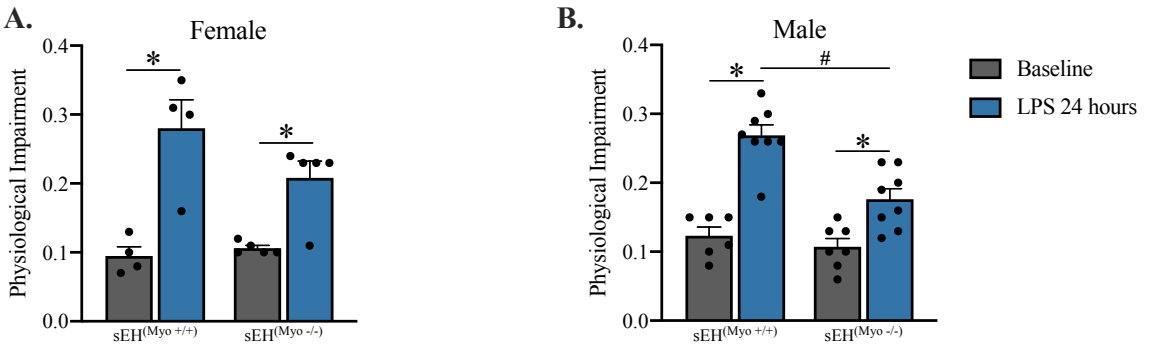

Figure 6.1.1. Level of physiological impairment in young **A.)** female and **B.)** male Cre lox mice at baseline and 24 hours after LPS administration. Data are means ± SEM, N = 4-8, $p < 0.05$; * vs baseline; # vs $sEH^{(Myo\ +/+)}$ LPS-24 hours.

	Female				Male			
	$sEH^{(Myo\ +/+)}$		$sEH^{(Myo\ -/-)}$		$sEH^{(Myo\ +/+)}$		$sEH^{(Myo\ -/-)}$	
	Baseline	LPS-24h	Baseline	LPS-24h	Baseline	LPS-24h	Baseline	LPS-24h
Heart rate (beats/min)	394 ± 14	376 ± 13	425 ± 16	400 ± 16	463 ± 19	390 ± 12	475 ± 22	420 ± 13
Wall Measurements								
Corrected LV mass, mg	75.30 ± 8.15	60.76 ± 8.32	69.31 ± 5.29	61.95 ± 5.20	88.55 ± 5.10	88.41 ± 5.53	80.00 ± 4.35	81.34 ± 2.74
IVS-diastole, mm	0.96 ± 0.10	0.82 ± 0.12	0.73 ± 0.07	1.05 ± 0.09	0.78 ± 0.03	0.88 ± 0.04	0.82 ± 0.03	0.85 ± 0.04
IVS-systole, mm	1.50 ± 0.07	1.20 ± 0.22	1.12 ± 0.11	1.43 ± 0.11	1.18 ± 0.07	1.05 ± 0.05	1.26 ± 0.04	1.13 ± 0.05
LVPW-diastole, mm	0.84 ± 0.03	0.73 ± 0.09	0.76 ± 0.04	0.81 ± 0.06	0.79 ± 0.04	0.73 ± 0.06	0.73 ± 0.03	0.72 ± 0.03
LVPW-systole, mm	1.28 ± 0.06	0.98 ± 0.12	1.18 ± 0.05	1.11 ± 0.06	1.28 ± 0.06	0.86 ± 0.05*	1.15 ± 0.03	0.97 ± 0.04*
LVID-diastole, mm	3.11 ± 0.17	3.16 ± ± 0.26	3.51 ± 0.10	2.67 ± 0.19*	3.90 ± 0.10	3.83 ± 0.15	3.73 ± 0.09	3.74 ± 0.13
LVID-systole, mm	1.87 ± 0.13	2.32 ± 0.32	2.30 ± 0.10	1.96 ± 0.14	2.58 ± 0.11	3.43 ± 0.12*	2.49 ± 0.11	3.04 ± 0.14*
Cardiac Function								
Ejection Fraction (%)	72.73 ± 4.22	55.13 ± 7.14	66.34 ± 1.43	59.31 ± 4.18	64.90 ± 2.41	26.89 ± 2.53*	63.13 ± 2.53	42. 03 ± 3.40*#
Fractional Shortening (%)	41.03 ± 3.81	28.40 ± 4.87	35.84 ± 1.05	30.49 ± 2.79	35.38 ± 1.82	12.38 ± 1.35*	34.17 ± 1.95	20.86 ± 1.98*#
LVEDV, µl	37.29 ± 4.76	41.42 ± 8.10	53.30 ± 3.05	28.58 ± 4.59*	69.77 ± 6.97	64.76 ± 5.52	61.45 ± 3.13	63.11 ± 4.86
LVESV, µl	10.07 ± 2.10	20.27 ± 5.79	18.00 ± 1.47	11.83 ± 2.05	24.66 ± 3.08	46.33 ± 2.97*	23.30 ± 2.27	37.60 ± 4.21*
CO, ml/min	10.05 ± 0.60	6.55 ± 1.07	10.30 ± 1.84	5.87 ± 1.24	14.08 ± 2.57	5.20 ± 0.85*	13.65 ± 1.17	8.44 ± 0.86*
SV, µl	30.12 ± 3.77	21.16 ± 2.34	35.30 ± 1.83	16.75 ± 2.87*	45.11 ± 4.67	18.44 ± 3.28*	38.16 ± 1.73	25.51 ± 2.00*
Doppler Imaging								
IVRT, ms	19.42 ± 1.42	23.28 ± 5.80	14.06 ± 1.95	22.69 ± 3.04	12.56 ± 1.24	26.21 ± 3.83*	14.99 ± 1.03	22.17 ± 2.39
IVCT, ms	13.89 ± 1.42	18.59 ± 2.82	10.89 ± 2.04	15.32 ± 2.70	10.51 ± 1.88	15.63 ± 2.28	11.34 ± 1.74	13.20 ± 1.77
ET, ms	53.33 ± 5.24	47.14 ± 5.35	41.67 ± 1.80	37.82 ± 3.28	47.04 ± 2.93	36.39 ± 1.88*	44.77 ± 1.48	38.86 ± 1.38
Mitral E/A ratio	1.55 ± 0.13	1.41 ± 0.15	1.75 ± 0.20	1.51 ± 0.15	1.44 ± 0.08	1.05 ± 0.08	1.60 ± 0.11	1.26 ± 0.05
E/E' ratio	25.75 ± 3.56	47.17 ± 11.17	22.16 ± 2.82	46.00 ± 7.35	31.75 ± 3.51	25.69 ± 3.96	32.19 ± 2.75	38.50 ± 2.87
Tei index	0.65 ± 0.12	0.96 ± 0.23	0.60 ± 0.07	1.13 ± 0.29	0.52 ± 0.06	1.19 ± 0.14*	0.60 ± 0.05	0.88 ± 0.10
Body Weight (g)	23.38 ± 0.60	21.60 ± 0.73	22.06 ± 0.68	20.24 ± 0.49	31.07 ± 0.55	27.11 ± 0.62*	27.88 ± 0.69	24.32 ± 0.59*
N value	4	4	5	6	12	10	16	17

Table 6.1.2. Cardiac functional parameters at baseline and after 24 hours post-LPS administration in young female and male Cre lox mice measured by 2D transthoracic echocardiography. Data are means ± SEM, N = 4-17, $p < 0.05$; * vs baseline; # vs $sEH^{(Myo\ +/+)}$ LPS-24h.

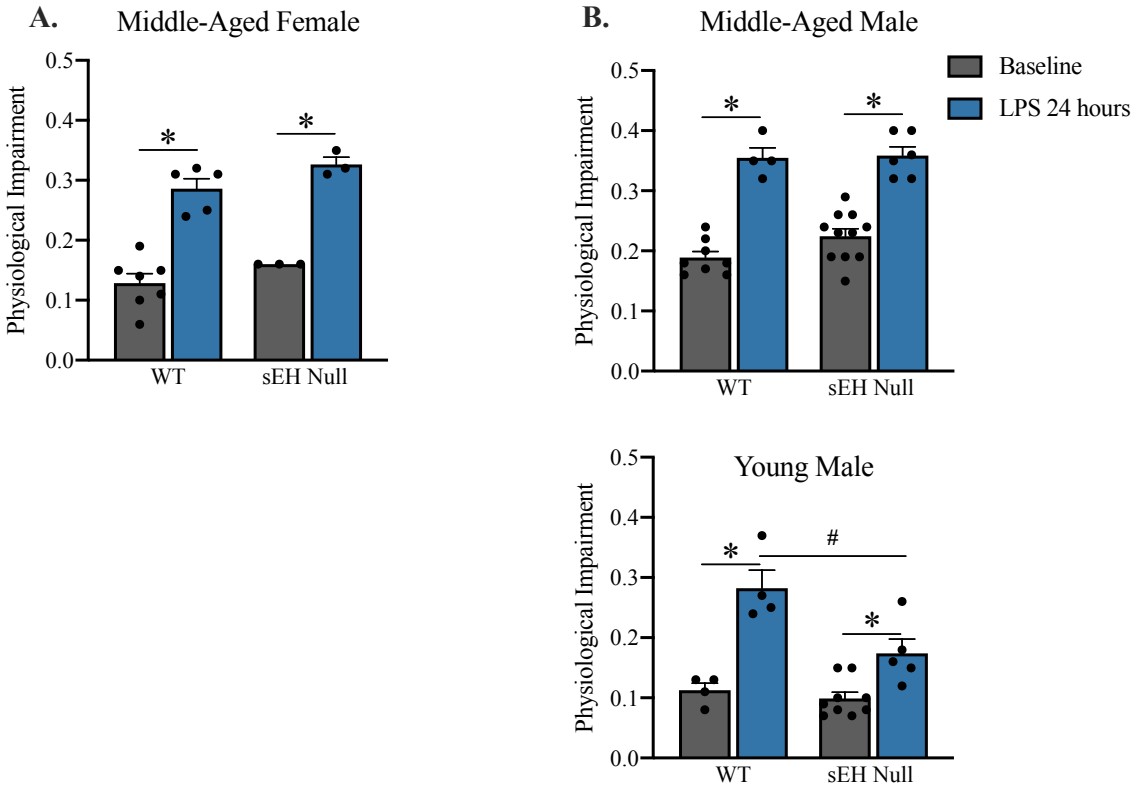

Figure 6.1.2. Level of physiological impairment in middle-aged **A.)** female and **B.)** male WT and sEH null mice at baseline and 24 hours after LPS administration. Data are means ± SEM, N = 3-11, $p < 0.05$; * vs baseline; # vs WT LPS-24h.

	Female				Male			
	WT		sEH Null		WT		sEH Null	
	Baseline	LPS-24h	Baseline	LPS-24h	Baseline	LPS-24h	Baseline	LPS-24h
Heart rate (beats/min)	456 ± 18	452 ± 15	492 ± 3	409 ± 42	480 ± 18	363 ± 18*	491 ± 14	406 ± 16*
Wall Measurements								
Corrected LV mass, mg	100.53 ± 2.59	101.51 ± 5.02	113.53 ± 4.87	117. ± 89 ± 5.32	123.87 ± 13.25	118.81 ± 14.55	112.90 ± 11.26	119.99 ± 6.50
IVS-diastole, mm	0.94 ± 0.06	0.87 ± 0.03	0.96 ± 0.06	1.02 ± 0.10	1.10 ± 0.06	1.00 ± 0.02	1.25 ± 0.14	0.97 ± 0.07
IVS-systole, mm	1.32 ± 0.12	1.20 ± 0.08	1.45 ± 0.08	1.27 ± 0.10	1.53 ± 0.09	1.29 ± 0.01	1.48 ± 0.12	1.16 ± 0.11
LVPW-diastole, mm	0.85 ± 0.04	0.88 ± 0.10	0.97 ± 0.08	1.11 ± 0.14	0.90 ± 0.07	0.95 ± 0.21	1.06 ± 0.08	0.83 ± 0.06
LVPW-systole, mm	1.29 ± 0.07	1.10 ± 0.17	1.44 ± 0.05	1.25 ± 0.17	1.35 ± 0.06	1.14 ± 0.27	1.36 ± 0.13	1.04 ± 0.07
LVID-diastole, mm	3.82 ± 0.18	3.91 ± 0.14	3.84 ± 0.17	3.61 ± 0.45	4.39 ± 0.55	3.96 ± 0.71	3.41 ± 0.18	4.22 ± 0.25
LVID-systole, mm	2.66 ± 0.16	3.19 ± 0.27	2.91 ± 0.33	3.13 ± 0.39	3.22 ± 0.58	3.50 ± 0.69	2.88 ± 0.36	3.66 ± 0.22
Cardiac Function								
Ejection Fraction (%)	57.94 ± 3.43	42.29 ± 7.65	65.07 ± 2.68	31.30 ± 4.39*	58.15 ± 7.70	26.92 ± 2.88*	65.09 ± 2.21	29.36 ± 3.34*
Fractional Shortening (%)	30.31 ± 2.39	20.89 ± 4.41	35.17 ± 2.06	14.46 ± 2.30*	31.28 ± 4.75	12.18 ± 1.21*	35.24 ± 1.61	13.69 ± 1.77*
LVEDV, µl	64.95 ± 7.74	66.63 ± 4.87	64.33 ± 6.74	57.92 ± 17.31	69.31 ± 11.20	72.88 ± 35.86	63.54 ± 5.15	76.92 ± 11.39
LVESV, µl	27.51 ± 4.15	39.50 ± 8.00	22.28 ± 2.03	39.30 ± 11.66	23.49 ± 3.30	54.99 ± 28.60	22.79 ± 3.04	53.84 ± 8.87
CO, ml/min	17.02 ± 1.95	11.34 ± 2.10	20.66 ± 2.66	8.07 ± 3.01*	20.98 ± 2.20	6.25 ± 2.90*	16.68 ± 2.96	9.55 ± 2.25
SV, µl	37.45 ± 4.43	27.13 ± 3.32	42.05 ± 5.63	18.62 ± 6.06	48.91 ± 7.63	17.89 ± 7.27*	40.74 ± 2.24	23.92 ± 4.14
Doppler Imaging								
IVRT, ms	15.24 ± 1.31	18.08 ± 2.66	13.45 ± 1.66	22.94 ± 3.45	15.81 ± 1.74	34.63 ± 1.61*	14.33 ± 1.43	30.95 ± 5.16*
IVCT, ms	12.76 ± 3.89	10.78 ± 2.64	13.58 ± 3.94	17.92 ± 1.88	17.72 ± 5.67	26.30 ± 8.21	18.24 ± 1.93	16.59 ± 3.01
ET, ms	41.12 ± 1.87	29.32 ± 2.40*	40.76 ± 2.33	25.05 ± 0.90*	37.91 ± 2.39	33.43 ± 2.25	40.31 ± 1.97	32.28 ± 1.68*
Mitral E/A ratio	1.39 ± 0.10	1.17 ± 0.15	1.26 ± 0.09	1.10 ± 0.04	1.42 ± 0.24	0.64 ± 0.10	1.44 ± 0.11	1.14 ± 0.17
E/E' ratio	28.45 ± 4.70	30.94 ± 6.13	30.09 ± 0.84	70.81 ± 35.49	28.96 ± 4.46	26.94 ± 9.24	24.55 ± 3.60	52.81 ± 7.31*
Tei index	0.68 ± 0.06	1.06 ± 0.26	0.65 ± 0.10	1.65 ± 0.25*	0.87 ± 0.11	1.84 ± 0.31*	0.83 ± 0.09	1.57 ± 0.26*
Body Weight (g)	34.73 ± 1.51	32.70 ± 2.04	45.30 ± 2.52#	43.90 ± 2.41#	42.28 ± 2.00	40.73 ± 2.99	47.76 ± 1.09	46.40 ± 0.90
N value	6	5	3	3	5	3	7	6

Table 6.1.3. Cardiac functional parameters at baseline and after 24 hours post-LPS administration in middle-aged female and male WT and sEH null mice measured by 2D transthoracic echocardiography. Data are means ± SEM, N = 3-7, $p < 0.05$; * vs baseline; # vs WT counterpart.

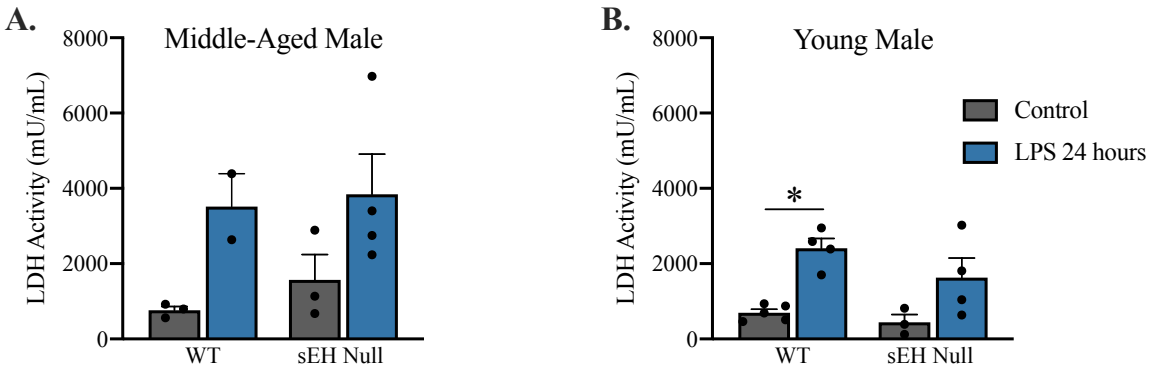

Figure 6.1.3. Plasma levels of LDH activity in **A.)** middle-aged male and **B.)** young male control mice and in mice exposed to LPS for 24 hours. Data are means ± SEM, N = 2-4.

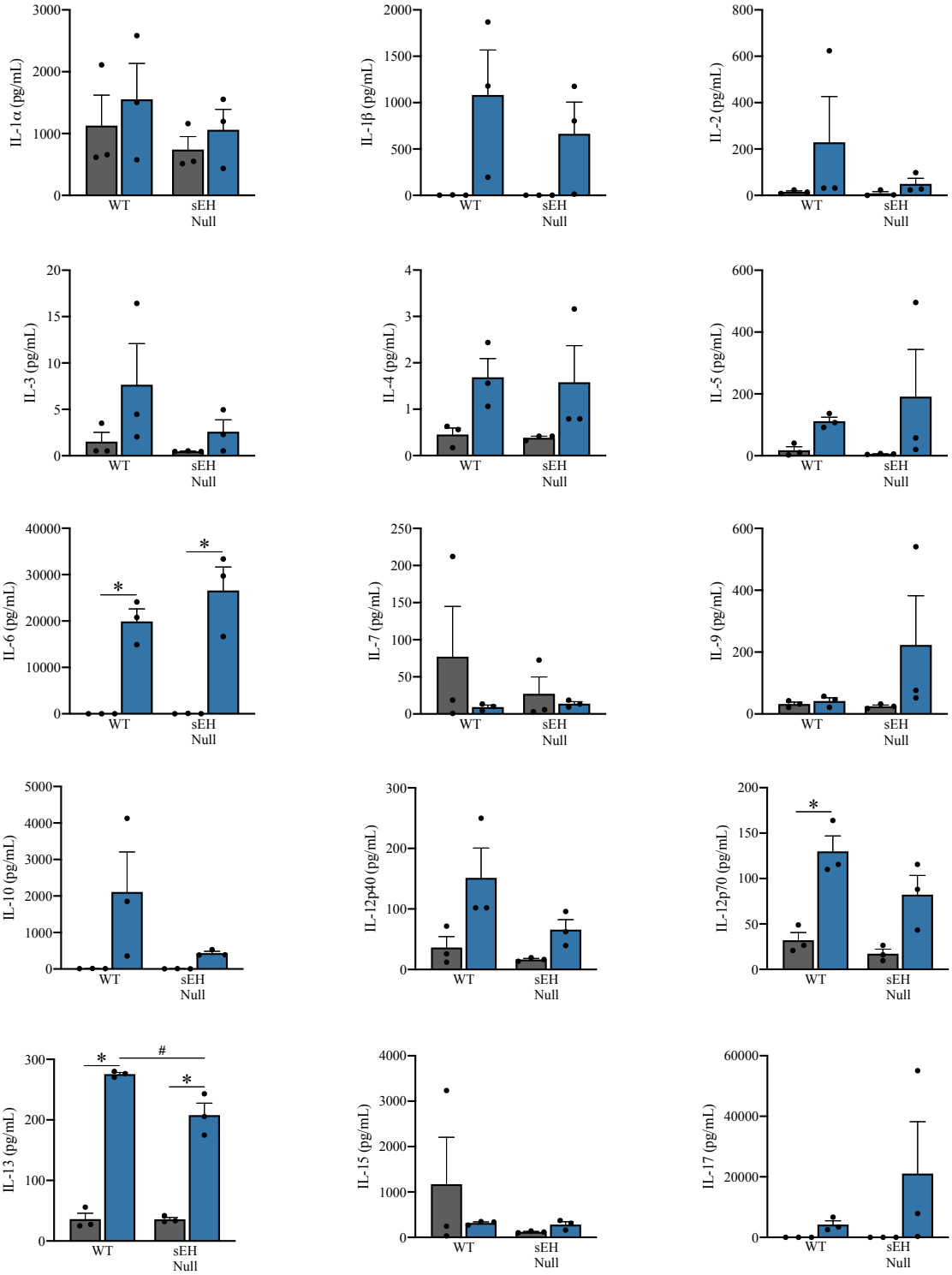

Figure 6.1.4. Plasma levels of interleukins in middle-aged male control mice and mice treated with LPS for 24 hours measured using a multi-plex assay. Data are means ± SEM, N = 3, $p < 0.05$; * vs control; # vs WT post LPS-24 hours.

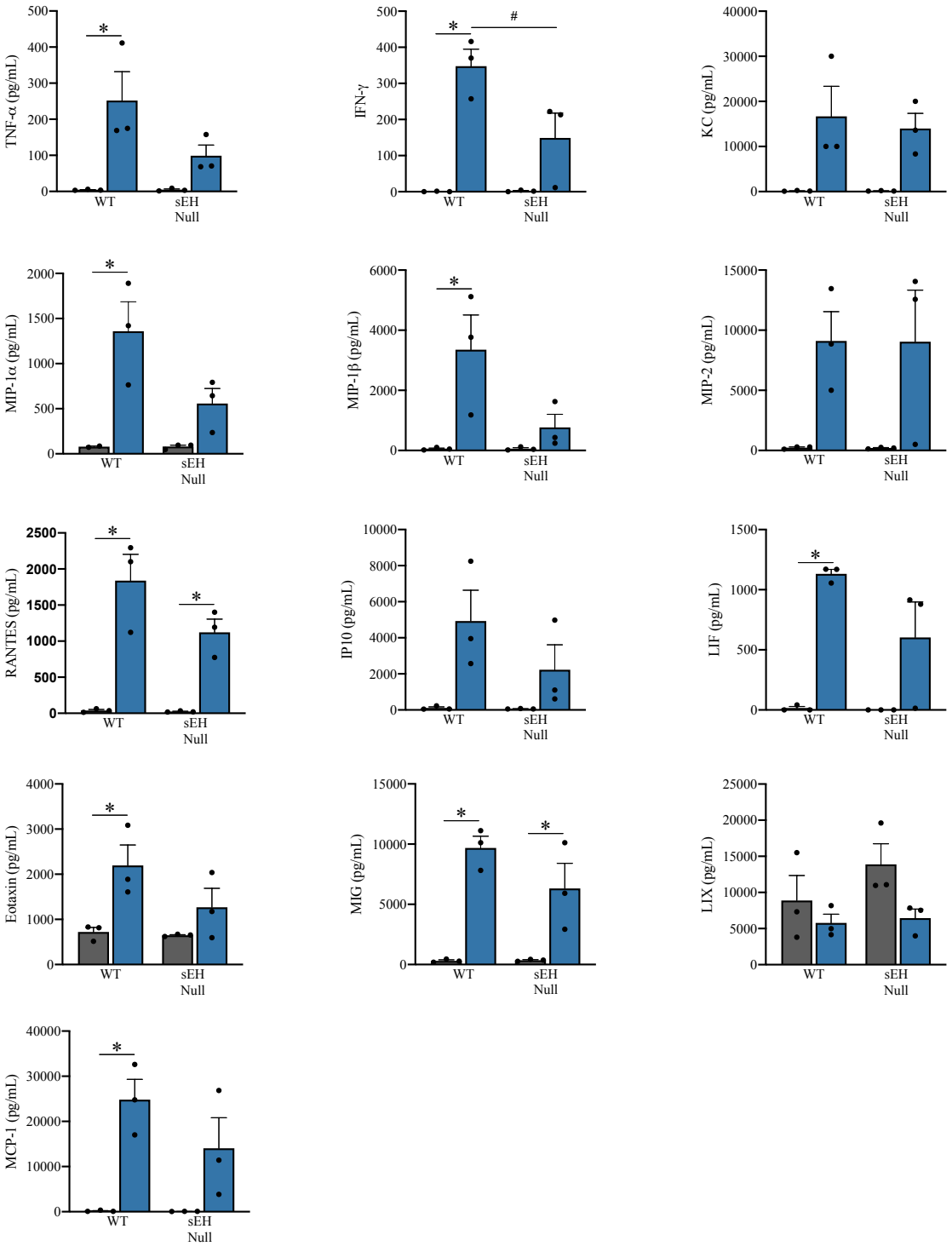

Figure 6.1.5. Plasma levels of inflammatory mediators in middle-aged male control mice and mice treated with LPS for 24 hours measured using a multi-plex assay. Data are means ± SEM, N = 3, $p < 0.05$; * vs control; # vs WT post LPS-24 hours.

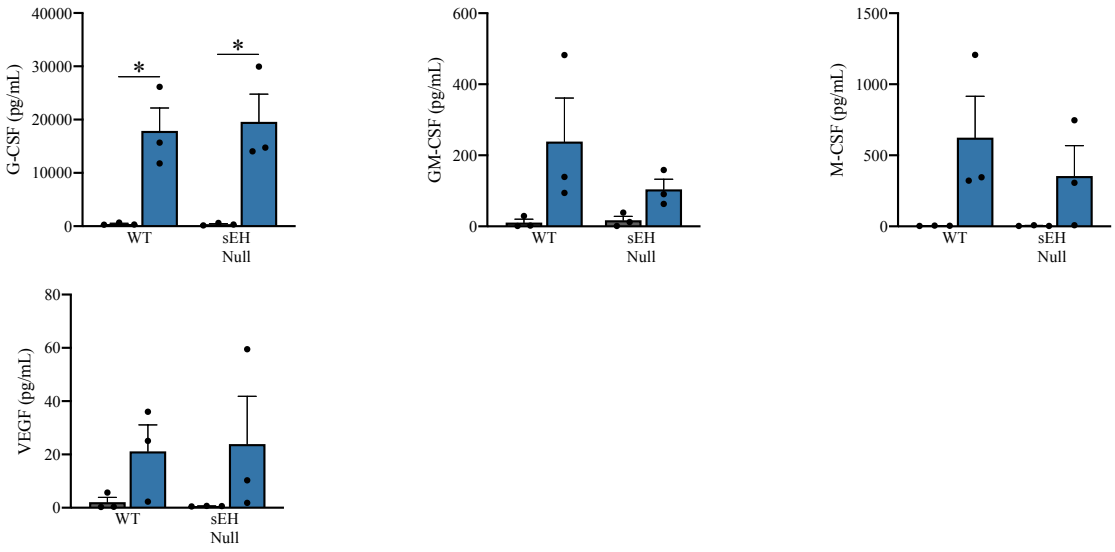

Figure 6.1.6. Plasma levels of growth factors and stimulating factors in middle-aged male control mice and mice treated with LPS for 24 hours measured using a multi-plex assay. Data are means ± SEM, N = 3, $p < 0.05$; * vs control.

6.2 BASELINE PHENOTYPIC CHARACTERIZATION OF CRE LOX MICE

6.2.1 Baseline alterations may occur in Myh6-Cre$^{+/-}$sEH$^{(Myo\ +/+)}$ and Myh6-Cre$^{+/-}$sEH$^{(Myo\ -/-)}$ mice

Through our biochemical analysis of heart and plasma tissue, we serendipitously discovered that mice from our Cre lox colony may have differences in protein expression and cytokine levels at baseline (after enduring the tamoxifen administration protocol) compared to WT and sEH null mouse colonies.

Preliminary data shows cytosolic p62 expression is dramatically increased in saline control and LPS-treated sEH$^{(Myo\ +/+)}$ and sEH$^{(Myo\ -/-)}$ mice compared to WT and sEH null colonies. (Figure 6.2). p62 is a cytosolic protein associated with autophagy. Autophagy is a regulated cellular process which allows for the removal of damaged organelles, dysfunctional proteins, and other macromolecules through the formation of autophagosomes.[482] Autophagy allows the cell to remove these debris without the need to initiate apoptosis and other cell death pathways, thus promoting cell survival.[482] As acute LPS exposure can cause mitochondrial and other organelle damage, assessing markers of autophagy may provide indication as to how well the heart is coping with the acute stress.[164, 483] The interpretation of this initial finding is complex. During autophagy, p62 is found on the outer membrane of autophagosomes destined to rid the cell of debris.[482] However, the autophagosome is shuttled to lysosomes where fusion promotes the formation of autophagolysosomes and lysosomal enzymes can then digest the debris.[482] Critically, when the autophagosome fuses with the lysosome, p62 is also degraded in the process.[482] Thus elevated levels of p62 may be interpreted in two ways. Higher levels of p62 expression may mean that the autophagic process is enhanced as there may be more formation of autophagosomes. Conversely, it may also suggest that the dynamic autophagic process has become stagnant and that autophagosomes are not efficiently fusing with the lysosomes.[482] Nonetheless this may suggest that perturbations exists in the autophagic process in Cre lox hearts. Because autophagy is an active process, use of live cell imaging may be useful to understand changes in autophagic flux occurring in Cre lox heart tissue.

We also assessed the cardiac levels of phosphorylated (Tyr14) caveolin-1 (p-Cav-1) in the crude microsomal fractions. Briefly, caveolins are the structural components of caveolae, membrane invaginations which play important roles in regulating cholesterol transport, cell signalling, surface protein expression, and plasma membrane organization.[484, 485] We observed changes in p-Cav-1 expression in human dilated cardiomyopathy (DCM) hearts (Appendix), which prompted us to further explore this protein in other models of CVD, including our acute LPS model. We found a marked increase in the phosphorylation of Cav-1 in saline control-treated Cre lox heart tissue, and which was significantly increased in $sEH^{(Myo\ +/+)}$ control hearts (Figure 6.2). There is limited mechanistic understanding about caveolin-1 and its phosphorylation in CVD pathogenesis. Some studies have shown that Cav-1 accumulates at the endoplasmic reticulum (ER) and mitochondrial membrane interface in response to cellular stress to preserve mitochondrial bioenergetics and cell viability.[486] Cav-1 deficient mice have enhanced endothelial cell mitochondrial ROS production and activation of autophagic processes. Hence, increased levels of Cav-1 may be a compensatory protective mechanism by cells experiencing stressful stimuli.[487] Src-dependent phosphorylation at tyrosine 14 residue of Cav-1 enhances NF-*k*B activation and inflammatory mediator generation in LPS-treated endothelial cells.[488] It can also promote the release of caveolae structures from the plasma membrane. Phosphorylation can also enhance endothelial cell permeability and barrier dysfunction in response to ROS.[489] Therefore, enhanced phosphorylation may be indicative of underlying oxidative stress or inflammatory processes occurring in the heart tissue from our Cre lox colony. Currently, it is difficult to draw any conclusions with such a small sample size, so further analysis of p62 and p-Cav-1 protein expression is necessary to validate these preliminary data.

Assessment of cytokines levels in the plasma also revealed some baseline anomalies in control Cre lox mice compared to WT and sEH null controls. Lipopolysaccharide-induced CXC chemokine (LIX) in mice, or CXCL5 in humans, was also elevated in our Cre lox colony (Figure 6.2). This chemokine has potent effects on neutrophil activation, chemoattraction, and cell migration.[490] Expression of LIX can be stimulated by other cytokines including TNF-α and IL-1.[491] As well, cardiac endothelial cells exposed to LIX can promote the expression of TNF-α and IL-1β, igniting a vicious cycle of inflammation.[492] Lastly, the numbers of $CD68^{+}$ cells were also greater in cross-sections of saline control-

treated Cre lox hearts compared to the corresponding WT and sEH null controls(Figure 6.2). $CD68^+$ is expressed on the surface of immune cells including macrophages.[433] Therefore, these initial findings suggest that Cre lox mice may be experiencing local inflammation in the myocardium as well as activation of underlying systemic inflammatory processes at baseline.

Importantly, all experimental mice underwent a baseline echocardiography assessment to ensure normal cardiac function before LPS or saline injection. It was confirmed that baseline cardiac function was indeed similar between our Cre lox, WT, and sEH null colonies before their use experimentally. Thus, these potential biochemical and cellular baseline alterations in protein expression and LIX plasma levels may not impact cardiac function. However, this gives rise to the speculation that other underlying processes may be altered. Investigation into what may be causing these changes and their impact on physiological functions will be critical to investigate.

6.2.2 Tamoxifen administration, cardiac CreER recombinase activation, and off-target implications

The advancement in murine models to include the use of the Cre lox system has allowed research to make enormous strides in the understanding of tissue and cell specific effects of individual genes and proteins in *in vivo* models.[337] The use of an inducible CreER recombinase conveniently allows the targeted knockdown of gene expression at a desired point in time.[337] In our model, CreER recombinase is bound by a mutant estrogen receptor (ER) in the cytosol and remains inactive until the addition of tamoxifen. Tamoxifen allows the translocation of Cre to the nucleus which excises the portion of the *Ephx2* gene flanked by LoxP sites. Importantly, the expression of the *CreER* recombinase gene is driven by the alpha myosin heavy chain 6 (Myh6) promoter.[493] Protein expression of CreER recombinase occurs in cardiomyocytes, thus upon its induction by tamoxifen, the *Ephx2* gene is also selectively removed only from the cardiomyocyte and remains functional in all other cells of the body.

Despite the usefulness of this system, it also comes with challenges and setbacks to be overcome. First, tamoxifen can have toxic effects, especially at high doses.[494, 495] We

administer 6 doses of 45 mg/kg over a period of 8 days. On average, we see a 30% mortality rate with each cohort undergoing the tamoxifen protocol. Surviving mice are given a 5 week wash-out period to recover before their use experimentally. One study found that the injection of tamoxifen into C57/BL6 mice did not induce cardiac dysfunction or mortality regardless of the dose.[495] Conversely, another study reports that use of raloxifene to induce CreER activation is less cardiotoxic.[496] However, whether tamoxifen incites changes in baseline cardiac protein expression and inflammation in the absence of CreER recombinase is unknown. Hence, toxic effects of high dose tamoxifen administration may contribute to some of the changes we have observed. We have plans to inject C57/BL6 mice with our tamoxifen protocol and will then assess cardiac function and well as p62, p-Cav-1, and serum cytokine levels. This will provide information as to whether the changes seen in our Cre lox colony are due to long-term effects of tamoxifen.

Another challenge is posed by the cardiotoxicity of CreER recombinase activation. Induction of CreER can cause a transient heart failure phenotype.[495, 496] Ejection fraction can be reduced by more than 30% during the acute activation period.[495] This can also result in cardiomyocyte apoptosis and mitochondrial damage. Again, this phenotype is supposedly transient and baseline echocardiography 5 weeks post-tamoxifen ensures that cardiac function has recovered in our mice. However, whether remodeling on the cellular or protein level in response to the acute stress occurs will need to be determined. The insertion of the CreER recombinase transgene into the murine genome can also alter expression of genes around the site of insertion.[494] To control for this, we used CreER expressing mice lacking *Ephx2* LoxP sites. Since these preliminary phenotypic abnormalities are observed in $sEH^{(Myo\ +/+)}$ and $sEH^{(Myo\ -/-)}$ mice, which both express CreER, suggests that the *CreER* recombinase transgene may be a contributing factor to our observed baseline alterations. Importantly, a separate study undertaking the characterization of this Cre lox colony will provide important information about underlying biochemical and cellular alterations in this model, physiological processes consequently effected, and thus the implications and limitations for the use of this mouse colony in other experiments.

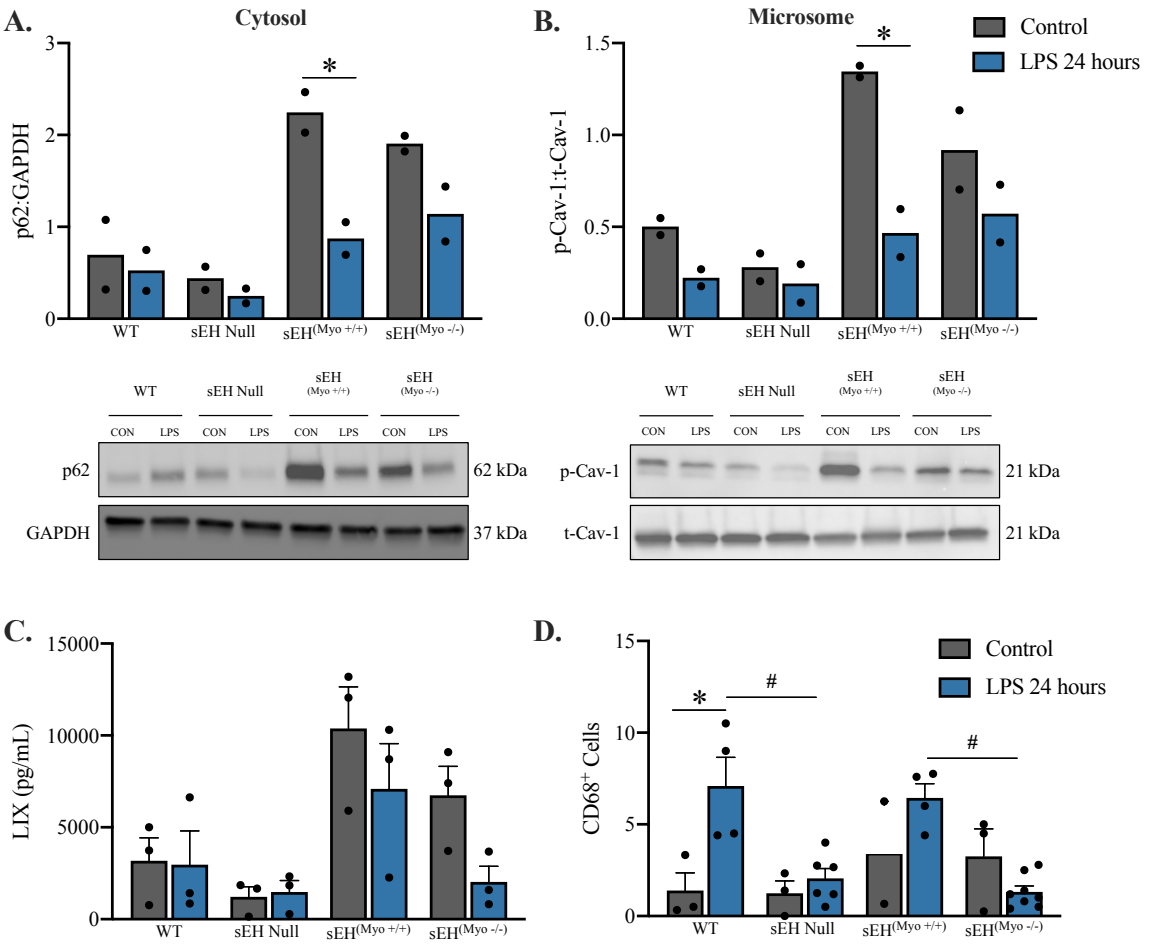

Figure 6.2.1. Preliminary changes in baseline parameters of Cre lox mice. Western immunoblot of **A.)** p62 expression in the cytosol and **B.)** p-Cav-1 expression in microsomal fractions of control and 24 hour LPS-treated mice. Data are displayed as the mean, N = 2. **C.**) Plasma levels of LIX in control and mice treated with LPS for 24 hours determined by multi-plex assay. **D.**) Quantitation of $CD68^{+}$ cells in myocardial slices. Each point (N) represents the average number of $CD68^{+}$ cells from all images (4-6) taken of a heart from each individual mouse. Data are means ± SEM, N = 2-8, $p < 0.05$; * vs respective control; # vs true control WT or $sEH^{(Myo\ +/+)}$ post-LPS.

REFERENCES

1. Chen L, Deng H, Cui H, Fang J, Zuo Z, Deng J, Li Y, Wang X and Zhao L. Inflammatory responses and inflammation-associated diseases in organs. *Oncotarget*. 2018;9:7204-7218.
2. Nedeva C, Menassa J and Puthalakath H. Sepsis: Inflammation Is a Necessary Evil. *Front Cell Dev Biol*. 2019;7:108.
3. Jarczak D, Kluge S and Nierhaus A. Sepsis-Pathophysiology and Therapeutic Concepts. *Front Med (Lausanne)*. 2021;8:628302.
4. Merx MW and Weber C. Sepsis and the heart. *Circulation*. 2007;116:793-802.
5. Celes MR, Prado CM and Rossi MA. Sepsis: going to the heart of the matter. *Pathobiology*. 2013;80:70-86.
6. Jamieson KL, Endo T, Darwesh AM, Samokhvalov V and Seubert JM. Cytochrome P450-derived eicosanoids and heart function. *Pharmacol Ther*. 2017;179:47-83.
7. Dennis EA and Norris PC. Eicosanoid storm in infection and inflammation. *Nat Rev Immunol*. 2015;15:511-23.
8. Tam VC. Lipidomic profiling of bioactive lipids by mass spectrometry during microbial infections. *Semin Immunol*. 2013;25:240-8.
9. McReynolds C, Morisseau C, Wagner K and Hammock B. Epoxy Fatty Acids Are Promising Targets for Treatment of Pain, Cardiovascular Disease and Other Indications Characterized by Mitochondrial Dysfunction, Endoplasmic Stress and Inflammation. *Adv Exp Med Biol*. 2020;1274:71-99.
10. Gilroy DW, Edin ML, De Maeyer RP, Bystrom J, Newson J, Lih FB, Stables M, Zeldin DC and Bishop-Bailey D. CYP450-derived oxylipins mediate inflammatory resolution. *Proc Natl Acad Sci U S A*. 2016;113:E3240-9.
11. Samokhvalov V, Vriend J, Jamieson KL, Akhnokh MK, Manne R, Falck JR and Seubert JM. PPARgamma signaling is required for mediating EETs protective effects in neonatal cardiomyocytes exposed to LPS. *Front Pharmacol*. 2014;5:242.
12. Hunter JD and Doddi M. Sepsis and the heart. *Br J Anaesth*. 2010;104:3-11.
13. Rudd KE, Johnson SC, Agesa KM, Shackelford KA, Tsoi D, Kievlan DR, Colombara DV, Ikuta KS, Kissoon N, Finfer S, Fleischmann-Struzek C, Machado FR, Reinhart KK, Rowan K, Seymour CW, Watson RS, West TE, Marinho F, Hay SI, Lozano R, Lopez AD, Angus DC, Murray CJL and Naghavi M. Global, regional, and national sepsis incidence and mortality, 1990-2017: analysis for the Global Burden of Disease Study. *Lancet*. 2020;395:200-211.
14. Rhee C, Jones TM, Hamad Y, Pande A, Varon J, O'Brien C, Anderson DJ, Warren DK, Dantes RB, Epstein L, Klompas M, Centers for Disease C and Prevention Prevention Epicenters P. Prevalence, Underlying Causes, and Preventability of Sepsis-Associated Mortality in US Acute Care Hospitals. *JAMA Netw Open*. 2019;2:e187571.
15. Chu M, Gao Y, Zhang Y, Zhou B, Wu B, Yao J and Xu D. The role of speckle tracking echocardiography in assessment of lipopolysaccharide-induced myocardial dysfunction in mice. *J Thorac Dis*. 2015;7:2253-61.
16. Doi K, Leelahavanichkul A, Yuen PS and Star RA. Animal models of sepsis and sepsis-induced kidney injury. *J Clin Invest*. 2009;119:2868-78.
17. Lin H, Wang W, Lee M, Meng Q and Ren H. Current Status of Septic Cardiomyopathy: Basic Science and Clinical Progress. *Front Pharmacol*. 2020;11:210.

18. Martin L, Derwall M, Al Zoubi S, Zechendorf E, Reuter DA, Thiemermann C and Schuerholz T. The Septic Heart: Current Understanding of Molecular Mechanisms and Clinical Implications. *Chest*. 2019;155:427-437.
19. Vieillard-Baron A, Caille V, Charron C, Belliard G, Page B and Jardin F. Actual incidence of global left ventricular hypokinesia in adult septic shock. *Crit Care Med*. 2008;36:1701-6.
20. Fisher CJ, Jr., Agosti JM, Opal SM, Lowry SF, Balk RA, Sadoff JC, Abraham E, Schein RM and Benjamin E. Treatment of septic shock with the tumor necrosis factor receptor:Fc fusion protein. The Soluble TNF Receptor Sepsis Study Group. *N Engl J Med*. 1996;334:1697-702.
21. Abraham E, Laterre PF, Garbino J, Pingleton S, Butler T, Dugernier T, Margolis B, Kudsk K, Zimmerli W, Anderson P, Reynaert M, Lew D, Lesslauer W, Passe S, Cooper P, Burdeska A, Modi M, Leighton A, Salgo M, Van der Auwera P and Lenercept Study G. Lenercept (p55 tumor necrosis factor receptor fusion protein) in severe sepsis and early septic shock: a randomized, double-blind, placebo-controlled, multicenter phase III trial with 1,342 patients. *Crit Care Med*. 2001;29:503-10.
22. Opal SM, Fisher CJ, Jr., Dhainaut JF, Vincent JL, Brase R, Lowry SF, Sadoff JC, Slotman GJ, Levy H, Balk RA, Shelly MP, Pribble JP, LaBrecque JF, Lookabaugh J, Donovan H, Dubin H, Baughman R, Norman J, DeMaria E, Matzel K, Abraham E and Seneff M. Confirmatory interleukin-1 receptor antagonist trial in severe sepsis: a phase III, randomized, double-blind, placebo-controlled, multicenter trial. The Interleukin-1 Receptor Antagonist Sepsis Investigator Group. *Crit Care Med*. 1997;25:1115-24.
23. Kakihana Y, Ito T, Nakahara M, Yamaguchi K and Yasuda T. Sepsis-induced myocardial dysfunction: pathophysiology and management. *J Intensive Care*. 2016;4:22.
24. Hotchkiss RS and Karl IE. Reevaluation of the role of cellular hypoxia and bioenergetic failure in sepsis. *JAMA*. 1992;267:1503-10.
25. Cunnion RE, Schaer GL, Parker MM, Natanson C and Parrillo JE. The coronary circulation in human septic shock. *Circulation*. 1986;73:637-44.
26. Kumar A, Thota V, Dee L, Olson J, Uretz E and Parrillo JE. Tumor necrosis factor alpha and interleukin 1beta are responsible for in vitro myocardial cell depression induced by human septic shock serum. *J Exp Med*. 1996;183:949-58.
27. Finkel MS, Oddis CV, Jacob TD, Watkins SC, Hattler BG and Simmons RL. Negative inotropic effects of cytokines on the heart mediated by nitric oxide. *Science*. 1992;257:387-9.
28. Suliman HB, Welty-Wolf KE, Carraway M, Tatro L and Piantadosi CA. Lipopolysaccharide induces oxidative cardiac mitochondrial damage and biogenesis. *Cardiovasc Res*. 2004;64:279-88.
29. Stanzani G, Duchen MR and Singer M. The role of mitochondria in sepsis-induced cardiomyopathy. *Biochim Biophys Acta Mol Basis Dis*. 2019;1865:759-773.
30. Joseph LC, Kokkinaki D, Valenti MC, Kim GJ, Barca E, Tomar D, Hoffman NE, Subramanyam P, Colecraft HM, Hirano M, Ratner AJ, Madesh M, Drosatos K and Morrow JP. Inhibition of NADPH oxidase 2 (NOX2) prevents sepsis-induced cardiomyopathy by improving calcium handling and mitochondrial function. *JCI Insight*. 2017;2.
31. Trumbeckaite S, Opalka JR, Neuhof C, Zierz S and Gellerich FN. Different sensitivity of rabbit heart and skeletal muscle to endotoxin-induced impairment of mitochondrial function. *Eur J Biochem*. 2001;268:1422-9.

32. Larche J, Lancel S, Hassoun SM, Favory R, Decoster B, Marchetti P, Chopin C and Neviere R. Inhibition of mitochondrial permeability transition prevents sepsis-induced myocardial dysfunction and mortality. *J Am Coll Cardiol*. 2006;48:377-85.
33. Bohm M, Kirchmayr R, Gierschik P and Erdmann E. Increase of myocardial inhibitory G-proteins in catecholamine-refractory septic shock or in septic multiorgan failure. *Am J Med*. 1995;98:183-6.
34. Shepherd RE, Lang CH and McDonough KH. Myocardial adrenergic responsiveness after lethal and nonlethal doses of endotoxin. *Am J Physiol*. 1987;252:H410-6.
35. Chousterman BG, Swirski FK and Weber GF. Cytokine storm and sepsis disease pathogenesis. *Semin Immunopathol*. 2017;39:517-528.
36. Raeburn CD, Calkins CM, Zimmerman MA, Song Y, Ao L, Banerjee A, Harken AH and Meng X. ICAM-1 and VCAM-1 mediate endotoxemic myocardial dysfunction independent of neutrophil accumulation. *Am J Physiol Regul Integr Comp Physiol*. 2002;283:R477-86.
37. Raeburn CD, Calkins CM, Zimmerman MA, Song Y, Ao L, Banerjee A, Meng X and Harken AH. Vascular cell adhesion molecule--1 expression is obligatory for endotoxin-induced myocardial neutrophil accumulation and contractile dysfunction. *Surgery*. 2001;130:319-25.
38. Delano MJ and Ward PA. The immune system's role in sepsis progression, resolution, and long-term outcome. *Immunol Rev*. 2016;274:330-353.
39. Wang C, Wang Z, Wang G, Lau JY, Zhang K and Li W. COVID-19 in early 2021: current status and looking forward. *Signal Transduct Target Ther*. 2021;6:114.
40. Simonsen L and Viboud C. A comprehensive look at the COVID-19 pandemic death toll. *Elife*. 2021;10.
41. Polito MV, Silverio A, Bellino M, Iuliano G, Di Maio M, Alfano C, Iannece P, Esposito N and Galasso G. Cardiovascular Involvement in COVID-19: What Sequelae Should We Expect? *Cardiol Ther*. 2021;10:377-396.
42. Ferrucci L and Fabbri E. Inflammageing: chronic inflammation in ageing, cardiovascular disease, and frailty. *Nat Rev Cardiol*. 2018;15:505-522.
43. Lopez-Candales A, Hernandez Burgos PM, Hernandez-Suarez DF and Harris D. Linking Chronic Inflammation with Cardiovascular Disease: From Normal Aging to the Metabolic Syndrome. *J Nat Sci*. 2017;3.
44. Willerson JT and Ridker PM. Inflammation as a cardiovascular risk factor. *Circulation*. 2004;109:II2-10.
45. Luscher TF. Inflammation: the new cardiovascular risk factor. *Eur Heart J*. 2018;39:3483-3487.
46. Dhingra R and Vasan RS. Age as a risk factor. *Med Clin North Am*. 2012;96:87-91.
47. Yazdanyar A and Newman AB. The burden of cardiovascular disease in the elderly: morbidity, mortality, and costs. *Clin Geriatr Med*. 2009;25:563-77, vii.
48. Keller KM and Howlett SE. Sex Differences in the Biology and Pathology of the Aging Heart. *Can J Cardiol*. 2016;32:1065-73.
49. Rodgers JL, Jones J, Bolleddu SI, Vanthenapalli S, Rodgers LE, Shah K, Karia K and Panguluri SK. Cardiovascular Risks Associated with Gender and Aging. *J Cardiovasc Dev Dis*. 2019;6.

50. Zhou D, Borsa M and Simon AK. Hallmarks and detection techniques of cellular senescence and cellular ageing in immune cells. *Aging Cell*. 2021;20:e13316.
51. Hulsmans M, Sager HB, Roh JD, Valero-Munoz M, Houstis NE, Iwamoto Y, Sun Y, Wilson RM, Wojtkiewicz G, Tricot B, Osborne MT, Hung J, Vinegoni C, Naxerova K, Sosnovik DE, Zile MR, Bradshaw AD, Liao R, Tawakol A, Weissleder R, Rosenzweig A, Swirski FK, Sam F and Nahrendorf M. Cardiac macrophages promote diastolic dysfunction. *J Exp Med*. 2018;215:423-440.
52. Wang Y, Zhu S, Wei W, Tu Y, Chen C, Song J, Li J, Wang C, Xu Z and Sun S. Interleukin-6 knockout reverses macrophage differentiation imbalance and alleviates cardiac dysfunction in aging mice. *Aging (Albany NY)*. 2020;12:20184-20197.
53. Conti P and Shaik-Dasthagirisaeb Y. Atherosclerosis: a chronic inflammatory disease mediated by mast cells. *Cent Eur J Immunol*. 2015;40:380-6.
54. Rosenfeld ME. Inflammation and atherosclerosis: direct versus indirect mechanisms. *Curr Opin Pharmacol*. 2013;13:154-60.
55. Gombozhapova A, Rogovskaya Y, Shurupov V, Rebenkova M, Kzhyshkowska J, Popov SV, Karpov RS and Ryabov V. Macrophage activation and polarization in post-infarction cardiac remodeling. *J Biomed Sci*. 2017;24:13.
56. Han YL, Li YL, Jia LX, Cheng JZ, Qi YF, Zhang HJ and Du J. Reciprocal interaction between macrophages and T cells stimulates IFN-gamma and MCP-1 production in Ang II-induced cardiac inflammation and fibrosis. *PLoS One*. 2012;7:e35506.
57. Harel-Adar T, Ben Mordechai T, Amsalem Y, Feinberg MS, Leor J and Cohen S. Modulation of cardiac macrophages by phosphatidylserine-presenting liposomes improves infarct repair. *Proc Natl Acad Sci U S A*. 2011;108:1827-32.
58. Hohmann C, Pfister R, Mollenhauer M, Adler C, Kozlowski J, Wodarz A, Drebber U, Wippermann J and Michels G. Inflammatory cell infiltration in left atrial appendageal tissues of patients with atrial fibrillation and sinus rhythm. *Sci Rep*. 2020;10:1685.
59. Riehle C and Bauersachs J. Key inflammatory mechanisms underlying heart failure. *Herz*. 2019;44:96-106.
60. Dick SA and Epelman S. Chronic Heart Failure and Inflammation: What Do We Really Know? *Circ Res*. 2016;119:159-76.
61. Bertani B and Ruiz N. Function and Biogenesis of Lipopolysaccharides. *EcoSal Plus*. 2018;8.
62. Raetz CR and Whitfield C. Lipopolysaccharide endotoxins. *Annu Rev Biochem*. 2002;71:635-700.
63. Kalynych S, Morona R and Cygler M. Progress in understanding the assembly process of bacterial O-antigen. *FEMS Microbiol Rev*. 2014;38:1048-65.
64. Silipo A and Molinaro A. The diversity of the core oligosaccharide in lipopolysaccharides. *Subcell Biochem*. 2010;53:69-99.
65. Suffredini AF, Fromm RE, Parker MM, Brenner M, Kovacs JA, Wesley RA and Parrillo JE. The cardiovascular response of normal humans to the administration of endotoxin. *N Engl J Med*. 1989;321:280-7.
66. Dickson K and Lehmann C. Inflammatory Response to Different Toxins in Experimental Sepsis Models. *Int J Mol Sci*. 2019;20.

67. Copeland S, Warren HS, Lowry SF, Calvano SE, Remick D, Inflammation and the Host Response to Injury I. Acute inflammatory response to endotoxin in mice and humans. *Clin Diagn Lab Immunol*. 2005;12:60-7.
68. Seok J, Warren HS, Cuenca AG, Mindrinos MN, Baker HV, Xu W, Richards DR, McDonald-Smith GP, Gao H, Hennessy L, Finnerty CC, Lopez CM, Honari S, Moore EE, Minei JP, Cuschieri J, Bankey PE, Johnson JL, Sperry J, Nathens AB, Billiar TR, West MA, Jeschke MG, Klein MB, Gamelli RL, Gibran NS, Brownstein BH, Miller-Graziano C, Calvano SE, Mason PH, Cobb JP, Rahme LG, Lowry SF, Maier RV, Moldawer LL, Herndon DN, Davis RW, Xiao W, Tompkins RG, Inflammation and Host Response to Injury LSCRP. Genomic responses in mouse models poorly mimic human inflammatory diseases. *Proc Natl Acad Sci U S A*. 2013;110:3507-12.
69. Li D and Wu M. Pattern recognition receptors in health and diseases. *Signal Transduct Target Ther*. 2021;6:291.
70. Palsson-McDermott EM and O'Neill LA. Signal transduction by the lipopolysaccharide receptor, Toll-like receptor-4. *Immunology*. 2004;113:153-62.
71. Yang Y, Lv J, Jiang S, Ma Z, Wang D, Hu W, Deng C, Fan C, Di S, Sun Y and Yi W. The emerging role of Toll-like receptor 4 in myocardial inflammation. *Cell Death Dis*. 2016;7:e2234.
72. Charalambous BM, Stephens RC, Feavers IM and Montgomery HE. Role of bacterial endotoxin in chronic heart failure: the gut of the matter. *Shock*. 2007;28:15-23.
73. Kiechl S, Egger G, Mayr M, Wiedermann CJ, Bonora E, Oberhollenzer F, Muggeo M, Xu Q, Wick G, Poewe W and Willeit J. Chronic infections and the risk of carotid atherosclerosis: prospective results from a large population study. *Circulation*. 2001;103:1064-70.
74. Anker SD, Egerer KR, Volk HD, Kox WJ, Poole-Wilson PA and Coats AJ. Elevated soluble CD14 receptors and altered cytokines in chronic heart failure. *Am J Cardiol*. 1997;79:1426-30.
75. Peschel T, Schonauer M, Thiele H, Anker SD, Schuler G and Niebauer J. Invasive assessment of bacterial endotoxin and inflammatory cytokines in patients with acute heart failure. *Eur J Heart Fail*. 2003;5:609-14.
76. Krack A, Sharma R, Figulla HR and Anker SD. The importance of the gastrointestinal system in the pathogenesis of heart failure. *Eur Heart J*. 2005;26:2368-74.
77. Lequier LL, Nikaidoh H, Leonard SR, Bokovoy JL, White ML, Scannon PJ and Giroir BP. Preoperative and postoperative endotoxemia in children with congenital heart disease. *Chest*. 2000;117:1706-12.
78. Sharma R, Bolger AP, Li W, Davlouros PA, Volk HD, Poole-Wilson PA, Coats AJ, Gatzoulis MA and Anker SD. Elevated circulating levels of inflammatory cytokines and bacterial endotoxin in adults with congenital heart disease. *Am J Cardiol*. 2003;92:188-93.
79. Moludi J, Maleki V, Jafari-Vayghyan H, Vaghef-Mehrabany E and Alizadeh M. Metabolic endotoxemia and cardiovascular disease: A systematic review about potential roles of prebiotics and probiotics. *Clin Exp Pharmacol Physiol*. 2020;47:927-939.
80. Niebauer J, Volk HD, Kemp M, Dominguez M, Schumann RR, Rauchhaus M, Poole-Wilson PA, Coats AJ and Anker SD. Endotoxin and immune activation in chronic heart failure: a prospective cohort study. *Lancet*. 1999;353:1838-42.

81. Karagiannakis DS, Vlachogiannakos J, Anastasiadis G, Vafiadis-Zouboulis I and Ladas SD. Frequency and severity of cirrhotic cardiomyopathy and its possible relationship with bacterial endotoxemia. *Dig Dis Sci*. 2013;58:3029-36.
82. Wiedermann CJ, Kiechl S, Dunzendorfer S, Schratzberger P, Egger G, Oberhollenzer F and Willeit J. Association of endotoxemia with carotid atherosclerosis and cardiovascular disease: prospective results from the Bruneck Study. *J Am Coll Cardiol*. 1999;34:1975-81.
83. McIntyre CW, Harrison LE, Eldehni MT, Jefferies HJ, Szeto CC, John SG, Sigrist MK, Burton JO, Hothi D, Korsheed S, Owen PJ, Lai KB and Li PK. Circulating endotoxemia: a novel factor in systemic inflammation and cardiovascular disease in chronic kidney disease. *Clin J Am Soc Nephrol*. 2011;6:133-41.
84. Karnoutsos K, Papastergiou P, Stefanidis S and Vakaloudi A. Periodontitis as a risk factor for cardiovascular disease: the role of anti-phosphorylcholine and anti-cardiolipin antibodies. *Hippokratia*. 2008;12:144-9.
85. Beck JD, Offenbacher S, Williams R, Gibbs P and Garcia R. Periodontitis: a risk factor for coronary heart disease? *Ann Periodontol*. 1998;3:127-41.
86. Chaplin DD. Overview of the immune response. *J Allergy Clin Immunol*. 2010;125:S3-23.
87. Mann DL. The emerging role of innate immunity in the heart and vascular system: for whom the cell tolls. *Circ Res*. 2011;108:1133-45.
88. Frodermann V and Nahrendorf M. Neutrophil-macrophage cross-talk in acute myocardial infarction. *Eur Heart J*. 2017;38:198-200.
89. Sansonetti M, Waleczek FJG, Jung M, Thum T and Perbellini F. Resident cardiac macrophages: crucial modulators of cardiac (patho)physiology. *Basic Res Cardiol*. 2020;115:77.
90. Hulsmans M, Clauss S, Xiao L, Aguirre AD, King KR, Hanley A, Hucker WJ, Wulfers EM, Seemann G, Courties G, Iwamoto Y, Sun Y, Savol AJ, Sager HB, Lavine KJ, Fishbein GA, Capen DE, Da Silva N, Miquerol L, Wakimoto H, Seidman CE, Seidman JG, Sadreyev RI, Naxerova K, Mitchell RN, Brown D, Libby P, Weissleder R, Swirski FK, Kohl P, Vinegoni C, Milan DJ, Ellinor PT and Nahrendorf M. Macrophages Facilitate Electrical Conduction in the Heart. *Cell*. 2017;169:510-522 e20.
91. Heidt T, Courties G, Dutta P, Sager HB, Sebas M, Iwamoto Y, Sun Y, Da Silva N, Panizzi P, van der Laan AM, Swirski FK, Weissleder R and Nahrendorf M. Differential contribution of monocytes to heart macrophages in steady-state and after myocardial infarction. *Circ Res*. 2014;115:284-95.
92. Mantovani A, Cassatella MA, Costantini C and Jaillon S. Neutrophils in the activation and regulation of innate and adaptive immunity. *Nat Rev Immunol*. 2011;11:519-31.
93. Vafadarnejad E, Rizzo G, Krampert L, Arampatzi P, Arias-Loza AP, Nazzal Y, Rizakou A, Knochenhauer T, Bandi SR, Nugroho VA, Schulz DJJ, Roesch M, Alayrac P, Vilar J, Silvestre JS, Zernecke A, Saliba AE and Cochain C. Dynamics of Cardiac Neutrophil Diversity in Murine Myocardial Infarction. *Circ Res*. 2020;127:e232-e249.
94. Hotchkiss RS, Monneret G and Payen D. Sepsis-induced immunosuppression: from cellular dysfunctions to immunotherapy. *Nat Rev Immunol*. 2013;13:862-74.

95. Guo RF, Sun L, Gao H, Shi KX, Rittirsch D, Sarma VJ, Zetoune FS and Ward PA. In vivo regulation of neutrophil apoptosis by C5a during sepsis. *J Leukoc Biol*. 2006;80:1575-83.
96. Delano MJ, Kelly-Scumpia KM, Thayer TC, Winfield RD, Scumpia PO, Cuenca AG, Harrington PB, O'Malley KA, Warner E, Gabrilovich S, Mathews CE, Laface D, Heyworth PG, Ramphal R, Strieter RM, Moldawer LL and Efron PA. Neutrophil mobilization from the bone marrow during polymicrobial sepsis is dependent on CXCL12 signaling. *J Immunol*. 2011;187:911-8.
97. Demaret J, Venet F, Friggeri A, Cazalis MA, Plassais J, Jallades L, Malcus C, Poitevin-Later F, Textoris J, Lepape A and Monneret G. Marked alterations of neutrophil functions during sepsis-induced immunosuppression. *J Leukoc Biol*. 2015;98:1081-90.
98. Zucoloto AZ and Jenne CN. Platelet-Neutrophil Interplay: Insights Into Neutrophil Extracellular Trap (NET)-Driven Coagulation in Infection. *Front Cardiovasc Med*. 2019;6:85.
99. Carvalho-Tavares J, Hickey MJ, Hutchison J, Michaud J, Sutcliffe IT and Kubes P. A role for platelets and endothelial selectins in tumor necrosis factor-alpha-induced leukocyte recruitment in the brain microvasculature. *Circ Res*. 2000;87:1141-8.
100. Clark SR, Ma AC, Tavener SA, McDonald B, Goodarzi Z, Kelly MM, Patel KD, Chakrabarti S, McAvoy E, Sinclair GD, Keys EM, Allen-Vercoe E, Devinney R, Doig CJ, Green FH and Kubes P. Platelet TLR4 activates neutrophil extracellular traps to ensnare bacteria in septic blood. *Nat Med*. 2007;13:463-9.
101. Maugeri N, Campana L, Gavina M, Covino C, De Metrio M, Panciroli C, Maiuri L, Maseri A, D'Angelo A, Bianchi ME, Rovere-Querini P and Manfredi AA. Activated platelets present high mobility group box 1 to neutrophils, inducing autophagy and promoting the extrusion of neutrophil extracellular traps. *J Thromb Haemost*. 2014;12:2074-88.
102. Shi C and Pamer EG. Monocyte recruitment during infection and inflammation. *Nat Rev Immunol*. 2011;11:762-74.
103. Murray PJ, Allen JE, Biswas SK, Fisher EA, Gilroy DW, Goerdt S, Gordon S, Hamilton JA, Ivashkiv LB, Lawrence T, Locati M, Mantovani A, Martinez FO, Mege JL, Mosser DM, Natoli G, Saeij JP, Schultze JL, Shirey KA, Sica A, Suttles J, Udalova I, van Ginderachter JA, Vogel SN and Wynn TA. Macrophage activation and polarization: nomenclature and experimental guidelines. *Immunity*. 2014;41:14-20.
104. Mantovani A, Sica A, Sozzani S, Allavena P, Vecchi A and Locati M. The chemokine system in diverse forms of macrophage activation and polarization. *Trends Immunol*. 2004;25:677-86.
105. Verreck FA, de Boer T, Langenberg DM, Hoeve MA, Kramer M, Vaisberg E, Kastelein R, Kolk A, de Waal-Malefyt R and Ottenhoff TH. Human IL-23-producing type 1 macrophages promote but IL-10-producing type 2 macrophages subvert immunity to (myco)bacteria. *Proc Natl Acad Sci U S A*. 2004;101:4560-5.
106. Mosser DM. The many faces of macrophage activation. *J Leukoc Biol*. 2003;73:209-12.
107. Honold L and Nahrendorf M. Resident and Monocyte-Derived Macrophages in Cardiovascular Disease. *Circ Res*. 2018;122:113-127.

108. Dai M, Wu L, He Z, Zhang S, Chen C, Xu X, Wang P, Gruzdev A, Zeldin DC and Wang DW. Epoxyeicosatrienoic acids regulate macrophage polarization and prevent LPS-induced cardiac dysfunction. *J Cell Physiol*. 2015;230:2108-19.
109. Mahbub S, Deburghgraeve CR and Kovacs EJ. Advanced age impairs macrophage polarization. *J Interferon Cytokine Res*. 2012;32:18-26.
110. Karuppagounder V, Giridharan VV, Arumugam S, Sreedhar R, Palaniyandi SS, Krishnamurthy P, Quevedo J, Watanabe K, Konishi T and Thandavarayan RA. Modulation of Macrophage Polarization and HMGB1-TLR2/TLR4 Cascade Plays a Crucial Role for Cardiac Remodeling in Senescence-Accelerated Prone Mice. *PLoS One*. 2016;11:e0152922.
111. Epelman S, Lavine KJ, Beaudin AE, Sojka DK, Carrero JA, Calderon B, Brija T, Gautier EL, Ivanov S, Satpathy AT, Schilling JD, Schwendener R, Sergin I, Razani B, Forsberg EC, Yokoyama WM, Unanue ER, Colonna M, Randolph GJ and Mann DL. Embryonic and adult-derived resident cardiac macrophages are maintained through distinct mechanisms at steady state and during inflammation. *Immunity*. 2014;40:91-104.
112. Leid J, Carrelha J, Boukarabila H, Epelman S, Jacobsen SE and Lavine KJ. Primitive Embryonic Macrophages are Required for Coronary Development and Maturation. *Circ Res*. 2016;118:1498-511.
113. Molawi K, Wolf Y, Kandalla PK, Favret J, Hagemeyer N, Frenzel K, Pinto AR, Klapproth K, Henri S, Malissen B, Rodewald HR, Rosenthal NA, Bajenoff M, Prinz M, Jung S and Sieweke MH. Progressive replacement of embryo-derived cardiac macrophages with age. *J Exp Med*. 2014;211:2151-8.
114. Gomez Perdiguero E, Klapproth K, Schulz C, Busch K, Azzoni E, Crozet L, Garner H, Trouillet C, de Bruijn MF, Geissmann F and Rodewald HR. Tissue-resident macrophages originate from yolk-sac-derived erythro-myeloid progenitors. *Nature*. 2015;518:547-51.
115. Hashimoto D, Chow A, Noizat C, Teo P, Beasley MB, Leboeuf M, Becker CD, See P, Price J, Lucas D, Greter M, Mortha A, Boyer SW, Forsberg EC, Tanaka M, van Rooijen N, Garcia-Sastre A, Stanley ER, Ginhoux F, Frenette PS and Merad M. Tissue-resident macrophages self-maintain locally throughout adult life with minimal contribution from circulating monocytes. *Immunity*. 2013;38:792-804.
116. Chakarov S, Lim HY, Tan L, Lim SY, See P, Lum J, Zhang XM, Foo S, Nakamizo S, Duan K, Kong WT, Gentek R, Balachander A, Carbajo D, Bleriot C, Malleret B, Tam JKC, Baig S, Shabeer M, Toh SES, Schlitzer A, Larbi A, Marichal T, Malissen B, Chen J, Poidinger M, Kabashima K, Bajenoff M, Ng LG, Angeli V and Ginhoux F. Two distinct interstitial macrophage populations coexist across tissues in specific subtissular niches. *Science*. 2019;363.
117. Pinto AR, Paolicelli R, Salimova E, Gospocic J, Slonimsky E, Bilbao-Cortes D, Godwin JW and Rosenthal NA. An abundant tissue macrophage population in the adult murine heart with a distinct alternatively-activated macrophage profile. *PLoS One*. 2012;7:e36814.
118. Bajpai G, Schneider C, Wong N, Bredemeyer A, Hulsmans M, Nahrendorf M, Epelman S, Kreisel D, Liu Y, Itoh A, Shankar TS, Selzman CH, Drakos SG and Lavine KJ. The human heart contains distinct macrophage subsets with divergent origins and functions. *Nat Med*. 2018;24:1234-1245.

119. Grazioli S and Pugin J. Mitochondrial Damage-Associated Molecular Patterns: From Inflammatory Signaling to Human Diseases. *Front Immunol*. 2018;9:832.
120. Mogensen TH. Pathogen recognition and inflammatory signaling in innate immune defenses. *Clin Microbiol Rev*. 2009;22:240-73, Table of Contents.
121. Roh JS and Sohn DH. Damage-Associated Molecular Patterns in Inflammatory Diseases. *Immune Netw*. 2018;18:e27.
122. Amarante-Mendes GP, Adjemian S, Branco LM, Zanetti LC, Weinlich R and Bortoluci KR. Pattern Recognition Receptors and the Host Cell Death Molecular Machinery. *Front Immunol*. 2018;9:2379.
123. Lien E, Means TK, Heine H, Yoshimura A, Kusumoto S, Fukase K, Fenton MJ, Oikawa M, Qureshi N, Monks B, Finberg RW, Ingalls RR and Golenbock DT. Toll-like receptor 4 imparts ligand-specific recognition of bacterial lipopolysaccharide. *J Clin Invest*. 2000;105:497-504.
124. Yang RB, Mark MR, Gray A, Huang A, Xie MH, Zhang M, Goddard A, Wood WI, Gurney AL and Godowski PJ. Toll-like receptor-2 mediates lipopolysaccharide-induced cellular signalling. *Nature*. 1998;395:284-8.
125. Gong T, Liu L, Jiang W and Zhou R. DAMP-sensing receptors in sterile inflammation and inflammatory diseases. *Nat Rev Immunol*. 2020;20:95-112.
126. Morrell CN, Aggrey AA, Chapman LM and Modjeski KL. Emerging roles for platelets as immune and inflammatory cells. *Blood*. 2014;123:2759-67.
127. Boyd JH, Mathur S, Wang Y, Bateman RM and Walley KR. Toll-like receptor stimulation in cardiomyoctes decreases contractility and initiates an NF-kappaB dependent inflammatory response. *Cardiovasc Res*. 2006;72:384-93.
128. Fallach R, Shainberg A, Avlas O, Fainblut M, Chepurko Y, Porat E and Hochhauser E. Cardiomyocyte Toll-like receptor 4 is involved in heart dysfunction following septic shock or myocardial ischemia. *J Mol Cell Cardiol*. 2010;48:1236-44.
129. Katare PB, Nizami HL, Paramesha B, Dinda AK and Banerjee SK. Activation of toll like receptor 4 (TLR4) promotes cardiomyocyte apoptosis through SIRT2 dependent p53 deacetylation. *Sci Rep*. 2020;10:19232.
130. Altan-Bonnet G and Mukherjee R. Cytokine-mediated communication: a quantitative appraisal of immune complexity. *Nat Rev Immunol*. 2019;19:205-217.
131. Comstock KL, Krown KA, Page MT, Martin D, Ho P, Pedraza M, Castro EN, Nakajima N, Glembotski CC, Quintana PJ and Sabbadini RA. LPS-induced TNF-alpha release from and apoptosis in rat cardiomyocytes: obligatory role for CD14 in mediating the LPS response. *J Mol Cell Cardiol*. 1998;30:2761-75.
132. Chaudhry H, Zhou J, Zhong Y, Ali MM, McGuire F, Nagarkatti PS and Nagarkatti M. Role of cytokines as a double-edged sword in sepsis. *In Vivo*. 2013;27:669-84.
133. Thijs LG and Hack CE. Time course of cytokine levels in sepsis. *Intensive Care Med*. 1995;21 Suppl 2:S258-63.
134. Mera S, Tatulescu D, Cismaru C, Bondor C, Slavcovici A, Zanc V, Carstina D and Oltean M. Multiplex cytokine profiling in patients with sepsis. *APMIS*. 2011;119:155-63.
135. Gogos CA, Drosou E, Bassaris HP and Skoutelis A. Pro- versus anti-inflammatory cytokine profile in patients with severe sepsis: a marker for prognosis and future therapeutic options. *J Infect Dis*. 2000;181:176-80.
136. Deshmane SL, Kremlev S, Amini S and Sawaya BE. Monocyte chemoattractant protein-1 (MCP-1): an overview. *J Interferon Cytokine Res*. 2009;29:313-26.

137. Roche JK, Keepers TR, Gross LK, Seaner RM and Obrig TG. CXCL1/KC and CXCL2/MIP-2 are critical effectors and potential targets for therapy of Escherichia coli O157:H7-associated renal inflammation. *Am J Pathol*. 2007;170:526-37.
138. Ness TL, Carpenter KJ, Ewing JL, Gerard CJ, Hogaboam CM and Kunkel SL. CCR1 and CC chemokine ligand 5 interactions exacerbate innate immune responses during sepsis. *J Immunol*. 2004;173:6938-48.
139. Dorner BG, Scheffold A, Rolph MS, Huser MB, Kaufmann SH, Radbruch A, Flesch IE and Kroczek RA. MIP-1alpha, MIP-1beta, RANTES, and ATAC/lymphotactin function together with IFN-gamma as type 1 cytokines. *Proc Natl Acad Sci U S A*. 2002;99:6181-6.
140. Kelley N, Jeltema D, Duan Y and He Y. The NLRP3 Inflammasome: An Overview of Mechanisms of Activation and Regulation. *Int J Mol Sci*. 2019;20.
141. Swanson KV, Deng M and Ting JP. The NLRP3 inflammasome: molecular activation and regulation to therapeutics. *Nat Rev Immunol*. 2019;19:477-489.
142. He Y, Hara H and Nunez G. Mechanism and Regulation of NLRP3 Inflammasome Activation. *Trends Biochem Sci*. 2016;41:1012-1021.
143. Bauernfeind FG, Horvath G, Stutz A, Alnemri ES, MacDonald K, Speert D, Fernandes-Alnemri T, Wu J, Monks BG, Fitzgerald KA, Hornung V and Latz E. Cutting edge: NF-kappaB activating pattern recognition and cytokine receptors license NLRP3 inflammasome activation by regulating NLRP3 expression. *J Immunol*. 2009;183:787-91.
144. Franchi L, Eigenbrod T and Nunez G. Cutting edge: TNF-alpha mediates sensitization to ATP and silica via the NLRP3 inflammasome in the absence of microbial stimulation. *J Immunol*. 2009;183:792-6.
145. Munoz-Planillo R, Kuffa P, Martinez-Colon G, Smith BL, Rajendiran TM and Nunez G. K(+) efflux is the common trigger of NLRP3 inflammasome activation by bacterial toxins and particulate matter. *Immunity*. 2013;38:1142-53.
146. Liu M, Zhang SS, Liu DN, Yang YL, Wang YH and Du GH. Chrysomycin A Attenuates Neuroinflammation by Down-Regulating NLRP3/Cleaved Caspase-1 Signaling Pathway in LPS-Stimulated Mice and BV2 Cells. *Int J Mol Sci*. 2021;22.
147. Shi J, Zhao Y, Wang K, Shi X, Wang Y, Huang H, Zhuang Y, Cai T, Wang F and Shao F. Cleavage of GSDMD by inflammatory caspases determines pyroptotic cell death. *Nature*. 2015;526:660-5.
148. Sborgi L, Ruhl S, Mulvihill E, Pipercevic J, Heilig R, Stahlberg H, Farady CJ, Muller DJ, Broz P and Hiller S. GSDMD membrane pore formation constitutes the mechanism of pyroptotic cell death. *EMBO J*. 2016;35:1766-78.
149. Evavold CL, Ruan J, Tan Y, Xia S, Wu H and Kagan JC. The Pore-Forming Protein Gasdermin D Regulates Interleukin-1 Secretion from Living Macrophages. *Immunity*. 2018;48:35-44 e6.
150. Broz P, Pelegrin P and Shao F. The gasdermins, a protein family executing cell death and inflammation. *Nat Rev Immunol*. 2020;20:143-157.
151. Gaidt MM and Hornung V. Pore formation by GSDMD is the effector mechanism of pyroptosis. *EMBO J*. 2016;35:2167-2169.
152. Liu X, Zhang Z, Ruan J, Pan Y, Magupalli VG, Wu H and Lieberman J. Inflammasome-activated gasdermin D causes pyroptosis by forming membrane pores. *Nature*. 2016;535:153-8.

153. Kayagaki N, Stowe IB, Lee BL, O'Rourke K, Anderson K, Warming S, Cuellar T, Haley B, Roose-Girma M, Phung QT, Liu PS, Lill JR, Li H, Wu J, Kummerfeld S, Zhang J, Lee WP, Snipas SJ, Salvesen GS, Morris LX, Fitzgerald L, Zhang Y, Bertram EM, Goodnow CC and Dixit VM. Caspase-11 cleaves gasdermin D for non-canonical inflammasome signalling. *Nature*. 2015;526:666-71.
154. Ruhl S and Broz P. Caspase-11 activates a canonical NLRP3 inflammasome by promoting K(+) efflux. *Eur J Immunol*. 2015;45:2927-36.
155. Shimada K, Crother TR, Karlin J, Dagvadorj J, Chiba N, Chen S, Ramanujan VK, Wolf AJ, Vergnes L, Ojcius DM, Rentsendorj A, Vargas M, Guerrero C, Wang Y, Fitzgerald KA, Underhill DM, Town T and Arditi M. Oxidized mitochondrial DNA activates the NLRP3 inflammasome during apoptosis. *Immunity*. 2012;36:401-14.
156. Dudek J. Role of Cardiolipin in Mitochondrial Signaling Pathways. *Front Cell Dev Biol*. 2017;5:90.
157. Iyer SS, He Q, Janczy JR, Elliott EI, Zhong Z, Olivier AK, Sadler JJ, Knepper-Adrian V, Han R, Qiao L, Eisenbarth SC, Nauseef WM, Cassel SL and Sutterwala FS. Mitochondrial cardiolipin is required for Nlrp3 inflammasome activation. *Immunity*. 2013;39:311-323.
158. Luo H, Mu WC, Karki R, Chiang HH, Mohrin M, Shin JJ, Ohkubo R, Ito K, Kanneganti TD and Chen D. Mitochondrial Stress-Initiated Aberrant Activation of the NLRP3 Inflammasome Regulates the Functional Deterioration of Hematopoietic Stem Cell Aging. *Cell Rep*. 2019;26:945-954 e4.
159. Park S, Won JH, Hwang I, Hong S, Lee HK and Yu JW. Defective mitochondrial fission augments NLRP3 inflammasome activation. *Sci Rep*. 2015;5:15489.
160. Ichinohe T, Yamazaki T, Koshiba T and Yanagi Y. Mitochondrial protein mitofusin 2 is required for NLRP3 inflammasome activation after RNA virus infection. *Proc Natl Acad Sci U S A*. 2013;110:17963-8.
161. Cimolai MC, Alvarez S, Bode C and Bugger H. Mitochondrial Mechanisms in Septic Cardiomyopathy. *Int J Mol Sci*. 2015;16:17763-78.
162. Haileselassie B, Mukherjee R, Joshi AU, Napier BA, Massis LM, Ostberg NP, Queliconi BB, Monack D, Bernstein D and Mochly-Rosen D. Drp1/Fis1 interaction mediates mitochondrial dysfunction in septic cardiomyopathy. *J Mol Cell Cardiol*. 2019;130:160-169.
163. Kapetanovic R, Afroz SF, Ramnath D, Lawrence GM, Okada T, Curson JE, de Bruin J, Fairlie DP, Schroder K, St John JC, Blumenthal A and Sweet MJ. Lipopolysaccharide promotes Drp1-dependent mitochondrial fission and associated inflammatory responses in macrophages. *Immunol Cell Biol*. 2020;98:528-539.
164. Samokhvalov V, Jamieson KL, Darwesh AM, Keshavarz-Bahaghighat H, Lee TYT, Edin M, Lih F, Zeldin DC and Seubert JM. Deficiency of Soluble Epoxide Hydrolase Protects Cardiac Function Impaired by LPS-Induced Acute Inflammation. *Front Pharmacol*. 2018;9:1572.
165. Zang QS, Sadek H, Maass DL, Martinez B, Ma L, Kilgore JA, Williams NS, Frantz DE, Wigginton JG, Nwariaku FE, Wolf SE and Minei JP. Specific inhibition of mitochondrial oxidative stress suppresses inflammation and improves cardiac function in a rat pneumonia-related sepsis model. *Am J Physiol Heart Circ Physiol*. 2012;302:H1847-59.
166. Church LD, Cook GP and McDermott MF. Primer: inflammasomes and interleukin 1beta in inflammatory disorders. *Nat Clin Pract Rheumatol*. 2008;4:34-42.

167. Chen G, Chelu MG, Dobrev D and Li N. Cardiomyocyte Inflammasome Signaling in Cardiomyopathies and Atrial Fibrillation: Mechanisms and Potential Therapeutic Implications. *Front Physiol*. 2018;9:1115.
168. Mezzaroma E, Toldo S, Farkas D, Seropian IM, Van Tassell BW, Salloum FN, Kannan HR, Menna AC, Voelkel NF and Abbate A. The inflammasome promotes adverse cardiac remodeling following acute myocardial infarction in the mouse. *Proc Natl Acad Sci U S A*. 2011;108:19725-30.
169. Luo B, Li B, Wang W, Liu X, Xia Y, Zhang C, Zhang M, Zhang Y and An F. NLRP3 gene silencing ameliorates diabetic cardiomyopathy in a type 2 diabetes rat model. *PLoS One*. 2014;9:e104771.
170. Yao C, Veleva T, Scott L, Jr., Cao S, Li L, Chen G, Jeyabal P, Pan X, Alsina KM, Abu-Taha ID, Ghezelbash S, Reynolds CL, Shen YH, LeMaire SA, Schmitz W, Muller FU, El-Armouche A, Tony Eissa N, Beeton C, Nattel S, Wehrens XHT, Dobrev D and Li N. Enhanced Cardiomyocyte NLRP3 Inflammasome Signaling Promotes Atrial Fibrillation. *Circulation*. 2018;138:2227-2242.
171. Coll RC, Robertson AA, Chae JJ, Higgins SC, Munoz-Planillo R, Inserra MC, Vetter I, Dungan LS, Monks BG, Stutz A, Croker DE, Butler MS, Haneklaus M, Sutton CE, Nunez G, Latz E, Kastner DL, Mills KH, Masters SL, Schroder K, Cooper MA and O'Neill LA. A small-molecule inhibitor of the NLRP3 inflammasome for the treatment of inflammatory diseases. *Nat Med*. 2015;21:248-55.
172. Shao BZ, Xu ZQ, Han BZ, Su DF and Liu C. NLRP3 inflammasome and its inhibitors: a review. *Front Pharmacol*. 2015;6:262.
173. van Hout GP, Bosch L, Ellenbroek GH, de Haan JJ, van Solinge WW, Cooper MA, Arslan F, de Jager SC, Robertson AA, Pasterkamp G and Hoefer IE. The selective NLRP3-inflammasome inhibitor MCC950 reduces infarct size and preserves cardiac function in a pig model of myocardial infarction. *Eur Heart J*. 2017;38:828-836.
174. van der Heijden T, Kritikou E, Venema W, van Duijn J, van Santbrink PJ, Slutter B, Foks AC, Bot I and Kuiper J. NLRP3 Inflammasome Inhibition by MCC950 Reduces Atherosclerotic Lesion Development in Apolipoprotein E-Deficient Mice-Brief Report. *Arterioscler Thromb Vasc Biol*. 2017;37:1457-1461.
175. Zhang L, Jiang YH, Fan C, Zhang Q, Jiang YH, Li Y and Xue YT. MCC950 attenuates doxorubicin-induced myocardial injury in vivo and in vitro by inhibiting NLRP3-mediated pyroptosis. *Biomed Pharmacother*. 2021;143:112133.
176. Li S, Guo Z and Zhang ZY. Protective effects of NLRP3 inhibitor MCC950 on sepsis-induced myocardial dysfunction. *J Biol Regul Homeost Agents*. 2021;35:141-150.
177. Anderson TJ, Gregoire J, Pearson GJ, Barry AR, Couture P, Dawes M, Francis GA, Genest J, Jr., Grover S, Gupta M, Hegele RA, Lau DC, Leiter LA, Lonn E, Mancini GB, McPherson R, Ngui D, Poirier P, Sievenpiper JL, Stone JA, Thanassoulis G and Ward R. 2016 Canadian Cardiovascular Society Guidelines for the Management of Dyslipidemia for the Prevention of Cardiovascular Disease in the Adult. *Can J Cardiol*. 2016;32:1263-1282.
178. Bang HO, Dyerberg J and Nielsen AB. Plasma lipid and lipoprotein pattern in Greenlandic West-coast Eskimos. *Lancet*. 1971;1:1143-5.
179. Dyerberg J and Bang HO. Haemostatic function and platelet polyunsaturated fatty acids in Eskimos. *Lancet*. 1979;2:433-5.
180. Dyerberg J, Bang HO, Stoffersen E, Moncada S and Vane JR. Eicosapentaenoic acid and prevention of thrombosis and atherosclerosis? *Lancet*. 1978;2:117-9.

181. Bang HO and Dyerberg J. Plasma lipids and lipoproteins in Greenlandic west coast Eskimos. *Acta Med Scand*. 1972;192:85-94.
182. Gryglewski RJ, Salmon JA, Ubatuba FB, Weatherly BC, Moncada S and Vane JR. Effects of all cis-5,8,11,14,17 eicosapentaenoic acid and PGH3 on platelet aggregation. *Prostaglandins*. 1979;18:453-78.
183. Bays HE, Ballantyne CM, Kastelein JJ, Isaacsohn JL, Braeckman RA and Soni PN. Eicosapentaenoic acid ethyl ester (AMR101) therapy in patients with very high triglyceride levels (from the Multi-center, plAcebo-controlled, Randomized, double-blINd, 12-week study with an open-label Extension [MARINE] trial). *Am J Cardiol*. 2011;108:682-90.
184. Investigators G-P. Dietary supplementation with n-3 polyunsaturated fatty acids and vitamin E after myocardial infarction: results of the GISSI-Prevenzione trial. Gruppo Italiano per lo Studio della Sopravvivenza nell'Infarto miocardico. *Lancet*. 1999;354:447-55.
185. Burr ML, Fehily AM, Gilbert JF, Rogers S, Holliday RM, Sweetnam PM, Elwood PC and Deadman NM. Effects of changes in fat, fish, and fibre intakes on death and myocardial reinfarction: diet and reinfarction trial (DART). *Lancet*. 1989;2:757-61.
186. Heydari B, Abdullah S, Pottala JV, Shah R, Abbasi S, Mandry D, Francis SA, Lumish H, Ghoshhajra BB, Hoffmann U, Appelbaum E, Feng JH, Blankstein R, Steigner M, McConnell JP, Harris W, Antman EM, Jerosch-Herold M and Kwong RY. Effect of Omega-3 Acid Ethyl Esters on Left Ventricular Remodeling After Acute Myocardial Infarction: The OMEGA-REMODEL Randomized Clinical Trial. *Circulation*. 2016;134:378-91.
187. Galan P, Briancon S, Blacher J, Czernichow S and Hercberg S. The SU.FOL.OM3 Study: a secondary prevention trial testing the impact of supplementation with folate and B-vitamins and/or Omega-3 PUFA on fatal and non fatal cardiovascular events, design, methods and participants characteristics. *Trials*. 2008;9:35.
188. Blacher J, Czernichow S, Paillard F, Ducimetiere P, Hercberg S, Galan P and Group SFOSR. Cardiovascular effects of B-vitamins and/or N-3 fatty acids: the SU.FOL.OM3 trial. *Int J Cardiol*. 2013;167:508-13.
189. Bowman L, Mafham M, Wallendszus K, Stevens W, Buck G, Barton J, Murphy K, Aung T, Haynes R, Cox J, Murawska A, Young A, Lay M, Chen F, Sammons E, Waters E, Adler A, Bodansky J, Farmer A, McPherson R, Neil A, Simpson D, Peto R, Baigent C, Collins R, Parish S, Armitage J and Group ASC. Effects of n-3 Fatty Acid Supplements in Diabetes Mellitus. *N Engl J Med*. 2018;379:1540-1550.
190. Investigators OT, Bosch J, Gerstein HC, Dagenais GR, Diaz R, Dyal L, Jung H, Maggiono AP, Probstfield J, Ramachandran A, Riddle MC, Ryden LE and Yusuf S. n-3 fatty acids and cardiovascular outcomes in patients with dysglycemia. *N Engl J Med*. 2012;367:309-18.
191. Siscovick DS, Barringer TA, Fretts AM, Wu JH, Lichtenstein AH, Costello RB, Kris-Etherton PM, Jacobson TA, Engler MB, Alger HM, Appel LJ, Mozaffarian D, American Heart Association Nutrition Committee of the Council on L, Cardiometabolic H, Council on E, Prevention, Council on Cardiovascular Disease in the Y, Council on C, Stroke N and Council on Clinical C. Omega-3 Polyunsaturated Fatty Acid (Fish Oil) Supplementation and the Prevention of Clinical Cardiovascular Disease: A Science Advisory From the American Heart Association. *Circulation*. 2017;135:e867-e884.

192. Endres S, Ghorbani R, Kelley VE, Georgilis K, Lonnemann G, van der Meer JW, Cannon JG, Rogers TS, Klempner MS, Weber PC and et al. The effect of dietary supplementation with n-3 polyunsaturated fatty acids on the synthesis of interleukin-1 and tumor necrosis factor by mononuclear cells. *N Engl J Med*. 1989;320:265-71.
193. Darwesh AM, Bassiouni W, Sosnowski DK and Seubert JM. Can N-3 polyunsaturated fatty acids be considered a potential adjuvant therapy for COVID-19-associated cardiovascular complications? *Pharmacol Ther*. 2021;219:107703.
194. Westphal C, Konkel A and Schunck WH. Cytochrome p450 enzymes in the bioactivation of polyunsaturated Fatty acids and their role in cardiovascular disease. *Adv Exp Med Biol*. 2015;851:151-87.
195. Blok WL, Katan MB and van der Meer JW. Modulation of inflammation and cytokine production by dietary (n-3) fatty acids. *J Nutr*. 1996;126:1515-33.
196. Yan A, Zhang T, Yang X, Shao J, Fu N, Shen F, Fu Y and Xia W. Thromboxane A2 receptor antagonist SQ29548 reduces ischemic stroke-induced microglia/macrophages activation and enrichment, and ameliorates brain injury. *Sci Rep*. 2016;6:35885.
197. Brouard C and Pascaud M. Effects of moderate dietary supplementations with n-3 fatty acids on macrophage and lymphocyte phospholipids and macrophage eicosanoid synthesis in the rat. *Biochim Biophys Acta*. 1990;1047:19-28.
198. Careaga-Houck M and Sprecher H. Effect of a fish oil diet on the composition of rat neutrophil lipids and the molecular species of choline and ethanolamine glycerophospholipids. *J Lipid Res*. 1989;30:77-87.
199. Gibney MJ and Hunter B. The effects of short- and long-term supplementation with fish oil on the incorporation of n-3 polyunsaturated fatty acids into cells of the immune system in healthy volunteers. *Eur J Clin Nutr*. 1993;47:255-9.
200. Browning LM, Walker CG, Mander AP, West AL, Madden J, Gambell JM, Young S, Wang L, Jebb SA and Calder PC. Incorporation of eicosapentaenoic and docosahexaenoic acids into lipid pools when given as supplements providing doses equivalent to typical intakes of oily fish. *Am J Clin Nutr*. 2012;96:748-58.
201. Chapkin RS, Akoh CC and Miller CC. Influence of dietary n-3 fatty acids on macrophage glycerophospholipid molecular species and peptidoleukotriene synthesis. *J Lipid Res*. 1991;32:1205-13.
202. Darwesh AM, Sosnowski DK, Lee TY, Keshavarz-Bahaghighat H and Seubert JM. Insights into the cardioprotective properties of n-3 PUFAs against ischemic heart disease via modulation of the innate immune system. *Chem Biol Interact*. 2019;308:20-44.
203. Hazen SL, Ford DA and Gross RW. Activation of a membrane-associated phospholipase A2 during rabbit myocardial ischemia which is highly selective for plasmalogen substrate. *J Biol Chem*. 1991;266:5629-33.
204. Corey EJ, Shih C and Cashman JR. Docosahexaenoic acid is a strong inhibitor of prostaglandin but not leukotriene biosynthesis. *Proc Natl Acad Sci U S A*. 1983;80:3581-4.
205. De Caterina R and Massaro M. Omega-3 fatty acids and the regulation of expression of endothelial pro-atherogenic and pro-inflammatory genes. *J Membr Biol*. 2005;206:103-16.
206. Calder PC. N-3 polyunsaturated fatty acids and inflammation: from molecular biology to the clinic. *Lipids*. 2003;38:343-52.
207. Duda MK, O'Shea KM, Tintinu A, Xu W, Khairallah RJ, Barrows BR, Chess DJ, Azimzadeh AM, Harris WS, Sharov VG, Sabbah HN and Stanley WC. Fish oil, but not

flaxseed oil, decreases inflammation and prevents pressure overload-induced cardiac dysfunction. *Cardiovasc Res*. 2009;81:319-27.
208. Lucas D, Goulitquer S, Marienhagen J, Fer M, Dreano Y, Schwaneberg U, Amet Y and Corcos L. Stereoselective epoxidation of the last double bond of polyunsaturated fatty acids by human cytochromes P450. *J Lipid Res*. 2010;51:1125-33.
209. Myasoedova KN. New findings in studies of cytochromes P450. *Biochemistry (Mosc)*. 2008;73:965-9.
210. Delozier TC, Kissling GE, Coulter SJ, Dai D, Foley JF, Bradbury JA, Murphy E, Steenbergen C, Zeldin DC and Goldstein JA. Detection of human CYP2C8, CYP2C9, and CYP2J2 in cardiovascular tissues. *Drug Metab Dispos*. 2007;35:682-8.
211. Hammer H, Schmidt F, Marx-Stoelting P, Potz O and Braeuning A. Cross-species analysis of hepatic cytochrome P450 and transport protein expression. *Arch Toxicol*. 2021;95:117-133.
212. Graves JP, Edin ML, Bradbury JA, Gruzdev A, Cheng J, Lih FB, Masinde TA, Qu W, Clayton NP, Morrison JP, Tomer KB and Zeldin DC. Characterization of four new mouse cytochrome P450 enzymes of the CYP2J subfamily. *Drug Metab Dispos*. 2013;41:763-73.
213. Zhou GL, Beloiartsev A, Yu B, Baron DM, Zhou W, Niedra R, Lu N, Tainsh LT, Zapol WM, Seed B and Bloch KD. Deletion of the murine cytochrome P450 Cyp2j locus by fused BAC-mediated recombination identifies a role for Cyp2j in the pulmonary vascular response to hypoxia. *PLoS Genet*. 2013;9:e1003950.
214. Seubert J, Yang B, Bradbury JA, Graves J, Degraff LM, Gabel S, Gooch R, Foley J, Newman J, Mao L, Rockman HA, Hammock BD, Murphy E and Zeldin DC. Enhanced postischemic functional recovery in CYP2J2 transgenic hearts involves mitochondrial ATP-sensitive K+ channels and p42/p44 MAPK pathway. *Circ Res*. 2004;95:506-14.
215. Ma B, Xiong X, Chen C, Li H, Xu X, Li X, Li R, Chen G, Dackor RT, Zeldin DC and Wang DW. Cardiac-specific overexpression of CYP2J2 attenuates diabetic cardiomyopathy in male streptozotocin-induced diabetic mice. *Endocrinology*. 2013;154:2843-56.
216. Westphal C, Spallek B, Konkel A, Marko L, Qadri F, DeGraff LM, Schubert C, Bradbury JA, Regitz-Zagrosek V, Falck JR, Zeldin DC, Muller DN, Schunck WH and Fischer R. CYP2J2 overexpression protects against arrhythmia susceptibility in cardiac hypertrophy. *PLoS One*. 2013;8:e73490.
217. Evangelista EA, Aliwarga T, Sotoodehnia N, Jensen PN, McKnight B, Lemaitre RN, Totah RA and Gharib SA. CYP2J2 Modulates Diverse Transcriptional Programs in Adult Human Cardiomyocytes. *Sci Rep*. 2020;10:5329.
218. Evangelista EA, Lemaitre RN, Sotoodehnia N, Gharib SA and Totah RA. CYP2J2 Expression in Adult Ventricular Myocytes Protects Against Reactive Oxygen Species Toxicity. *Drug Metab Dispos*. 2018;46:380-386.
219. Zarghi A and Arfaei S. Selective COX-2 Inhibitors: A Review of Their Structure-Activity Relationships. *Iran J Pharm Res*. 2011;10:655-83.
220. Blobaum AL and Marnett LJ. Structural and functional basis of cyclooxygenase inhibition. *J Med Chem*. 2007;50:1425-41.
221. Konkel A and Schunck WH. Role of cytochrome P450 enzymes in the bioactivation of polyunsaturated fatty acids. *Biochim Biophys Acta*. 2011;1814:210-22.

222. Schunck WH, Konkel A, Fischer R and Weylandt KH. Therapeutic potential of omega-3 fatty acid-derived epoxyeicosanoids in cardiovascular and inflammatory diseases. *Pharmacol Ther*. 2018;183:177-204.
223. Wang RX, Chai Q, Lu T and Lee HC. Activation of vascular BK channels by docosahexaenoic acid is dependent on cytochrome P450 epoxygenase activity. *Cardiovasc Res*. 2011;90:344-52.
224. Lauterbach B, Barbosa-Sicard E, Wang MH, Honeck H, Kargel E, Theuer J, Schwartzman ML, Haller H, Luft FC, Gollasch M and Schunck WH. Cytochrome P450-dependent eicosapentaenoic acid metabolites are novel BK channel activators. *Hypertension*. 2002;39:609-13.
225. Hercule HC, Salanova B, Essin K, Honeck H, Falck JR, Sausbier M, Ruth P, Schunck WH, Luft FC and Gollasch M. The vasodilator 17,18-epoxyeicosatetraenoic acid targets the pore-forming BK alpha channel subunit in rodents. *Exp Physiol*. 2007;92:1067-76.
226. Morin C, Sirois M, Echave V, Rizcallah E and Rousseau E. Relaxing effects of 17(18)-EpETE on arterial and airway smooth muscles in human lung. *Am J Physiol Lung Cell Mol Physiol*. 2009;296:L130-9.
227. Agbor LN, Walsh MT, Boberg JR and Walker MK. Elevated blood pressure in cytochrome P4501A1 knockout mice is associated with reduced vasodilation to omega-3 polyunsaturated fatty acids. *Toxicol Appl Pharmacol*. 2012;264:351-60.
228. Ye D, Zhang D, Oltman C, Dellsperger K, Lee HC and VanRollins M. Cytochrome p-450 epoxygenase metabolites of docosahexaenoate potently dilate coronary arterioles by activating large-conductance calcium-activated potassium channels. *J Pharmacol Exp Ther*. 2002;303:768-76.
229. Pfister SL, Gauthier KM and Campbell WB. Vascular pharmacology of epoxyeicosatrienoic acids. *Adv Pharmacol*. 2010;60:27-59.
230. Dhanasekaran A, Al-Saghir R, Lopez B, Zhu D, Gutterman DD, Jacobs ER and Medhora M. Protective effects of epoxyeicosatrienoic acids on human endothelial cells from the pulmonary and coronary vasculature. *Am J Physiol Heart Circ Physiol*. 2006;291:H517-31.
231. Oltman CL, Weintraub NL, VanRollins M and Dellsperger KC. Epoxyeicosatrienoic acids and dihydroxyeicosatrienoic acids are potent vasodilators in the canine coronary microcirculation. *Circ Res*. 1998;83:932-9.
232. Imig JD, Jankiewicz WK and Khan AH. Epoxy Fatty Acids: From Salt Regulation to Kidney and Cardiovascular Therapeutics: 2019 Lewis K. Dahl Memorial Lecture. *Hypertension*. 2020;76:3-15.
233. Darwesh AM, Jamieson KL, Wang C, Samokhvalov V and Seubert JM. Cardioprotective effects of CYP-derived epoxy metabolites of docosahexaenoic acid involve limiting NLRP3 inflammasome activation (1). *Can J Physiol Pharmacol*. 2019;97:544-556.
234. Nithipatikom K, Moore JM, Isbell MA, Falck JR and Gross GJ. Epoxyeicosatrienoic acids in cardioprotection: ischemic versus reperfusion injury. *Am J Physiol Heart Circ Physiol*. 2006;291:H537-42.
235. Gross GJ, Gauthier KM, Moore J, Falck JR, Hammock BD, Campbell WB and Nithipatikom K. Effects of the selective EET antagonist, 14,15-EEZE, on cardioprotection

produced by exogenous or endogenous EETs in the canine heart. *Am J Physiol Heart Circ Physiol*. 2008;294:H2838-44.
236. Darwesh AM, Bassiouni W, Adebesin AM, Mohammad AS, Falck JR and Seubert JM. A Synthetic Epoxydocosapentaenoic Acid Analogue Ameliorates Cardiac Ischemia/Reperfusion Injury: The Involvement of the Sirtuin 3-NLRP3 Pathway. *Int J Mol Sci*. 2020;21.
237. Katragadda D, Batchu SN, Cho WJ, Chaudhary KR, Falck JR and Seubert JM. Epoxyeicosatrienoic acids limit damage to mitochondrial function following stress in cardiac cells. *J Mol Cell Cardiol*. 2009;46:867-75.
238. El-Sikhry HE, Alsaleh N, Dakarapu R, Falck JR and Seubert JM. Novel Roles of Epoxyeicosanoids in Regulating Cardiac Mitochondria. *PLoS One*. 2016;11:e0160380.
239. Samokhvalov V, Alsaleh N, El-Sikhry HE, Jamieson KL, Chen CB, Lopaschuk DG, Carter C, Light PE, Manne R, Falck JR and Seubert JM. Epoxyeicosatrienoic acids protect cardiac cells during starvation by modulating an autophagic response. *Cell Death Dis*. 2013;4:e885.
240. Li A, Gao M, Jiang W, Qin Y and Gong G. Mitochondrial Dynamics in Adult Cardiomyocytes and Heart Diseases. *Front Cell Dev Biol*. 2020;8:584800.
241. Node K, Huo Y, Ruan X, Yang B, Spiecker M, Ley K, Zeldin DC and Liao JK. Anti-inflammatory properties of cytochrome P450 epoxygenase-derived eicosanoids. *Science*. 1999;285:1276-9.
242. Luo XQ, Duan JX, Yang HH, Zhang CY, Sun CC, Guan XX, Xiong JB, Zu C, Tao JH, Zhou Y and Guan CX. Epoxyeicosatrienoic acids inhibit the activation of NLRP3 inflammasome in murine macrophages. *J Cell Physiol*. 2020;235:9910-9921.
243. Falck JR, Kodela R, Manne R, Atcha KR, Puli N, Dubasi N, Manthati VL, Capdevila JH, Yi XY, Goldman DH, Morisseau C, Hammock BD and Campbell WB. 14,15-Epoxyeicosa-5,8,11-trienoic acid (14,15-EET) surrogates containing epoxide bioisosteres: influence upon vascular relaxation and soluble epoxide hydrolase inhibition. *J Med Chem*. 2009;52:5069-75.
244. Catella F, Lawson JA, Fitzgerald DJ and FitzGerald GA. Endogenous biosynthesis of arachidonic acid epoxides in humans: increased formation in pregnancy-induced hypertension. *Proc Natl Acad Sci U S A*. 1990;87:5893-7.
245. Decker M, Arand M and Cronin A. Mammalian epoxide hydrolases in xenobiotic metabolism and signalling. *Arch Toxicol*. 2009;83:297-318.
246. Hassett C, Robinson KB, Beck NB and Omiecinski CJ. The human microsomal epoxide hydrolase gene (EPHX1): complete nucleotide sequence and structural characterization. *Genomics*. 1994;23:433-42.
247. Falany CN, McQuiddy P and Kasper CB. Structure and organization of the microsomal xenobiotic epoxide hydrolase gene. *J Biol Chem*. 1987;262:5924-30.
248. Coller JK, Fritz P, Zanger UM, Siegle I, Eichelbaum M, Kroemer HK and Murdter TE. Distribution of microsomal epoxide hydrolase in humans: an immunohistochemical study in normal tissues, and benign and malignant tumours. *Histochem J*. 2001;33:329-36.
249. Hassett C, Aicher L, Sidhu JS and Omiecinski CJ. Human microsomal epoxide hydrolase: genetic polymorphism and functional expression in vitro of amino acid variants. *Hum Mol Genet*. 1994;3:421-8.
250. Gaedigk A, Leeder JS and Grant DM. Tissue-specific expression and alternative splicing of human microsomal epoxide hydrolase. *DNA Cell Biol*. 1997;16:1257-66.

251. Marowsky A, Meyer I, Erismann-Ebner K, Pellegrini G, Mule N and Arand M. Beyond detoxification: a role for mouse mEH in the hepatic metabolism of endogenous lipids. *Arch Toxicol*. 2017;91:3571-3585.
252. Morisseau C, Kodani SD, Kamita SG, Yang J, Lee KSS and Hammock BD. Relative Importance of Soluble and Microsomal Epoxide Hydrolases for the Hydrolysis of Epoxy-Fatty Acids in Human Tissues. *Int J Mol Sci*. 2021;22.
253. Edin ML and Zeldin DC. Regulation of cardiovascular biology by microsomal epoxide hydrolase. *Toxicol Res*. 2021;37:285-292.
254. Harris TR and Hammock BD. Soluble epoxide hydrolase: gene structure, expression and deletion. *Gene*. 2013;526:61-74.
255. Marowsky A, Haenel K, Bockamp E, Heck R, Rutishauser S, Mule N, Kindler D, Rudin M and Arand M. Genetic enhancement of microsomal epoxide hydrolase improves metabolic detoxification but impairs cerebral blood flow regulation. *Arch Toxicol*. 2016;90:3017-3027.
256. Vaclavikova R, Hughes DJ and Soucek P. Microsomal epoxide hydrolase 1 (EPHX1): Gene, structure, function, and role in human disease. *Gene*. 2015;571:1-8.
257. Hang J, Zhou W, Wang X, Zhang H, Sun B, Dai H, Su L and Christiani DC. Microsomal epoxide hydrolase, endotoxin, and lung function decline in cotton textile workers. *Am J Respir Crit Care Med*. 2005;171:165-70.
258. Morisseau C and Hammock BD. Impact of soluble epoxide hydrolase and epoxyeicosanoids on human health. *Annu Rev Pharmacol Toxicol*. 2013;53:37-58.
259. Sandberg M and Meijer J. Structural characterization of the human soluble epoxide hydrolase gene (EPHX2). *Biochem Biophys Res Commun*. 1996;221:333-9.
260. Enayetallah AE, French RA, Barber M and Grant DF. Cell-specific subcellular localization of soluble epoxide hydrolase in human tissues. *J Histochem Cytochem*. 2006;54:329-35.
261. Newman JW, Morisseau C, Harris TR and Hammock BD. The soluble epoxide hydrolase encoded by EPXH2 is a bifunctional enzyme with novel lipid phosphate phosphatase activity. *Proc Natl Acad Sci U S A*. 2003;100:1558-63.
262. Cronin A, Mowbray S, Durk H, Homburg S, Fleming I, Fisslthaler B, Oesch F and Arand M. The N-terminal domain of mammalian soluble epoxide hydrolase is a phosphatase. *Proc Natl Acad Sci U S A*. 2003;100:1552-7.
263. Gross GJ and Nithipatikom K. Soluble epoxide hydrolase: a new target for cardioprotection. *Curr Opin Investig Drugs*. 2009;10:253-8.
264. Moghaddam MF, Grant DF, Cheek JM, Greene JF, Williamson KC and Hammock BD. Bioactivation of leukotoxins to their toxic diols by epoxide hydrolase. *Nat Med*. 1997;3:562-6.
265. Fornage M, Boerwinkle E, Doris PA, Jacobs D, Liu K and Wong ND. Polymorphism of the soluble epoxide hydrolase is associated with coronary artery calcification in African-American subjects: The Coronary Artery Risk Development in Young Adults (CARDIA) study. *Circulation*. 2004;109:335-9.
266. Lee CR, Pretorius M, Schuck RN, Burch LH, Bartlett J, Williams SM, Zeldin DC and Brown NJ. Genetic variation in soluble epoxide hydrolase (EPHX2) is associated with forearm vasodilator responses in humans. *Hypertension*. 2011;57:116-22.
267. Lee CR, North KE, Bray MS, Fornage M, Seubert JM, Newman JW, Hammock BD, Couper DJ, Heiss G and Zeldin DC. Genetic variation in soluble epoxide hydrolase

(EPHX2) and risk of coronary heart disease: The Atherosclerosis Risk in Communities (ARIC) study. *Hum Mol Genet*. 2006;15:1640-9.
268. Fava C, Montagnana M, Danese E, Almgren P, Hedblad B, Engstrom G, Berglund G, Minuz P and Melander O. Homozygosity for the EPHX2 K55R polymorphism increases the long-term risk of ischemic stroke in men: a study in Swedes. *Pharmacogenet Genomics*. 2010;20:94-103.
269. Burdon KP, Lehtinen AB, Langefeld CD, Carr JJ, Rich SS, Freedman BI, Herrington D and Bowden DW. Genetic analysis of the soluble epoxide hydrolase gene, EPHX2, in subclinical cardiovascular disease in the Diabetes Heart Study. *Diab Vasc Dis Res*. 2008;5:128-34.
270. Ai D, Fu Y, Guo D, Tanaka H, Wang N, Tang C, Hammock BD, Shyy JY and Zhu Y. Angiotensin II up-regulates soluble epoxide hydrolase in vascular endothelium in vitro and in vivo. *Proc Natl Acad Sci U S A*. 2007;104:9018-23.
271. Ai D, Pang W, Li N, Xu M, Jones PD, Yang J, Zhang Y, Chiamvimonvat N, Shyy JY, Hammock BD and Zhu Y. Soluble epoxide hydrolase plays an essential role in angiotensin II-induced cardiac hypertrophy. *Proc Natl Acad Sci U S A*. 2009;106:564-9.
272. Alsaad AM, Zordoky BN, El-Sherbeni AA and El-Kadi AO. Chronic doxorubicin cardiotoxicity modulates cardiac cytochrome P450-mediated arachidonic acid metabolism in rats. *Drug Metab Dispos*. 2012;40:2126-35.
273. Althurwi HN, Tse MM, Abdelhamid G, Zordoky BN, Hammock BD and El-Kadi AO. Soluble epoxide hydrolase inhibitor, TUPS, protects against isoprenaline-induced cardiac hypertrophy. *Br J Pharmacol*. 2013;168:1794-807.
274. Zordoky BN, Aboutabl ME and El-Kadi AO. Modulation of cytochrome P450 gene expression and arachidonic acid metabolism during isoproterenol-induced cardiac hypertrophy in rats. *Drug Metab Dispos*. 2008;36:2277-86.
275. Imig JD, Zhao X, Capdevila JH, Morisseau C and Hammock BD. Soluble epoxide hydrolase inhibition lowers arterial blood pressure in angiotensin II hypertension. *Hypertension*. 2002;39:690-4.
276. Zhao X, Yamamoto T, Newman JW, Kim IH, Watanabe T, Hammock BD, Stewart J, Pollock JS, Pollock DM and Imig JD. Soluble epoxide hydrolase inhibition protects the kidney from hypertension-induced damage. *J Am Soc Nephrol*. 2004;15:1244-53.
277. Wang Q, Liang Y, Qiao Y, Zhao X, Yang Y, Yang S, Li B, Zhao Q, Dong L, Quan S, Tian R and Liu Z. Expression of soluble epoxide hydrolase in renal tubular epithelial cells regulates macrophage infiltration and polarization in IgA nephropathy. *Am J Physiol Renal Physiol*. 2018;315:F915-F926.
278. Wang Y, Yang J, Wang W, Sanidad KZ, Cinelli MA, Wan D, Hwang SH, Kim D, Lee KSS, Xiao H, Hammock BD and Zhang G. Soluble epoxide hydrolase is an endogenous regulator of obesity-induced intestinal barrier dysfunction and bacterial translocation. *Proc Natl Acad Sci U S A*. 2020;117:8431-8436.
279. Fife KL, Liu Y, Schmelzer KR, Tsai HJ, Kim IH, Morisseau C, Hammock BD and Kroetz DL. Inhibition of soluble epoxide hydrolase does not protect against endotoxin-mediated hepatic inflammation. *J Pharmacol Exp Ther*. 2008;327:707-15.
280. Hung TH, Chen SF, Wu CH, Kao CC and Wu CP. Increased Soluble Epoxide Hydrolase in Human Gestational Tissues from Pregnancies Complicated by Acute Chorioamnionitis. *Mediators Inflamm*. 2019;2019:8687120.

281. Inceoglu B, Jinks SL, Schmelzer KR, Waite T, Kim IH and Hammock BD. Inhibition of soluble epoxide hydrolase reduces LPS-induced thermal hyperalgesia and mechanical allodynia in a rat model of inflammatory pain. *Life Sci*. 2006;79:2311-9.
282. Schmelzer KR, Kubala L, Newman JW, Kim IH, Eiserich JP and Hammock BD. Soluble epoxide hydrolase is a therapeutic target for acute inflammation. *Proc Natl Acad Sci U S A*. 2005;102:9772-7.
283. Zhou Y, Liu T, Duan JX, Li P, Sun GY, Liu YP, Zhang J, Dong L, Lee KSS, Hammock BD, Jiang JX and Guan CX. Soluble Epoxide Hydrolase Inhibitor Attenuates Lipopolysaccharide-Induced Acute Lung Injury and Improves Survival in Mice. *Shock*. 2017;47:638-645.
284. Shen HC and Hammock BD. Discovery of inhibitors of soluble epoxide hydrolase: a target with multiple potential therapeutic indications. *J Med Chem*. 2012;55:1789-808.
285. Podolin PL, Bolognese BJ, Foley JF, Long E, 3rd, Peck B, Umbrecht S, Zhang X, Zhu P, Schwartz B, Xie W, Quinn C, Qi H, Sweitzer S, Chen S, Galop M, Ding Y, Belyanskaya SL, Israel DI, Morgan BA, Behm DJ, Marino JP, Jr., Kurali E, Barnette MS, Mayer RJ, Booth-Genthe CL and Callahan JF. In vitro and in vivo characterization of a novel soluble epoxide hydrolase inhibitor. *Prostaglandins Other Lipid Mediat*. 2013;104-105:25-31.
286. Bzowka M, Mitusinska K, Hopko K and Gora A. Computational insights into the known inhibitors of human soluble epoxide hydrolase. *Drug Discov Today*. 2021;26:1914-1921.
287. Morisseau C, Goodrow MH, Newman JW, Wheelock CE, Dowdy DL and Hammock BD. Structural refinement of inhibitors of urea-based soluble epoxide hydrolases. *Biochem Pharmacol*. 2002;63:1599-608.
288. Tao W, Li PS, Yang LQ and Ma YB. Effects of a Soluble Epoxide Hydrolase Inhibitor on Lipopolysaccharide-Induced Acute Lung Injury in Mice. *PLoS One*. 2016;11:e0160359.
289. Li J, Carroll MA, Chander PN, Falck JR, Sangras B and Stier CT. Soluble epoxide hydrolase inhibitor, AUDA, prevents early salt-sensitive hypertension. *Front Biosci*. 2008;13:3480-7.
290. Yeh CF, Chuang TY, Hung YW, Lan MY, Tsai CH, Huang HX and Lin YY. Inhibition of soluble epoxide hydrolase regulates monocyte/macrophage polarization and improves neurological outcome in a rat model of ischemic stroke. *Neuroreport*. 2019;30:567-572.
291. Chen Z, Tang Y, Yu J, Dong R, Yang Y, Fu M, Luo J, Hu S, Wang DW, Tu L and Xu X. sEH Inhibitor Tppu Ameliorates Cecal Ligation and Puncture-Induced Sepsis by Regulating Macrophage Functions. *Shock*. 2020;53:761-771.
292. Sun CP, Zhang XY, Morisseau C, Hwang SH, Zhang ZJ, Hammock BD and Ma XC. Discovery of Soluble Epoxide Hydrolase Inhibitors from Chemical Synthesis and Natural Products. *J Med Chem*. 2021;64:184-215.
293. Zhang YF, Sun CC, Duan JX, Yang HH, Zhang CY, Xiong JB, Zhong WJ, Zu C, Guan XX, Jiang HL, Hammock BD, Hwang SH, Zhou Y and Guan CX. A COX-2/sEH dual inhibitor PTUPB ameliorates cecal ligation and puncture-induced sepsis in mice via anti-inflammation and anti-oxidative stress. *Biomed Pharmacother*. 2020;126:109907.
294. Yang HH, Duan JX, Liu SK, Xiong JB, Guan XX, Zhong WJ, Sun CC, Zhang CY, Luo XQ, Zhang YF, Chen P, Hammock BD, Hwang SH, Jiang JX, Zhou Y and Guan CX.

A COX-2/sEH dual inhibitor PTUPB alleviates lipopolysaccharide-induced acute lung injury in mice by inhibiting NLRP3 inflammasome activation. *Theranostics*. 2020;10:4749-4761.
295. Batchu SN, Lee SB, Qadhi RS, Chaudhary KR, El-Sikhry H, Kodela R, Falck JR and Seubert JM. Cardioprotective effect of a dual acting epoxyeicosatrienoic acid analogue towards ischaemia reperfusion injury. *Br J Pharmacol*. 2011;162:897-907.
296. Liu JY, Tsai HJ, Hwang SH, Jones PD, Morisseau C and Hammock BD. Pharmacokinetic optimization of four soluble epoxide hydrolase inhibitors for use in a murine model of inflammation. *Br J Pharmacol*. 2009;156:284-96.
297. Hwang SH, Tsai HJ, Liu JY, Morisseau C and Hammock BD. Orally bioavailable potent soluble epoxide hydrolase inhibitors. *J Med Chem*. 2007;50:3825-40.
298. Akhnokh MK, Yang FH, Samokhvalov V, Jamieson KL, Cho WJ, Wagg C, Takawale A, Wang X, Lopaschuk GD, Hammock BD, Kassiri Z and Seubert JM. Inhibition of Soluble Epoxide Hydrolase Limits Mitochondrial Damage and Preserves Function Following Ischemic Injury. *Front Pharmacol*. 2016;7:133.
299. Darwesh AM, Keshavarz-Bahaghighat H, Jamieson KL and Seubert JM. Genetic Deletion or Pharmacological Inhibition of Soluble Epoxide Hydrolase Ameliorates Cardiac Ischemia/Reperfusion Injury by Attenuating NLRP3 Inflammasome Activation. *Int J Mol Sci*. 2019;20.
300. Jamieson KL, Darwesh AM, Sosnowski DK, Zhang H, Shah S, Zhabyeyev P, Yang J, Hammock BD, Edin ML, Zeldin DC, Oudit GY, Kassiri Z and Seubert JM. Soluble Epoxide Hydrolase in Aged Female Mice and Human Explanted Hearts Following Ischemic Injury. *Int J Mol Sci*. 2021;22.
301. Sinal CJ, Miyata M, Tohkin M, Nagata K, Bend JR and Gonzalez FJ. Targeted disruption of soluble epoxide hydrolase reveals a role in blood pressure regulation. *J Biol Chem*. 2000;275:40504-10.
302. Luria A, Weldon SM, Kabcenell AK, Ingraham RH, Matera D, Jiang H, Gill R, Morisseau C, Newman JW and Hammock BD. Compensatory mechanism for homeostatic blood pressure regulation in Ephx2 gene-disrupted mice. *J Biol Chem*. 2007;282:2891-8.
303. Jamieson KL, Samokhvalov V, Akhnokh MK, Lee K, Cho WJ, Takawale A, Wang X, Kassiri Z and Seubert JM. Genetic deletion of soluble epoxide hydrolase provides cardioprotective responses following myocardial infarction in aged mice. *Prostaglandins Other Lipid Mediat*. 2017;132:47-58.
304. Monti J, Fischer J, Paskas S, Heinig M, Schulz H, Gosele C, Heuser A, Fischer R, Schmidt C, Schirdewan A, Gross V, Hummel O, Maatz H, Patone G, Saar K, Vingron M, Weldon SM, Lindpaintner K, Hammock BD, Rohde K, Dietz R, Cook SA, Schunck WH, Luft FC and Hubner N. Soluble epoxide hydrolase is a susceptibility factor for heart failure in a rat model of human disease. *Nat Genet*. 2008;40:529-37.
305. Wang L, Zhao D, Tang L, Li H, Liu Z, Gao J, Edin ML, Zhang H, Zhang K, Chen J, Zhu X, Wang D, Zeldin DC, Hammock BD, Wang J and Huang H. Soluble epoxide hydrolase deficiency attenuates lipotoxic cardiomyopathy via upregulation of AMPK-mTORC mediated autophagy. *J Mol Cell Cardiol*. 2021;154:80-91.
306. Zhang H, Wang T, Zhang K, Liu Y, Huang F, Zhu X, Liu Y, Wang MH, Tang W, Wang J and Huang H. Deletion of soluble epoxide hydrolase attenuates cardiac hypertrophy via down-regulation of cardiac fibroblasts-derived fibroblast growth factor-2. *Crit Care Med*. 2014;42:e345-54.

307. Jamieson KL, Keshavarz-Bahaghighat H, Darwesh AM, Sosnowski DK and Seubert JM. Age and Sex Differences in Hearts of Soluble Epoxide Hydrolase Null Mice. *Front Physiol*. 2020;11:48.
308. Hildreth K, Kodani SD, Hammock BD and Zhao L. Cytochrome P450-derived linoleic acid metabolites EpOMEs and DiHOMEs: a review of recent studies. *J Nutr Biochem*. 2020;86:108484.
309. Edin ML, Wang Z, Bradbury JA, Graves JP, Lih FB, DeGraff LM, Foley JF, Torphy R, Ronnekleiv OK, Tomer KB, Lee CR and Zeldin DC. Endothelial expression of human cytochrome P450 epoxygenase CYP2C8 increases susceptibility to ischemia-reperfusion injury in isolated mouse heart. *FASEB J*. 2011;25:3436-47.
310. Viswanathan S, Hammock BD, Newman JW, Meerarani P, Toborek M and Hennig B. Involvement of CYP 2C9 in mediating the proinflammatory effects of linoleic acid in vascular endothelial cells. *J Am Coll Nutr*. 2003;22:502-10.
311. Chaudhary KR, Zordoky BN, Edin ML, Alsaleh N, El-Kadi AO, Zeldin DC and Seubert JM. Differential effects of soluble epoxide hydrolase inhibition and CYP2J2 overexpression on postischemic cardiac function in aged mice. *Prostaglandins Other Lipid Mediat*. 2013;104-105:8-17.
312. Moran JH, Mon T, Hendrickson TL, Mitchell LA and Grant DF. Defining mechanisms of toxicity for linoleic acid monoepoxides and diols in Sf-21 cells. *Chem Res Toxicol*. 2001;14:431-7.
313. Sisemore MF, Zheng J, Yang JC, Thompson DA, Plopper CG, Cortopassi GA and Hammock BD. Cellular characterization of leukotoxin diol-induced mitochondrial dysfunction. *Arch Biochem Biophys*. 2001;392:32-7.
314. Mitchell LA, Grant DF, Melchert RB, Petty NM and Kennedy RH. Linoleic acid metabolites act to increase contractility in isolated rat heart. *Cardiovasc Toxicol*. 2002;2:219-30.
315. Bannehr M, Lohr L, Gelep J, Haverkamp W, Schunck WH, Gollasch M and Wutzler A. Linoleic Acid Metabolite DiHOME Decreases Post-ischemic Cardiac Recovery in Murine Hearts. *Cardiovasc Toxicol*. 2019;19:365-371.
316. Lynes MD, Leiria LO, Lundh M, Bartelt A, Shamsi F, Huang TL, Takahashi H, Hirshman MF, Schlein C, Lee A, Baer LA, May FJ, Gao F, Narain NR, Chen EY, Kiebish MA, Cypess AM, Bluher M, Goodyear LJ, Hotamisligil GS, Stanford KI and Tseng YH. The cold-induced lipokine 12,13-diHOME promotes fatty acid transport into brown adipose tissue. *Nat Med*. 2017;23:631-637.
317. Stanford KI, Lynes MD, Takahashi H, Baer LA, Arts PJ, May FJ, Lehnig AC, Middelbeek RJW, Richard JJ, So K, Chen EY, Gao F, Narain NR, Distefano G, Shettigar VK, Hirshman MF, Ziolo MT, Kiebish MA, Tseng YH, Coen PM and Goodyear LJ. 12,13-diHOME: An Exercise-Induced Lipokine that Increases Skeletal Muscle Fatty Acid Uptake. *Cell Metab*. 2018;27:1111-1120 e3.
318. Pinckard KM, Shettigar VK, Wright KR, Abay E, Baer LA, Vidal P, Dewal RS, Das D, Duarte-Sanmiguel S, Hernandez-Saavedra D, Arts PJ, Lehnig AC, Bussberg V, Narain NR, Kiebish MA, Yi F, Sparks LM, Goodpaster BH, Smith SR, Pratley RE, Lewandowski ED, Raman SV, Wold LE, Gallego-Perez D, Coen PM, Ziolo MT and Stanford KI. A Novel Endocrine Role for the BAT-Released Lipokine 12,13-diHOME to Mediate Cardiac Function. *Circulation*. 2021;143:145-159.

319. Fromel T, Jungblut B, Hu J, Trouvain C, Barbosa-Sicard E, Popp R, Liebner S, Dimmeler S, Hammock BD and Fleming I. Soluble epoxide hydrolase regulates hematopoietic progenitor cell function via generation of fatty acid diols. *Proc Natl Acad Sci U S A*. 2012;109:9995-10000.
320. Ethridge AD, Bazzi MH, Lukacs NW and Huffnagle GB. Interkingdom Communication and Regulation of Mucosal Immunity by the Microbiome. *J Infect Dis*. 2021;223:S236-S240.
321. Levan SR, Stamnes KA, Lin DL, Panzer AR, Fukui E, McCauley K, Fujimura KE, McKean M, Ownby DR, Zoratti EM, Boushey HA, Cabana MD, Johnson CC and Lynch SV. Elevated faecal 12,13-diHOME concentration in neonates at high risk for asthma is produced by gut bacteria and impedes immune tolerance. *Nat Microbiol*. 2019;4:1851-1861.
322. Zimmer B, Angioni C, Osthues T, Toewe A, Thomas D, Pierre SC, Geisslinger G, Scholich K and Sisignano M. The oxidized linoleic acid metabolite 12,13-DiHOME mediates thermal hyperalgesia during inflammatory pain. *Biochim Biophys Acta Mol Cell Biol Lipids*. 2018;1863:669-678.
323. Thompson DA and Hammock BD. Dihydroxyoctadecamonoenoate esters inhibit the neutrophil respiratory burst. *J Biosci*. 2007;32:279-91.
324. McReynolds CB, Cortes-Puch I, Ravindran R, Khan IH, Hammock BG, Shih PB, Hammock BD and Yang J. Plasma Linoleate Diols Are Potential Biomarkers for Severe COVID-19 Infections. *Front Physiol*. 2021;12:663869.
325. Stimers JR, Dobretsov M, Hastings SL, Jude AR and Grant DF. Effects of linoleic acid metabolites on electrical activity in adult rat ventricular myocytes. *Biochim Biophys Acta*. 1999;1438:359-68.
326. Balvers MG, Verhoeckx KC, Meijerink J, Bijlsma S, Rubingh CM, Wortelboer HM and Witkamp RF. Time-dependent effect of in vivo inflammation on eicosanoid and endocannabinoid levels in plasma, liver, ileum and adipose tissue in C57BL/6 mice fed a fish-oil diet. *Int Immunopharmacol*. 2012;13:204-14.
327. Hamaguchi M, Wu HN, Tanaka M, Tsuda N, Tantengco OAG, Matsushima T, Nakao T, Ishibe T, Sakata I and Yanagihara I. A case series of the dynamics of lipid mediators in patients with sepsis. *Acute Med Surg*. 2019;6:413-418.
328. Campbell WB, Deeter C, Gauthier KM, Ingraham RH, Falck JR and Li PL. 14,15-Dihydroxyeicosatrienoic acid relaxes bovine coronary arteries by activation of K(Ca) channels. *Am J Physiol Heart Circ Physiol*. 2002;282:H1656-64.
329. Lu T, Katakam PV, VanRollins M, Weintraub NL, Spector AA and Lee HC. Dihydroxyeicosatrienoic acids are potent activators of Ca(2+)-activated K(+) channels in isolated rat coronary arterial myocytes. *J Physiol*. 2001;534:651-67.
330. Zuo D, Pi Q, Shi Y, Luo S and Xia Y. Dihydroxyeicosatrienoic Acid, a Metabolite of Epoxyeicosatrienoic Acids Upregulates Endothelial Nitric Oxide Synthase Expression Through Transcription: Mechanism of Vascular Endothelial Function Protection. *Cell Biochem Biophys*. 2021;79:289-299.
331. Fang X, Hu S, Xu B, Snyder GD, Harmon S, Yao J, Liu Y, Sangras B, Falck JR, Weintraub NL and Spector AA. 14,15-Dihydroxyeicosatrienoic acid activates peroxisome proliferator-activated receptor-alpha. *Am J Physiol Heart Circ Physiol*. 2006;290:H55-63.

332. Suzuki S, Oguro A, Osada-Oka M, Funae Y and Imaoka S. Epoxyeicosatrienoic acids and/or their metabolites promote hypoxic response of cells. *J Pharmacol Sci*. 2008;108:79-88.
333. Bergmann CB, Hammock BD, Wan D, Gogolla F, Goetzman H, Caldwell CC and Supp DM. TPPU treatment of burned mice dampens inflammation and generation of bioactive DHET which impairs neutrophil function. *Sci Rep*. 2021;11:16555.
334. Litvinukova M, Talavera-Lopez C, Maatz H, Reichart D, Worth CL, Lindberg EL, Kanda M, Polanski K, Heinig M, Lee M, Nadelmann ER, Roberts K, Tuck L, Fasouli ES, DeLaughter DM, McDonough B, Wakimoto H, Gorham JM, Samari S, Mahbubani KT, Saeb-Parsy K, Patone G, Boyle JJ, Zhang H, Zhang H, Viveiros A, Oudit GY, Bayraktar OA, Seidman JG, Seidman CE, Noseda M, Hubner N and Teichmann SA. Cells of the adult human heart. *Nature*. 2020;588:466-472.
335. Woodcock EA and Matkovich SJ. Cardiomyocytes structure, function and associated pathologies. *Int J Biochem Cell Biol*. 2005;37:1746-51.
336. Canadian Council on Animal Care. *Guide to the care and use of experimental animals*. Ottawa, Ont.: Canadian Council on Animal Care; 1980.
337. Feil S, Valtcheva N and Feil R. Inducible Cre mice. *Methods Mol Biol*. 2009;530:343-63.
338. Ussher JR, Baggio LL, Campbell JE, Mulvihill EE, Kim M, Kabir MG, Cao X, Baranek BM, Stoffers DA, Seeley RJ and Drucker DJ. Inactivation of the cardiomyocyte glucagon-like peptide-1 receptor (GLP-1R) unmasks cardiomyocyte-independent GLP-1R-mediated cardioprotection. *Mol Metab*. 2014;3:507-17.
339. Seemann S, Zohles F and Lupp A. Comprehensive comparison of three different animal models for systemic inflammation. *J Biomed Sci*. 2017;24:60.
340. Fink MP. Animal models of sepsis. *Virulence*. 2014;5:143-53.
341. Whitehead JC, Hildebrand BA, Sun M, Rockwood MR, Rose RA, Rockwood K and Howlett SE. A clinical frailty index in aging mice: comparisons with frailty index data in humans. *J Gerontol A Biol Sci Med Sci*. 2014;69:621-32.
342. Lindsey ML, Kassiri Z, Virag JAI, de Castro Bras LE and Scherrer-Crosbie M. Guidelines for measuring cardiac physiology in mice. *Am J Physiol Heart Circ Physiol*. 2018;314:H733-H752.
343. Kovacic S, Soltys CL, Barr AJ, Shiojima I, Walsh K and Dyck JR. Akt activity negatively regulates phosphorylation of AMP-activated protein kinase in the heart. *J Biol Chem*. 2003;278:39422-7.
344. Zhao G, Wang X, Edwards S, Dai M, Li J, Wu L, Xu R, Han J and Yuan H. NLRX1 knockout aggravates lipopolysaccharide (LPS)-induced heart injury and attenuates the anti-LPS cardioprotective effect of CYP2J2/11,12-EET by enhancing activation of NF-kappaB and NLRP3 inflammasome. *Eur J Pharmacol*. 2020;881:173276.
345. Veltman D, Laeremans T, Passante E and Huber HJ. Signal transduction analysis of the NLRP3-inflammasome pathway after cellular damage and its paracrine regulation. *J Theor Biol*. 2017;415:125-136.
346. Jakobs C, Bartok E, Kubarenko A, Bauernfeind F and Hornung V. Immunoblotting for active caspase-1. *Methods Mol Biol*. 2013;1040:103-15.
347. Polster BM, Nicholls DG, Ge SX and Roelofs BA. Use of potentiometric fluorophores in the measurement of mitochondrial reactive oxygen species. *Methods Enzymol*. 2014;547:225-50.

348. Presley AD, Fuller KM and Arriaga EA. MitoTracker Green labeling of mitochondrial proteins and their subsequent analysis by capillary electrophoresis with laser-induced fluorescence detection. *J Chromatogr B Analyt Technol Biomed Life Sci*. 2003;793:141-50.
349. Meneses G, Rosetti M, Espinosa A, Florentino A, Bautista M, Diaz G, Olvera G, Barcena B, Fleury A, Adalid-Peralta L, Lamoyi E, Fragoso G and Sciutto E. Recovery from an acute systemic and central LPS-inflammation challenge is affected by mouse sex and genetic background. *PLoS One*. 2018;13:e0201375.
350. Kang HE and Park DW. Lactate as a Biomarker for Sepsis Prognosis? *Infect Chemother*. 2016;48:252-253.
351. van der Flier M, van Leeuwen HJ, van Kessel KP, Kimpen JL, Hoepelman AI and Geelen SP. Plasma vascular endothelial growth factor in severe sepsis. *Shock*. 2005;23:35-8.
352. Pickkers P, Sprong T, Eijk L, Hoeven H, Smits P and Deuren M. Vascular endothelial growth factor is increased during the first 48 hours of human septic shock and correlates with vascular permeability. *Shock*. 2005;24:508-12.
353. Radziwon-Balicka A, Moncada de la Rosa C and Jurasz P. Platelet-associated angiogenesis regulating factors: a pharmacological perspective. *Can J Physiol Pharmacol*. 2012;90:679-88.
354. Sato R and Nasu M. A review of sepsis-induced cardiomyopathy. *J Intensive Care*. 2015;3:48.
355. Hoffman M, Kyriazis ID, Lucchese AM, de Lucia C, Piedepalumbo M, Bauer M, Schulze PC, Bonios MJ, Koch WJ and Drosatos K. Myocardial Strain and Cardiac Output are Preferable Measurements for Cardiac Dysfunction and Can Predict Mortality in Septic Mice. *J Am Heart Assoc*. 2019;8:e012260.
356. Graves JP, Bradbury JA, Gruzdev A, Li H, Duval C, Lih FB, Edin ML and Zeldin DC. Expression of Cyp2c/Cyp2j subfamily members and oxylipin levels during LPS-induced inflammation and resolution in mice. *FASEB J*. 2019;33:14784-14797.
357. Theken KN, Deng Y, Kannon MA, Miller TM, Poloyac SM and Lee CR. Activation of the acute inflammatory response alters cytochrome P450 expression and eicosanoid metabolism. *Drug Metab Dispos*. 2011;39:22-9.
358. Willenberg I, Rund K, Rong S, Shushakova N, Gueler F and Schebb NH. Characterization of changes in plasma and tissue oxylipin levels in LPS and CLP induced murine sepsis. *Inflamm Res*. 2016;65:133-42.
359. Yang L, Chen C, Lv B, Gao Y and Li G. Epoxyeicosatrienoic acids prevent cardiomyocytes against sepsis by A2AR-induced activation of PI3K and PPARgamma. *Prostaglandins Other Lipid Mediat*. 2021;157:106595.
360. Du F, Sun W, Morisseau C, Hammock BD, Bao X, Liu Q, Wang C, Zhang T, Yang H, Zhou J, Xiao W, Liu Z and Chen G. Discovery of memantyl urea derivatives as potent soluble epoxide hydrolase inhibitors against lipopolysaccharide-induced sepsis. *Eur J Med Chem*. 2021;223:113678.
361. Schroder K, Sagulenko V, Zamoshnikova A, Richards AA, Cridland JA, Irvine KM, Stacey KJ and Sweet MJ. Acute lipopolysaccharide priming boosts inflammasome activation independently of inflammasome sensor induction. *Immunobiology*. 2012;217:1325-9.

362. Kalbitz M, Fattahi F, Grailer JJ, Jajou L, Malan EA, Zetoune FS, Huber-Lang M, Russell MW and Ward PA. Complement-induced activation of the cardiac NLRP3 inflammasome in sepsis. *FASEB J*. 2016;30:3997-4006.
363. Makrecka-Kuka M, Korzh S, Videja M, Vilskersts R, Sevostjanovs E, Zharkova-Malkova O, Arsenyan P, Kuka J, Dambrova M and Liepinsh E. Inhibition of CPT2 exacerbates cardiac dysfunction and inflammation in experimental endotoxaemia. *J Cell Mol Med*. 2020;24:11903-11911.
364. Sun CC, Zhang CY, Duan JX, Guan XX, Yang HH, Jiang HL, Hammock BD, Hwang SH, Zhou Y, Guan CX, Liu SK and Zhang J. PTUPB ameliorates high-fat diet-induced non-alcoholic fatty liver disease via inhibiting NLRP3 inflammasome activation in mice. *Biochem Biophys Res Commun*. 2020;523:1020-1026.
365. Li PS, Tao W, Yang LQ and Shu YS. Effect of Soluble Epoxide Hydrolase in Hyperoxic Acute Lung Injury in Mice. *Inflammation*. 2018;41:1065-1072.
366. Samokhvalov V, Jamieson KL, Vriend J, Quan S and Seubert JM. CYP-epoxygenase metabolites of docosahexaenoic acid protect HL-1 cardiac cells against LPS-induced cytotoxicity Through SIRT1. *Cell Death Discov*. 2015;1.
367. Butler TAJ, Paul JW, Chan EC, Smith R and Tolosa JM. Misleading Westerns: Common Quantification Mistakes in Western Blot Densitometry and Proposed Corrective Measures. *Biomed Res Int*. 2019;2019:5214821.
368. Cheng Z, Teo G, Krueger S, Rock TM, Koh HW, Choi H and Vogel C. Differential dynamics of the mammalian mRNA and protein expression response to misfolding stress. *Mol Syst Biol*. 2016;12:855.
369. Dagvadorj J, Mikulska-Ruminska K, Tumurkhuu G, Ratsimandresey RA, Carriere J, Andres AM, Marek-Iannucci S, Song Y, Chen S, Lane M, Dorfleutner A, Gottlieb RA, Stehlik C, Cassel S, Sutterwala FS, Bahar I, Crother TR and Arditi M. Recruitment of pro-IL-1alpha to mitochondrial cardiolipin, via shared LC3 binding domain, inhibits mitophagy and drives maximal NLRP3 activation. *Proc Natl Acad Sci U S A*. 2021;118.
370. Fu MH, Chen IC, Lee CH, Wu CW, Lee YC, Kung YC, Hung CY and Wu KLH. Anti-neuroinflammation ameliorates systemic inflammation-induced mitochondrial DNA impairment in the nucleus of the solitary tract and cardiovascular reflex dysfunction. *J Neuroinflammation*. 2019;16:224.
371. Gu J, Luo L, Wang Q, Yan S, Lin J, Li D, Cao B, Mei H, Ying B, Bin L, Smith FG and Jin SW. Maresin 1 attenuates mitochondrial dysfunction through the ALX/cAMP/ROS pathway in the cecal ligation and puncture mouse model and sepsis patients. *Lab Invest*. 2018;98:715-733.
372. Hickson-Bick DL, Jones C and Buja LM. Stimulation of mitochondrial biogenesis and autophagy by lipopolysaccharide in the neonatal rat cardiomyocyte protects against programmed cell death. *J Mol Cell Cardiol*. 2008;44:411-8.
373. Joseph LC, Reyes MV, Lakkadi KR, Gowen BH, Hasko G, Drosatos K and Morrow JP. PKCdelta causes sepsis-induced cardiomyopathy by inducing mitochondrial dysfunction. *Am J Physiol Heart Circ Physiol*. 2020;318:H778-H786.
374. Liu D, Yi B, Liao Z, Tang L, Yin D, Zeng S, Yao J and He M. 14-3-3gamma protein attenuates lipopolysaccharide-induced cardiomyocytes injury through the Bcl-2 family/mitochondria pathway. *Int Immunopharmacol*. 2014;21:509-15.
375. Vico TA, Marchini T, Ginart S, Lorenzetti MA, Adan Arean JS, Calabro V, Garces M, Ferrero MC, Mazo T, D'Annunzio V, Gelpi RJ, Corach D, Evelson P, Vanasco V and

Alvarez S. Mitochondrial bioenergetics links inflammation and cardiac contractility in endotoxemia. *Basic Res Cardiol*. 2019;114:38.
376. Wang Y, Jasper H, Toan S, Muid D, Chang X and Zhou H. Mitophagy coordinates the mitochondrial unfolded protein response to attenuate inflammation-mediated myocardial injury. *Redox Biol*. 2021;45:102049.
377. Yao X, Carlson D, Sun Y, Ma L, Wolf SE, Minei JP and Zang QS. Mitochondrial ROS Induces Cardiac Inflammation via a Pathway through mtDNA Damage in a Pneumonia-Related Sepsis Model. *PLoS One*. 2015;10:e0139416.
378. Zhang T, Liu CF, Zhang TN, Wen R and Song WL. Overexpression of Peroxisome Proliferator-Activated Receptor gamma Coactivator 1-alpha Protects Cardiomyocytes from Lipopolysaccharide-Induced Mitochondrial Damage and Apoptosis. *Inflammation*. 2020;43:1806-1820.
379. Molagoda IMN, Athapaththu A, Choi YH, Park C, Jin CY, Kang CH, Lee MH and Kim GY. Fisetin Inhibits NLRP3 Inflammasome by Suppressing TLR4/MD2-Mediated Mitochondrial ROS Production. *Antioxidants (Basel)*. 2021;10.
380. Xu Y, Zhang S, Rong J, Lin Y, Du L, Wang Y and Zhang Z. Sirt3 is a novel target to treat sepsis induced myocardial dysfunction by acetylated modulation of critical enzymes within cardiac tricarboxylic acid cycle. *Pharmacol Res*. 2020;159:104887.
381. Fock EM and Parnova RG. Protective Effect of Mitochondria-Targeted Antioxidants against Inflammatory Response to Lipopolysaccharide Challenge: A Review. *Pharmaceutics*. 2021;13.
382. Liu Y, Lian K, Zhang L, Wang R, Yi F, Gao C, Xin C, Zhu D, Li Y, Yan W, Xiong L, Gao E, Wang H and Tao L. TXNIP mediates NLRP3 inflammasome activation in cardiac microvascular endothelial cells as a novel mechanism in myocardial ischemia/reperfusion injury. *Basic Res Cardiol*. 2014;109:415.
383. Kawaguchi M, Takahashi M, Hata T, Kashima Y, Usui F, Morimoto H, Izawa A, Takahashi Y, Masumoto J, Koyama J, Hongo M, Noda T, Nakayama J, Sagara J, Taniguchi S and Ikeda U. Inflammasome activation of cardiac fibroblasts is essential for myocardial ischemia/reperfusion injury. *Circulation*. 2011;123:594-604.
384. Batchu SN, Lee SB, Samokhvalov V, Chaudhary KR, El-Sikhry H, Weldon SM and Seubert JM. Novel soluble epoxide hydrolase inhibitor protects mitochondrial function following stress. *Can J Physiol Pharmacol*. 2012;90:811-23.
385. Jiang XS, Xiang XY, Chen XM, He JL, Liu T, Gan H and Du XG. Inhibition of soluble epoxide hydrolase attenuates renal tubular mitochondrial dysfunction and ER stress by restoring autophagic flux in diabetic nephropathy. *Cell Death Dis*. 2020;11:385.
386. Wang L, Chen M, Yuan L, Xiang Y, Zheng R and Zhu S. 14,15-EET promotes mitochondrial biogenesis and protects cortical neurons against oxygen/glucose deprivation-induced apoptosis. *Biochem Biophys Res Commun*. 2014;450:604-9.
387. Liu L, Chen C, Gong W, Li Y, Edin ML, Zeldin DC and Wang DW. Epoxyeicosatrienoic acids attenuate reactive oxygen species level, mitochondrial dysfunction, caspase activation, and apoptosis in carcinoma cells treated with arsenic trioxide. *J Pharmacol Exp Ther*. 2011;339:451-63.
388. Zhang CH, Zheng L, Gui L, Lin JY, Zhu YM, Deng WS and Luo M. Soluble epoxide hydrolase inhibition with t-TUCB alleviates liver fibrosis and portal pressure in carbon tetrachloride-induced cirrhosis in rats. *Clin Res Hepatol Gastroenterol*. 2018;42:118-125.

389. Bettaieb A, Koike S, Chahed S, Zhao Y, Bachaalany S, Hashoush N, Graham J, Fatima H, Havel PJ, Gruzdev A, Zeldin DC, Hammock BD and Haj FG. Podocyte-specific soluble epoxide hydrolase deficiency in mice attenuates acute kidney injury. *FEBS J*. 2017;284:1970-1986.
390. Muller-Werdan U, Buerke M, Ebelt H, Heinroth KM, Herklotz A, Loppnow H, Russ M, Schlegel F, Schlitt A, Schmidt HB, Soffker G and Werdan K. Septic cardiomyopathy - A not yet discovered cardiomyopathy? *Exp Clin Cardiol*. 2006;11:226-36.
391. Chagnon F, Metz CN, Bucala R and Lesur O. Endotoxin-induced myocardial dysfunction: effects of macrophage migration inhibitory factor neutralization. *Circ Res*. 2005;96:1095-102.
392. Hobai IA, Morse JC, Siwik DA and Colucci WS. Lipopolysaccharide and cytokines inhibit rat cardiomyocyte contractility in vitro. *J Surg Res*. 2015;193:888-901.
393. Yucel G, Zhao Z, El-Battrawy I, Lan H, Lang S, Li X, Buljubasic F, Zimmermann WH, Cyganek L, Utikal J, Ravens U, Wieland T, Borggrefe M, Zhou XB and Akin I. Lipopolysaccharides induced inflammatory responses and electrophysiological dysfunctions in human-induced pluripotent stem cell derived cardiomyocytes. *Sci Rep*. 2017;7:2935.
394. Kawa K, Tsutsui H, Uchiyama R, Kato J, Matsui K, Iwakura Y, Matsumoto T and Nakanishi K. IFN-gamma is a master regulator of endotoxin shock syndrome in mice primed with heat-killed Propionibacterium acnes. *Int Immunol*. 2010;22:157-66.
395. Paludan SR. Synergistic action of pro-inflammatory agents: cellular and molecular aspects. *J Leukoc Biol*. 2000;67:18-25.
396. Torzewski M, Wenzel P, Kleinert H, Becker C, El-Masri J, Wiese E, Brandt M, Pautz A, Twardowski L, Schmitt E, Munzel T and Reifenberg K. Chronic inflammatory cardiomyopathy of interferon gamma-overexpressing transgenic mice is mediated by tumor necrosis factor-alpha. *Am J Pathol*. 2012;180:73-81.
397. Reifenberg K, Lehr HA, Torzewski M, Steige G, Wiese E, Kupper I, Becker C, Ott S, Nusser P, Yamamura K, Rechtsteiner G, Warger T, Pautz A, Kleinert H, Schmidt A, Pieske B, Wenzel P, Munzel T and Lohler J. Interferon-gamma induces chronic active myocarditis and cardiomyopathy in transgenic mice. *Am J Pathol*. 2007;171:463-72.
398. Sun X, Delbridge LM and Dusting GJ. Cardiodepressant effects of interferon-gamma and endotoxin reversed by inhibition of NO synthase 2 in rat myocardium. *J Mol Cell Cardiol*. 1998;30:989-97.
399. Levick SP and Goldspink PH. Could interferon-gamma be a therapeutic target for treating heart failure? *Heart Fail Rev*. 2014;19:227-36.
400. Hung TH, Shyue SK, Wu CH, Chen CC, Lin CC, Chang CF and Chen SF. Deletion or inhibition of soluble epoxide hydrolase protects against brain damage and reduces microglia-mediated neuroinflammation in traumatic brain injury. *Oncotarget*. 2017;8:103236-103260.
401. Muller-Werdan U, Schumann H, Loppnow H, Fuchs R, Darmer D, Stadler J, Holtz J and Werdan K. Endotoxin and tumor necrosis factor alpha exert a similar proinflammatory effect in neonatal rat cardiomyocytes, but have different cardiodepressant profiles. *J Mol Cell Cardiol*. 1998;30:1027-36.

402. Zhang H, Wang HY, Bassel-Duby R, Maass DL, Johnston WE, Horton JW and Tao W. Role of interleukin-6 in cardiac inflammation and dysfunction after burn complicated by sepsis. *Am J Physiol Heart Circ Physiol*. 2007;292:H2408-16.
403. Shen YL, Shi YZ, Chen GG, Wang LL, Zheng MZ, Jin HF and Chen YY. TNF-alpha induces Drp1-mediated mitochondrial fragmentation during inflammatory cardiomyocyte injury. *Int J Mol Med*. 2018;41:2317-2327.
404. Liu W, Wang B, Ding H, Wang DW and Zeng H. A potential therapeutic effect of CYP2C8 overexpression on anti-TNF-alpha activity. *Int J Mol Med*. 2014;34:725-32.
405. Hong T, Li S, Guo X, Wei Y, Zhang J, Su X, Zhou M, Jin H, Miao Q, Shen L, Zhu M and He B. IL-13 Derived Type 2 Innate Lymphocytes Ameliorates Cardiomyocyte Apoptosis Through STAT3 Signaling Pathway. *Front Cell Dev Biol*. 2021;9:742662.
406. Guo X, Hong T, Zhang S, Wei Y, Jin H, Miao Q, Wang K, Zhou M, Wang C and He B. IL-13 Alleviates Cardiomyocyte Apoptosis by Improving Fatty Acid Oxidation in Mitochondria. *Front Cell Dev Biol*. 2021;9:736603.
407. Gomez-Jimenez J, Martin MC, Sauri R, Segura RM, Esteban F, Ruiz JC, Nuvials X, Boveda JL, Peracaula R and Salgado A. Interleukin-10 and the monocyte/macrophage-induced inflammatory response in septic shock. *J Infect Dis*. 1995;171:472-5.
408. Teixeira JM, Abdalla HB, Basting RT, Hammock BD, Napimoga MH and Clemente-Napimoga JT. Peripheral soluble epoxide hydrolase inhibition reduces hypernociception and inflammation in albumin-induced arthritis in temporomandibular joint of rats. *Int Immunopharmacol*. 2020;87:106841.
409. Yeh CF, Chuang TY, Hung YW, Lan MY, Tsai CH, Huang HX and Lin YY. Soluble epoxide hydrolase inhibition enhances anti-inflammatory and antioxidative processes, modulates microglia polarization, and promotes recovery after ischemic stroke. *Neuropsychiatr Dis Treat*. 2019;15:2927-2941.
410. Lee HT, Lee KI, Chen CH and Lee TS. Genetic deletion of soluble epoxide hydrolase delays the progression of Alzheimer's disease. *J Neuroinflammation*. 2019;16:267.
411. Hamilton JA. Colony-stimulating factors in inflammation and autoimmunity. *Nat Rev Immunol*. 2008;8:533-44.
412. Hacham M, Cristal N, White RM, Segal S and Apte RN. Complementary organ expression of IL-1 vs. IL-6 and CSF-1 activities in normal and LPS-injected mice. *Cytokine*. 1996;8:21-31.
413. Hohensinner PJ, Kaun C, Rychli K, Ben-Tal Cohen E, Kastl SP, Demyanets S, Pfaffenberger S, Speidl WS, Rega G, Ullrich R, Maurer G, Huber K and Wojta J. Monocyte chemoattractant protein (MCP-1) is expressed in human cardiac cells and is differentially regulated by inflammatory mediators and hypoxia. *FEBS Lett*. 2006;580:3532-8.
414. Zhang J, Wang M, Ye J, Liu J, Xu Y, Wang Z, Ye D, Zhao M and Wan J. The Anti-inflammatory Mediator Resolvin E1 Protects Mice Against Lipopolysaccharide-Induced Heart Injury. *Front Pharmacol*. 2020;11:203.
415. Kundu S, Roome T, Bhattacharjee A, Carnevale KA, Yakubenko VP, Zhang R, Hwang SH, Hammock BD and Cathcart MK. Metabolic products of soluble epoxide hydrolase are essential for monocyte chemotaxis to MCP-1 in vitro and in vivo. *J Lipid Res*. 2013;54:436-47.

416. Ghigo A, Franco I, Morello F and Hirsch E. Myocyte signalling in leucocyte recruitment to the heart. *Cardiovasc Res*. 2014;102:270-80.
417. Slimani H, Zhai Y, Yousif NG, Ao L, Zeng Q, Fullerton DA and Meng X. Enhanced monocyte chemoattractant protein-1 production in aging mice exaggerates cardiac depression during endotoxemia. *Crit Care*. 2014;18:527.
418. Page AV and Liles WC. Biomarkers of endothelial activation/dysfunction in infectious diseases. *Virulence*. 2013;4:507-16.
419. Hauschildt J, Schrimpf C, Thamm K, Retzlaff J, Idowu TO, von Kaisenberg C, Haller H and David S. Dual Pharmacological Inhibition of Angiopoietin-2 and VEGF-A in Murine Experimental Sepsis. *J Vasc Res*. 2020;57:34-45.
420. Nolan A, Weiden MD, Thurston G and Gold JA. Vascular endothelial growth factor blockade reduces plasma cytokines in a murine model of polymicrobial sepsis. *Inflammation*. 2004;28:271-8.
421. Rand AA, Rajamani A, Kodani SD, Harris TR, Schlatt L, Barnych B, Passerini AG and Hammock BD. Epoxyeicosatrienoic acid (EET)-stimulated angiogenesis is mediated by epoxy hydroxyeicosatrienoic acids (EHETs) formed from COX-2. *J Lipid Res*. 2019;60:1996-2005.
422. Panigrahy D, Greene ER, Pozzi A, Wang DW and Zeldin DC. EET signaling in cancer. *Cancer Metastasis Rev*. 2011;30:525-40.
423. Sommer K, Jakob H, Badjlan F, Henrich D, Frank J, Marzi I and Sander AL. 11,12 and 14,15 epoxyeicosatrienoic acid rescue deteriorated wound healing in ischemia. *PLoS One*. 2019;14:e0209158.
424. Panigrahy D, Kalish BT, Huang S, Bielenberg DR, Le HD, Yang J, Edin ML, Lee CR, Benny O, Mudge DK, Butterfield CE, Mammoto A, Mammoto T, Inceoglu B, Jenkins RL, Simpson MA, Akino T, Lih FB, Tomer KB, Ingber DE, Hammock BD, Falck JR, Manthati VL, Kaipainen A, D'Amore PA, Puder M, Zeldin DC and Kieran MW. Epoxyeicosanoids promote organ and tissue regeneration. *Proc Natl Acad Sci U S A*. 2013;110:13528-33.
425. Wang Y, Wei X, Xiao X, Hui R, Card JW, Carey MA, Wang DW and Zeldin DC. Arachidonic acid epoxygenase metabolites stimulate endothelial cell growth and angiogenesis via mitogen-activated protein kinase and phosphatidylinositol 3-kinase/Akt signaling pathways. *J Pharmacol Exp Ther*. 2005;314:522-32.
426. Hou HH, Hammock BD, Su KH, Morisseau C, Kou YR, Imaoka S, Oguro A, Shyue SK, Zhao JF and Lee TS. N-terminal domain of soluble epoxide hydrolase negatively regulates the VEGF-mediated activation of endothelial nitric oxide synthase. *Cardiovasc Res*. 2012;93:120-9.
427. Xu DY, Davis BB, Wang ZH, Zhao SP, Wasti B, Liu ZL, Li N, Morisseau C, Chiamvimonvat N and Hammock BD. A potent soluble epoxide hydrolase inhibitor, t-AUCB, acts through PPARgamma to modulate the function of endothelial progenitor cells from patients with acute myocardial infarction. *Int J Cardiol*. 2013;167:1298-304.
428. Zhang G, Panigrahy D, Mahakian LM, Yang J, Liu JY, Stephen Lee KS, Wettersten HI, Ulu A, Hu X, Tam S, Hwang SH, Ingham ES, Kieran MW, Weiss RH, Ferrara KW and Hammock BD. Epoxy metabolites of docosahexaenoic acid (DHA) inhibit angiogenesis, tumor growth, and metastasis. *Proc Natl Acad Sci U S A*. 2013;110:6530-5.
429. Ibrahim A, Mbodji K, Hassan A, Aziz M, Boukhettala N, Coeffier M, Savoye G, Dechelotte P and Marion-Letellier R. Anti-inflammatory and anti-angiogenic effect of long

chain n-3 polyunsaturated fatty acids in intestinal microvascular endothelium. *Clin Nutr*. 2011;30:678-87.
430. Dong R, Hu D, Yang Y, Chen Z, Fu M, Wang DW, Xu X and Tu L. EETs reduces LPS-induced hyperpermeability by targeting GRP78 mediated Src activation and subsequent Rho/ROCK signaling pathway. *Oncotarget*. 2017;8:50958-50971.
431. Cai R, Hao Y, Liu YY, Huang L, Yao Y and Zhou MS. Tumor Necrosis Factor Alpha Deficiency Improves Endothelial Function and Cardiovascular Injury in Deoxycorticosterone Acetate/Salt-Hypertensive Mice. *Biomed Res Int*. 2020;2020:3921074.
432. Danielski LG, Giustina AD, Bonfante S, Barichello T and Petronilho F. The NLRP3 Inflammasome and Its Role in Sepsis Development. *Inflammation*. 2020;43:24-31.
433. Chistiakov DA, Killingsworth MC, Myasoedova VA, Orekhov AN and Bobryshev YV. CD68/macrosialin: not just a histochemical marker. *Lab Invest*. 2017;97:4-13.
434. Ma Y, Mouton AJ and Lindsey ML. Cardiac macrophage biology in the steady-state heart, the aging heart, and following myocardial infarction. *Transl Res*. 2018;191:15-28.
435. Tavener SA, Long EM, Robbins SM, McRae KM, Van Remmen H and Kubes P. Immune cell Toll-like receptor 4 is required for cardiac myocyte impairment during endotoxemia. *Circ Res*. 2004;95:700-7.
436. Humeres C, Vivar R, Boza P, Munoz C, Bolivar S, Anfossi R, Osorio JM, Olivares-Silva F, Garcia L and Diaz-Araya G. Cardiac fibroblast cytokine profiles induced by proinflammatory or profibrotic stimuli promote monocyte recruitment and modulate macrophage M1/M2 balance in vitro. *J Mol Cell Cardiol*. 2016.
437. Salas-Hernandez A, Espinoza-Perez C, Vivar R, Espitia-Corredor J, Lillo J, Parra-Flores P, Sanchez-Ferrer CF, Peiro C and Diaz-Araya G. Resolvin D1 and E1 promote resolution of inflammation in rat cardiac fibroblast in vitro. *Mol Biol Rep*. 2021;48:57-66.
438. Sawa Y, Sugimoto Y, Ueki T, Ishikawa H, Sato A, Nagato T and Yoshida S. Effects of TNF-alpha on leukocyte adhesion molecule expressions in cultured human lymphatic endothelium. *J Histochem Cytochem*. 2007;55:721-33.
439. Turner NA, Das A, O'Regan DJ, Ball SG and Porter KE. Human cardiac fibroblasts express ICAM-1, E-selectin and CXC chemokines in response to proinflammatory cytokine stimulation. *Int J Biochem Cell Biol*. 2011;43:1450-8.
440. Xia P, Gamble JR, Rye KA, Wang L, Hii CS, Cockerill P, Khew-Goodall Y, Bert AG, Barter PJ and Vadas MA. Tumor necrosis factor-alpha induces adhesion molecule expression through the sphingosine kinase pathway. *Proc Natl Acad Sci U S A*. 1998;95:14196-201.
441. Wang T, Tian J and Jin Y. VCAM1 expression in the myocardium is associated with the risk of heart failure and immune cell infiltration in myocardium. *Sci Rep*. 2021;11:19488.
442. Ponten A, Walsh S, Malan D, Xian X, Scheele S, Tarnawski L, Fleischmann BK and Jovinge S. FACS-based isolation, propagation and characterization of mouse embryonic cardiomyocytes based on VCAM-1 surface marker expression. *PLoS One*. 2013;8:e82403.
443. Kim J, Yoon SP, Toews ML, Imig JD, Hwang SH, Hammock BD and Padanilam BJ. Pharmacological inhibition of soluble epoxide hydrolase prevents renal interstitial fibrogenesis in obstructive nephropathy. *Am J Physiol Renal Physiol*. 2015;308:F131-9.

444. Li D, Liu Y, Zhang X, Lv H, Pang W, Sun X, Gan LM, Hammock BD, Ai D and Zhu Y. Inhibition of soluble epoxide hydrolase alleviated atherosclerosis by reducing monocyte infiltration in Ldlr(-/-) mice. *J Mol Cell Cardiol*. 2016;98:128-37.
445. Dai M, Wu L, Wang P, Wen Z, Xu X and Wang DW. CYP2J2 and Its Metabolites EETs Attenuate Insulin Resistance via Regulating Macrophage Polarization in Adipose Tissue. *Sci Rep*. 2017;7:46743.
446. Davis BB, Liu JY, Tancredi DJ, Wang L, Simon SI, Hammock BD and Pinkerton KE. The anti-inflammatory effects of soluble epoxide hydrolase inhibitors are independent of leukocyte recruitment. *Biochem Biophys Res Commun*. 2011;410:494-500.
447. Capozzi ME, Hammer SS, McCollum GW and Penn JS. Epoxygenated Fatty Acids Inhibit Retinal Vascular Inflammation. *Sci Rep*. 2016;6:39211.
448. Gao M, Wang X, Zhang X, Ha T, Ma H, Liu L, Kalbfleisch JH, Gao X, Kao RL, Williams DL and Li C. Attenuation of Cardiac Dysfunction in Polymicrobial Sepsis by MicroRNA-146a Is Mediated via Targeting of IRAK1 and TRAF6 Expression. *J Immunol*. 2015;195:672-82.
449. Hoyer FF, Naxerova K, Schloss MJ, Hulsmans M, Nair AV, Dutta P, Calcagno DM, Herisson F, Anzai A, Sun Y, Wojtkiewicz G, Rohde D, Frodermann V, Vandoorne K, Courties G, Iwamoto Y, Garris CS, Williams DL, Breton S, Brown D, Whalen M, Libby P, Pittet MJ, King KR, Weissleder R, Swirski FK and Nahrendorf M. Tissue-Specific Macrophage Responses to Remote Injury Impact the Outcome of Subsequent Local Immune Challenge. *Immunity*. 2019;51:899-914 e7.
450. Wang L, Li Y, Wang X, Wang P, Essandoh K, Cui S, Huang W, Mu X, Liu Z, Wang Y, Peng T and Fan GC. GDF3 Protects Mice against Sepsis-Induced Cardiac Dysfunction and Mortality by Suppression of Macrophage Pro-Inflammatory Phenotype. *Cells*. 2020;9.
451. Sharma A, Yang WL, Matsuo S and Wang P. Differential alterations of tissue T-cell subsets after sepsis. *Immunol Lett*. 2015;168:41-50.
452. Liu LP, Li B, Shuai TK, Zhu L and Li YM. Deletion of soluble epoxide hydrolase attenuates mice Hyperoxic acute lung injury. *BMC Anesthesiol*. 2018;18:48.
453. Kumar P, Nagarajan A and Uchil PD. Analysis of Cell Viability by the Lactate Dehydrogenase Assay. *Cold Spring Harb Protoc*. 2018;2018.
454. Nemzek JA, Hugunin KM and Opp MR. Modeling sepsis in the laboratory: merging sound science with animal well-being. *Comp Med*. 2008;58:120-8.
455. Lewis AJ, Seymour CW and Rosengart MR. Current Murine Models of Sepsis. *Surg Infect (Larchmt)*. 2016;17:385-93.
456. Korneev KV. [Mouse Models of Sepsis and Septic Shock]. *Mol Biol (Mosk)*. 2019;53:799-814.
457. Li Y, Deng S, Wang X, Huang W, Chen J, Robbins N, Mu X, Essandoh K, Peng T, Jegga AG, Rubinstein J, Adams DE, Wang Y, Peng J and Fan GC. Sectm1a deficiency aggravates inflammation-triggered cardiac dysfunction through disruption of LXRalpha signalling in macrophages. *Cardiovasc Res*. 2021;117:890-902.
458. Ly OT, Brown GE, Han YD, Darbar D and Khetani SR. Bioengineering approaches to mature induced pluripotent stem cell-derived atrial cardiomyocytes to model atrial fibrillation. *Exp Biol Med (Maywood)*. 2021;246:1816-1828.

459. Bekkevold CM, Robertson KL, Reinhard MK, Battles AH and Rowland NE. Dehydration parameters and standards for laboratory mice. *J Am Assoc Lab Anim Sci*. 2013;52:233-9.
460. Morita-Takemura S, Nakahara K, Hasegawa-Ishii S, Isonishi A, Tatsumi K, Okuda H, Tanaka T, Kitabatake M, Ito T and Wanaka A. Responses of perivascular macrophages to circulating lipopolysaccharides in the subfornical organ with special reference to endotoxin tolerance. *J Neuroinflammation*. 2019;16:39.
461. Jamali F and Kunz-Dober CM. Pain-mediated altered absorption and metabolism of ibuprofen: an explanation for decreased serum enantiomer concentration after dental surgery. *Br J Clin Pharmacol*. 1999;47:391-6.
462. van Haren FM, Sleigh JW, Pickkers P and Van der Hoeven JG. Gastrointestinal perfusion in septic shock. *Anaesth Intensive Care*. 2007;35:679-94.
463. Nasa P, Juneja D and Singh O. Severe sepsis and septic shock in the elderly: An overview. *World J Crit Care Med*. 2012;1:23-30.
464. Zhou M, Wu R, Dong W, Leong J and Wang P. Accelerated apoptosis contributes to aging-related hyperinflammation in endotoxemia. *Int J Mol Med*. 2010;25:929-35.
465. Lufrano M, Jacob A, Zhou M and Wang P. Sphingosine kinase1 mediates endotoxemiainduced hyperinflammation in aged animals. *Mol Med Rep*. 2013;8:645-9.
466. Leong J, Zhou M, Jacob A and Wang P. Aging-related hyperinflammation in endotoxemia is mediated by the alpha2A-adrenoceptor and CD14/TLR4 pathways. *Life Sci*. 2010;86:740-6.
467. Saito H, Sherwood ER, Varma TK and Evers BM. Effects of aging on mortality, hypothermia, and cytokine induction in mice with endotoxemia or sepsis. *Mech Ageing Dev*. 2003;124:1047-58.
468. Kumar AT, Sudhir U, Punith K, Kumar R, Ravi Kumar VN and Rao MY. Cytokine profile in elderly patients with sepsis. *Indian J Crit Care Med*. 2009;13:74-8.
469. Saito H and Papaconstantinou J. Age-associated differences in cardiovascular inflammatory gene induction during endotoxic stress. *J Biol Chem*. 2001;276:29307-12.
470. Zhang J, Zhao P, Quan N, Wang L, Chen X, Cates C, Rousselle T and Li J. The endotoxemia cardiac dysfunction is attenuated by AMPK/mTOR signaling pathway regulating autophagy. *Biochem Biophys Res Commun*. 2017;492:520-527.
471. Qin J, Le Y, Froogh G, Kandhi S, Jiang H, Luo M, Sun D and Huang A. Sexually dimorphic adaptation of cardiac function: roles of epoxyeicosatrienoic acid and peroxisome proliferator-activated receptors. *Physiol Rep*. 2016;4.
472. Stice JP, Lee JS, Pechenino AS and Knowlton AA. Estrogen, aging and the cardiovascular system. *Future Cardiol*. 2009;5:93-103.
473. Hobai IA, Aziz K, Buys ES, Brouckaert P, Siwik DA and Colucci WS. Distinct Myocardial Mechanisms Underlie Cardiac Dysfunction in Endotoxemic Male and Female Mice. *Shock*. 2016;46:713-722.
474. Goncalves RP, Guarido KL, Assreuy J and da Silva-Santos JE. Gender-specific differences in the in situ cardiac function of endotoxemic rats detected by pressure-volume catheter. *Shock*. 2014;42:415-23.
475. El-Lakany MA, Fouda MA, El-Gowelli HM, El-Gowilly SM and El-Mas MM. Gonadal hormone receptors underlie the resistance of female rats to inflammatory and cardiovascular complications of endotoxemia. *Eur J Pharmacol*. 2018;823:41-48.

476. Meldrum DR. Estrogen increases protective proteins following trauma and hemorrhage. *Am J Physiol Regul Integr Comp Physiol*. 2006;290:R809-11.
477. Vandereyken MM, Singh P, Wathieu CP, Jacques S, Zurashvilli T, Dejager L, Amand M, Musumeci L, Singh M, Moutschen MP, Libert CRF and Rahmouni S. Dual-Specificity Phosphatase 3 Deletion Protects Female, but Not Male, Mice from Endotoxemia-Induced and Polymicrobial-Induced Septic Shock. *J Immunol*. 2017;199:2515-2527.
478. Zhu H, Shan L and Peng T. Rac1 mediates sex difference in cardiac tumor necrosis factor-alpha expression via NADPH oxidase-ERK1/2/p38 MAPK pathway in endotoxemia. *J Mol Cell Cardiol*. 2009;47:264-74.
479. Eachempati SR, Hydo L and Barie PS. Gender-based differences in outcome in patients with sepsis. *Arch Surg*. 1999;134:1342-7.
480. Schroder J, Kahlke V, Staubach KH, Zabel P and Stuber F. Gender differences in human sepsis. *Arch Surg*. 1998;133:1200-5.
481. Adrie C, Azoulay E, Francais A, Clec'h C, Darques L, Schwebel C, Nakache D, Jamali S, Goldgran-Toledano D, Garrouste-Orgeas M, Timsit JF and OutcomeRea Study G. Influence of gender on the outcome of severe sepsis: a reappraisal. *Chest*. 2007;132:1786-93.
482. Klionsky DJ, Abdalla FC, Abeliovich H, Abraham RT, Acevedo-Arozena A, Adeli K, Agholme L, Agnello M, Agostinis P, Aguirre-Ghiso JA, Ahn HJ, Ait-Mohamed O, Ait-Si-Ali S, Akematsu T, Akira S, Al-Younes HM, Al-Zeer MA, Albert ML, Albin RL, Alegre-Abarrategui J, Aleo MF, Alirezaei M, Almasan A, Almonte-Becerril M, Amano A, Amaravadi R, Amarnath S, Amer AO, Andrieu-Abadie N, Anantharam V, Ann DK, Anoopkumar-Dukie S, Aoki H, Apostolova N, Arancia G, Aris JP, Asanuma K, Asare NY, Ashida H, Askanas V, Askew DS, Auberger P, Baba M, Backues SK, Baehrecke EH, Bahr BA, Bai XY, Bailly Y, Baiocchi R, Baldini G, Balduini W, Ballabio A, Bamber BA, Bampton ET, Banhegyi G, Bartholomew CR, Bassham DC, Bast RC, Jr., Batoko H, Bay BH, Beau I, Bechet DM, Begley TJ, Behl C, Behrends C, Bekri S, Bellaire B, Bendall LJ, Benetti L, Berliocchi L, Bernardi H, Bernassola F, Besteiro S, Bhatia-Kissova I, Bi X, Biard-Piechaczyk M, Blum JS, Boise LH, Bonaldo P, Boone DL, Bornhauser BC, Bortoluci KR, Bossis I, Bost F, Bourquin JP, Boya P, Boyer-Guittaut M, Bozhkov PV, Brady NR, Brancolini C, Brech A, Brenman JE, Brennand A, Bresnick EH, Brest P, Bridges D, Bristol ML, Brookes PS, Brown EJ, Brumell JH, Brunetti-Pierri N, Brunk UT, Bulman DE, Bultman SJ, Bultynck G, Burbulla LF, Bursch W, Butchar JP, Buzgariu W, Bydlowski SP, Cadwell K, Cahova M, Cai D, Cai J, Cai Q, Calabretta B, Calvo-Garrido J, Camougrand N, Campanella M, Campos-Salinas J, Candi E, Cao L, Caplan AB, Carding SR, Cardoso SM, Carew JS, Carlin CR, Carmignac V, Carneiro LA, Carra S, Caruso RA, Casari G, Casas C, Castino R, Cebollero E, Cecconi F, Celli J, Chaachouay H, Chae HJ, Chai CY, Chan DC, Chan EY, Chang RC, Che CM, Chen CC, Chen GC, Chen GQ, Chen M, Chen Q, Chen SS, Chen W, Chen X, Chen X, Chen X, Chen YG, Chen Y, Chen Y, Chen YJ, Chen Z, Cheng A, Cheng CH, Cheng Y, Cheong H, Cheong JH, Cherry S, Chess-Williams R, Cheung ZH, Chevet E, Chiang HL, Chiarelli R, Chiba T, Chin LS, Chiou SH, Chisari FV, Cho CH, Cho DH, Choi AM, Choi D, Choi KS, Choi ME, Chouaib S, Choubey D, Choubey V, Chu CT, Chuang TH, Chueh SH, Chun T, Chwae YJ, Chye ML, Ciarcia R, Ciriolo MR, Clague MJ, Clark RS, Clarke PG, Clarke R, Codogno P, Coller HA, Colombo MI, Comincini S, Condello M, Condorelli F, Cookson MR, Coombs GH,

Coppens I, Corbalan R, Cossart P, Costelli P, Costes S, Coto-Montes A, Couve E, Coxon FP, Cregg JM, Crespo JL, Cronje MJ, Cuervo AM, Cullen JJ, Czaja MJ, D'Amelio M, Darfeuille-Michaud A, Davids LM, Davies FE, De Felici M, de Groot JF, de Haan CA, De Martino L, De Milito A, De Tata V, Debnath J, Degterev A, Dehay B, Delbridge LM, Demarchi F, Deng YZ, Dengjel J, Dent P, Denton D, Deretic V, Desai SD, Devenish RJ, Di Gioacchino M, Di Paolo G, Di Pietro C, Diaz-Araya G, Diaz-Laviada I, Diaz-Meco MT, Diaz-Nido J, Dikic I, Dinesh-Kumar SP, Ding WX, Distelhorst CW, Diwan A, Djavaheri-Mergny M, Dokudovskaya S, Dong Z, Dorsey FC, Dosenko V, Dowling JJ, Doxsey S, Dreux M, Drew ME, Duan Q, Duchosal MA, Duff K, Dugail I, Durbeej M, Duszenko M, Edelstein CL, Edinger AL, Egea G, Eichinger L, Eissa NT, Ekmekcioglu S, El-Deiry WS, Elazar Z, Elgendy M, Ellerby LM, Eng KE, Engelbrecht AM, Engelender S, Erenpreisa J, Escalante R, Esclatine A, Eskelinen EL, Espert L, Espina V, Fan H, Fan J, Fan QW, Fan Z, Fang S, Fang Y, Fanto M, Fanzani A, Farkas T, Farre JC, Faure M, Fechheimer M, Feng CG, Feng J, Feng Q, Feng Y, Fesus L, Feuer R, Figueiredo-Pereira ME, Fimia GM, Fingar DC, Finkbeiner S, Finkel T, Finley KD, Fiorito F, Fisher EA, Fisher PB, Flajolet M, Florez-McClure ML, Florio S, Fon EA, Fornai F, Fortunato F, Fotedar R, Fowler DH, Fox HS, Franco R, Frankel LB, Fransen M, Fuentes JM, Fueyo J, Fujii J, Fujisaki K, Fujita E, Fukuda M, Furukawa RH, Gaestel M, Gailly P, Gajewska M, Galliot B, Galy V, Ganesh S, Ganetzky B, Ganley IG, Gao FB, Gao GF, Gao J, Garcia L, Garcia-Manero G, Garcia-Marcos M, Garmyn M, Gartel AL, Gatti E, Gautel M, Gawriluk TR, Gegg ME, Geng J, Germain M, Gestwicki JE, Gewirtz DA, Ghavami S, Ghosh P, Giammarioli AM, Giatromanolaki AN, Gibson SB, Gilkerson RW, Ginger ML, Ginsberg HN, Golab J, Goligorsky MS, Golstein P, Gomez-Manzano C, Goncu E, Gongora C, Gonzalez CD, Gonzalez R, Gonzalez-Estevez C, Gonzalez-Polo RA, Gonzalez-Rey E, Gorbunov NV, Gorski S, Goruppi S, Gottlieb RA, Gozuacik D, Granato GE, Grant GD, Green KN, Gregorc A, Gros F, Grose C, Grunt TW, Gual P, Guan JL, Guan KL, Guichard SM, Gukovskaya AS, Gukovsky I, Gunst J, Gustafsson AB, Halayko AJ, Hale AN, Halonen SK, Hamasaki M, Han F, Han T, Hancock MK, Hansen M, Harada H, Harada M, Hardt SE, Harper JW, Harris AL, Harris J, Harris SD, Hashimoto M, Haspel JA, Hayashi S, Hazelhurst LA, He C, He YW, Hebert MJ, Heidenreich KA, Helfrich MH, Helgason GV, Henske EP, Herman B, Herman PK, Hetz C, Hilfiker S, Hill JA, Hocking LJ, Hofman P, Hofmann TG, Hohfeld J, Holyoake TL, Hong MH, Hood DA, Hotamisligil GS, Houwerzijl EJ, Hoyer-Hansen M, Hu B, Hu CA, Hu HM, Hua Y, Huang C, Huang J, Huang S, Huang WP, Huber TB, Huh WK, Hung TH, Hupp TR, Hur GM, Hurley JB, Hussain SN, Hussey PJ, Hwang JJ, Hwang S, Ichihara A, Ilkhanizadeh S, Inoki K, Into T, Iovane V, Iovanna JL, Ip NY, Isaka Y, Ishida H, Isidoro C, Isobe K, Iwasaki A, Izquierdo M, Izumi Y, Jaakkola PM, Jaattela M, Jackson GR, Jackson WT, Janji B, Jendrach M, Jeon JH, Jeung EB, Jiang H, Jiang H, Jiang JX, Jiang M, Jiang Q, Jiang X, Jiang X, Jimenez A, Jin M, Jin S, Joe CO, Johansen T, Johnson DE, Johnson GV, Jones NL, Joseph B, Joseph SK, Joubert AM, Juhasz G, Juillerat-Jeanneret L, Jung CH, Jung YK, Kaarniranta K, Kaasik A, Kabuta T, Kadowaki M, Kagedal K, Kamada Y, Kaminskyy VO, Kampinga HH, Kanamori H, Kang C, Kang KB, Kang KI, Kang R, Kang YA, Kanki T, Kanneganti TD, Kanno H, Kanthasamy AG, Kanthasamy A, Karantza V, Kaushal GP, Kaushik S, Kawazoe Y, Ke PY, Kehrl JH, Kelekar A, Kerkhoff C, Kessel DH, Khalil H, Kiel JA, Kiger AA, Kihara A, Kim DR, Kim DH, Kim DH, Kim EK, Kim HR, Kim JS, Kim JH, Kim JC, Kim JK, Kim PK, Kim SW, Kim YS, Kim Y, Kimchi A, Kimmelman AC, King JS, Kinsella TJ, Kirkin

V, Kirshenbaum LA, Kitamoto K, Kitazato K, Klein L, Klimecki WT, Klucken J, Knecht E, Ko BC, Koch JC, Koga H, Koh JY, Koh YH, Koike M, Komatsu M, Kominami E, Kong HJ, Kong WJ, Korolchuk VI, Kotake Y, Koukourakis MI, Kouri Flores JB, Kovacs AL, Kraft C, Krainc D, Kramer H, Kretz-Remy C, Krichevsky AM, Kroemer G, Kruger R, Krut O, Ktistakis NT, Kuan CY, Kucharczyk R, Kumar A, Kumar R, Kumar S, Kundu M, Kung HJ, Kurz T, Kwon HJ, La Spada AR, Lafont F, Lamark T, Landry J, Lane JD, Lapaquette P, Laporte JF, Laszlo L, Lavandero S, Lavoie JN, Layfield R, Lazo PA, Le W, Le Cam L, Ledbetter DJ, Lee AJ, Lee BW, Lee GM, Lee J, Lee JH, Lee M, Lee MS, Lee SH, Leeuwenburgh C, Legembre P, Legouis R, Lehmann M, Lei HY, Lei QY, Leib DA, Leiro J, Lemasters JJ, Lemoine A, Lesniak MS, Lev D, Levenson VV, Levine B, Levy E, Li F, Li JL, Li L, Li S, Li W, Li XJ, Li YB, Li YP, Liang C, Liang Q, Liao YF, Liberski PP, Lieberman A, Lim HJ, Lim KL, Lim K, Lin CF, Lin FC, Lin J, Lin JD, Lin K, Lin WW, Lin WC, Lin YL, Linden R, Lingor P, Lippincott-Schwartz J, Lisanti MP, Liton PB, Liu B, Liu CF, Liu K, Liu L, Liu QA, Liu W, Liu YC, Liu Y, Lockshin RA, Lok CN, Lonial S, Loos B, Lopez-Berestein G, Lopez-Otin C, Lossi L, Lotze MT, Low P, Lu B, Lu B, Lu B, Lu Z, Luciano F, Lukacs NW, Lund AH, Lynch-Day MA, Ma Y, Macian F, MacKeigan JP, Macleod KF, Madeo F, Maiuri L, Maiuri MC, Malagoli D, Malicdan MC, Malorni W, Man N, Mandelkow EM, Manon S, Manov I, Mao K, Mao X, Mao Z, Marambaud P, Marazziti D, Marcel YL, Marchbank K, Marchetti P, Marciniak SJ, Marcondes M, Mardi M, Marfe G, Marino G, Markaki M, Marten MR, Martin SJ, Martinand-Mari C, Martinet W, Martinez-Vicente M, Masini M, Matarrese P, Matsuo S, Matteoni R, Mayer A, Mazure NM, McConkey DJ, McConnell MJ, McDermott C, McDonald C, McInerney GM, McKenna SL, McLaughlin B, McLean PJ, McMaster CR, McQuibban GA, Meijer AJ, Meisler MH, Melendez A, Melia TJ, Melino G, Mena MA, Menendez JA, Menna-Barreto RF, Menon MB, Menzies FM, Mercer CA, Merighi A, Merry DE, Meschini S, Meyer CG, Meyer TF, Miao CY, Miao JY, Michels PA, Michiels C, Mijaljica D, Milojkovic A, Minucci S, Miracco C, Miranti CK, Mitroulis I, Miyazawa K, Mizushima N, Mograbi B, Mohseni S, Molero X, Mollereau B, Mollinedo F, Momoi T, Monastyrska I, Monick MM, Monteiro MJ, Moore MN, Mora R, Moreau K, Moreira PI, Moriyasu Y, Moscat J, Mostowy S, Mottram JC, Motyl T, Moussa CE, Muller S, Muller S, Munger K, Munz C, Murphy LO, Murphy ME, Musaro A, Mysorekar I, Nagata E, Nagata K, Nahimana A, Nair U, Nakagawa T, Nakahira K, Nakano H, Nakatogawa H, Nanjundan M, Naqvi NI, Narendra DP, Narita M, Navarro M, Nawrocki ST, Nazarko TY, Nemchenko A, Netea MG, Neufeld TP, Ney PA, Nezis IP, Nguyen HP, Nie D, Nishino I, Nislow C, Nixon RA, Noda T, Noegel AA, Nogalska A, Noguchi S, Notterpek L, Novak I, Nozaki T, Nukina N, Nurnberger T, Nyfeler B, Obara K, Oberley TD, Oddo S, Ogawa M, Ohashi T, Okamoto K, Oleinick NL, Oliver FJ, Olsen LJ, Olsson S, Opota O, Osborne TF, Ostrander GK, Otsu K, Ou JH, Ouimet M, Overholtzer M, Ozpolat B, Paganetti P, Pagnini U, Pallet N, Palmer GE, Palumbo C, Pan T, Panaretakis T, Pandey UB, Papackova Z, Papassideri I, Paris I, Park J, Park OK, Parys JB, Parzych KR, Patschan S, Patterson C, Pattingre S, Pawelek JM, Peng J, Perlmutter DH, Perrotta I, Perry G, Pervaiz S, Peter M, Peters GJ, Petersen M, Petrovski G, Phang JM, Piacentini M, Pierre P, Pierrefite-Carle V, Pierron G, Pinkas-Kramarski R, Piras A, Piri N, Platanias LC, Poggeler S, Poirot M, Poletti A, Pous C, Pozuelo-Rubio M, Praetorius-Ibba M, Prasad A, Prescott M, Priault M, Produit-Zengaffinen N, Progulske-Fox A, Proikas-Cezanne T, Przedborski S, Przyklenk K, Puertollano R, Puyal J, Qian SB, Qin L, Qin ZH, Quaggin SE, Raben N, Rabinowich H,

Rabkin SW, Rahman I, Rami A, Ramm G, Randall G, Randow F, Rao VA, Rathmell JC, Ravikumar B, Ray SK, Reed BH, Reed JC, Reggiori F, Regnier-Vigouroux A, Reichert AS, Reiners JJ, Jr., Reiter RJ, Ren J, Revuelta JL, Rhodes CJ, Ritis K, Rizzo E, Robbins J, Roberge M, Roca H, Roccheri MC, Rocchi S, Rodemann HP, Rodriguez de Cordoba S, Rohrer B, Roninson IB, Rosen K, Rost-Roszkowska MM, Rouis M, Rouschop KM, Rovetta F, Rubin BP, Rubinsztein DC, Ruckdeschel K, Rucker EB, 3rd, Rudich A, Rudolf E, Ruiz-Opazo N, Russo R, Rusten TE, Ryan KM, Ryter SW, Sabatini DM, Sadoshima J, Saha T, Saitoh T, Sakagami H, Sakai Y, Salekdeh GH, Salomoni P, Salvaterra PM, Salvesen G, Salvioli R, Sanchez AM, Sanchez-Alcazar JA, Sanchez-Prieto R, Sandri M, Sankar U, Sansanwal P, Santambrogio L, Saran S, Sarkar S, Sarwal M, Sasakawa C, Sasnauskiene A, Sass M, Sato K, Sato M, Schapira AH, Scharl M, Schatzl HM, Scheper W, Schiaffino S, Schneider C, Schneider ME, Schneider-Stock R, Schoenlein PV, Schorderet DF, Schuller C, Schwartz GK, Scorrano L, Sealy L, Seglen PO, Segura-Aguilar J, Seiliez I, Seleverstov O, Sell C, Seo JB, Separovic D, Setaluri V, Setoguchi T, Settembre C, Shacka JJ, Shanmugam M, Shapiro IM, Shaulian E, Shaw RJ, Shelhamer JH, Shen HM, Shen WC, Sheng ZH, Shi Y, Shibuya K, Shidoji Y, Shieh JJ, Shih CM, Shimada Y, Shimizu S, Shintani T, Shirihai OS, Shore GC, Sibirny AA, Sidhu SB, Sikorska B, Silva-Zacarin EC, Simmons A, Simon AK, Simon HU, Simone C, Simonsen A, Sinclair DA, Singh R, Sinha D, Sinicrope FA, Sirko A, Siu PM, Sivridis E, Skop V, Skulachev VP, Slack RS, Smaili SS, Smith DR, Soengas MS, Soldati T, Song X, Sood AK, Soong TW, Sotgia F, Spector SA, Spies CD, Springer W, Srinivasula SM, Stefanis L, Steffan JS, Stendel R, Stenmark H, Stephanou A, Stern ST, Sternberg C, Stork B, Stralfors P, Subauste CS, Sui X, Sulzer D, Sun J, Sun SY, Sun ZJ, Sung JJ, Suzuki K, Suzuki T, Swanson MS, Swanton C, Sweeney ST, Sy LK, Szabadkai G, Tabas I, Taegtmeyer H, Tafani M, Takacs-Vellai K, Takano Y, Takegawa K, Takemura G, Takeshita F, Talbot NJ, Tan KS, Tanaka K, Tanaka K, Tang D, Tang D, Tanida I, Tannous BA, Tavernarakis N, Taylor GS, Taylor GA, Taylor JP, Terada LS, Terman A, Tettamanti G, Thevissen K, Thompson CB, Thorburn A, Thumm M, Tian F, Tian Y, Tocchini-Valentini G, Tolkovsky AM, Tomino Y, Tonges L, Tooze SA, Tournier C, Tower J, Towns R, Trajkovic V, Travassos LH, Tsai TF, Tschan MP, Tsubata T, Tsung A, Turk B, Turner LS, Tyagi SC, Uchiyama Y, Ueno T, Umekawa M, Umemiya-Shirafuji R, Unni VK, Vaccaro MI, Valente EM, Van den Berghe G, van der Klei IJ, van Doorn W, van Dyk LF, van Egmond M, van Grunsven LA, Vandenabeele P, Vandenberghe WP, Vanhorebeek I, Vaquero EC, Velasco G, Vellai T, Vicencio JM, Vierstra RD, Vila M, Vindis C, Viola G, Viscomi MT, Voitsekhovskaja OV, von Haefen C, Votruba M, Wada K, Wade-Martins R, Walker CL, Walsh CM, Walter J, Wan XB, Wang A, Wang C, Wang D, Wang F, Wang F, Wang G, Wang H, Wang HG, Wang HD, Wang J, Wang K, Wang M, Wang RC, Wang X, Wang X, Wang YJ, Wang Y, Wang Z, Wang ZC, Wang Z, Wansink DG, Ward DM, Watada H, Waters SL, Webster P, Wei L, Weihl CC, Weiss WA, Welford SM, Wen LP, Whitehouse CA, Whitton JL, Whitworth AJ, Wileman T, Wiley JW, Wilkinson S, Willbold D, Williams RL, Williamson PR, Wouters BG, Wu C, Wu DC, Wu WK, Wyttenbach A, Xavier RJ, Xi Z, Xia P, Xiao G, Xie Z, Xie Z, Xu DZ, Xu J, Xu L, Xu X, Yamamoto A, Yamamoto A, Yamashina S, Yamashita M, Yan X, Yanagida M, Yang DS, Yang E, Yang JM, Yang SY, Yang W, Yang WY, Yang Z, Yao MC, Yao TP, Yeganeh B, Yen WL, Yin JJ, Yin XM, Yoo OJ, Yoon G, Yoon SY, Yorimitsu T, Yoshikawa Y, Yoshimori T, Yoshimoto K, You HJ, Youle RJ, Younes A, Yu L, Yu L, Yu SW, Yu WH, Yuan ZM, Yue Z, Yun CH, Yuzaki M, Zabirnyk

O, Silva-Zacarin E, Zacks D, Zacksenhaus E, Zaffaroni N, Zakeri Z, Zeh HJ, 3rd, Zeitlin SO, Zhang H, Zhang HL, Zhang J, Zhang JP, Zhang L, Zhang L, Zhang MY, Zhang XD, Zhao M, Zhao YF, Zhao Y, Zhao ZJ, Zheng X, Zhivotovsky B, Zhong Q, Zhou CZ, Zhu C, Zhu WG, Zhu XF, Zhu X, Zhu Y, Zoladek T, Zong WX, Zorzano A, Zschocke J and Zuckerbraun B. Guidelines for the use and interpretation of assays for monitoring autophagy. *Autophagy*. 2012;8:445-544.
483. Yin X, Xin H, Mao S, Wu G and Guo L. The Role of Autophagy in Sepsis: Protection and Injury to Organs. *Front Physiol*. 2019;10:1071.
484. Parton RG and del Pozo MA. Caveolae as plasma membrane sensors, protectors and organizers. *Nat Rev Mol Cell Biol*. 2013;14:98-112.
485. Williams TM and Lisanti MP. The caveolin proteins. *Genome Biol*. 2004;5:214.
486. Bravo-Sagua R, Parra V, Ortiz-Sandoval C, Navarro-Marquez M, Rodriguez AE, Diaz-Valdivia N, Sanhueza C, Lopez-Crisosto C, Tahbaz N, Rothermel BA, Hill JA, Cifuentes M, Simmen T, Quest AFG and Lavandero S. Caveolin-1 impairs PKA-DRP1-mediated remodelling of ER-mitochondria communication during the early phase of ER stress. *Cell Death Differ*. 2019;26:1195-1212.
487. Zimnicka AM, Husain YS, Shajahan AN, Sverdlov M, Chaga O, Chen Z, Toth PT, Klomp J, Karginov AV, Tiruppathi C, Malik AB and Minshall RD. Src-dependent phosphorylation of caveolin-1 Tyr-14 promotes swelling and release of caveolae. *Mol Biol Cell*. 2016;27:2090-106.
488. Jiao H, Zhang Y, Yan Z, Wang ZG, Liu G, Minshall RD, Malik AB and Hu G. Caveolin-1 Tyr14 phosphorylation induces interaction with TLR4 in endothelial cells and mediates MyD88-dependent signaling and sepsis-induced lung inflammation. *J Immunol*. 2013;191:6191-9.
489. Sun Y, Hu G, Zhang X and Minshall RD. Phosphorylation of caveolin-1 regulates oxidant-induced pulmonary vascular permeability via paracellular and transcellular pathways. *Circ Res*. 2009;105:676-85, 15 p following 685.
490. Choong ML, Yong YP, Tan AC, Luo B and Lodish HF. LIX: a chemokine with a role in hematopoietic stem cells maintenance. *Cytokine*. 2004;25:239-45.
491. Chang MS, McNinch J, Basu R and Simonet S. Cloning and characterization of the human neutrophil-activating peptide (ENA-78) gene. *J Biol Chem*. 1994;269:25277-82.
492. Chandrasekar B, Melby PC, Sarau HM, Raveendran M, Perla RP, Marelli-Berg FM, Dulin NO and Singh IS. Chemokine-cytokine cross-talk. The ELR+ CXC chemokine LIX (CXCL5) amplifies a proinflammatory cytokine response via a phosphatidylinositol 3-kinase-NF-kappa B pathway. *J Biol Chem*. 2003;278:4675-86.
493. Kim H, Kim M, Im SK and Fang S. Mouse Cre-LoxP system: general principles to determine tissue-specific roles of target genes. *Lab Anim Res*. 2018;34:147-159.
494. Doetschman T and Azhar M. Cardiac-specific inducible and conditional gene targeting in mice. *Circ Res*. 2012;110:1498-512.
495. Bersell K, Choudhury S, Mollova M, Polizzotti BD, Ganapathy B, Walsh S, Wadugu B, Arab S and Kuhn B. Moderate and high amounts of tamoxifen in alphaMHC-MerCreMer mice induce a DNA damage response, leading to heart failure and death. *Dis Model Mech*. 2013;6:1459-69.
496. Koitabashi N, Bedja D, Zaiman AL, Pinto YM, Zhang M, Gabrielson KL, Takimoto E and Kass DA. Avoidance of transient cardiomyopathy in cardiomyocyte-targeted tamoxifen-induced MerCreMer gene deletion models. *Circ Res*. 2009;105:12-5.

497. Schultheiss HP, Fairweather D, Caforio ALP, Escher F, Hershberger RE, Lipshultz SE, Liu PP, Matsumori A, Mazzanti A, McMurray J and Priori SG. Dilated cardiomyopathy. *Nat Rev Dis Primers*. 2019;5:32.
498. Zhang H, Viveiros A, Nikhanj A, Nguyen Q, Wang K, Wang W, Freed DH, Mullen JC, MacArthur R, Kim DH, Tymchak W, Sergi CM, Kassiri Z, Wang S and Oudit GY. The Human Explanted Heart Program: A translational bridge for cardiovascular medicine. *Biochim Biophys Acta Mol Basis Dis*. 2020;1867:165995.
499. Vangaveti V, Baune BT and Kennedy RL. Hydroxyoctadecadienoic acids: novel regulators of macrophage differentiation and atherogenesis. *Ther Adv Endocrinol Metab*. 2010;1:51-60.
500. Li WP, Liu P, Pilcher BK and Anderson RG. Cell-specific targeting of caveolin-1 to caveolae, secretory vesicles, cytoplasm or mitochondria. *J Cell Sci*. 2001;114:1397-408.
501. Fridolfsson HN, Kawaraguchi Y, Ali SS, Panneerselvam M, Niesman IR, Finley JC, Kellerhals SE, Migita MY, Okada H, Moreno AL, Jennings M, Kidd MW, Bonds JA, Balijepalli RC, Ross RS, Patel PM, Miyanohara A, Chen Q, Lesnefsky EJ, Head BP, Roth DM, Insel PA and Patel HH. Mitochondria-localized caveolin in adaptation to cellular stress and injury. *FASEB J*. 2012;26:4637-49.
502. Chaudhary KR, Cho WJ, Yang F, Samokhvalov V, El-Sikhry HE, Daniel EE and Seubert JM. Effect of ischemia reperfusion injury and epoxyeicosatrienoic acids on caveolin expression in mouse myocardium. *J Cardiovasc Pharmacol*. 2013;61:258-63.
503. Bosch M, Mari M, Herms A, Fernandez A, Fajardo A, Kassan A, Giralt A, Colell A, Balgoma D, Barbero E, Gonzalez-Moreno E, Matias N, Tebar F, Balsinde J, Camps M, Enrich C, Gross SP, Garcia-Ruiz C, Perez-Navarro E, Fernandez-Checa JC and Pol A. Caveolin-1 deficiency causes cholesterol-dependent mitochondrial dysfunction and apoptotic susceptibility. *Curr Biol*. 2011;21:681-6.
504. Chen YH, Lin WW, Liu CS, Hsu LS, Lin YM and Su SL. Caveolin-1 provides palliation for adverse hepatic reactions in hypercholesterolemic rabbits. *PLoS One*. 2014;9:e71862.
505. Shiroto T, Romero N, Sugiyama T, Sartoretto JL, Kalwa H, Yan Z, Shimokawa H and Michel T. Caveolin-1 is a critical determinant of autophagy, metabolic switching, and oxidative stress in vascular endothelium. *PLoS One*. 2014;9:e87871.
506. Asterholm IW, Mundy DI, Weng J, Anderson RG and Scherer PE. Altered mitochondrial function and metabolic inflexibility associated with loss of caveolin-1. *Cell Metab*. 2012;15:171-85.

Schematics created with BioRender.com

APPENDIX

An adapted version of the following manuscript: Deanna K. Sosnowski, K. Lockhart Jamieson, Ahmed M. Darwesh, Hao Zhang, Matthew L. Edin, Darryl C. Zeldin, Gavin Y. Oudit, John M. Seubert. *Alterations to the N-3 and N-6 PUFA metabolome and mitochondrial quality in heart tissue from human dilated cardiomyopathy patients* has been submitted to JMCC, November 2021.

This project was led in collaboration by Dr. Gavin Oudit from the Faculty of Medicine and principle investigator Dr. John Seubert from the Faculty of Pharmacy and Pharmaceutical Sciences. Gavin Y. Oudit is the director of the Human Explanted Heart Program (HELP) and Human Organ Procurement and Exchange Program (HOPE) and the University of Alberta and the Mazankowski Heart Institute and provided the human heart tissue as well as guidance for this study. K. Lockhart Jamieson collected initial Western immunoblot data and conducted and analyzed mitochondrial enzyme complex activity data. Ahmed M. Darwesh performed and analyzed the results of cardiac fibre mitochondrial respiration. Hao Zhang performed electron microscopy. Matthew L. Edin, a member of the research group of Darryl C. Zeldin conducted LCMS/MS on heart tissue to generate the oxylipin profiles.

ABSTRACT

Dilated cardiomyopathy (DCM) is characterized by impaired cardiac function due to dilation of the ventricles. N-3 and N-6 polyunsaturated fatty acid (PUFA)-derived lipid mediators have beneficial and detrimental effects on the heart. However, contribution of these lipid mediators to DCM pathobiology remains under-explored. Using left ventricle tissues from DCM patients, we identified marked disturbances in the oxylipid metabolome. These alterations are accompanied by severe impairments in mitochondrial ultrastructure, function, and caveolin-1 protein expression. Exogenous oxylipid administration was able to improve mitochondrial function from DCM cardiac fibres, highlighting a critical link between DCM pathogenesis, mitochondrial health, and the PUFA metabolome.

A.1. INTRODUCTION

Dilated cardiomyopathy (DCM) is a disease characterized by dilation of the ventricles accompanied by systolic dysfunction and reduced cardiac output.[497] In addition to ventricular remodeling and fibrosis, DCM is associated with impaired cardiac mitochondrial function and bioenergetics; however, the pathophysiological mechanism(s) of disease development and progression remain poorly understood.[497] Dietary lipids play a critical role in maintaining cardiac function and cellular homeostasis but they can contribute to the pathogenesis of numerous cardiovascular disorders.[6] To date, only a limited number of studies have examined lipid profiles in cardiac tissue from human DCM patients. N-3 and N-6 polyunsaturated fatty acids (PUFAs) can be metabolised by cyclooxygenase (COX), lipoxygenase (LOX) and cytochrome P450 (CYP)-epoxygenase enzymes into a plethora of biologically active lipid mediators.[6] CYP-epoxygenase-derived metabolites of N-3 and N-6 PUFAs, termed as oxylipids, have known cardioprotective and anti-inflammatory effects in various cardiac disease models, yet have not been fully explored in the context of DCM.[6] Importantly, CYP-derived oxylipids, such as epoxyeicosatrienoic acids (EETs) and epoxydocosapentaenoic acids (EDPs), exert cardioprotective effects.[6] In this study, we characterize the PUFA metabolome profiles obtained from human patients with DCM and examine correlations with biomarkers of cardiac mitochondrial quality. These data provide

preliminary but novel mechanistic insight into DCM pathogenesis and identify new therapeutic avenues to explore in further detail.

A.2. MATERIALS AND METHODS

A.2.1 Patient clinical data and donor heart tissue procurement

Left ventricular (LV) biopsies from male and female non-failing control (NFC) donors with no history of CVD were obtained from the Human Organ Procurement and Exchange (HOPE) at the University of Alberta. Additionally, biopsies from DCM patients with end-stage heart failure were procured as part of the Human Explanted Heart Program (HELP) during transplant procedures at the Mazankowski Alberta Heart Institute.[498] Tissue collection followed protocols approved by the Health Research and Ethics Board of the University of Alberta. Both the demographic and clinical data from NFC and DCM patients is summarized in Table 1.A. Data from DCM patients corresponds to clinical assessment prior to when heart transplant was performed.

A.2.2 Oxylipid and metabolomic profile

Levels of oxylipins and their metabolites were quantified by LCMS/MS. Analysis of heart tissue was performed in accordance with previously established protocols.[309]

A.2.3 Protein expression and immunoblot analysis

Heart tissue was homogenized, fractionated, and prepared for Western immunoblot according to the following detailed protocol.[300] Primary antibodies were used at a concentration of 1:1000 (sEH, sc25797; GAPDH, cs5174; mEH, sc135984; CYP2J2, ABS1605; CYP2C8, ab88904; β Actin, sc47778; Caveolin-1, cs3267s; VDAC, ab14734). Densitometry was performed with ImageJ software and protein expressions were normalized to their respective loading controls.

A.2.4 Mitochondrial enzyme activities

Complex I (NADH:ubiquinone oxidoreductase), complex II (succinate dehydrogenase) and citrate synthase activities were determined in mitochondrial tissue fractions as previously described.[300] Briefly, individual cuvettes containing sample and substrates for complex I (NADH 100 μM, ubiquinone 60 μM), complex II (succinate 20 mM, DCPIP 80 μM, decylubiquinone 50 μM) or citrate synthase (DTNB 100 μM, acetyl coenzyme A 300 μM) were prepared. Specific inhibitors for complex I (rotenone 10 μM) and complex II (malonate 10 mM) were added in a separate assay to account for non-specific complex activity. Absorbance (complex I, 340 nm; complex II, 600 nm; citrate synthase, 412 nm) was monitored spectrophotometrically over 2-3 minutes. Complex activity was calculated using linear absorbance, substrate extinction coefficient, sample volume, and protein concentration.

A.2.5 Mitochondrial respiration

Determination of mitochondrial oxygen consumption was performed using a Clark electrode connected to an Oxygraph Plus recorder (Hansatech Instruments Ltd., Norfolk, England). Non-frozen, fresh cardiac fibres were isolated from hearts within 30-minutes post-transplant. Fibres were permeabilized with isolation buffer containing saponin (100 μg/mL), and added to the 30°C respiration chamber containing 2 mL of respiration buffer. Basal and ADP-stimulated (0.5 mmol/L) respiratory rates using malate (5 mmol/L) and glutamate (10 mmol/L) as substrates were recorded followed by the addition of vehicle or 19,20-EDP (1 μM). Respiratory control ratio (RCR) was calculated as the ratio between basal and ADP-stimulated respiration rates to indicate efficiency of ATP production.

2.6 Mitochondrial ultrastructure

Transmission electron microscopy (TEM) was used to assess mitochondrial morphology and ultrastructure in myocardial tissue.[307] Slices were imaged within 1 week of staining at 60 kV using a transmission electron microscope (Hitachi H-7650 TEM, Hitachi

High-Technologies Canada, Inc) with a 16-megapixel EMCCD camera (XR111, Advanced Microscopy Technique, MA, United States) at the University of Alberta, Faculty of Medicine and Dentistry, EM Core Facility. A qualitative scoring tool was used to assess the presence and severity of inclusion bodies and cristae disorganization. Images were randomly scored in triplicate by two blinded, independent investigators.

A.3. RESULTS AND DISCUSSION

A.3.1 DCM left ventricles have marked changes in oxylipid and metabolism profiles

CYP-derived oxylipids in DCM hearts including epoxyoctadecenoic acid (EpOME) and epoxyeicosatrienoic acid (EET) were significantly elevated (Table 2.A). Oxylipids, such as EETs, have known cardioprotective effects, including preservation of mitochondrial quality and function.[6] These data suggest a compensatory upregulation of protective oxylipid metabolites within the failing heart. Metabolism of oxylipids to their corresponding less active, and potentially detrimental, diol metabolites occurs by soluble epoxide hydrolase (sEH) and microsomal epoxide hydrolase (mEH).[6] For example, DiHOMEs promote inflammation, impact mitochondrial quality and attenuate cardiac function.[6] Increased diol metabolites including, dihydroxyeicosatrienoic acids (DHET) and dihydroxyoctadecanoic acids (DiHOME), indicate enhanced metabolic capacity of sEH and mEH in DCM hearts. Further metabolic shifts observed in DCM tissues demonstrate enhanced COX-derived inflammatory mediators, PGE_2, PGD_2 and TXB_2 indicating robust inflammation in the failing hearts. Interestingly, LOX-derived stable oxidation products of the N-6 PUFA linoleic acid, 9- and 13-hydroxyoctadecadienoic acid (HODE) were strikingly increased. HODEs, known to possess proinflammatory properties, are involved in atherosclerosis, resident macrophage lipid uptake, and plaque progression.[499] Their role in heart failure and DCM remain unknown, highlighting necessary future exploration. Alterations in cardiac PUFA-metabolising enzymes revealed trending elevation in expression of the CYP450 epoxygenases, CYP2J2, but not CYP2C8, in DCM hearts consistent with marked increase in oxylipid levels (Figure A.1). Importantly both sEH and mEH were markedly increased in DCM tissues consistent with the observed increase in diol metabolites (Table A.2) and

(Figure A.1). Furthermore, no differences in expression were observed between male and female DCM patients.

A.3.2 Impaired mitochondrial quality in DCM hearts can be partially rescued by oxylipids

Assessment of damaged mitochondria in DCM hearts from images using a 60kV transmission electron microscope highlights distinct ultrastructural changes, such as loss of circular morphology and cristae organization as well as the presence of inclusion bodies. (Figure A.1). The morphological changes were accompanied by significant decreases in activity of electron transport chain enzymes, complex I and II, as well as citrate synthase (Figure A.1). Freshly isolated cardiac fibres demonstrated a reduced respiratory control ratio (RCR) in male and female DCM tissues compared to NFC suggesting a diminished ability to produce ATP and impaired mitochondrial function (Figure A.1). Importantly, treatment of permeabilized DCM cardiac fibres with the oxylipid 19,20-EDP (1 μM) partially rescued the mitochondrial RCR indicating a protective role for oxylipids in DCM hearts (Figure A.1).

A.3.3 Reduced mitochondrial caveolin-1 correlates with impaired mitochondrial function and oxylipid disturbances

Caveolae are invaginations in the plasma membrane forming lipid rafts rich in proteins and lipids critical for endocytosis, signal transduction, and lipid transport.[484] Caveolae are composed of structural proteins called caveolins, including caveolin-1 (Cav-1).[484] Given the importance of caveolae and caveolins in basic cellular functions, their role in CVD pathobiology is under-explored. Studies have shown that Cav-1 not only forms caveolins at the plasma membrane but can also localize to organelles, including the mitochondrial membrane.[500, 501] Levels of Cav-1 are reduced following ischemia-reperfusion injury correlating with damage to mitochondrial morphology.[502] Genetic deletion of Cav-1 causes mitochondrial dysfunction including hyperpolarization, reactive oxygen species production, and impairment in respiratory chain complex activity.[503-506] In male DCM hearts, Cav-1 expression was significantly reduced in mitochondrial fractions, suggesting a link to impaired mitochondrial quality and function (Figure A.1). Our previous work

demonstrated that genetic deletion of sEH or treatment with the beneficial oxylipid, EET, preserves cardiac mitochondrial Cav-1 levels and ultrastructure following IR injury.[502] Similarly in this current study, enhanced sEH expression and oxylipid metabolism correlates with reduced mitochondrial Cav-1 expression and impaired mitochondrial quality. These findings suggest an intricate relationship between Cav-1, oxylipid metabolism, and mitochondrial function, in the pathogenesis and progression of DCM.

A.4. CONCULSION

Together these data demonstrate a marked shift in the N-3 and N-6 PUFA metabolome in LV tissues from DCM patients compared to NFC, which was correlated with a decline in Cav-1 expression and mitochondrial function. Despite a compensatory increase in beneficial CYP-derived oxylipids, there was also a marked elevation of detrimental and pro-inflammatory metabolites in DCM hearts (Figure A.2), which suggests compensatory elevation of oxylipid levels may not be sufficient to protect the failing heart. Preliminary experimental data indicate oxylipids, such as 19,20-EDP, can improve mitochondrial respiration rates in DCM fibres. Moreover, as 19, 20-EDP levels were not increased in the DCM tissues these observations suggest the exogenous administration of oxylipids may circumvent the effects of detrimental metabolites. Limited research has investigated the role of lipid mediators and their metabolites in DCM. This study provides the novel, preliminary findings to fuel future mechanistic studies to decipher the relationship between Cav-1, mitochondrial quality, and oxylipids in DCM pathogenesis; henceforth, providing insight into novel therapeutic strategies for individuals with DCM.

NFC

	Male n= 5	Female n= 6	P Value
Demographics			
Age, yrs	38 (27-38)	51 (44-56)	0.11
BMI, kg/m^2	23.1 (21.9-24.4)	25.5 (24.2-27.6)	0.20
Echocardiography			
LVEF (%)	45 (40-50)	55 (43-60)	0.35

DCM

	Male n= 12	Female n= 3	P Value		Male n= 12	Female n= 3	P Value
Demographics				**Functional Class**			
Age, yrs	52 (47-56)	55 (46-56)	0.86	NYHA II	1 (8.3)	1 (33.3)	0.37
BMI, kg/m^2	24.7 (22.6-25.2)	27.6 (24.2-33.5)	0.45	NYHA III	7 (58.3)	1 (33.3)	0.57
Laboratory Tests				NYHA IV	4 (33.3)	1 (33.3)	>0.99
Hemoglobin, g/L	119 (113-134)	115 (112-121)	0.72	**Comorbidities**			
eGFR, mL/min/m2	57 (51-62)	62 (59-92)	0.28	Atrial fibrillation	2 (16.7)	0	>0.99
Medications				Kidney disease	9 (75.0)	1 (33.3)	0.24
ACE inhibitor	7 (58.3)	3 (100)	0.51	Diabetes mellitus	2 (16.7)	1 (33.3)	0.52
ARB	2 (16.7)	1 (33.3)	0.52	Hypertension	1 (8.3)	0	>0.99
β-blocker	9 (75.0)	3 (100)	>0.99	COPD/Asthma	2 (16.7)	3 (100)	0.022*
Loop diuretics	11 (91.7)	1 (33.3)	0.081	Dyslipidemia	1 (8.3)	0	>0.99
MRA	8 (66.7)	1 (33.3)	0.53	Liver disease	3 (25.0)	0	>0.99
Antiplatelet	7 (58.3)	2 (66.7)	>0.99	**Devices**			
Anticoagulant	8 (66.7)	3 (100)	0.52	AICD/ICD	5 (41.7)	1 (33.3)	>0.99
Statin	3 (25)	1 (33.3)	>0.99	BiV-ICD	2 (16.7)	1 (33.3)	0.52
Antiarrhythmics				CRT	2 (16.7)	1 (33.3)	0.52
Class I	1 (8.3)	0	>0.99	**Vitals**			
Class III	3 (25.0)	2 (66.7)	0.24	Heart rate, bpm	96 (74-103)	108 (101-114)	0.33
Echocardiography				Systolic BP, mmHg	101 (91-116)	113 (110-117)	0.50
LVEF (%)	18 (13-20)	20 (16-26)	0.68	Diastolic BP, mmHg	64 (56-73)	71 (69-73)	0.45

Table A.1. Demographic and clinical parameters of patients from electronic medical records. Descriptive data is expressed as median (interquartile range, IQR) and analyzed using non-parametric Mann Whitney t-test. Categorical data is expressed as absolute number (%) and analyzed using standard chi square with Fisher's exact test (each individual patient = N, male NFC N = 5, male DMC N = 12, female NFC N = 6, female DCM N = 3, $*p<0.05$).

	Male		Female	
	NFC	**DCM**	**NFC**	**DCM**
CYP dependent				
9,10-EpOME	63.7 ± 22.1	411.6 ± 71.6*	92.4 ± 36.0	245.8 ± 87.4
12,13-EpOME	17.5 ± 3.9	106.2 ± 20.7*	28.7 ± 9.9	61.1 ± 24.0
8,9-EET	11.6 ± 1.4	20.9 ± 2.5*	12.6 ± 1.9	12.8 ± 3.3
11,12-EET	5.6 ± 0.9	14.0 ± 2.7*	6.7 ± 0.9	5.0 ± 2.0#
14,15-EET	8.8 ± 1.0	13.9 ± 1.3*	10.9 ± 1.2	8.5 ± 2.23
19,20-EDP	47.9 ± 14.3	47.8 ± 11.8	35.6 ± 2.3	35.94± 9.6
sEH dependent				
9,10-DiHOME	8.7 ± 2.3	74.0 ± 10.8*	12.0 ± 3.8	37.9 ± 10.9*
12,13-DiHOME	4.9 ± 0.7	17.8 ± 3.5*	6.1 ± 1.6	16.3 ± 4.7*
8,9-DHET	0.8 ± 0.1	1.6 ± 0.2*	0.7 ± 0.1	1.2 ± 0.4
11,12-DHET	0.8 ± 0.08	0.9 ± 0.1	0.9 ± 0.1	1.0 ± 0.4
14,15-DHET	0.6 ± 0.08	0.8 ± 0.1	0.5 ± 0.07	0.5 ± 0.04
COX dependent				
6-keto $PGF_{1\alpha}$	5.4 ± 2.1	2.4 ± 0.9	5.7 ± 1.1	2.7 ± 2.3
TXB_2	0.2 ± 0.06	0.08 ± 0.02*	0.2 ± 0.06	0.05 ± 0.04
$PGF_{2\alpha}$	5.1 ± 3.1	7.7 ± 4.4	1.1 ± 0.5	2.6 ± 0.4
PGE_2	6.0 ± 1.5	27.5 ± 4.3*	9.0 ± 2.7	13.8 ± 4.8
PGD_2	10.6 ± 2.9	43.1 ± 4.6*	16.5 ± 4.4	23.9 ± 8.3
8iso$PGF_{2\alpha}$	1.0 ± 0.09	1.8 ± 0.3	1.1 ± 0.09	1.1 ± 0.2
LOX dependent				
9-HODE	159.5 ± 25.0	1074.4 ± 207.3*	359.4 ± 154.5	675.7 ± 417.9
13-HODE	282.5 ± 37.6	1488.7 ± 278.6*	542.2 ± 204.6	970.3 ± 527.1
5-HETE	26.8 ± 6.7	35.5 ± 8.0	36.0 ± 5.8	17.6 ± 5.1
11-HETE	29.6 ± 7.6	33.2 ± 6.4	33.8 ± 5.8	18.2 ± 8.2
12-HETE	40.9 ± 12.4	34.0 ± 7.2	45.6 ± 7.9	18.5 ± 8.1
15-HETE	39.9 ± 9.9	53.1 ± 13.2	48.8 ± 8.0	23.7 ± 9.7

Table A.2. N-3 and N-6 oxylipin profile (ng/g tissue) from LV heart biopsies measured by LCMS/MS. Data were analyzed using ordinary one-way ANOVA with Tukey's multiple comparisons test and are expressed as mean ± SEM (male NFC N = 5, male DCM N = 10, female NFC N = 4, female DCM N = 3, *$p<0.05$ vs. NFC, $^{\#}p<0.05$ vs. male counterpart).

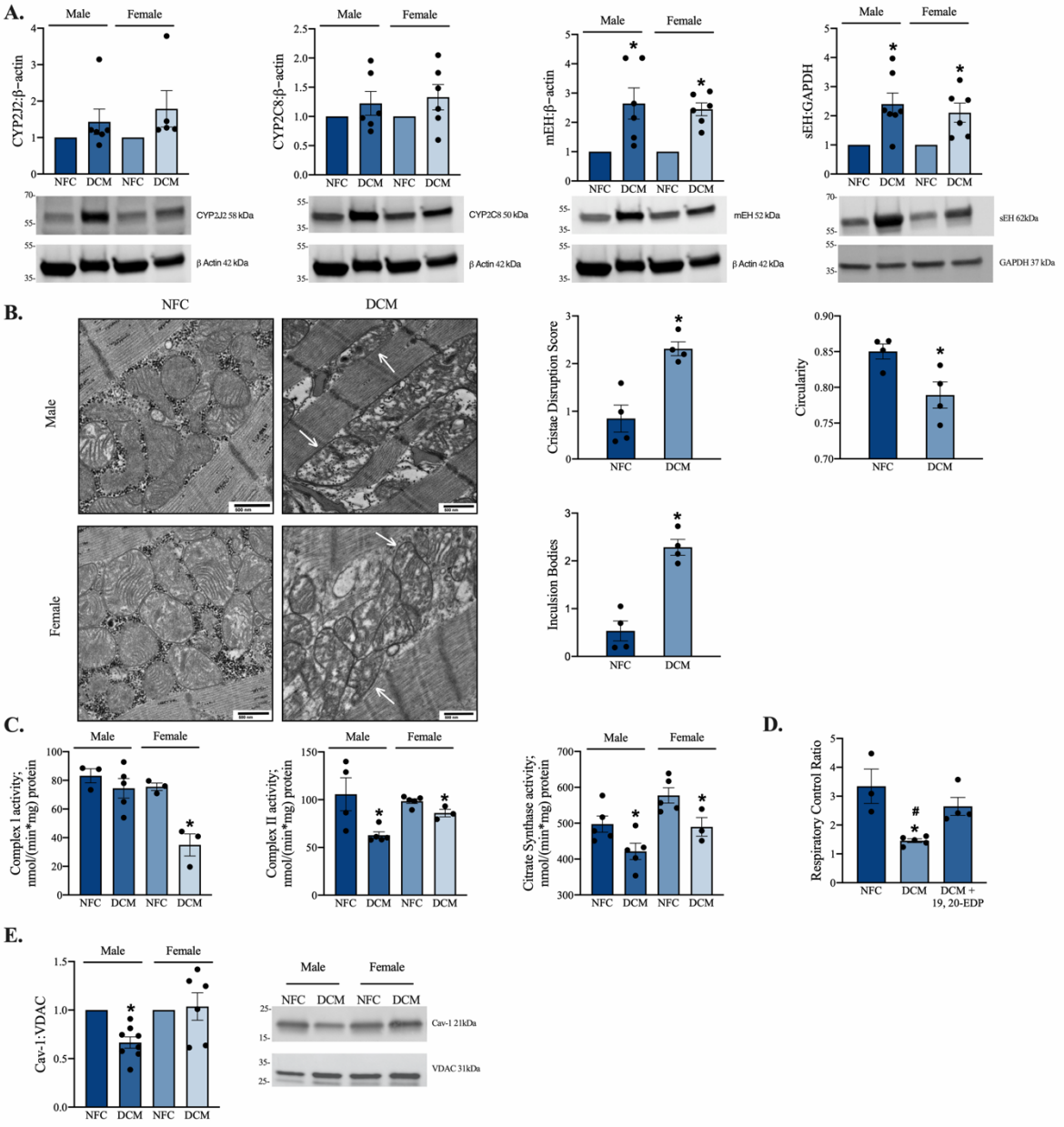

Figure A.1. A) Western immunoblot of PUFA and oxylipid metabolizing enzymes in microsomal and cytosolic fractions. **B)** Representative images of mitochondrial morphology by transmission electron microscopy. White arrows indicate damaged mitochondria **C)** Enzymatic activities of mitochondrial electron transport chain complexes. **D)** Mitochondrial oxygen consumption in LV tissue. **E)** Western immunoblot of caveolin-1 expression in mitochondrial fractions. Data are expressed as means ± SEM and analyzed using one-way ANOVA with Tukey's multiple comparisons test (male NFC N = 6, female NFC N = 6, male DCM N = 6, female DCM N = 6, * $p<0.05$ vs. NFC, # $p<0.05$ vs. DCM + 19,20-EDP).

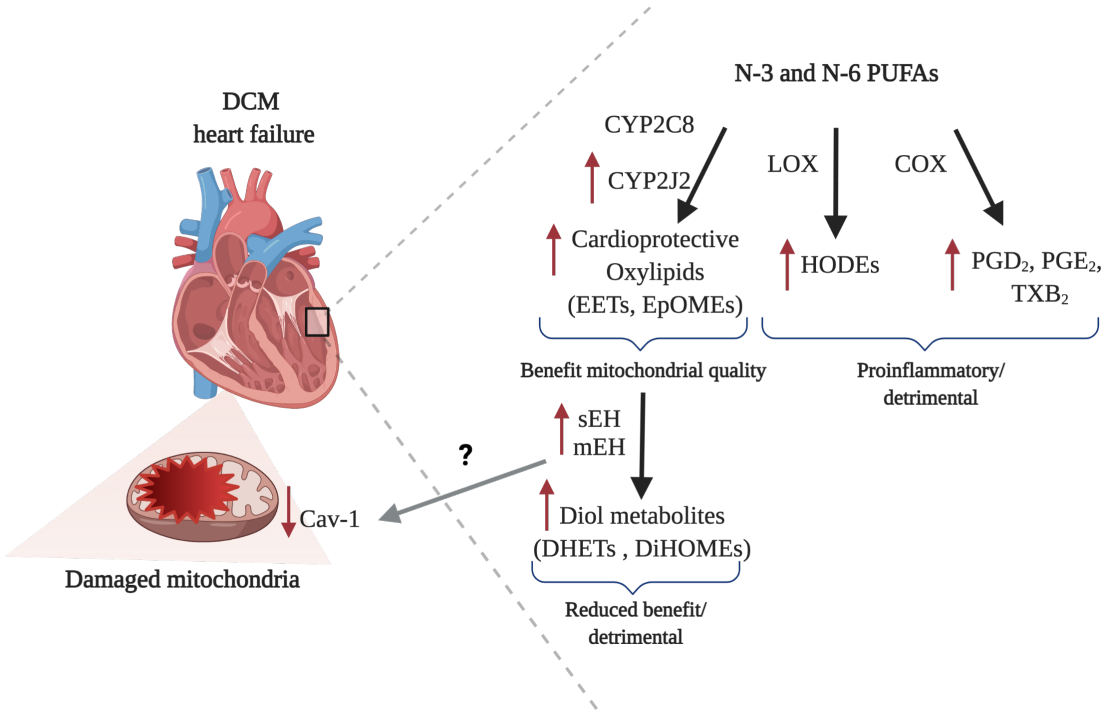

Figure A.2. Graphical schematic of data.